






Universitat Autònoma de Barcelona

**Control of abiotic stress
responses by brassinosteroids
receptors in Arabidopsis thaliana**

Fidel Lozano Elena

ADVERTIMENT. L'accés als continguts d'aquesta tesi queda condicionat a l'acceptació de les condicions d'ús establertes per la següent llicència Creative Commons:  http://cat.creativecommons.org/?page_id=184

ADVERTENCIA. El acceso a los contenidos de esta tesis queda condicionado a la aceptación de las condiciones de uso establecidas por la siguiente licencia Creative Commons:  <http://es.creativecommons.org/blog/licencias/>

WARNING. The access to the contents of this doctoral thesis it is limited to the acceptance of the use conditions set by the following Creative Commons license:  <https://creativecommons.org/licenses/?lang=en>

UNIVERSITAT AUTÒNOMA DE BARCELONA

CENTER FOR RESEARCH IN AGRICULTURAL
GENOMICS (CRAG)

Control of abiotic stress
responses by brassinosteroids
receptors in *Arabidopsis thaliana*

Author:

Fidel

Lozano Elena

Supervisor:

Dr. Ana I.

Caño-Delgado

September 3, 2019

Universitat Autònoma de Barcelona

Animal biology, Plant biology and Ecology department

Plant Biology and Biotechnology PhD program

**Center for Research in Agricultural Genomics
(CRAG)**

Molecular Genetics department

**Control of abiotic stress
responses by brassinosteroids
receptors in *Arabidopsis thaliana***

Dissertation submitted in partial fulfillment of the requirements for obtaining
the degree of Doctor (PhD) by Universitat Autònoma de Barcelona
(Barcelona, Spain)

Author:

Fidel

Lozano Elena

Supervisor:

Dr. Ana I.

Caño-Delgado

September 3, 2019

”Caminante no hay camino, se hace camino al andar...

Caminante no hay camino, sino estelas en la mar.”

Antonio Machado

A la libertad de perderse...

y al orgullo de encontrarse.

Abstract

The present PhD thesis dissertation reports new functions for Brassinosteroids receptors controlling abiotic stress responses in *Arabidopsis thaliana*.

Brassinosteroids (BRs) are the steroid hormones of plants. BRs play essential roles in plant growth and development and plant adaptation to stress. In this direction, exogenous application of BRs provide crop protection against abiotic stresses, such as salt, cold or drought stress, yet the mechanisms governing these responses have remained unknown. Activation of downstream signaling components failed to provide the resistance observed with exogenous applications. The putative roles of BR receptors under stress stand out as key information for dissecting the BR-driven mechanism of stress adaptation but they have remained very unexplored. Here, we use an interdisciplinary approach, including genetics, multiomics analyses and bioinformatics, to decipher the roles of BR receptors in front of abiotic stresses such as DNA damage, osmotic stress and drought.

The results presented in this thesis uncover a role for the spatiotemporal control of BR signaling in response to abiotic stress. Physiological analysis of *Arabidopsis* roots revealed that BR receptors are required for cellular regeneration of the root stem cells after DNA damage. Moreover, the multiomic analysis of plants exposed to drought showed that the overexpression of the vascular-specific BRI1-like 3 (BRL3) receptor lead to an altered transcriptional

and metabolic signature that alleviate the detrimental effects of drought and decouple drought tolerance from growth arrest. A major part of omics hallmarks found in these plants are phloem-specific. The bioinformatic approach used to disentangle tissue-specific transcriptional control was further implemented in a web tool, expandable to any plant specie. Finally, through a structural biology approach we found a small Receptor-Like Kinase (RLK) whose interaction with BRL3 is more favorable than the canonical co-receptor BAK1. Indeed, this candidate has been recently involved in response to osmotic stress, which suggest alternative BR-activated pathways that control abiotic stress responses.

Overall, the present PhD thesis advances the roles of BR receptors to support plant growth and survival under abiotic stress. BRs paracrine signaling at the root stem cell niche and the metabolic adaptation driven from vascular tissues illustrate the importance of dissecting plant tissue-specific responses. The study presented here, also opens new windows for further investigation on mechanisms triggered by BR-receptor that contribute to plant adaptation.

Contents

1	General Introduction	1
1.1	Brassinosteroids are plant growth regulators	3
1.2	Brassinosteroid perception at plasma membrane	9
1.3	Common and specific roles of BRLs	17
1.4	Brassinsteroids impact on abiotic stress responses	20
1.5	Conclusions and perspectives	27
	Objectives	29
2	Brassinosteroid signaling and perception at Arabidopsis root stem cell niche	31
2.1	Introduction	33
2.2	Active BES1 can trigger QC divisions cell-autonomously	35
2.3	The hormone is the limiting factor for QC divisions	37
2.4	BRI1 is necessary but not sufficient to promote QC division	42
2.5	BR signaling acts in a paracrine manner to trigger QC divisions	49
3	Vascular receptor BRL3 mediates drought stress responses	55
3.1	Introduction	57
3.2	BR receptors control osmotic stress sensitivity in the root	60
3.3	BRL3 overexpression confers drought resistance without penalizing growth	69
3.4	BRL3 overexpressor plants accumulate osmoprotectant metabolites	73
3.5	Transcriptional control of metabolite production by BRL3	81

4	TOTEM: A web <u>T</u>ool for <u>T</u>issue-<u>E</u>nrichment analysis on gene lists	99
4.1	Introduction	101
4.2	Basic usage and implementation	102
4.3	Tissue-enrichment analysis of deregulated genes in <i>BRL3ox</i> roots	108
4.4	Tissue-enrichment analysis of BR-regulated drought stress genes in maturing tomato fruits	113
4.5	Future perspectives	113
5	Computational modeling of BRL3 interactors	117
5.1	Introduction	119
5.2	High-throughput modeling of protein-protein interactions with BR-receptors	124
5.3	BRL3 has a more favorable LRR-RLK interactor than BAK1 . .	131
5.4	Identification of critical residues for the interaction	134
5.5	Modeling of ligand-mediated interaction at extracellular part . .	138
5.6	Future perspectives	143
6	General Discussion	147
6.1	Brassinosteroid perception at the stem cell niche is necessary for QC division and cellular regeneration	150
6.2	The vascular brassinosteroid receptor BRL3 confers drought resistance through metabolite production	155
6.3	Information on tissue-specific expression is a valuable resource to identify specific responses	162
6.4	KIN7 is a probable co-receptor of BRL3 implicated in abiotic stress responses	163
6.5	Future perspectives	168
	Conclusions	171
	Materials and methods	175
	Plant material and growth conditions	177

Plant physiology	179
Imaging	183
Methods in molecular biology	185
Bioinformatics and statistics	191
Structural bioinformatics	196
Bibliography	201
Acknowledgements	231
List of Figures	235
List of Tables	239
CV and Publications	241

Abbreviations

- 3DiD:** DATABASE OF THREE-DIMENSIONAL INTERACTING DOMAINS
- ABA:** ABSICIC ACID
- amiRNA:** ARTIFICIAL MICRO-INTERFERENCE RNA
- BAK1:** BRI1-ASSOCIATED KINASE 1
- BKI1:** BRI1-KINASE INHIBITOR 1
- BES1:** BRI1-EMS-SUPPRESSOR 1
- BIN2:** BRASSINOSTEROID INSENSITIVE 2
- BL:** BRASSINOLIDE
- BR(s):** BRASSINOSTEROID(S)
- BRAVO:** BRASSINOSTEROID AT VASCULAR AND ORGANIZING CENTER
- BRI1:** BRASINOSTEROID INSENSITIVE 1
- BRL1/2/3:** BRI1-LIKE 1/2/3
- BRZ:** BRASSINAZOLE
- BSKs:** BRASSINOSTEROIDS-SIGNALING KINASES
- BZR1:** BRASSINAZOLE RESISTANT 1
- CaMV35S:** CAULIFLOWER MOSAIC VIRUS 35S PROMOTER
- CoIP:** CO-IMMUNO PRECIPITATION
- CPD:** CONSTITUTIVE PHOTOMORPHOGENIC DWARF
- CS:** CASTASTERONE
- ddG:** VARIATION IN GIBBS' FREE ENERGY
- DWF4:** DWARF 4

EdU: 5-ETHYNYL-2'-DEOXYURIDINE
ERF115: ETHYLENE-RESPONSE FACTOR 115
FACS: FLUORESCENCE-ACTIVATED CELL SORTING
GCI: GRATING-COUPLED INTERFEROMETRY
GO: GENE ONTOLOGY
GalS2: GALACTINOL SYNTHASE 2
ITC: ISOTHERMAL TITRATION CALORIMETRY
JA: JASMONIC ACID
LEA: LATE EMBRYOGENESIS ABUNDANT
LRR: LEUCINE RICH REPEATS
PCD: PROGRAMMED CELL DEATH
PDB: PROTEIN DATA BANK
PI: PROPIDIUM IODINE
PPI: PROTEIN-PROTEIN INTERACTION
QC: QUISCENT CENTER
RAB18: RESPONSIVE TO ABA 18
RD22/26: RESPONSE TO DESSICATION 22/26
RFO: RAFFINOSE FAMILY OF OLIGOSACCHARIDES
RLK(s): RECEPTOR LIKE KINASE(S)
ROS: REACTIVE OXYGEN SPECIES
RPKM: READS PER KILOBASE MILLION
RWC: RELATIVE WATER CONTENT
SCR: SCARECROW (ENDODEMIS-SPECIFIC TRANSCRIPTION FACTOR)
SERKs: SOMATIC EMBRYOGENESIS RECEPTOR-LIKE KINASES
SVG: SCALABLE VECTOR GRAPH
TPP: TREHALOSE PHOSPHATE PHOSPHATASE
WOX5: WUSCHEL-RELATED HOMEBOX 5 (QC-SPECIFIC TRANSCRIPTION FACTOR)
Y2H: YEAST TWO HYBRID

Chapter 1

General Introduction

Part of this chapter published as:

Emerging roles of vascular brassinosteroid receptors of the BRI1-like family

Lozano-Elena, F. and Caño-Delgado, AI. (2019) *Current Opinion in Plant Biology*, 51:105-113.

General Introduction

1.1 Brassinosteroids are plant growth regulators

Brassinosteroids (BR) are plant steroid hormones essential for plant growth and development. BRs are a group of naturally occurring polyhydroxysteroids, originally purified from rape pollen (*Brassica napus*) because their ability to promote growth in small amounts when applied exogenously to other plants (Mandava, 1988; Mitchell et al., 1970). BR molecules are composed of a steroid nucleus (some with the oxygen function in the B ring) but they generally differ in the radicals bound to the C17, in the steroid D ring (Mandava, 1988) (Figure 1.1). Strikingly, plant BRs resemble animal steroids, not only in terms of chemical structure, but also in the functions they regulate, for example embryonic development or homeostasis in mature organisms (Thummel and Chory, 2002).

Brassinosteroids control growth and development

Since their original discovery, BRs have been linked to growth processes, especially to cell division and elongation (Mandava, 1988). BRs were rapidly associated to mutants that had impaired photomorphogenesis or defective

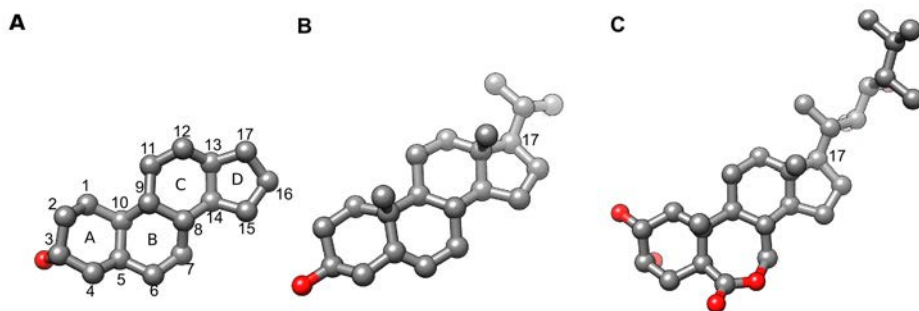


Figure 1.1: Chemical structures of sterol and brassinosteroids

(A) Sterol: This is basic steroid structure common to all BRs (B) Campesterol: Common precursor for the synthesis of all BRs (C) Brassinolide: The most active BR. Note the different radicals bound to the C17 of the steroid structure. Carbon in gray, Oxygen in red. Hydrogens are not represented.

light-dependent development (Li et al., 1996; Szekeres et al., 1996). Further screening for BR-insensitivity mutants (putative receptor mutants) identified plants showing dark-green leaves with a packed rosette of very small size (Clouse et al., 1996; Kauschmann et al., 1996; Li and Chory, 1997). Later studies have revealed direct interactions of components of the BR signaling pathway with the light signaling machinery of the plant, supporting their role in light-dependent development (Oh et al., 2012).

Additional evidences of the BRs control over development were found in the reproductive phase of plants. For example, BRs modulate the levels of the floral repressor FL, which controls the flowering time (Domagalska et al., 2007). BRs are also critical for the stamen growth and pollen development. Accordingly, strong loss-of-function mutants on genes involved in BR perception or synthesis show reduced pollen fertility (Ye et al., 2010). Moreover, BRs determine the sex in plants with unisexual flowers (Hartwig et al., 2011).

In a more local level, BRs promote cell growth and elongation. The exact mechanisms that BRs use to induce cell elongation are still controversial.

Some of these mechanisms, even though are BR-regulated, use independent signaling pathways (Guo et al., 2009). However, BRs can directly alter cell wall composition and promote the production of cellulose, phenomena that is required for cell wall expansion and cell elongation (Hossain et al., 2012; Minami et al., 2019; Sánchez-Rodríguez et al., 2017; Wolf et al., 2012; Xie et al., 2011). BRs also regulate the cell division of plant cells, specially in growing tissues such as meristems. This is accomplish through the direct control of cell cycle (Cheon et al., 2010; Espinosa-Ruiz et al., 2017; González-García et al., 2011; Hacham et al., 2011; Zhiponova et al., 2013). The fine modulation of the division rate by BRs determines organ growth and the definition of its boundaries. Therefore, BRs are also involved in organ morphogenesis. Defects in BR signaling lead to defects in organ separation (Bell et al., 2012; Espinosa-Ruiz et al., 2017; Gendron et al., 2012). The control of cell division becomes particularly relevant in stem cell niches, where BRs regulate the stem cells renewal and their differentiation (Heyman et al., 2013; Kang et al., 2017; Lee et al., 2015; Vilarrasa-Blasi et al., 2014; Vragović et al., 2015). Alterations in the stem cell division and differentiation programs are directly reflected in the vascular development. Indeed BRs promote the differentiation of the highly specialized vascular tissues (Caño-Delgado et al., 2004; Ibañes et al., 2009) and both, receptors and downstream components of BR signaling pathway, directly affect the xylem (Fukuda, 2004; Nagata et al., 2001) and phloem differentiation in *Arabidopsis* (Anne et al., 2015; Kang et al., 2017). Interestingly, these studies also support differential roles of BRs in different plant tissues and revealed the importance of the spatial localization and regulation of the BRs biosynthesis and signaling machinery (Chaiwanon and Wang, 2015; Fàbregas et al., 2013; Savaldi-Goldstein et al., 2007; Vragović et al., 2015).

It is noteworthy the fact that BRs hardly ever have the exclusive control of a particular process. Instead, crosstalk between the signaling components of BRs and other hormones is common and has repeatedly been reported. In

some cases they establish cooperative relationships and in others antagonistic (Choudhary et al., 2012). Furthermore some processes are independent from the hormone (ligand) itself although BR signaling components are required, like phloem and xylem maturation in plant leaves or vascular cell-fate maintenance through phytosulfokine signaling (Holzwardt et al., 2018; Saito et al., 2018).

The Brassinosteroid signaling pathway

Despite the similarities of BRs with animal steroids, the signaling mechanisms differ. The perception of animal steroids occurs in the nucleus directly by members of the superfamily of nuclear receptor transcription factors (Aranda and Pascual, 2001). Conversely in plants this perception takes place in the cytoplasmic membrane through Leucine-Rich Repeats Receptor-Like Kinases (LRR-RLKs). The principal receptor involved in BR perception and signal transduction is BRI1 (BRassinosteroid-Insensitive 1), identified due to its insensitivity to exogenous application of Brassinolide (BL), the most active BR compound (Clouse et al., 1996; Li and Chory, 1997; Wang et al., 2001).

The canonical BR signaling components are currently well known. Upon perception of BL by BRI1 (Kinoshita et al., 2005), this heterodimerizes with a smaller LRR-RLK that is essential for BR signaling, the Brassinosteroid-Associated Kinase 1 (BAK1), (Li et al., 2002b; Nam and Li, 2002; Russinova et al., 2004). During this interaction, kinase domains of the both LRR-RLKs are transphosphorylated and further activated (Wang et al., 2005a; Yun et al., 2009). Additional early events that activate BR pathway take place in the plasmatic membrane. These involve the phosphorylation and subsequent detachment from BRI1 and dissociation from the membrane of the BRI1-Kinase Inhibitor 1 (BKI1) that allow the transphosphorylation with BAK1 (Jaillais et al., 2011; Wang and Chory, 2006). The dissociated form of BKI1 also can interact with downstream components, further regulating BR signaling (Wang et al., 2011). Upon its total activation BRI1 phosphorylates members of two groups of plasma membrane-anchored

cytoplasmic kinases, Brassinosteroid-Signaling Kinase (BSKs) and Constitutive Differential Growth 1 (CDG1) (Kim et al., 2011; Tang et al., 2008). These two proteins, when activated (phosphorylated) can bind and activate (by phosphorylation) the phosphatase BRI1-Suppressor 1 (BSU1) (Mora-García et al., 2004). The active form of BSU1 dephosphorylates another kinase, the Brassinosteroids Insensitive 2 (BIN2) (Li et al., 2002a). The inactive form (dephosphorylated) of BIN2 is sent to proteasome degradation (Peng et al., 2008).

In absence of BR or when their levels are low, active BIN2 maintains the phosphorylation state of two homologous transcription factors, BrassinaZole Resistant 1 (BZR1) and BRI1-EMS-Suppressor 1) (Wang et al., 2002; Yin et al., 2002). The phosphorylation of these two transcription factors inhibits their DNA-binding capacity and causes their cytosolic retention by 14-3-3 proteins (Gampala et al., 2007; Vert and Chory, 2006). The 14-3-3 proteins can also interact with the membrane-released BKI1, which provokes a competition with BZR1/BES1 transcription factor for their binding (Wang et al., 2011).

With increased levels of BR, BIN2 is degraded so the BES1/BZR1 transcription factors are no longer kept phosphorylated and are dephosphorylated by Protein Phosphatases 2A (PP2A) (Tang et al., 2011). Dephosphorylated BES1/BZR1 can then translocate to the nucleus where they bind to BR-regulated promoters (He et al., 2005; Ryu et al., 2007; Yin et al., 2005). Actually the specific DNA sequences where BZR1 and BES1 bind are known: The BR-response elements (BRRE, CGTG^C/_TG) and E-boxes (CANNTG) (He et al., 2005; Sun et al., 2010; Yu et al., 2011).

In summary, the BR signaling pathways initiates at the plasma membrane with the steroid binding to the extracellular part of BR receptors. This triggers a series of phosphorylation events that leads to the activation of the BES1/BZR1 transcription factors and the regulation of thousands of genes. The complete signaling pathway is represented in [Figure 1.2](#). More recently the detailed molecular mechanisms of BL perception and receptor activation have been elucidated.

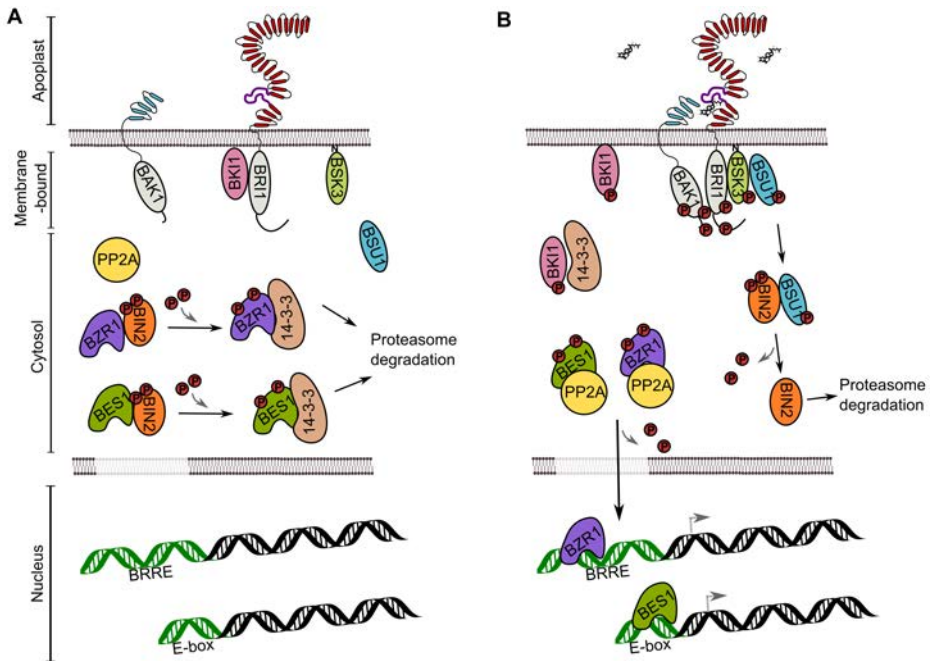


Figure 1.2: Brassinosteroids signaling pathway

(A) When there is not BR molecules available in the apoplast the signaling pathway is off. The membrane receptor BRI1 is kept dephosphorylated and its kinase activity is inhibited by its C-terminal tail and the binding of BKI1. The transcription factors BES1 and BZR1 are kept in a phosphorylated state by the BIN2 kinase and retained in the cytoplasm. 14-3-3 proteins bind the phosphorylated forms of BES1/BZR1 and send them to proteasome degradation. (B) Upon BR binding at the extracellular part of the BRI1 receptor, BAK1 and BRI1 heterodimerize and transphosphorylate. Then BKI1 is released from plasma membrane completely activating BRI1 kinase activity. Subsequent phosphorylation of BSKs take place (BSK3 is represented because it acts as membrane scaffold for the binding and phosphorylation of many proteins, including other BSKs and BSU1 (Ryu et al., 2019)), which lead to the phosphorylation and activation of the BSU1 phosphatase. BSU1 dephosphorylates the BIN2 kinase, which is sent to proteasome degradation. With reduced levels of BIN2, BES1 and BZR1 cannot be phosphorylated anymore and the phosphatases PP2A find no competition for the BES1/BZR1 binding, dephosphorylating them. The BES1/BZR1 transcription factors can then move to the nucleus where they bind specific sequences (BRRE and E-boxes) and modulate the transcription of thousand of genes. The multiple phosphorylation and dephosphorylation events along the pathway allow the crosstalk with other hormones and allow the BR signaling to be controlled at several points.

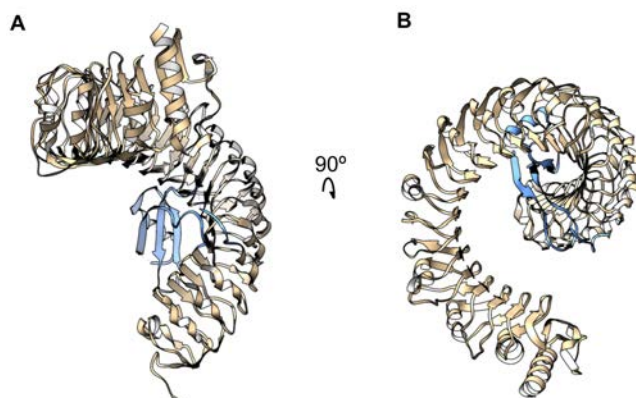


Figure 1.3: Extracellular structure of the BRI1 receptor

(A) Side view of the crystal structure of BRI1 extracellular part (PDB: 3RIZ; [Hothorn et al. \(2011\)](#)). The island domain is highlighted in blue. The transmembrane domain would be situated at the bottom of the representation whereas the N-terminal would be at the top. (B) Top view of the same crystal, upon a 90° rotation in the x axis.

1.2 Brassinosteroid perception at plasma membrane

The BR signaling pathway starts with the steroid-hormone binding at the extracellular part of the BRI1 receptor. The extracellular part of BRI1 is principally composed by 25 tandem LRRs ([Li and Chory, 1997](#)). The LRR domain confers structural strength to the extracellular part and force it adopt a horseshoe-like shape with parallel β -sheets in the concave face and α -helix on the convex face ([Enkhbayar et al., 2003](#)). The LRR array is interrupted near the plasma membrane, between LRRs 21 and 22, by a stretch of 70 aminoacids named “island domain” ([Figure 1.3](#)). The island domain is critical for the receptor binding of the ligand ([Kinoshita et al., 2005](#)). The rest of the protein is composed by a transmembrane domain (and a juxta-membrane domain in the intracellular part) and an intracellular kinase domain ([Kinoshita et al., 2005](#); [Li and Chory, 1997](#)).

Brassinosteroid receptor BRI1 has three homologs

In Arabidopsis, apart from BRI1 there are three more receptor, the BRI1-Like family of receptors (BRLs), composed by BRL1-3. BRLs share at least 47% homology in their protein sequences and have structures similar to BRI1. During postembryonic development, BRI1 receptors are present in the majority of plant tissues (especially in the outer cell layers) (Friedrichsen et al., 2000) whereas the BRLs receptor localization is associated to vascular tissues (particularly in phloem-pole pericycle) and stem cell niches (Caño-Delgado et al., 2004; Ceserani et al., 2009; Fàbregas et al., 2013; Salazar-Henao et al., 2016). And transcriptionally, the BRI1 expression domain does not overlap with the expression domains of BRLs, at least for root stem cell niche and quiescent center (Fàbregas et al., 2013; Wilma van Esse et al., 2011) (Figure 1.4). From BRLs family, only BRL1 and BRL3 are functional BR receptors able to complement the dwarf phenotype of *bri1* mutants (Caño-Delgado et al., 2004). And indeed BRL1 and BRL3 have a higher binding affinity for the BR hormone than BRI1 (Caño-Delgado et al., 2004; Zhou et al., 2004). However, BRL2 (aka VASCULAR HIGHWAY 1, VH1) is not able to bind the hormone (Kinoshita et al., 2005) but strikingly, *brl2* mutants do display vascular-defective phenotypes (Ceserani et al., 2009; Clay and Nelson, 2002). Thus, the roles attributed to BRL2 are very likely BR-independent. BRLs appear not to play major role in plant growth, as *brl* single mutants plant are not dwarf. This last point suggests that BRLs carry out very specific roles in the plant and/or play redundant roles with BRI1 (Hacham et al., 2011). Actually, this lack of growth phenotype and their cell-specific expression have discouraged the study of BRLs functions in the plant. Even though, BRLs have been proposed to play roles in fine-tuning and connecting other responses with BRs (Gendron et al., 2012; Savaldi-Goldstein et al., 2007; Wu et al., 2018a) and evidence supports that different BR receptor complexes play different roles in different plant tissues or conditions. However fundamental questions concerning the mechanism for such signaling coordination between tissues remain very elusive (Caño-Delgado

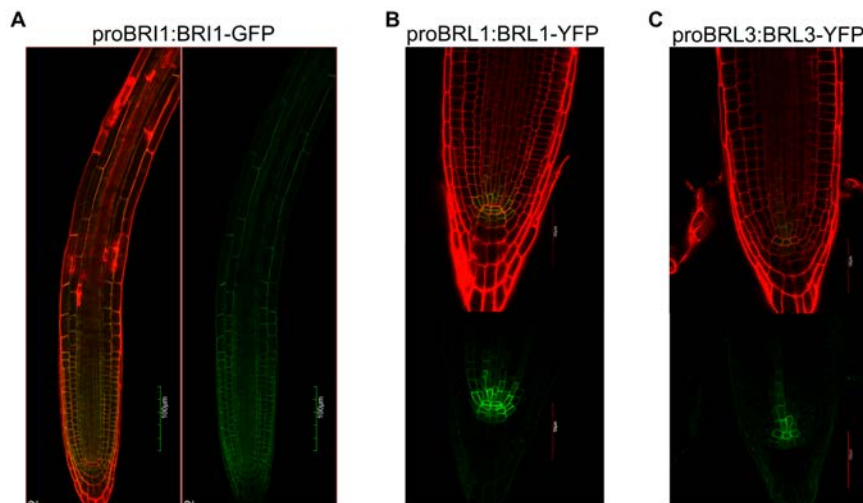


Figure 1.4: Confocal microscopy pictures of BR receptor reporter lines

Confocal microscopy images of the primary root of *Arabidopsis*. Images show translational reporter lines of (A) BRI1, (B) BRL1 and (C) BRL3. Merged (red: PI counter-staining; green: GFP) and green channels are shown separately. Scale bars = 100 μm for BRI1 (A) and 50 μm for BRL1 and BRL3 (B-C).

et al., 2004; Gendron et al., 2012; González-García et al., 2011; Hacham et al., 2011; Lozano-Elena et al., 2018; Savaldi-Goldstein et al., 2007; Vilarrasa-Blasi et al., 2014; Vukašinović and Russinova, 2018).

Along with the BRLs compartmentalization in different plant tissues, their conservation across plant species also supports a role in specialized processes of the plant. Indeed in rice, molecular analysis of BRLs already suggested specific functions in roots (Nakamura et al., 2006). The structure of the *Arabidopsis* BR receptor family, including the non-functional BRL2 receptor, is highly conserved across the superior plants (Wang and Mao, 2014) (Figure 1.5). Protein sequence comparisons of BRs receptors across different plant species reveals a sequential diversification in clades of the BRI1-BRLs family. First, a division between BRL2 clade and the rest of the family members and then division between the BRI1 and the BRL1,3 clades (Wang and Mao, 2014) (Figure 1.5). Remarkably, the complete receptor structure that includes the island domain, LRRs and

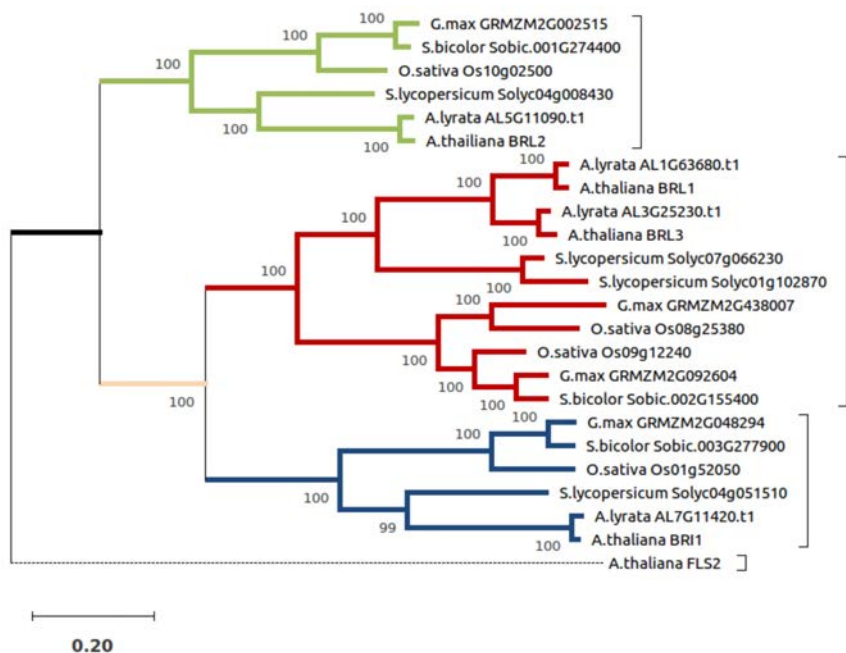


Figure 1.5: Phylogenetic tree of BR receptors across different plant species

Maximum-Likelihood tree including all four *Arabidopsis* BR receptors and its orthologs in species of agronomic interest. Different colors denote the different clades: Green for the BRL2 clade, red for the BRL1-BRL3 clade and blue for the BRI1 clade. *Arabidopsis* LRR receptor FLS2 was included as outgroup. Scale represents the number of substitutions per site. Numbers over the tree nodes denote the bootstrap support. Orthologs protein sequences were retrieved from Phytozome, aligned with *MUSCLE* and the tree constructed with *MEGAX*.

the intracellular kinase appeared only in angiosperms and gymnosperms (Wang and Mao, 2014). This last point opens an interesting question given that BRs have been detected and quantified in non-seed plants (Yokota et al., 2017) but their receptor lacks the island domain. Perhaps these plants have a different (ancestral) mechanism to sense and respond to steroids hormones.

The reason why plants harbor several receptors for BR remains elusive but at the same time intriguing. Even more shadowy is if BRL1 and BRL3 possess different roles. Specific studies on this topic would shed light on the evolutive advantage of maintaining three additional BRs receptors to BRI1.

Structural basis for steroid perception

The crystallization of BRI1 ectodomain and its resolved structure revealed a hydrophobic pocket formed by the island domain that folds back into the interior of the LRR-superhelix against the LRRs 21-25, and where the steroid hormone is bound (Hothorn et al., 2011; She et al., 2011) (Figure 1.6). However no major conformational changes occur upon the binding of the hormone, only a discrete fixing of the island domain loop, which lets part of the bound hormone exposed to the solvent (Hothorn et al., 2011; She et al., 2011). Mechanisms governing the hormone binding in BRI1 are likely conserved in BRLs, given their sequence similarity. In fact the BRL1 ectodomain bound to brassinolide (BL), display a similar structure than BRI1 (She et al., 2013). The higher affinity of BRL1 to BL could be explained by a larger buried surface and very subtle residues changes in the island domain (Caño-Delgado et al., 2004; She et al., 2013) (Figure 1.6) and similarly to BRI1, the conformational changes are limited to the island domain (She et al., 2013). Homology-based models show similar mechanism for BRL3 hormone binding. Conversely, for the case of BRL2, models revealed that its inability to bind the hormone is mainly attributed to the presence of a bulky charged aminoacid substitution at the inner end of the cavity that prevent the steroid from entering the pocket (She et al., 2013) (Figure 1.6).

The structural resolution of the BR receptors ectodomains uncovered two interesting things: i) There is no major conformational changes upon hormone binding and ii) hormone binding to the island domain creates a docking platform for other proteins, that is BL acting as "molecular glue" (Hothorn et al., 2011; She et al., 2013). These new insights rationalized all the previous evidences for the critical role of BAK1 in brassinosteroid signaling.

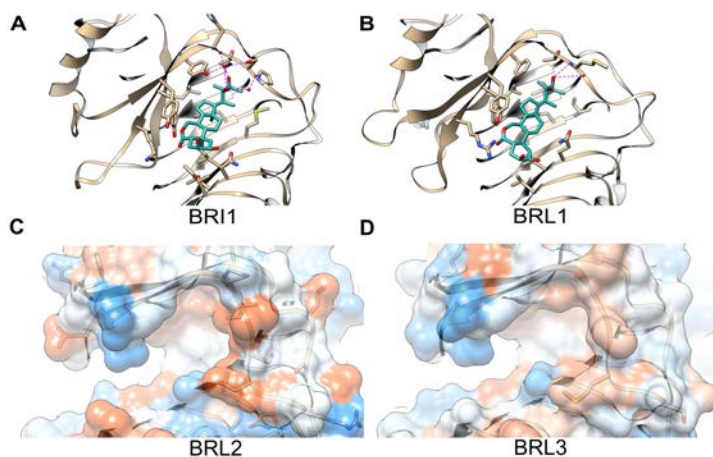


Figure 1.6: Brassinosteroids binding pocket of BR receptors

(A) Island domain of BRI1 bound to brassinolide (PDB: 3RGZ; [Hothorn et al. \(2011\)](#)). (B) Island domain of BRL1 bound to brassinolide (PDB: 4J0M; [She et al. \(2013\)](#)). Purple dashed lines depict H-bonds. Full-represented residues have hydrophobic contacts with the hormone. (C) Coulombic surface of the island domain of BRL2 homology model. (D) Coulombic surface of the island domain of BRL3 homology model. Note the higher positive potential at the bottom of the hydrophobic pocket in BRL2. This probably avoid the hormone entering into the pocket. Full-represented residues differ from the template, the BRL1 crystal. Homology models created with Modeller v9.2 and molecular representations with UCSF Chimera.

Membrane co-receptors

In addition to BRI1 and BRI1-like receptors, BR signaling depends on additional components, such as BAK1, a small (5 LRR) LRR-RLK ([Li et al., 2002b](#); [Nam and Li, 2002](#)). BAK1 is considered a co-receptor because it is unable to bind hormone itself ([Kinoshita et al., 2005](#); [Wang et al., 2005b](#)). BAK1 interacts with BRI1 in a BL-dependent manner and their kinase domains transphosphorylates each other, triggering then the signaling pathway ([Wang et al., 2008](#)). BAK1 binds to the complex formed by BRI1-BL at its inner surface, completely burying the exposed ligand part and interacting with the inner part of the last LRR-repeats. No notable conformational changes take place neither, at least in the extracellular part ([Sun et al., 2013a](#)). So the current model, which is firmly supported by structural data, is that the extracellular part of BRI1 receptor and BAK1 co-receptor get in close proximity upon the

perception of the steroid hormone. This brings closer the kinase domains and allows their subsequent transphosphorylation. Additionally to BAK1 (aka. SERK3), BRI1 function also depends on other co-receptors. This is the case of the family of LRR kinases known as Somatic Embryogenesis Receptor-like Kinases (SERKs). Four out five members of the family have impact on BR signaling that can actually bind BRI1 (Gou et al., 2012; He et al., 2007; Karlova et al., 2006), sharing similar activation mechanisms (Santiago et al., 2013). SERKs can also bind other receptors to support other signal transduction pathways (Hohmann et al., 2018b; Sun et al., 2013b; Wu et al., 2018a). The versatility of SERKs supports a new vision of plant signal transduction as an interconnected network, where the hormone receptor can associate with several co-receptors to transduce the same signal and conversely, a single co-receptor can support the signaling of several pathways through the association with different receptors. In agreement with this notion, additional receptor proteins can also modulate the BR signal transduction (Smakowska-Luzan et al., 2018). Indeed, a complete *in vitro* LRR-RLKs interaction network revealed an important implication of small co-receptor in signaling robustness and that small multi-functional RLKs, such as BAK1, transduce more information (for several signaling pathways) but at the same time are less essential due their redundancy (Ahmed et al., 2018; Smakowska-Luzan et al., 2018).

Regarding to BRLs, due to their structural similarity to BRI1, it is plausible that specialized functions may rely more on additional partners than in BRLs themselves. In fact, the in planta BRL3 signalosome revealed interactions with several unannotated RLKs, BAK1 and BRL1 but not with BRI1 (Fàbregas et al., 2013). Specific interactors of BRLs are potential factors determining its functional specificity (Fàbregas, 2013; Fàbregas et al., 2013).

Given that the current model of membrane signaling implies a high degree of "promiscuity" between the receptors (attribute that supports network robust-

ness and balanced signaling), signal specificity may be provided also by kinase domains and their downstream interactors (Hohmann et al., 2018b). Indeed, different parts of BAK1 kinase domain with different phosphocodes are required for the different pathways in which it is involved (Perraki et al., 2018; Wu et al., 2018b). Taken together, these studies support that specialized roles of BRLs apart of being determined by their tissue-specific localization, are also highly determined by their specific subset of interactors.

Kinase domains and further signal transduction

Upon the ligand-dependent binding of receptor and co-receptor, further signal transmission depends on kinase activities. BRs induce the BRI1 phosphorylation (Wang et al., 2001). Although BRI1 kinase domain has autophosphorylation capability (Oh et al., 2015, 2000; Wang and Chory, 2006), this is kept inactive through homodimerisation, auto-inhibition by its C-terminal part (Wang et al., 2005a) and the binding of the inhibitory kinase BKI1 (Jaillais et al., 2011; Wang and Chory, 2006; Wang et al., 2008). The transphosphorylation between BAK1 and BRI1 and detachment of BKI1 are requisites for BRI1 kinase activation (Jaillais et al., 2011; Wang et al., 2014; Yun et al., 2009). The existence of receptor homodimers is attributed to a resting state while heterodimerization occurs only upon BR binding and results in transphosphorylation and pathway activation (Bojar et al., 2014; Hink et al., 2008; Jaillais et al., 2011; Wang et al., 2008). Even though the kinases activation mechanisms are known (Bojar et al., 2014; Wang et al., 2014; Yan et al., 2012), how these allow for further phosphorylation on downstream components, as the BR-Signaling Kinases BSKs, remain poorly understood (Sreeramulu et al., 2013; Tang et al., 2008). New evidences suggest that BSKs may act merely as scaffolds for the binding and phosphorylation of other components by BRI1 (Ren et al., 2019).

While no specific studies on BRLs are available, it is also reasonable propose similar mechanisms given that their kinase domains share a minimum identity of 64% (without BRL2, 74%). Accordingly, BSKs are present in the BRL3 signalosome (Fàbregas et al., 2013). Interestingly, the kinase domain of BRL1 does not interact with BKI1 inhibitor, at least through the BKI1 patch that binds BRI1 (Jaillais et al., 2011), which could yield notable differences. The same residues that avoid BKI1 binding to BRL1 are also found in BRL3. If BRLs activate a different set of downstream components is currently unknown, but it could contribute to specific functions. Future studies on specific BRLs phosphorylation substrates would be a starting point for the dissection of specific BRLs molecular pathways.

1.3 Common and specific roles of BRLs

Since the discovery of BRI1, this receptor pathway has not only been linked to overall plant growth and developmental processes, but also to the stress response. The roles of BRI1 in plant development and stress have been recently reviewed elsewhere (Planas-Riverola et al., 2019). Recent studies are narrowing down the exact tissue-specific mechanisms that are triggered by BRI1 to promote plant development (such as root growth, hypocotyl elongation (Minami et al., 2019)) and responses to stress (such as stomata opening (Inoue et al., 2017)). Interestingly new evidence attributes a function for BRI1 in vascular tissues differentiation that is independent of BRs (Holzwardt et al., 2018). Conversely, xylem and phloem differentiation requires the canonical transcription factors BES1 and BZR1 but independently of BRI1 (Saito et al., 2018). Therefore, the notion of a canonical signaling pathway triggered by BRI1 and exclusively devoted to BRs should be reviewed.

However, the discrete localization of BRLs and the lack of any evident growth phenotypes in the mutants have hampered the understanding of the specific

roles of BRLs. Interestingly, the xylem maturation phenotype of *bri1* mutants is enhanced when combined with *bri1bri3* mutants (Holzwardt et al., 2018). Accordingly, in other studies that account for BRLs, *bri1* vascular phenotypes are always enhanced when combined with *bri1* mutants, although single or double *bri1* mutants have no phenotypes themselves (Fàbregas et al., 2013; Kang et al., 2017). Once again, the actual roles of BRLs are masked by the predominance of BRI1. Literature on the specific roles of BRL is extremely scarce. However, some clues of BRLs regulating vascular development and responses to stress can be extracted, for example, from BRL3 transcriptional activation under low oxygen stress (Klok et al., 2002), from induction of a differentiation regulator in xylem (Ohashi-Ito et al., 2005), or from the drought-resistance phenotype of BRL3 overexpression and its transcriptional fingerprint (Fàbregas et al., 2018), (chapter 3).

Based on the present findings, and given the sequence and structural similarity of the BRI1 and BRL receptors, the functional specificity of BRLs may reside on: (i) specific residues in their interaction interfaces, especially in the kinase domain, that define a specific subset of interactors, and (ii) its specific localization within particular tissues, with the latter likely being the most determinant factor.

With regards to the first point, the inability of BRL1 to bind BKI1 exemplifies how BRLs could gather different subsets of interactors (Jaillais et al., 2011). In fact, a specific interactor of BRL3, RGS1 (Regulator of G-protein signaling), has already been described. RGS1, which is specifically phosphorylated *in vivo* by BRL3 (Tunc-Ozdemir and Jones, 2017), works downstream of BRL3 in sugar sensing and ROS production and has a vascular expression pattern that highly overlaps with those of BRL3 and BRL1 (Tunc-Ozdemir and Jones, 2017; Tunc-Ozdemir et al., 2017; Ullah et al., 2001). A role for BRL3 in sugar sensing fits well with its phloem localization. We have recently shown that BRL3 overexpressor plants accumulate osmoprotectant sugars in the root, which contribute to alleviating the effects of severe drought without penalizing growth (Fàbregas

et al., 2018), (chapter 3). The possible involvement of BRL3 in other stress responses is also supported by the fact that pathogen effectors and DNA-damage response transcription factors target BRL3 (Ahmed et al., 2018; Ogita et al., 2018).

The discrete spatial localization of BRLs is informative of their biological function in the vascular tissues. For example, *brl2* mutants (despite it does not bind BL), show specifically vascular phenotype (Ceserani et al., 2009; Clay and Nelson, 2002). BRL1 or BRL3 when expressed under the control of BRI1 promoter complement the *bri1* mutant phenotype (Caño-Delgado et al., 2004; Zhou et al., 2004). The fact that BR receptors are so interchangeable suggests that the control of different functions emanate from the compartmentalization. Conversely, *bri1*-impaired growth is not completely restored if BRI1 is expressed only in the inner root tissues or phloem (Hacham et al., 2011; Hategan et al., 2014). In addition, BR signaling from inner vascular tissues may have deep implications in development; BRI1 expressed only in protophloem cells is able to rescue most of the *bri1* dwarf phenotype in a *bri1brl1brl3* mutant background (Kang et al., 2017). This apparent incoherence really deserves further investigation. If similar effects are not observed in a simple *bri1* background, opposing roles for BRI1–BRLs are likely. Accordingly, tissue-specific transcriptomes in response to BR reveals opposite patterns that point to unique BRL functions (Vragović et al., 2015). When this tissue-specific expression data (Vragović et al., 2015) is combined with that derived from BRL3 overexpressors (Fàbregas et al., 2018)(chapter 3), we observed that BRL1 and BRL3 cluster together in a co-expression network. In contrast, BRI1 and BRL2 cluster in different modules. Interestingly, the BRL1-3 module was enriched in the cell wall metabolism and the xylem and phloem development categories. These biological processes are of special importance in vascular tissues.

Furthermore, BRL2 receptor mutants that are unable to bind BL show a specific vascular phenotype (Ceserani et al., 2009; Clay and Nelson, 2002), whereas a vascular phenotype only arises in BRL knockouts when they are combined with

bri1 mutants (Caño-Delgado et al., 2004; Fàbregas et al., 2013; Kang et al., 2017). As such, we hypothesize that BRI1 can take over BRL1 and BRL3 functions in their absence. This suggests a BRI1–BRL mutual regulation to limit their expression domains. Indeed, the expression pattern of BRL3 is regulated by the canonical BR pathway (Salazar-Henao et al., 2016), and strikingly we found a strong transcriptional activation of BRI1 in plants overexpressing BRL3 (Fàbregas et al., 2018)(chapter 3). Future work on the BRI1–BRL mutual regulation will shed light on the specific roles of BRLs, and could help to clarify the role of BRI1 signaling in inner root tissues (Hacham et al., 2011; Kang et al., 2017; Vragović et al., 2015).

In conclusion, BRL signaling has only just begun to emerge as a key factor for carrying out specialized functions such as vascular development or signaling to neighboring cells to promote recovery after genomic or environmental stresses. This kind of receptor redundancy may act to finetune plant adaptation to environmental responses. Future work aiming to elucidate specialized roles of BRLs is important because the BRI1–BRL case might be paradigmatic, with analogous examples in other pathways.

1.4 Brassinosteroids impact on abiotic stress responses

Brassinosteroids have been repeatedly reported to have protective effects against stresses in many in crops (Khripach et al., 2000) but the exact mechanisms to promote stress are still unclear. These protective effects are observed against stresses of both natures, abiotic and biotic. The roles of BRs in front of biotic stresses are well known (Ahmed et al., 2018; Lozano-Durán and Zipfel, 2015), however these are out of scope for this thesis and will not be presented. Abiotic stress is defined as the negative impact of non-living factors on the living organisms in a specific environment. In the case of

plants, due to their sessile nature, they are especially susceptible to a wide range of abiotic stresses, for example high light intensity, too hot or too cold temperatures or high salinity or heavy metal presence in the soil. Many of these particular stresses can be consequences of the same phenomena and tend to happen at the same time in the environment. This is the case of drought, which normally is accompanied by increased temperatures and soil salinity. Furthermore, in front of the actual panorama of global warming, abiotic stresses are predicted to become more severe and unpredictable with very harmful consequences for agriculture (Lesk et al., 2016). Understanding the plant response mechanisms to abiotic stress is a priority, which makes BRs stand as a promising biotechnological target to achieve robustness in the worldwide agricultural system.

BRs exert a protective effect against abiotic stresses. For example, plants treated with BRs show increased thermotolerance (Dhaubhadel et al., 2002; Kagale et al., 2007). BRs the translational machinery and promote heat-shock protein synthesis (Dhaubhadel et al., 2002). In addition, plants respond to heat stress with the endocytosis of BRI1 receptor, which reduces BR signaling favoring root elongation in detriment of cell division (Martins et al., 2017), although this effect is not in agreement the protective effects observed with the exogenous application of BR and suggest a more complex mode of action. Downstream components of BR signaling cascade also promote heat stress tolerance, for example through the control of Reactive-Oxygen Species (ROS) and other membrane components (Yin et al., 2018). Low temperatures also suppose a strong stress to plants. The constitutive activation of BR signaling enhances freezing resistance through the activation of cold-responsive genes (Eremina et al., 2016). Interestingly BRs have some structural properties with associated protective effects. Given their steroid nature, they can potentially be incorporated into lipidic membranes increases its fluidity, which contributes to freezing tolerance (Filek et al., 2017). Large amounts of heavy metals in

the soil suppose another kind of abiotic stress. The toxicity of heavy metals emanate basically from the overproduction of ROS and subsequent oxidative damage, which causes protein, membranes or DNA disruption (genotoxicity) (Rajewska et al., 2016). Application of BRs protects the plant by reducing the plant absorption and accumulation of heavy metals and the production of chelating agents and antioxidants that neutralize the ROS overproduction (Rajewska et al., 2016). Genotoxic stress particularly damage plant stem cells because their constant division, which increase their susceptibility to incorporate mutations. In this context, BRs have a special role mobilizing the stem cell reservoirs for the replenishment of damaged or dead stem cells (Fulcher and Sablowski, 2009; Heyman et al., 2013; Vilarrasa-Blasi et al., 2014). A very relevant abiotic stress given its agricultural implications is salt stress. Saline soils stop plant growth and eventually yield early senescence and plant death. Salt stress provokes a dramatic collapse of plant osmotic pressure, generating an osmotic stress. It also yields detrimental effects due to the uptake of ions such as Na^+ , K^+ or Cl^- and the generation of high amounts of ROS that create severe oxidative stress (Isayenkov and Maathuis, 2019). Multiple studies have reported the increased tolerance and germination rates of BR-treated plants under high soil salinity (Kagale et al., 2007; Tanveer et al., 2018). BRs ameliorate the chlorophyll degradation due to salinity and promote the production of antioxidant enzymes and osmolytes (Tanveer et al., 2018). BRs are also able to buffer the stress effects through modification of membrane properties to prevent ion leakage (Azhar et al., 2017). Salt stress entails different physiological effects on the plant and although BR-triggered physiological responses are well described, the exact molecular mechanisms remains without deep investigation.

Part of the bases for the BR-provided protection against abiotic stress might be derived from its control over plant development. A common response to abiotic stress in plants is the cell wall remodeling (Tenhaken, 2015) and BRs

have a prominent role regulating cell wall components (Sánchez-Rodríguez et al., 2017; Wolf et al., 2012; Xie et al., 2011). Although it is still not clear if cell wall stiffen or loosen in response to abiotic stress, it seems that some degree of flexibility in cell walls is required to reduce membrane damage due to decreased cell turgor (salt, osmotic, drought stresses) and maintain the organ growth under stress (Tenhaken, 2015). The control of cell wall properties could be a way for BR to positively impact on abiotic stress responses (Rao and Dixon, 2017). Interestingly, cell wall modification is highly dependent on ROS homeostasis and components controlling it, such as peroxidases and expansins, are also controlled by BRs (Rao and Dixon, 2017).

A shared feature of most of the abiotic stresses is the generation of high amounts of ROS. The levels of accumulated ROS determine if they act as signaling molecules (needed for example in cell wall remodeling) or create a severe oxidative damage (Mittler, 2017; Tenhaken, 2015). BRs can induce moderate levels of ROS that are important for plant development and activation of stress responses (Nie et al., 2013; Xia et al., 2009, 2015) and indeed some ROS levels necessary for proper BR signaling (Tian et al., 2018). Conversely, if levels of ROS are high enough, it can lead to oxidative damage and BRs have been shown to stimulate antioxidant production (Tanveer et al., 2018).

Some abiotic stresses provoke similar physiological effects and probably share the same response mechanisms (Figure 1.7). Likewise, BRs probably ameliorate the abiotic stress detrimental effects by enhancing these common mechanism, as redox homeostasis, photosynthesis or antioxidant and osmolyte production. However the specific molecular mechanisms are still very unknown. Yet, from the large number of studies of plants submitted to abiotic stress and BRs applications it could be inferred that BRs are capable to induce plant changes at a systemic level. Better understanding of how BRs activate this systemic

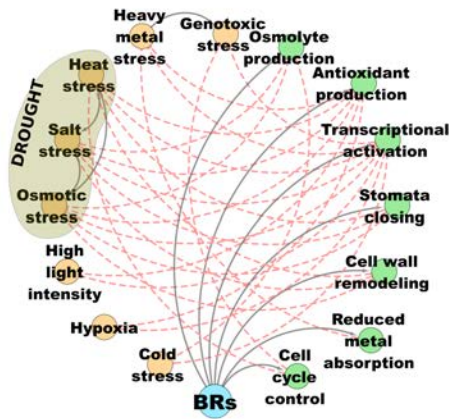


Figure 1.7: Network of abiotic stresses and the BR-induced protective effects

Summary of reported abiotic stresses in which BRs has a protective effect. Stresses are denoted as orange nodes whereas genetic and physiological changes induced by BRs are denoted by green nodes. Gray and solid edges represent a positive regulation. Conversely, dashed red edges represent the negative (protective) effect of the BR-induced effects on abiotic stresses. Relationships between abiotic stresses are also denoted, like the drought stress that is normally accompanied of increased salinity, osmotic and heat stress.

response and the stress sensing pathways can serve for better engineer plants to specific scenarios.

BR connection with ABA responses

Abcisic Acid (ABA) is a phytohormone that has a predominant role in plant responses to stress. Its levels are rapidly increased upon abiotic stress (Kuromori et al., 2018). Apart of controlling many stress-responsive genes, ABA is also involved in developmental processes like seed dormancy and accumulation of nutrients in storage organs. Nevertheless, ABA main role in response to stress, especially response to water deficit, is due to its control over stomata opening and overall plant hydraulics (Kuromori et al., 2018).

BRs signaling pathway crosstalks with ABA just after ligand perception by BR receptors (Gui et al., 2016; Zhang et al., 2009). In developmental processes, ABA and BR largely antagonizes, as it is the case of the Quiescent Center (QC) division or seed dormancy (Chung et al., 2014; Hu and Yu, 2014; Zhang et al., 2010). However in the activation of abiotic stress responses, both hormones appears to have a positive effect. Indeed BRs are required for the ABA-induced stomata closure (Ha et al., 2016) and both hormone share strategies to provide stress protection (Zhou et al., 2014). It is possible that these specific cooperation is dependent of the tissue or organ, given that specific ABA production is required to stomata closing or vascular hydraulic adaptation to osmotic stress (Kuromori et al., 2018). Additionally it is also plausible that BRs activate mechanisms of stress tolerance that are totally ABA-independent (Yoshida et al., 2014).

The case of drought

Drought can be understood as a combination of closely associated stresses such as osmotic, salt or heat (normally derived from the same natural or anthropogenic phenomena, Figure 1.7), that results in dehydration. That is, reduced amount of water availability for the cells. For that reason drought is considered a complex and multi-trait stress (Todaka et al., 2015). Drought is probably the most important of the abiotic stresses regarding to agriculture (Boyer, 1982) and the negative impact of drought in crop production is becoming more prominent due to climate change (Lesk et al., 2016). Moreover the situation is complex given agriculture is a major driver of the global warming and it is predicted to increase in absolute numbers in order to sustain population growth (Springmann et al., 2018). Political and sociological changes urge to reduce the global warming effects in a close future (Springmann et al., 2018) but more efficient crops also have the potential to ameliorate these adverse effects. For that reason, understanding how plants respond to drought is a

key point. Crop adaptation to overcome drought periods without compromising growth and productivity is a major goal, in which BRs have promising roles.

Exogenous applications of BRs are known to provide drought protection to plants (Kagale et al., 2007; Shakirova et al., 2016) through the modulation of multiple physiological processes (Tanveer et al., 2019) but the exact molecular mechanisms are still not clear. In agreement, the stimulation of endogenous BR levels also increases plant tolerance to drought (Kagale et al., 2007; Krishna, 2003; Sahni et al., 2016). Surprisingly, increasing the BR sensitivity through increased expression of BRI1 receptor can reduce drought tolerance (Nie et al., 2019), although it increases tolerance to cold (Eremina et al., 2016). Furthermore the suppression of BRI1 receptor results in drought-resistant phenotypes (Feng et al., 2015; Ye et al., 2017), though these involve growth arrest and likely imply reduced drought exposure (Chaves et al., 2002). Apart from BRI1 receptor, which seems to have a predominant role regulating growth, other BR receptors as BRL3 interact with proteins that strongly respond to drought, as dehydrins (Fàbregas et al., 2013). Importantly, dehydrins levels are also increased upon exogenous application of BRs (Shakirova et al., 2016). The lack of clear linearity in BR-induced drought responses (more BR signaling more BR drought tolerance) suggests a complex regulation at the level of hormone perception. Indeed the constitutive activation of the downstream transcription factor BES1, yields drought sensitive plants, which reveals a mechanism that antagonizes growth and drought adaptation (Nolan et al., 2017; Ye et al., 2017). Downstream players regulated by BES1 also have a negative effect on drought responses (Chen et al., 2017), therefore pushing the canonical BR pathway exclusively to growth regulation. The fact that either exogenous BRs application or increased biosynthesis promotes drought tolerance does not match with the BES1 repression of drought-responsive elements. This incoherence suggests additional signaling events upstream the classical BR transcription factors and

raises the question of what are the specific roles of BR receptors in front of drought.

1.5 Conclusions and perspectives

The last two decades of studies on BR signaling in *Arabidopsis* have provided a clear picture of their mechanisms for growth and development regulation. In addition structural studies have revealed the exact activation mechanisms of the pathway activation upon ligand perception. Conversely, even though the beneficial role of BR application to protect the plant against abiotic stress have been known since long time ago, the mechanisms leading this protection remain very obscure. Besides, activation of BR signaling pathway in different points lead to different outputs, so it still exists a gap in the understanding of BR-activated stress machinery. In this context, the study of BR receptor in front of abiotic stresses can supply valuable information needed to understand the mechanisms triggered by BRs to overcome the stress and supposes a great opportunity to decouple stress responses from growth.

Previous works in the laboratory of Dr. Caño-Delgado have led to the discovery of new roles for BRs receptors in root and shoot vascular development (Caño-Delgado et al., 2004; Fàbregas et al., 2013; González-García et al., 2011; Ibañez et al., 2009). The composition of the membrane signalosome of the vascular specific BR receptors BRL3 and BRL1 revealed a prominent presence of drought responsive proteins (Fàbregas, 2013; Fàbregas et al., 2013). However, it is not known if BR receptors are able to associate with special components and/or with tissue-specific proteins to carry on specific tasks under stress. The identification of specific roles for the BRI1-like receptors will shed light on what is the evolutionary advantage of such receptor redundancy. Furthermore, additional

membrane components may be necessary to deviate part of the BR signaling towards specific pathways needed to overcome abiotic stress.

Objectives

The general objective of this PhD thesis was to investigate the roles of brassinosteroid receptors in front of abiotic stress in the plant model *Arabidopsis thaliana*.

In particular, the following specific objectives have been accomplished:

1. Investigate the contribution of brassinosteroids receptors to stem cell division triggered by DNA-damaging agents at the root quiescent center.
2. Characterize the contribution of the BR vascular receptors to overall plant drought adaptation and tolerance, through a combination of genetics, physiology and multi-omics analyses.
3. Search for new interactors of BR receptors at plasma membrane, combining biochemical data with computational analyses for the modeling of direct protein-protein interactions.

Chapter 2

Brassinosteroid signaling and perception at Arabidopsis root stem cell niche

Part of this chapter published as:

Paracrine brassinosteroid signalling at the stem cell niche controls cellular regeneration

Lozano-Elena, F.*, Planas-Riverola, A.*, Vilarrasa-Blasi, J., Schwab, R. and Caño-Delgado, AI. (2018) *Journal of Cell Science*, 131:2.

Brassinosteroid signaling and perception at Arabidopsis root stem cell niche

2.1 Introduction

Stem cells are primarily involved in sustaining growth and replacing damaged tissues, through the provision of a continuous supply of precursor cells, (Sablowski, 2004). In Arabidopsis roots, stem cells, also known as root initials, are located at the root apex and surround the Quiescent Center (QC) (Dolan et al., 1993) (Figure 2.1 A,B). The QC, which comprises a small group of cells with very low mitotic activity, not only acts as a cell reservoir for the surrounding actively dividing stem cells (Dolan et al., 1993; Scheres, 2007) but is also responsible for maintaining the stem cells in their undifferentiated state (Sabatini et al., 2003; van den Berg et al., 1997). However upon cellular damage, the QC loses its quiescence and enters into a state of cell division to enable stem cell replenishment (Cruz-Ramírez et al., 2013; Heyman et al., 2013; Vilarrasa-Blasi

et al., 2014). Hormonal stimulation also plays an important role in governing cell division in the QC (González-García et al., 2011; Heyman et al., 2013; Zhang et al., 2010). For instance, BRs are known to promote both cell division in the QC and differentiation of the surrounding columella stem cells (Fàbregas et al., 2013; González-García et al., 2011; Vilarrasa-Blasi et al., 2014). More specifically, the Ethylene-Response Factor 115 (ERF115) transcription factor, which is activated by BRs, promotes QC division and stem cell regeneration after DNA damage (Heyman et al., 2016, 2013). In contrast BRassinosteroids At Vascular and Organizing Center (BRAVO), a transcription factor identified using cell-specific transcriptomics, acts as repressor of QC divisions (Vilarrasa-Blasi et al., 2014). Interestingly, BRAVO is a direct transcriptional target of BES1 transcription factor but also interacts with BES1 at protein level, forming a feedback loop that antagonistically regulates QC divisions (Vilarrasa-Blasi et al., 2014). Despite the importance of these transcription factors for locally safeguarding QC divisions, it is still unknown whether BR-regulated QC function is maintained in a cell-autonomous fashion or requires external signaling. Moreover, although BR receptor collectively modulate QC cell division and differentiation of surrounding stem cells under normal conditions (Fàbregas et al., 2013), the specific contribution of each receptor within the stem cell niche is not known. These question prompted us to investigate BR-mediated regulation of quiescence and its impact on stem cell regeneration after DNA damage at a local level. Accordingly, we used a tissue-specific approach in order to determine the ability of QC cells to integrate exogenous steroid signals. For this purpose we specifically overexpressed two BR signaling components, the BRI1 membrane receptor and the BES1 transcription factor, in the QC cells. We also specifically knocked out BRI1 in the stem cell niche using an artificial microRNA (amiRNA) (Dolan et al., 1993; Schwab et al., 2006). Altogether in this chapter it is shown that:

1. Active BES1 is necessary for cell-autonomous QC divisions.

2. The BR hormone itself (and not the receptors) is the limiting factor for BR-induced QC division in the root apex.
3. BRI1 is required at the stem cell niche for mediating BR-dependent QC divisions.
4. Upon stem cell death, paracrine BR signaling is required for QC divisions.

These results establish a hierarchy for the different BR receptors within the stem cell niche, indicating that under normal conditions, BRI1 receptor rather than its homologous acts as the main player controlling QC divisions.

2.2 Active BES1 can trigger QC divisions cell-autonomously

Whether the BR-induced division signals of the QC are transduced in a cell-autonomous manner through the canonical BR signaling was still unclear. To investigate this we used *bes1-D*, a constitutively active mutant version of BES1, as gain of function (Yin et al., 2002). The *bes1-D* mutant was previously cloned under the control of the QC-specific promoter WOX5 (Sarkar et al., 2007) and fused to YFP in its C-terminus (Vilarrasa-Blasi et al., 2014). This construct, pWOX5:*bes1-D*-YFP, was transformed into both Col-0 wild-type (WT) and the null BRI1 mutant *bri1-116* (Li and Chory, 1997) (Figure 2.1 C,D,G,H).

Confocal microscopy of 6-day-old root tips revealed an increase in the number of QC divisions in both, the WT and *bri1-116* mutant backgrounds, when *bes1-D* is expressed under the WOX5 promoter (Figure 2.2 A,D,F). This indicates that active BES1 locally promotes division at the QC in a cell-autonomous manner. Interestingly, however, the QC division rates in the *bri1-116* background were lower than those in the WT background (Figure 2.3), suggesting that BR

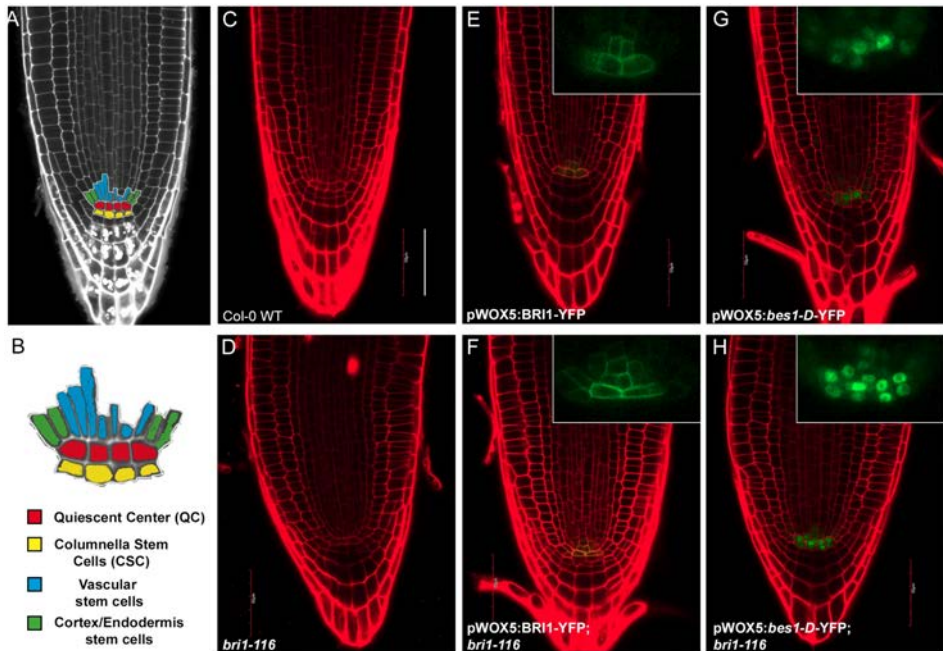


Figure 2.1: The stem cell niche of Arabidopsis roots and QC-specific expression of BR pathway components

(A) A stereotypical Arabidopsis (wild-type) primary root under confocal microscopy. The root stem cell niche is highlighted, and the different cell lineages depicted in colors. (B) Detailed representation of the root stem cell niche. (C-H) Confocal images of 6-day-old WT and mutant Arabidopsis roots in control conditions. Green represents YFP-tagged pathway components. Red is Propidium Iodide (PI) counter-staining. Insets show the YFP channel at higher magnification. Scale bar: 50 μm .

signaling from surrounding tissues also participates in the activation of QC divisions. It is noteworthy that BRI1 might also activate other downstream components besides BES1. For example one potential downstream target could be the transcription factor BZR1, which is also able to promote autonomous QC divisions when activated (Chaiwanon and Wang, 2015; Lee et al., 2015).

In addition, treatment of WT plants harboring the pWOX5:*bes1-D*-YFP construct with brassinolide (BL) did not result in a significant increase in cell division rates (Figure 2.2 D,J; Figure 2.3). Fact that is probably due to a saturated BR signal contributed also by basal receptor-transduced signaling. Conversely, upon BL treatment, a significant increase in cell division rate

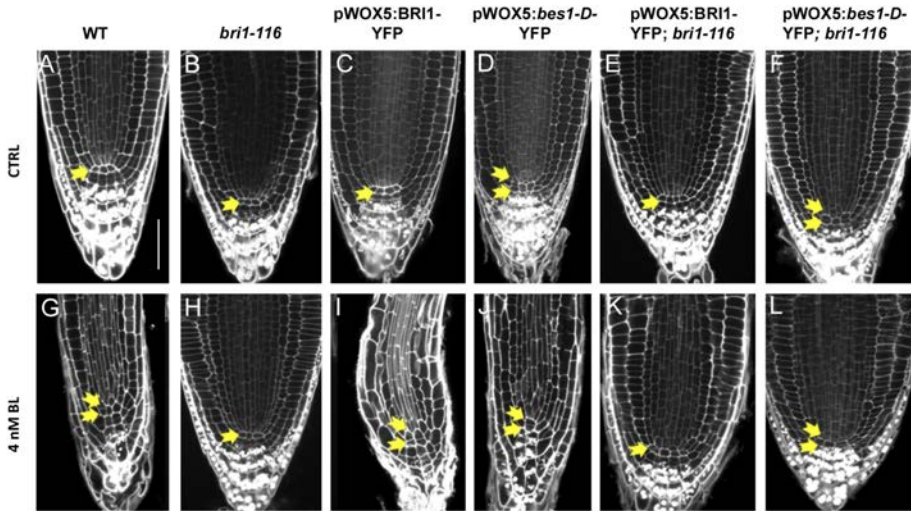


Figure 2.2: BES1 transcription factor promotes QC division cell-autonomously

(A-F) Confocal images of fixed 6-day-old Arabidopsis roots in control conditions. (G-L) Root anatomy of 6-day-old seedlings grown in media supplemented with 4nM BL. Yellow arrows mark the QC cell layers.

was observed for the *bri1-116* plants containing the pWOX5:*bes1-D*-YFP construct (Figure 2.2 F,L; Figure 2.3). This suggest that signal is not saturated in these plants and that the BRLs receptors are also contributing factors.

2.3 The hormone is the limiting factor for QC divisions

Next, by introducing the pWOX5:BRI1-YFP transgene into both WT and *bri1-116* backgrounds, the local contribution of the BRI1 to QC divisions was evaluated (Figure 2.1 C-F). As the WOX5 promoter drives relatively high expression compared with endogenous BRI1 promoter (Geldner et al., 2007), WOX5-controlled expression of the BRI1 receptor results in a local QC overexpression (Figure 2.4). In addition, the fact that the roots showed signs

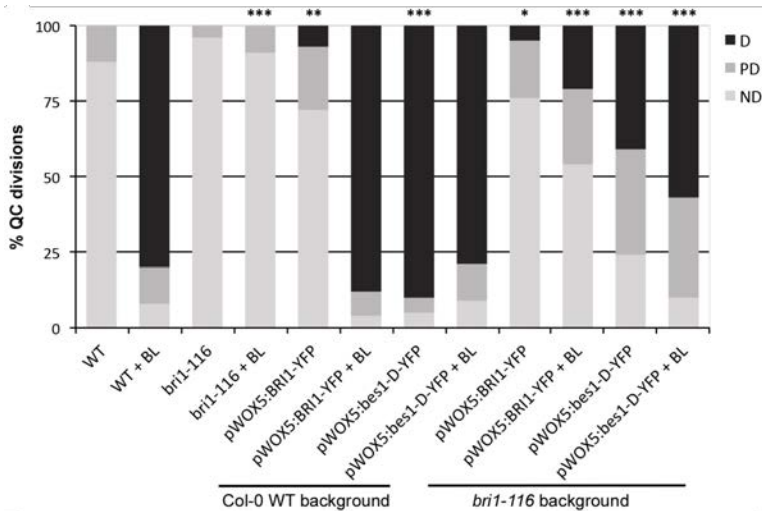


Figure 2.3: Quantification of QC division rates in QC-specific over-expression lines

Quantification of QC division rates for lines in Figure 2.2. ND, non-divided QC; PD, partially-divided QC; D, totally divided QC. Asterisks indicate statistically significant differences due to genotype, comparing against WT either in control or with 4 nM BL. Frequencies in division occurrence were assessed with a two-sided Fisher's test. Data generated from three independent replicates ($n > 21$). * $P < 0.05$, ** $P < 0.01$, *** $P < 0.005$. Scale bar: 50 μm .

of recovery in the *bri1* background (i.e. longer roots) confirmed that BRI1 was still functional when fused to YFP (Figure 2.5).

When BRI1 is locally overexpressed using the WOX5 promoter, a small increase in QC division rate was observed in both WT and *bri1-116* backgrounds (Figure 2.2 C,E; Figure 2.3). This increase, however, was substantially smaller than the observed with the expression of *bes1-D* using the same promoter (Figure 2.2 D,F; Figure 2.3). Upon application of exogenous BL, we observed a dramatic increase in the QC division rate for those plants expressing pWOX5:BRI1-YFP in the WT background but not in the *bri1-116* background (Figure 2.2 C,E,I,K; Figure 2.3). This result implies that BRI1 signaling in the QC alone is not sufficient to promote QC divisions. It requires additional external signaling. The fact that overexpression of BRI1 in the QC does not result in a large

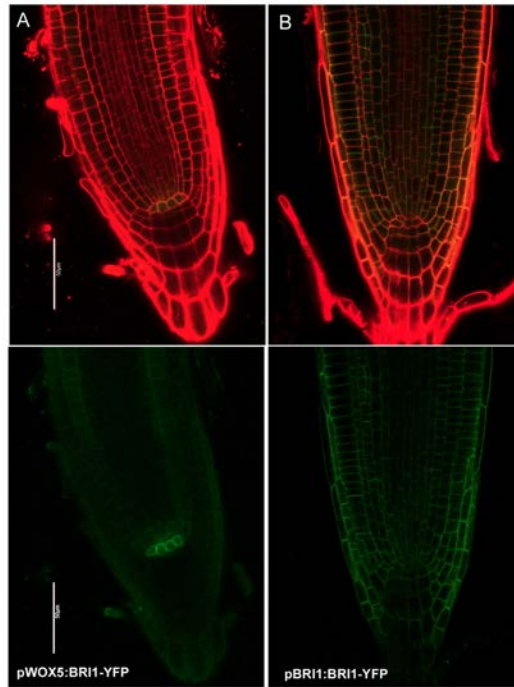


Figure 2.4: WOX5-controlled BRI1 expression is QC-specific

Confocal images of 6-day-old *Arabidopsis* roots grown under control conditions. (A) pWOX5:BRI1-YFP root (B) pBRI1:BRI1-GFP (Geldner et al., 2007). Green depicts GFP or YFP-tagged BRI1 protein and red depicts cell walls PI counter stain. Scale bar: 50 μm .

increase in QC division until exogenous BL is applied indicates that the BR hormone itself is the limiting factor for QC division. Furthermore, only after applying BL a dramatic reduction in meristem cell number could be observed in the *bri1-116* with the pWOX5:BRI1-YFP transgene. This typical effect of exogenous BL application was not seen when just BRI1 is overexpressed (Figure 2.5). Together, these results suggest two possible scenarios: (i) there is an insufficient pool of free BR in the root stem cell niche to promote QC divisions, or (ii) BRI1-like receptors (i.e. BRL1 and BRL3) act as competitors for ligand binding.

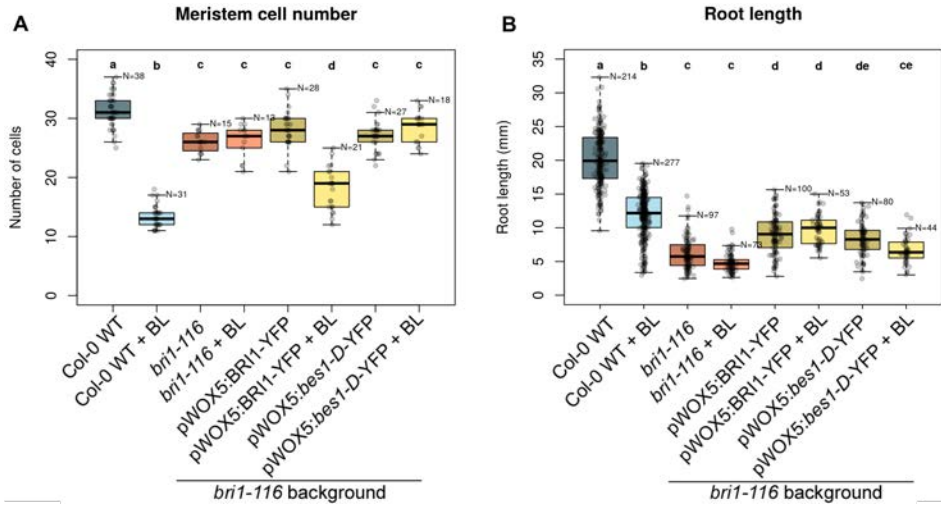


Figure 2.5: QC-specific expression of BR components has an impact on the growth of primary roots

(A) Quantification of meristem cell number of QC-overexpression lines in control and upon BL application. Note that expression of BRI1 exclusively in the QC partially recovers the sensitivity to BL application, thus showing that BRI1 is active in the WOX5 domain. (B) Quantification of root length of QC-overexpression lines. The partial alleviation of *bri1-116* dwarf phenotype in pWOX5:BRI1-YFP lines suggest that BR signaling in the QC accounts for overall root growth. Differences evaluated through one-way ANOVA plus a Tukey post-hoc test. Different letters mean significant differences. Data from three independent replicates. Number of individuals analyzed in for each genotype is depicted next to the upper whisker of each boxplot.

To address the second scenario, pWOX5:BRI1-YFP plants were crossed with double and triple mutants lacking two (*brl1brl3*) or all three functional receptors (*bri1-116brl1brl3*). The occurrence of spontaneous QC divisions or an increased sensitivity to BL was assessed. If BRLs receptors were competing with BRI1 for hormone binding, an increase in QC division would be expected already in control conditions in the pWOX5:BRI1-YFP plants crossed with the *brl1brl3* double mutant. However this effect was not observed (Figure 2.6; Figure 2.7). Application of BL to pWOX5:BRI1-YFP plants in the *brl1brl3* double mutant backgrounds yielded similar effects to those in the WT background, showing that the loss of these genes does not increase the QC division rates, not with small doses (it would mean increased sensitivity) neither with

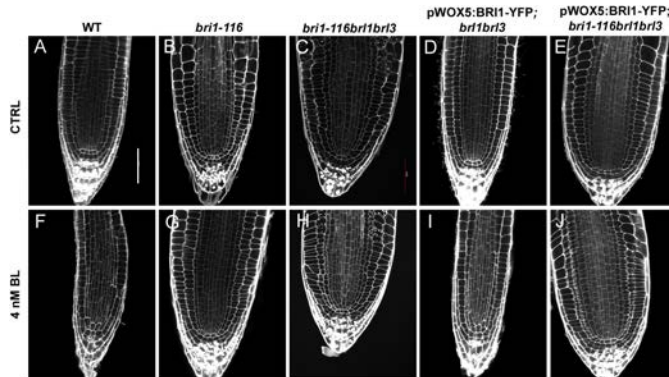


Figure 2.6: BRL1 and BRL3 receptors do not compete with BRI1 for ligand binding in the QC microenvironment

(A-E) Phenotype of 6-day-old roots grown under control conditions. (F-J) Phenotype of 6-day-old seedlings treated with BL.

high doses (Figure 2.6; Figure 2.7). With respect to the triple mutant, similar results than in the *bri1-116* background were obtained (Figure 2.6; Figure 2.7). Altogether, these results indicate that the BRL1/3 receptors do not compete with the BRI1 receptor for hormone binding. And interestingly, the lack of BRLs receptors attenuates the slight increase in QC division that is observed with the BRI1 expression in the QC (Figure 2.3; Figure 2.7), in agreement with previously reported data (Fàbregas et al., 2013). These results support a marginal role for BRL1 and BRL3 receptors in promoting BR-mediated QC division under normal conditions. All together, we concluded that the stem cell niche microenvironment must be characterized by an excess of BRI1 and a limited amount of free hormone. We discounted competition for the ligand between BRI1 and BRLs and hypothesize that, in the root stem cell niche, a threshold of available hormone has to be reached in order to promote QC divisions.

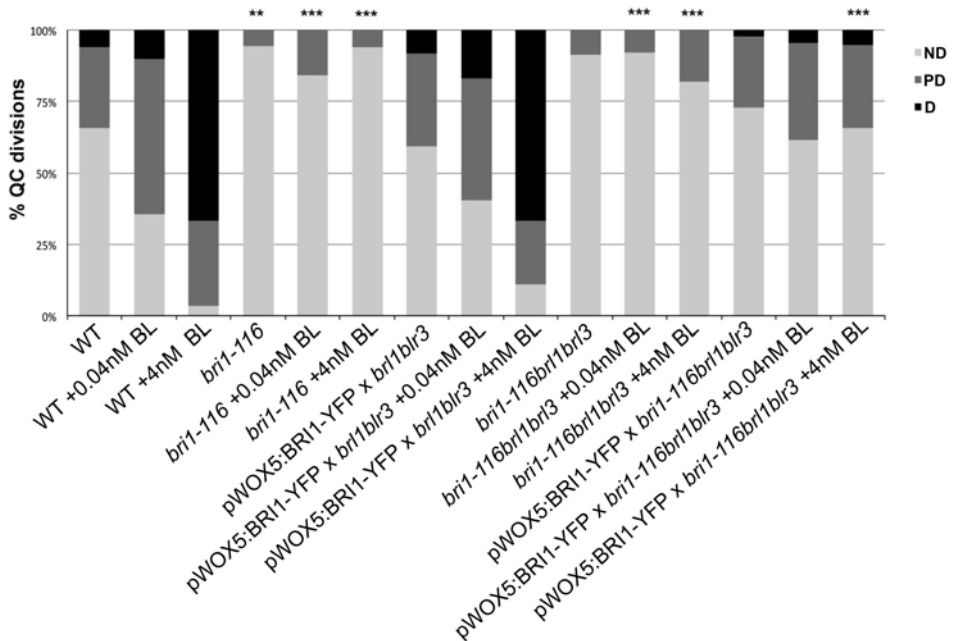


Figure 2.7: Quantification of QC division rates of QC-specific over-expressors lines in the *bri1bri3* null background

Quantification of QC division rates. ND, non-divided QC; PD, partially-divided QC; D, totally divided QC. Asterisks indicate statistically significant differences due to genotype, comparing against WT either in control or with 4 nM BL. Frequencies in division occurrence were assessed with a two-sided Fisher's test. Data generated from three independent replicates ($n > 21$). * $P < 0.05$, ** $P < 0.01$, *** $P < 0.005$. Scale bar: 50 μm .

2.4 BRI1 is necessary but not sufficient to promote QC division

According to the results exposed in the previous section, the presence of BRI1 in the QC is not the limiting factor for the QC division process. In fact, very low amounts of BRI1 receptor are present in these cells (Wilma van Esse et al., 2011). Furthermore, BRL1 and BRL3, both of which bind the hormone with higher affinity than BRI1, are also present in these cells (Caño-Delgado et al., 2004; Fàbregas et al., 2013). Accordingly, we wondered whether BRI1 was absolutely necessary in this domain. To answer this question we sought to knockout

BRI1 specifically in the QC. For this purpose, an Artificial Micro-Interference RNA (amiRNA) against the BRI1 transcript was designed and cloned under the control of the WOX5 promoter (Figure 2.8). To validate the ability of the amiRNA to knock out BRI1 expression, it was also placed under the control of the constitutive promoter of Cauliflower Mosaic Virus 35S (CaMV35S). This resulted in dwarf plants similar to null *bri1* mutants (Li and Chory, 1997), confirming the effectiveness of the amiRNA (Figure 2.8 C). Crosses of pWOX5:BRI1-amiRNA plants with plants expressing BRI1-GFP under the control of the endodermis-specific promoter scarecrow (SCR) (Hacham et al., 2011) revealed that inhibition of BRI1 expression was not limited to QC cells but also occurred in nearby surrounding cells (Figure 2.9 A,B). This implies that the small size of the mature amiRNA enables it to diffuse to adjacent cells. Importantly, YFP signal in plants that overexpressed BRI1-YFP in the QC completely disappeared when crossed with pWOX5:BRI1-amiRNA plants, indicating that the amiRNA expressed under WOX5 promoter is indeed effective at knocking out all BRI1 expression (Figure 2.9 C,D). Finally, genetic crosses between the pWOX5:BRI1-amiRNA lines and the translational reporter lines pBRL1:BRL1-GFP and pBRL3:BRL3-GFP (Fàbregas et al., 2013) showed that the BRI1-amiRNA is partially depleting *BRL1* and *BRL3* transcripts, probably as consequence of sequence similarity (Figure 2.9 E-H). A GFP intensity reduction of ~40% was detected in the crosses (Figure 2.10).

Next, two independent pWOX5:BRI1-amiRNA transgenic lines were analyzed in terms of sensitivity to exogenous BL application. Based on root length, meristem cell number and stele width, it was found that lines expressing the amiRNA retain BL sensitivity at closely similar levels than WT plants, while null mutants *bri1-116* plants are totally insensitive to hormone application (Figure 2.11), thereby suggesting that the effect of the mature amiRNA is strongly limited to a local level. Interestingly, we found that both pWOX5:BRI1-amiRNA lines are completely insensitive to BL application in

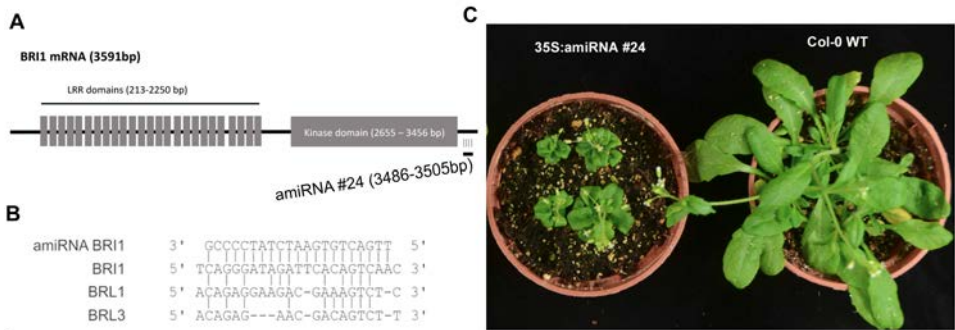


Figure 2.8: Design and testing of BRI1 amiRNA lines

(A) Schematic representation of the BRI1 transcript and the binding coordinates of the designed amiRNA. (B) Sequence of the amiRNA and its base pairing with the mRNA of BRI1, BRL1 and BRL3. (C) Images showing mature WT and 35S:BRI1-amiR#24 plants. The amiRNA#24 was chosen because its dwarf phenotype strongly resembles the *bri1* mutant.

terms of QC division (Figure 2.12; Figure 2.13). Taken together, these results indicate that the presence of BRI1 receptors in the QC is essential for QC division.

Additionally, pWOX5:BRI1-amiRNA lines exhibited impaired root growth, having slightly but significantly shorter roots than WT plants starting from 5 days after germination (Figure 2.11; Figure 2.14). This result reveals that QC division frequency has an impact on the primary root growth and that the presence of BR receptor in root stem cell niche contributes to optimal root growth. Accordingly, *bri1-116* plants overexpressing BRI1 or BES1 in the QC partially recovered the short root length observed in the *bri1-116* mutant (Figure 2.5 B). These observations suggest that some spontaneous QC divisions are required under basal conditions to sustain optimal root growth, presumably for the replenishment of the stem cell niche.

We next asked ourselves if the reduction in QC division found in pWOX5:BRI1-amiRNA lines might be just a consequence of a slower cell cycle progression in the meristem rather than a specific BRI1 effect in the QC. To rule out this question, roots were stained with 5-ethynyl-2'-deoxyuridine (EdU), a thymidine

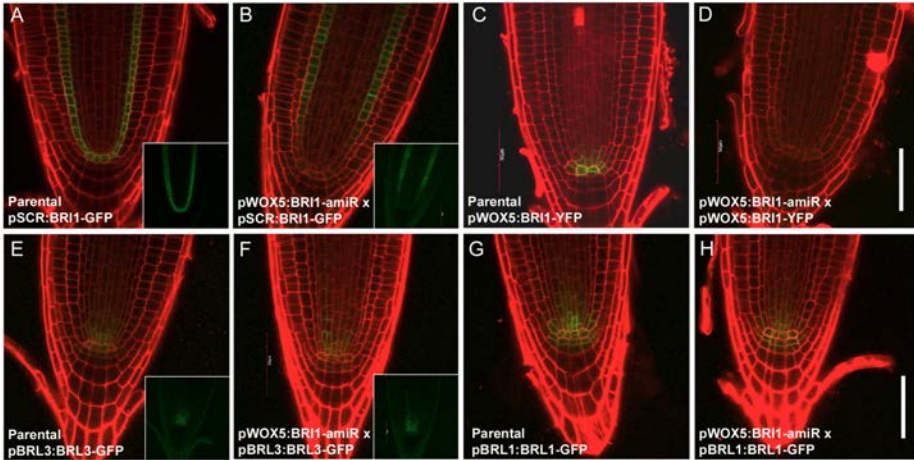


Figure 2.9: The pWOX5:BRI1-amiR construct downregulates BRI1 transcription in the root stem cell microenvironment

Confocal images of 6-days-old Arabidopsis roots. (A,B) Genetic crosses between pWOX5:BRI1-amiR and pSCR:BRI1-GFP lines reveal that BRI1 is knocked down in the stem cell microenvironment. (C,D) Genetic crosses between pWOX5:BRI1-YFP and pWOX5:BRI1-amiR lines show that the amiRNA completely depletes BRI1 around the QC domain. (E-H) Genetic crosses of pWOX5:BRI1-amiR lines with pBRL1:BRL1-GFP and pBRL3:BRL3-GFP. Insets show the GFP channel separately. All crosses are F3 double homozygous plants. Scale bar: 50 μm .

analogue that is incorporated into actively dividing cells (Salic and Mitchison, 2008). In WT plants EdU uniformly stains the entire root meristem except for the QC, which due to its quiescence barely incorporates EdU (Figure 2.15 A). The same staining than WT is obtained in the pWOX5:BRI1-amiRNA lines, which indicates a normal cell cycle (Figure 2.15 B,C). Thus, QC remains quiescent because of the absence of BRI1 and not because of a meristem-wide deceleration of the cell cycle. In contrast, the *bri1-116* mutant shows way lower EdU incorporation, confirming that it has a slower cell cycle compared with WT plants (Figure 2.15 D). Fluorescent intensity quantification confirms that pWOX5:BRI1-amiRNA lines incorporate EdU at the same levels as in the WT, whereas *bri1-116* does at lower rates (Figure 2.16). These observations agree with the previously reported slow cell cycle progression of *bri1-116*

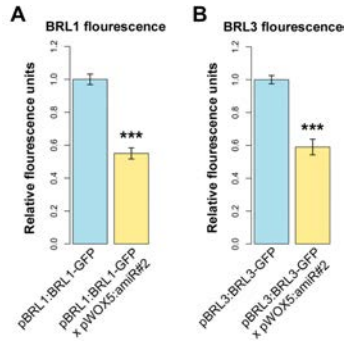


Figure 2.10: pWOX5:BRI1-amiR lines partially off-target BRL1 and BRL3 expression

(A,B) Fluorescence quantification of BRL1 and BRL3 proteins in the parental lines (pBRL1:BRL1-GFP, pBRL3:BRL3-GFP) and in the same lines crossed with the pWOX5:BRI1-amiR lines. GFP quantification shows partial downregulation in the crosses as a consequence of the amiRNA off-targeting, likely due to sequence homology. Asterisks depict statistically significant differences respect parental lines in a two-tailed t-test. Data generated from three independent replicates ($n > 22$).

(González-García et al., 2011).

Furthermore, pWOX5:BRI1-amiRNA plants were treated with BL in order to evaluate if BL promotes QC division in these lines. Upon BL treatment, WT roots incorporate EdU into the QC (Figure 2.15 E), confirming that QC cells were actually undergoing division. In contrast, pWOX5:BRI1-amiRNA lines do not incorporate EdU into the QC after being subjected to identical BL treatment (Figure 2.15 F,G). This result clearly supports that pWOX5:BRI1-amiRNA lines are insensitive to BR signals in the QC. On the other hand, plants with a constitutively dividing QC due to an active BES1 overexpression, the pWOX5:*bes1-D*-YFP line, exhibited EdU incorporation in the QC at basal conditions (without BL treatment) (Figure 2.15 H). This last result further confirms that activated downstream components of BR receptors are capable of triggering QC division in a cell-autonomous manner.

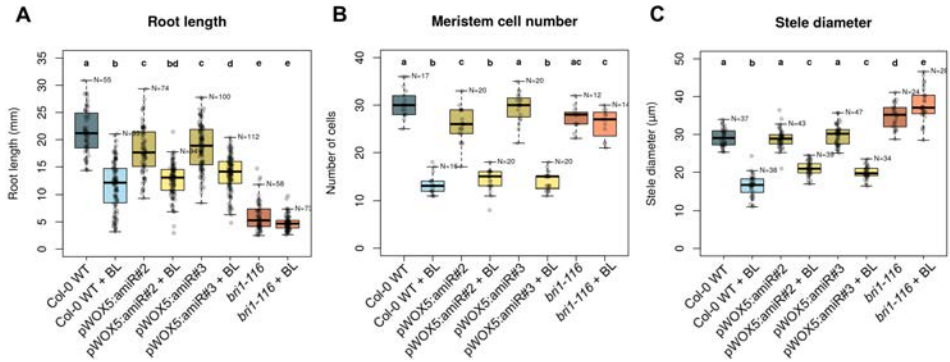


Figure 2.11: pWOX5:BRI1-amiR lines retain sensitivity to BL

(A) Quantification of root length of pWOX5:BRI1-amiR lines shows that the depletion of BRI1 in QC and surrounding cells negatively affects overall root growth. (B) Quantification of meristem cell number of pWOX5:BRI1-amiR lines shows that seedlings retain sensitivity to exogenous BL applications. (C) Quantification of stele width of pWOX5:BRI1-amiR lines. Data shows that pWOX5:BRI1-amiR lines do not have affected stele width. However they are slightly less sensitive to BL applications. Interestingly, *bri1-116* null mutant has a wider stele, which is even more expanded upon BL application. Different letters above the boxplots depict statistically significant differences. All pairwise comparisons evaluated through one-way ANOVA plus a Tukey post-hoc test. Data generated from three independent replicates. The number of individuals analyzed in each case is indicated next to the upper whisker of each boxplot.

Because pWOX5:BRI1-amiR lines totally abolish QC divisions while BRI1 acting exclusively in the QC (i.e. pWOX5:BRI1-YFP in *bri1-116*) do not totally recover BL-induced QC division to WT levels [Figure 2.3](#), we concluded that BRI1 signaling in the QC is necessary but not sufficient to promote QC self-renewal. It also highlights BRI1 as the main driving factor for this process. Despite the fact that BRLs activity is also partially downregulated in pWOX5:BRI1-amiR lines, previous results showed that *bri1brl3* double mutants have a normal BR-induced QC division ([Fàbregas et al., 2013](#)), which is in agreement with our results. On the other hand, *bri1-116* mutants, that have intact *BRL1* and *BRL3* genes, retain a quiescent QC even with application of high doses of BL ([Figure 2.3](#)) ([González-García et al., 2011](#)). Altogether, these results indicate the BRI1 signaling in the QC is necessary but not sufficient to promote its division.

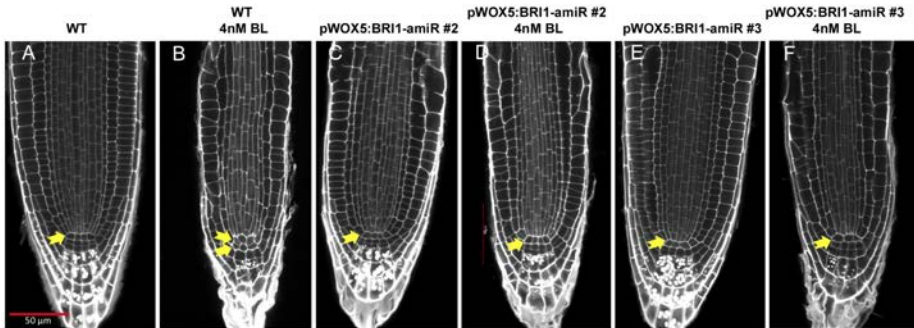


Figure 2.12: BRI1 is required in the stem cell niche to promote QC divisions

(A-B) Confocal images of fixed 6-day-old *Arabidopsis* roots grown in either control conditions or in media supplemented with 4 nM BL show the changes in the QC organization. (C-F) Two independent pWOX5:BRI1-amiR transgenic lines grown in control conditions or with 4 nM BL. Arrows indicate the number of QC cell layers identified. Scale bar: 50 μm .

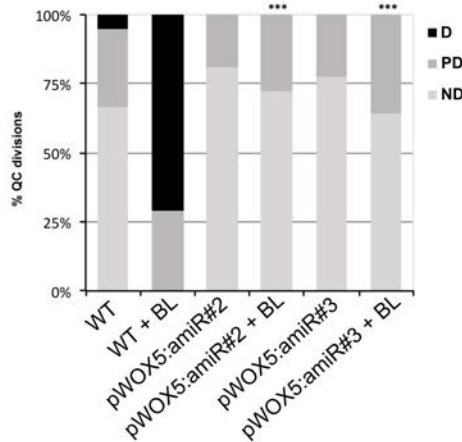


Figure 2.13: Quantification of QC division rates in pWOX5:BRI1-amiR lines

Quantification of QC divisions of WT and pWOX5:BRI1-amiR plants. ND, non-divided QC; PD, partially-divided QC; D, totally divided QC. Asterisks indicate statistically significant differences due to genotype, comparing against WT either in control or with 4 nM BL ($***P < 0.005$). Frequencies in division occurrence were assessed with a two-sided Fisher's test. Data generated from three independent replicates ($n > 39$).

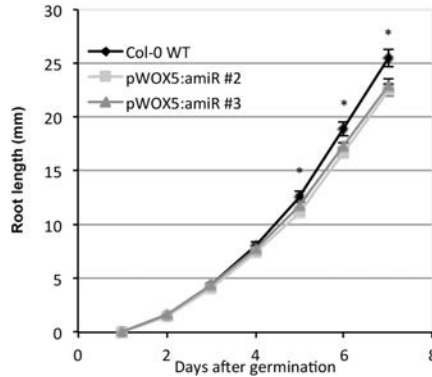


Figure 2.14: Root growth dynamics of pWOX5:BRI1-amiR lines

One week root growth curve of WT and pWOX5:BRI1-amiR lines. Asterisk denote statistically significant differences with respect WT in a two-tailed t-test ($*P < 0.05$). Data generated from three independent replicates ($n > 46$).

2.5 BR signaling acts in a paracrine manner to trigger QC divisions

The QC acts as a stem cell reservoir and it is known to divide in front of environmental stresses, such as the presence of DNA-damaging agents (Vilarrasa-Blasi et al., 2014) or changes in the homeostasis of reactive oxygen species (ROS) (Yu et al., 2016). In the root, DNA-damaging agents preferentially harm vascular and columella stem cells. Cells that are unable to repair this damage activate programmed cell death (PCD) and undergo apoptosis (Fulcher and Sablowski, 2009), which subsequently promotes QC division to replenish the stem cell niche and maintain meristematic activities (Heyman et al., 2016; Vilarrasa-Blasi et al., 2014). We took advantage of this property to analyze the receptor requirements of the signaling that causes QC divisions upon DNA damage. Whether BR receptors are essential for carrying out such stress-induced division was tested. For this, we used bleomycin, a chemotherapeutic drug that preferentially harms root vascular stem cells and induce QC divisions (Fulcher and Sablowski, 2009; Vilarrasa-Blasi et al., 2014). Therefore this system induces QC divisions independently of exogenous BR applications.

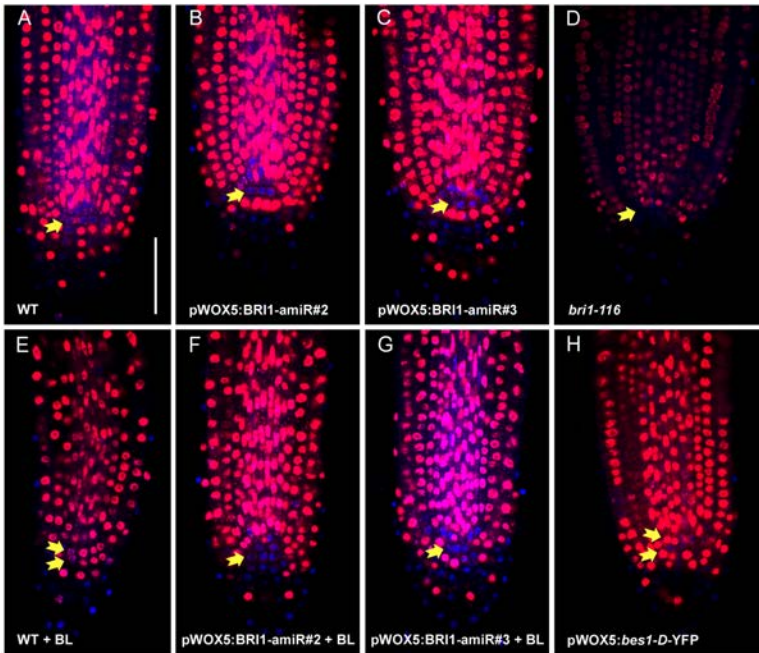


Figure 2.15: pWOX5:BRI1-amiR seedlings exhibit normal meristem divisions

Confocal images of fixed and EdU-stained 6-day-old Arabidopsis roots. (A-C) WT, pWOX5:BRI1-amiR#2 and pWOX5:BRI1-amiR#3 lines grown in control conditions. (D) *bri1-116* line grown in control conditions as a negative control for QC division. (E-G) WT, pWOX5:BRI1-amiR#2 and pWOX5:BRI1-amiR#3 lines grown for 4 days in control conditions plus 2 days in media supplemented with 4 nM BL. (H) pWOX5:*bes1-D-YFP* line grown in control condition as a positive control for QC divisions. Arrows indicate the number of QC cell layers identified. Scale bar: 50 μm .

The local knockout lines (pWOX5:BRI1-amiRNA) were compared against both, the null *bri1* mutant and WT roots. While the pWOX5:BRI1-amiRNA lines incorporate damage at the same rate as the WT plants, the *bri1* mutant remained free of any visible damage (Figure 2.17 A-D). As previously described, this is probably due to the slow cell cycle progression (González-García et al., 2011; Vilarrasa-Blasi et al., 2014). Interestingly, in contrast to what observed in WT roots, the QC of pWOX5:BRI1-amiRNA lines remained undivided following 24h of bleomycin treatment plus 24h of recovery (Figure 2.17 E-F; Figure 2.18). In the case of *bri1*, the QC also remains undivided but as

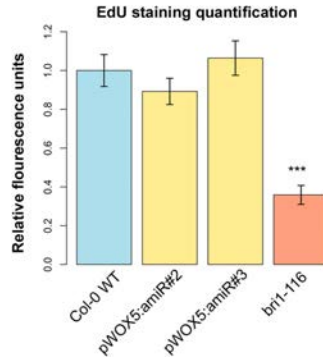


Figure 2.16: Quantification of EdU staining in pWOX5:BRI1-amiR lines

Fluorescence quantification due to EdU incorporation in the lines shown in Figure 2.15. Results reveal no differences in meristem cell cycle progression between WT and pWOX5:BRI1-amiR lines. Asterisk depict statistically significant differences respect WT in a two-tailed t-test (***) ($P < 0.005$). Data generated from two independent replicates ($n > 15$).

mentioned above, the roots were not damaged by bleomycin. Given that the pWOX5:BRI1-amiRNA lines and WT show similar levels of provascular cell death after 24h of bleomycin treatment (Figure 2.17 A-C, Figure 2.18), as well as the same amount of EdU staining (Figure 2.15), it was deduced that the absence of QC division in bleomycin-treated pWOX5:BRI1-amiRNA lines is not due to an inherent resistance against DNA damage nor a slow cell cycle progression. Interestingly, results reveal the paracrine nature of this DNA damage response: a signal that should emerge from damaged stem cells triggers cell division in the adjacent QC. And according to the results, this signal must be of steroid nature that is locally and mainly transduced by BRI1 in the stem cell niche.

Even if we cannot discern between BRI1 and the BRLs perceiving this signal, results reveal that the signal should be of a steroid nature and act in a paracrine manner. It is known that by stimulating paracrine signaling, human stem cells can promote wound healing and cancer progression (Dittmer and Leyh, 2014) but in plants the mechanisms behind autocrine and paracrine signaling are just

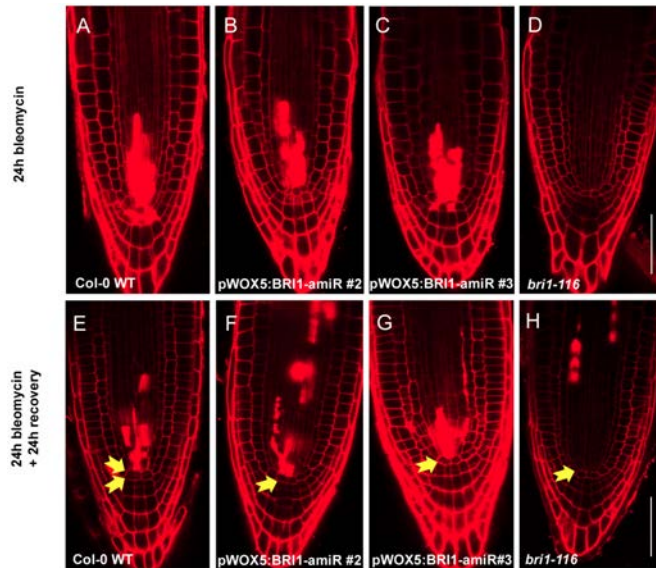


Figure 2.17: BR receptors in the stem cell niche modulate QC divisions upon DNA damage

(A-D) Confocal images of 5-day-old *Arabidopsis* seedlings treated with bleomycin for 24h. (E-H) Confocal images of 5-day-old *Arabidopsis* seedlings subjected to 24h bleomycin treatment and a subsequent 24h recovery period. Intense red stains (PI) marks cell death. Arrows indicate the number of QC cell layers identified. Scale bar: 50 μm .

starting to be uncovered (Qi et al., 2017). It has been proposed that BRs can regulate stem cell division in the roots via long-range signals originating at the epidermis (Hacham et al., 2011). However, although changes in QC markers (e.g. AGL42) were observed in response to epidermal signaling, no effect on QC division was reported (Hacham et al., 2011). Therefore, this limits the direct readout of BR-mediated signaling in the QC to short-range signals. Indeed, in contrast to other hormones that act over long distances it is accepted that BRs act a more local level (Fridman et al., 2014) and our findings indicate that the signals that promote QC division come from the nearby stem cell microenvironment rather than from the outer cell layers. Nevertheless, where exactly the BR signals are driven from remains a controversy.

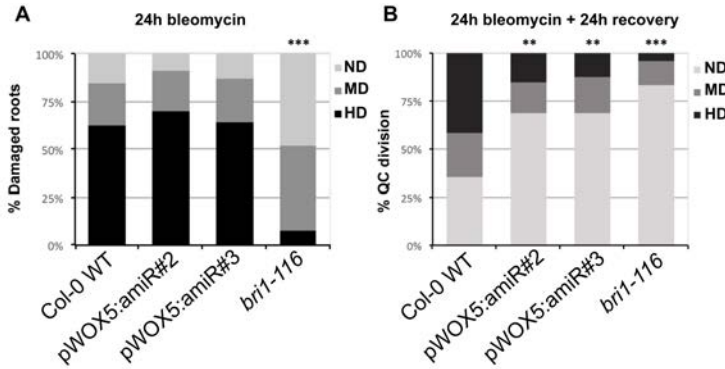


Figure 2.18: Quantification of cell damage and QC division following bleomycin treatments

(A) Proportion of roots from Figure 2.17 showing cell death in the root apex after 24h bleomycin treatment. HD, hard damage; MD, mild damage; ND, no damage. (B) Quantification of QC division of lines shown in Figure 2.17 after 24h bleomycin treatment and 24 additional hours of recovery. ND, non-divided QC; PD, partially-divided QC; D, totally divided QC. Asterisks indicate statistically significant differences respect WT (** $P < 0.01$, *** $P < 0.005$). Differences in proportion/frequencies were assessed with a two-sided Fisher's test. Data generated from three independent replicates ($n > 24$).

In summary, our findings show that: (i) QC cell division activity is promoted by BES1 transcription factor in the QC; (ii) BRI1 is required in both the QC and nearby cells to trigger division; and (iii) paracrine steroid signaling may be regulated by the hormone availability in the stem cell niche. A plausible way to control the hormone levels in the root stem cell niche of the root could be the upregulation of genes controlling its biosynthesis. However, the spatial regulation of the enzymes responsible for BR biosynthesis is still poorly understood. As such, further efforts in this area are crucial for elucidating the nature and origin of BR signals, where they are synthesized and where they are driven.

Chapter 3

Vascular receptor BRL3 mediates drought stress responses

Part of this chapter published as:

**Overexpression of the vascular brassinosteroid receptor BRL3
confers drought resistance without penalizing plant growth**

Fàbregas, N.*, Lozano-Elena, F.*, Blasco-Escámez, D., Toghe, T., et al.
(2018) *Nature Communications*, 9

Vascular receptor BRL3 mediates drought stress responses

3.1 Introduction

BRs modulate multiple developmental and environmental stress responses in plants but the exact role of BRs under stress conditions remains controversial. Because its wide localization across tissues, BRI1 is the central player regulating growth and adaptation to abiotic stress (Belkhadir and Jaillais, 2015; Eremina et al., 2016; Ye et al., 2017), whereas the functional relevance of vascular BRL1 and BRL3 is only just beginning to be explored (Fàbregas et al., 2013; Vragović et al., 2015). Moreover greater attention is being placed on the spatial regulation of hormonal signaling pathways in an attempt of further understand the coordination of plant growth and stress responses (Fàbregas et al., 2013; Lozano-Elena et al., 2018; Vilarrasa-Blasi et al., 2014; Ye et al., 2017) (chapter 2). In previous proteomic approaches in our laboratory, drought stress-related proteins were identified within the BRL3 signalosome complex (Fàbregas et al., 2013), but the exact role of the BRL3 pathway in drought

remained elusive.

Drought has been estimated to be responsible for at least 40% of crop losses worldwide (Boyer, 1982) and this proportion is dramatically increasing due to climate change. Understanding cellular responses to drought stress represents the first steps toward the development of better-adapted crops, which is currently a major challenge for plant biotechnology (Todaka et al., 2015). Classical approaches examining how plants cope with limited water led to the identification of components involved in the signal transduction cascades of both, ABA-dependent and ABA-independent pathways (Yoshida et al., 2014). Intriguingly ABA signaling, which is classically linked with most of the plant drought stress responses, inhibits the BR signaling pathway after BR perception and this crosstalk between the two pathways takes place upstream of the BIN2 kinase (Gui et al., 2016; Zhang et al., 2009). Further crosstalk has also been described downstream BIN2 but this is due to overlapped transcriptional control of BR-regulated and ABA-regulated genes (Chung et al., 2014; Huang et al., 2008), such as Response to Dessication 26 (RD26) (Ye et al., 2017).

Adaptation to drought stress also has been associated with the presence of proteins that protect cells from dehydration, such as Late-Embryogenesis-Abundant (LEA) proteins, osmoprotectants and detoxification enzymes (Graether and Boddington, 2014; Seki et al., 2007). Surprisingly LEA proteins are also abundant among BRL3-associated proteins, further supporting a role for BRL3 in drought responses (Fàbregas et al., 2013). These studies, along with many more, provided deeper insight into the molecular mechanisms underlying abiotic stress (Todaka et al., 2015), but at the same time showed that drought resistance is a complex trait simultaneously controlled by many genes. While genetic approaches have succeeded in conferring stress resistance to plants, this generally comes at the cost of reduced growth (Shao et al., 2008; Tardieu, 2012). Therefore, that a receptor of a hormone classically linked to

growth could have a role modulating drought responses, opens an interesting opportunity. Understanding how cellular growth is coupled to drought stress responses is essential for engineering plants with improved growth under drought. Especially in the water scarcity scenarios that are prognosticated along with the climate change.

In this chapter we show that knocking out or overexpressing different BR receptors modulate multiple drought stress-related traits in both roots and shoots. While the traits controlled by the BRI1 pathway are intimately linked to growth arrest, we found that overexpression of the vascular-enriched BRL3 receptor can confer drought resistance without penalizing overall plant growth. In addition, metabolite profiling revealed that the overexpression of the BRL3 receptor triggers the production of an osmoprotectant metabolic signature (i.e., proline, trehalose, sucrose and raffinose) in the whole plant and a specific accumulation of osmoprotectant metabolites in the roots during periods of drought. Subsequent transcriptomic profiling showed that this metabolic signature is transcriptionally regulated by the BRL3 pathway in response to drought. An enrichment of deregulated genes in root vascular tissues, especially in the phloem, further supports a preferential accumulation of osmoprotectant metabolites in the root. Overall, the study demonstrates that the overexpression of BRL3 receptor boosts the accumulation of sugar and osmoprotectant metabolites in the root and overcomes drought-associated growth arrest. These results uncover a new strategy to protect crops against drought.

3.2 BR receptors control osmotic stress sensitivity in the root

In order to determine the contribution of the BR complexes in the response to drought, we performed a comprehensive characterization of different combinations of mutants of all the BR receptors and the BAK1 co-receptor. We first phenotypically analyzed the primary root growth (Figure 3.1). Under control conditions, 7-day-old roots of *bak1*, *brl1brl3bak1*, *bri1-301* (hereafter *bri1*) and *bri1brl1brl3* displayed shorter roots than Col-0 wild-type (WT), as previously described (Fàbregas et al., 2013; González-García et al., 2011; Nam and Li, 2002). The primary roots of the quadruple mutant *bri1brl1brl3bak1* (hereafter *quad*) lacking all BR receptors and BAK1 were the shortest (Figure 3.1). Conversely, plants overexpressing BRL3 (CaMV35S:BRL3-GFP, hereafter *BRL3ox*) exhibited longer roots than WT (Figure 3.1). These results agree with the previously reported role of BR receptors in promoting root growth (González-García et al., 2011; Hacham et al., 2011). Interestingly we found that instead of the expected constitutive expression across all root tissues, *BRL3ox* showed increased receptor levels specifically in root vascular tissues (Figure 3.2) (Fàbregas et al., 2013).

We then subjected Arabidopsis seedlings to osmotic stress by transferring them to sorbitol-containing media. High concentrations of sorbitol in the media increase substantially the osmotic pressure, which raises the energy requirements of the plant for water uptake, thus *in vitro*-mimicking the drought water scarcity. We quantified the root lengths of 7-days-old seedlings that were transferred for 4 days to media 270 mM sorbitol and relativized them with the root lengths in control conditions. We defined the root growth inhibition caused by osmotic stress as:

$$\text{Root growth inhibition} = 1 - \frac{\text{Root length}_{\text{sorbitol}}}{\text{Root length}_{\text{control}}}$$

The *bri1*, *bri1brl1brl3* and *quad* showed a significantly lower root growth inhibition in sorbitol compared to WT (27, 28 and 27% respectively and 39% for WT) (Figure 3.1 B), revealing the capacity of these lines of avoiding the effects of osmotic stress. In contrast, no differences in terms of root growth inhibition were found in *brl1brl3*, *brl1brl3bak1* and *BRL3ox* compared to WT (Figure 3.1 B).

In order to describe more in detail what is happening in the primary roots exposed to such high osmotic pressure, we visualized sorbitol-treated roots under the confocal microscope. Previous experiments unveiled that water stress induces cell death in Arabidopsis roots, that this cell death is localized and it occurs via PCD, making it an actively controlled process (Duan et al., 2010). As shown by the incorporation of propidium iodine (PI) in the nuclei, just a short period of osmotic stress (24 h) caused massive cell death in the elongation zone of the roots (Figure 3.3 A). We quantified the red-stained area within a 500 μm window upwards the QC and relativized the values of sorbitol-treated roots respect the staining under control conditions to get rid of staining differences caused by other factors unrelated with the osmotic stress. When compared to WT, a reduced amount of cell death was observed in the roots of *bri1*, *bri1brl1brl3* and *quad* mutants (Figure 3.3), thereby indicating less sensitivity towards osmotic stress. Conversely, plants with increased levels of BRL3 showed a massive amount of cell death in root tips compared to WT (Figure 3.3). Because root growth inhibition in *BRL3ox* was not different from WT (Figure 3.1) these results are not indicative of a deleterious effect of BRL3 overexpression upon osmotic stress, but rather point towards a role for BR receptors in triggering osmotic stress responses in roots. Indeed the water stress-induced PCD has been proposed to modify the root system architecture and enhance drought tolerance (Cao and Li, 2010; Duan et al., 2010).

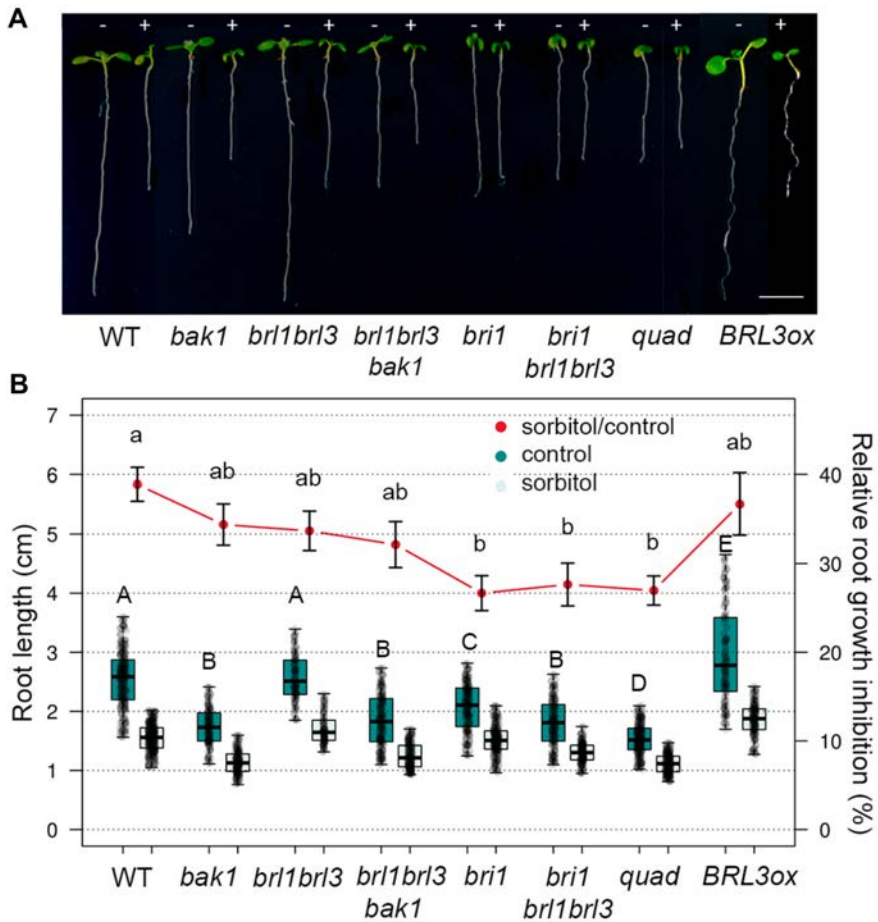


Figure 3.1: BR perception mutant's roots are less sensitive to osmotic stress

(A) Seven-day-old roots of WT, BR mutants *bak1*, *brl1brl3*, *brl1brl3bak1*, *bri1*, *bri1brl1brl3* and *quad*, and BR overexpressor line *BRL3ox* grown in control (-) or 270 mM sorbitol (+) conditions. Scale bar: 0.5 cm. (B) Boxplots depict the distribution of 7-day-old root lengths in control (dark green) or sorbitol (light green) conditions. Red line depicts relative root growth inhibition upon stress (ratio sorbitol/control \pm s.e.m). Data from five independent biological replicates ($n > 150$). Different letters represent significant differences (p -value < 0.05) in an one-way ANOVA plus Tukey post-hoc test.

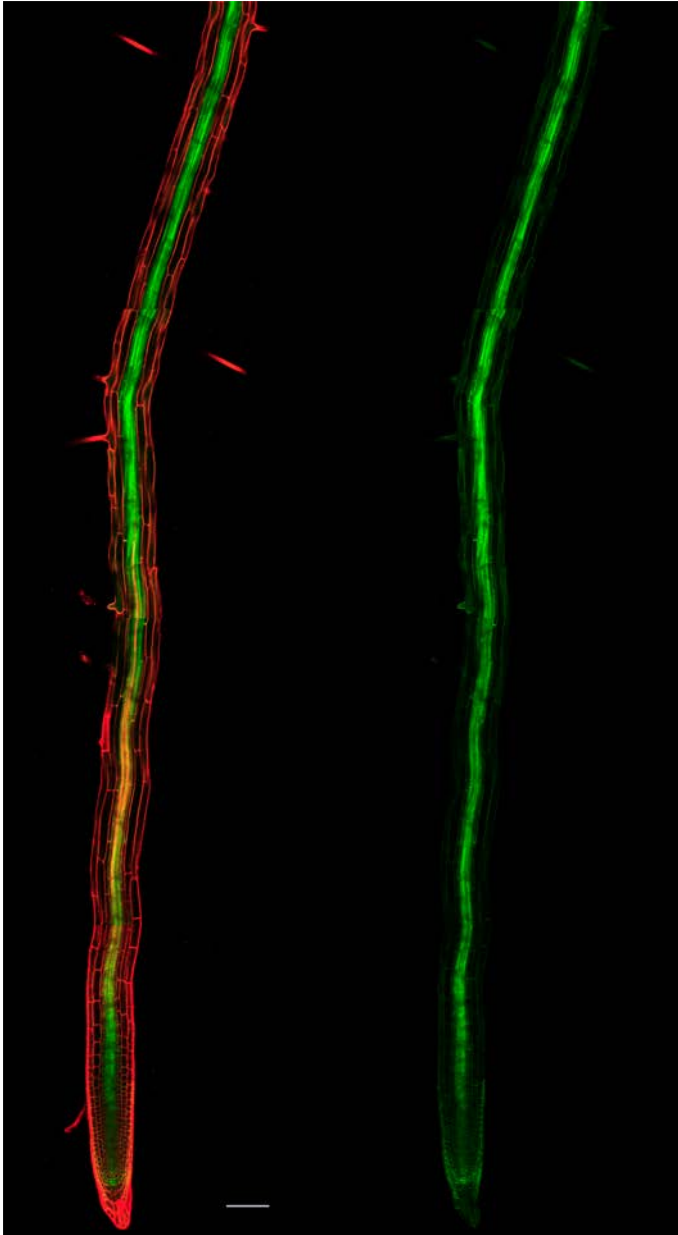


Figure 3.2: Localization pattern of BRL3 protein in the *BRL3ox* roots

Longitudinal section of a *35S:BRL3-GFP* (*BRL3ox*) roots in confocal microscope. The green channel depicts the GFP signal of the BRL3 receptor and the red channel shows the PI-stained cell walls. (Left) Merged image of both channels. (Right) Only green channel. Scale bar: 100 μm .

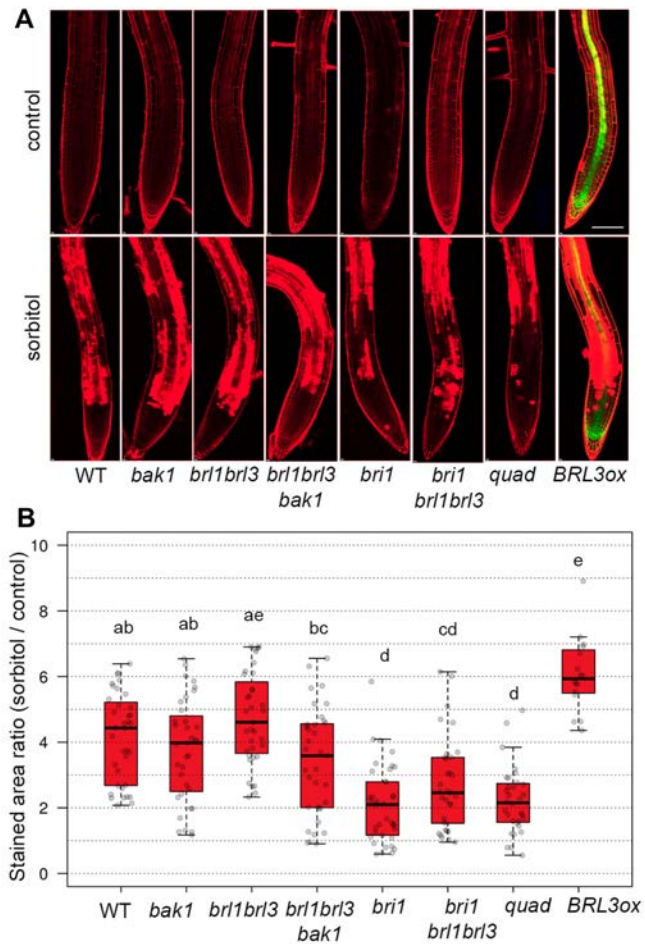


Figure 3.3: BR perception mutant roots are less sensitive to osmotic stress-induced PCD

(A) Four-day-old roots stained with PI after 24h in control (top) or sorbitol (bottom) media. Green channel shows the BRL3 localization (fused to GFP) and red channel show the cell wall and cell death staining by PI. Scale bar: 100 μm . (B) Quantification of cell death in sorbitol-treated root tips. Boxplots show the relative PI staining (sorbitol/control) for each genotype. Data from five independent replicates ($n > 31$). Different letters represent significant differences (p -values < 0.05) in an one-way ANOVA plus Tukey's post-hoc test.



Figure 3.4: BR perception mutant roots are less sensitive to hydrotropism

Root curvature (hydrotropic response) in 7-day-old roots after 24 h of sorbitol-induced osmotic stress (270 mM). The angle formed respect the vertical (considering the root before the media replacement) was measured. Scale bar: 0.2 cm.

We also explored the capacity of adaptation of BR receptor mutants in environments where the water is not equally distributed in the substrate. The adaptation of the plant root architecture to this kind of scenarios, which involves root bending towards zones with higher water content, is known as hydrotropism. Actually root hydrotropism represents a key feature for adaptation to environments scarce in water as it optimizes the root system growth (Iwata et al., 2013; Takahashi et al., 2002). We investigated the capacity of roots to escape imposed osmotic stress by replacing the bottom half of the plate with media containing 270 mM sorbitol and then quantifying the root angle formed respect the vertical after 24 h since media replacement (Takahashi et al., 2002) (Figure 3.4).

We found that BR receptor loss-of-function mutants have reduced hydrotropic responses compared to WT plants: Mutants roots grow straighter than WT roots towards sorbitol-containing media (Figure 3.5). This indicates that

hydrotropic responses in roots are, at least partially, dependent on BRs. Accordingly, the exogenous application of the BR synthesis inhibitor brassinazole (BRZ) (Asami et al., 2000) reverts almost the totality of the hydrotropic response in WT roots (Figure 3.6). Interestingly, the *brl1brl3bak1* mutants were the least sensitive to osmotic stress in terms of hydrotropism, showing lower root curvature angles than the *quad* roots (Figure 3.5). On the other hand, *BRL3ox* roots show an enhanced hydrotropic response in comparison to WT (Figure 3.5). To rule out if differences are due to a mechanical response because the media change rather than an actual hydrotropic response, we also replace the bottom half of the plate with control media (mock). No significant differences were found in such case, validating that the different root curvatures measured are actually differences in the root hydrotropic responses (Figure 3.7). Interestingly, the most extreme differences in hydrotropism angle are obtained either when the BRLs signalosome (Fàbregas et al., 2013) is completely disrupted or when the BRL3 receptor is overexpressed, specially in vascular tissues. Result suggest that this specific trait is mainly controlled by the BRL3 signalosome and from vascular tissues, unlinking it from BRI1, which would have its principal role in growth promotion. Importantly, better hydrotropic responses can modify root architecture for increased acquisition of water, favoring plant growth and survival under water-limited conditions (Iwata et al., 2013).

For better visualization of all traits analyzed, we generated and plotted a multi-traits matrix (Figure 3.8). We also included data from overall survival of BR mutants adult plants upon a drought period. This matrix highlights two different kind of responses:

1. The responses associated to BRI1 and/or dwarfism. These mutants clustered together at the right side of the matrix. They present decreased

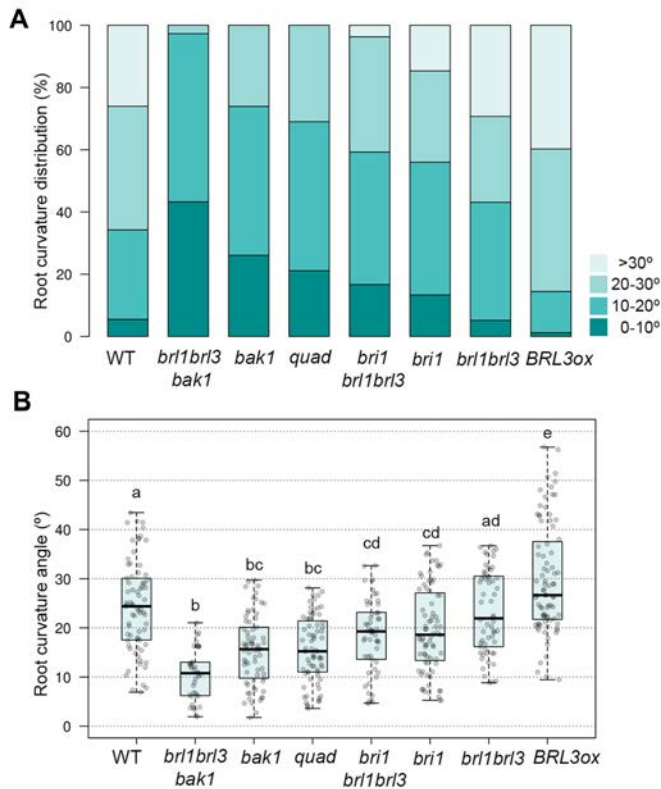


Figure 3.5: Overexpression of the BRL3 receptor promotes root hydrotropism

(A) Discrete distribution of root hydrotropic angles in the different genotypes after 24 h sorbitol treatment. Darkest green depicts root curved between 0° and 10°, and the lightest depicts roots with a curvature of more than 30°. (B) Boxplots representing the global angle distribution per genotype. Different letters indicate a significant difference (p -value < 0.05) in an one-way ANOVA plus Tukey's post-hoc test. Data from four independent replicates ($n > 50$).

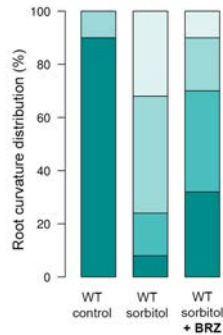


Figure 3.6: Brassinazole reverts the WT hydrotropic response

Distribution of root hydrotropic angles in wild type in control conditions (mock), sorbitol and sorbitol supplemented with the BR biosynthesis inhibitor brassinazole (BZR). The BZR application partially reverts the hydrotropic response observed with sorbitol alone, indicating that root hydrotropism is BR-dependent.

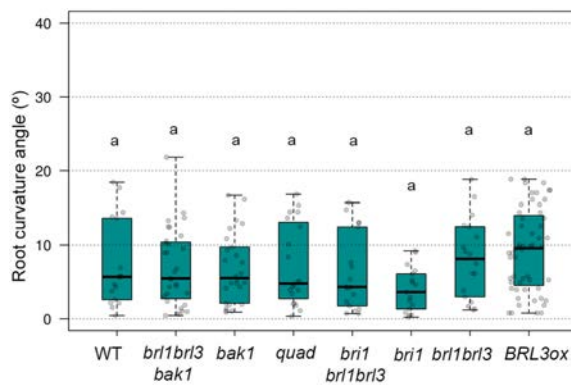


Figure 3.7: Differences in root curvature angles truly reflect differences in the hydrotropic response

Boxplots representing the global angle distribution per genotype when the bottom half of the is replaced with control media (mock). No significant differences (p -value <0.05) were found between genotypes in an one-way ANOVA plus Tukey's post-hoc test. ($n>35$).

root length, cell death and hydrotropism sensitivity but increased osmotic stress resistance.

- The responses associated to BRLs and/or vascular signalosomes. These clustered together with WT at the left side of the matrix. In the case of the mutants they present a WT-like response, except for hydrotropism. However in the case of the *BRL3ox*, it presents increased root length, cell death and hydrotropism response.

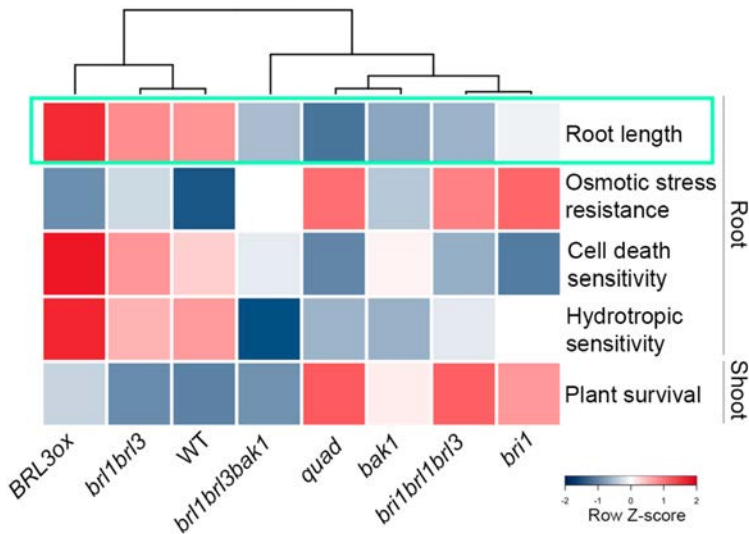


Figure 3.8: Stress multi-trait matrix

Stress trait matrix for all physiological assays performed on the roots and shoots of WT, BR loss-of-function mutants and *BRL3ox*. Root growth in control conditions is highlighted in green. Color bar depicts values for row-scaled data.

3.3 BRL3 overexpression confers drought resistance without penalizing growth

To further investigate if the impaired responses to abiotic stress observed in root seedling were preserved in mature plants, we next analyzed the phenotypes

of adult plants exposed to severe drought. After 12 days of withholding water, dramatic symptoms of drought stress were observed in WT, *brl1brl3* and *brl1brl3bak1* mutants. In contrast, other BR mutants showed a remarkable degree of drought resistance (Figure 3.9, middle column). To further confirm the survival rates after the drought period we examined the survival rates after re-watering for seven days (Figure 3.9, right column). In particular, *quad* mutant plants were the most resistant to the severe water-withholding regime, followed by *bak1*, *bri1*, *bri1brl1brl3* plants that had a significant increase in drought resistance respect WT. Interestingly *BRL3ox* plants also showed increased drought resistance compared to WT (Figure 3.9, rightmost bars), doubling the WT survival rates.

Because *bak1*, *bri1*, *bri1brl1brl3* and *quad* mutants exhibited different degrees of dwarfism (Figure 3.9, left column), drought resistance might be linked to growth retardation and decreased water necessities. In order to correct for the delayed growth, plants were submitted to a time course of drought stress in which relative water content (RWC), photosynthesis and transpiration parameters were monitored under similar soil water contents, even if this meant sampling at different timings (Figure 3.10). The WT plants took a total of 9 days to use 70% of the maximum water content that the soil can retain (field capacity). In comparison, BR loss-of-function mutant plants *bri1*, *bri1brl1brl3* and *quad* took 15 days, which indicates decreased water necessities of these plants. All subsequent measurements were done at the same soil water content for each genotype.

We found that the RWC in WT plants was reduced during drought, while RWC in BR mutant leaves remained as in well-watered conditions (Figure 3.11). This likely is consequence of the impaired growth, as these plants have very small water requirements in growth so they can conserve water during drought periods. Interestingly *BRL3ox* plants had increased RWC already in basal conditions, however the RWC decreases along the drought as in WT plants

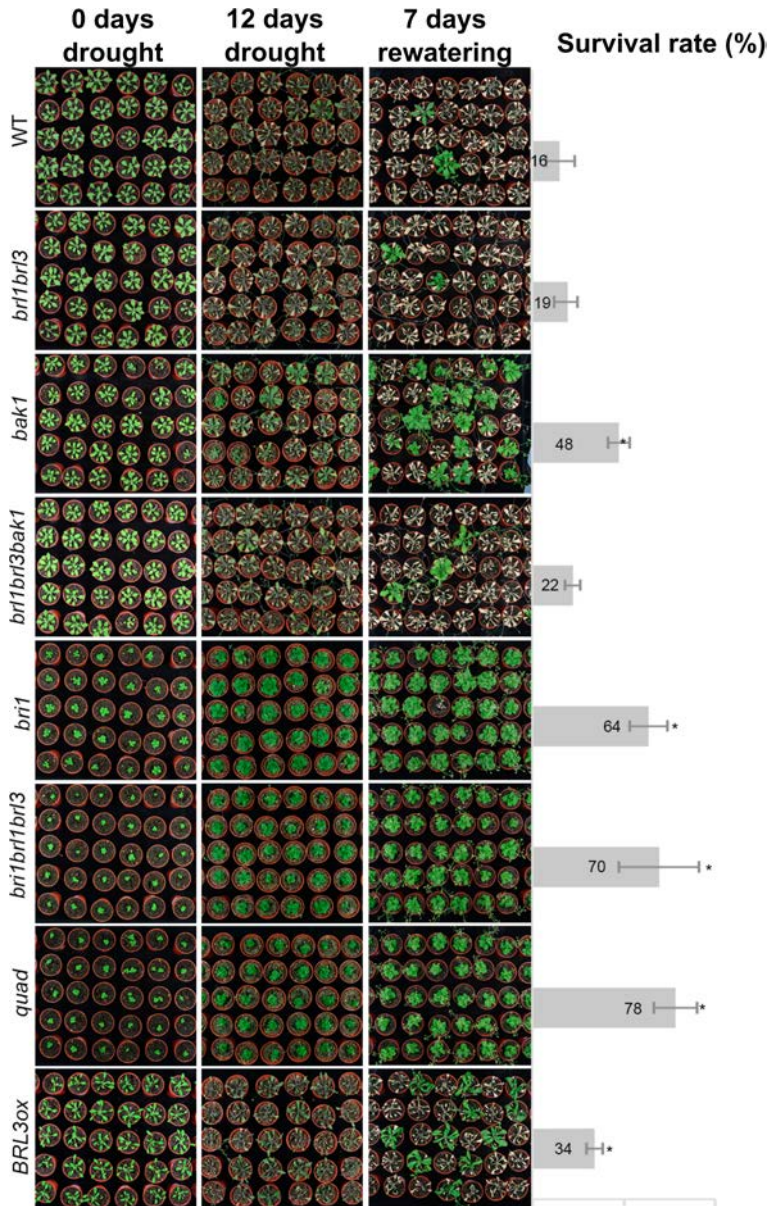


Figure 3.9: BRL3 overexpression confers drought tolerance

3-week-old plant rosettes phenotypes of WT, BR receptor mutants and *BRL3ox* grown in control conditions (left column), after 12 days of drought stress (middle column) and after 7 days of rewatering (right column). The bars at the left represent the survival rates quantified after 7 days of re-watering. Averages of five independent replicates \pm s.e.m. Asterisks indicate a significant difference (p -value < 0.05) in a χ^2 test for survival ratios compared to WT.

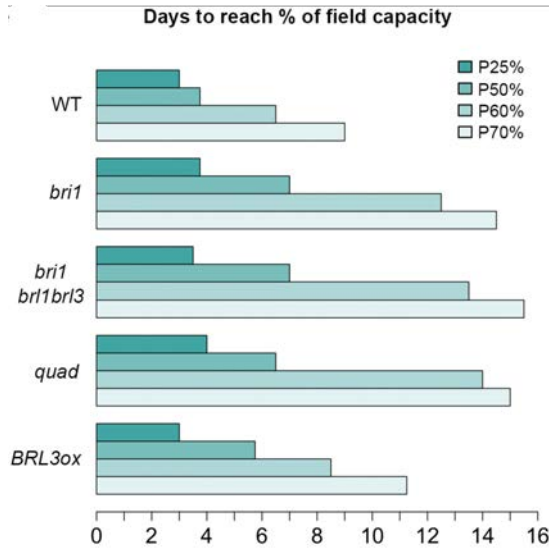


Figure 3.10: Days required to loose the same soil water content

The barplot shows the days needed to reach different percentages of soil water loss (from field capacity, P0%) for each genotype used in the study.

(Figure 3.11). In addition, compared to WT plants, BR mutants sustained higher levels of photosynthesis and transpiration during the drought period (Figure 3.12). The same trend was observed in *BRL3ox* plants, although the difference respect WT were only visible at early stages of drought (Figure 3.12). Interestingly the rate of photosynthesis was lower in *BRL3ox* than in WT at basal conditions but it showed softer decay than WT during drought (similar slopes than in BR mutants) (Figure 3.12 D).

Taken together our results indicate that the dwarf BR-receptors mutant plants are more resistant while consuming less water, likely through avoiding the effects of drought. These high survival rates observed are consequence of physiological effects and growth impairment and suppose a passive mechanism of protection against drought. Despite the small size of the BR receptor mutants, we consider that they still conserve potential for agriculture, especially in very arid contexts as long as they seed productivity was not very compromised.

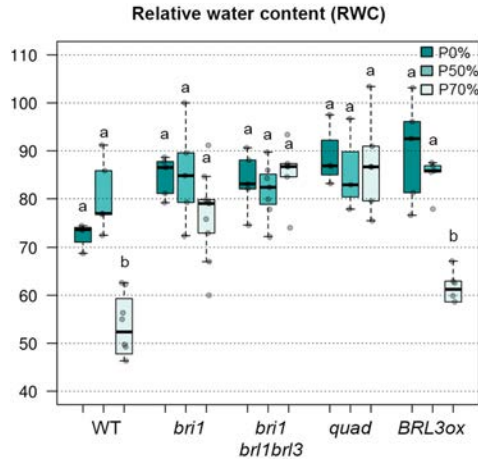


Figure 3.11: Relative water content of plants at comparable soil water contents

RWC of mature rosettes at 0% (field capacity), 50% and 70% soil water loss. Points within boxplots represent experimental observations (n=6). Different letters depict significant differences within each genotype in a one-way ANOVA plus Tukey's pos hoc test.

On the other hand *BRL3ox* plants are healthier than WT under the same water consumption conditions and do not show deleterious growth effects in terms of plant size, so results suggest that the BRL3 overexpression actively promotes drought tolerance. To better explain these two opposite resistance mechanisms we outlined a small model, where increased BR signaling supports active drought tolerance mechanisms that do not compromise growth whereas decreased BR signaling lead to impaired growth that as consequence, it permits the plants avoiding the drought (Figure 3.13).

3.4 BRL3 overexpressor plants accumulate osmoprotectant metabolites

Because several sugar transporter proteins were identified in the BRL3 signalosome (Fàbregas et al., 2013) and BRL3 has been linked already with

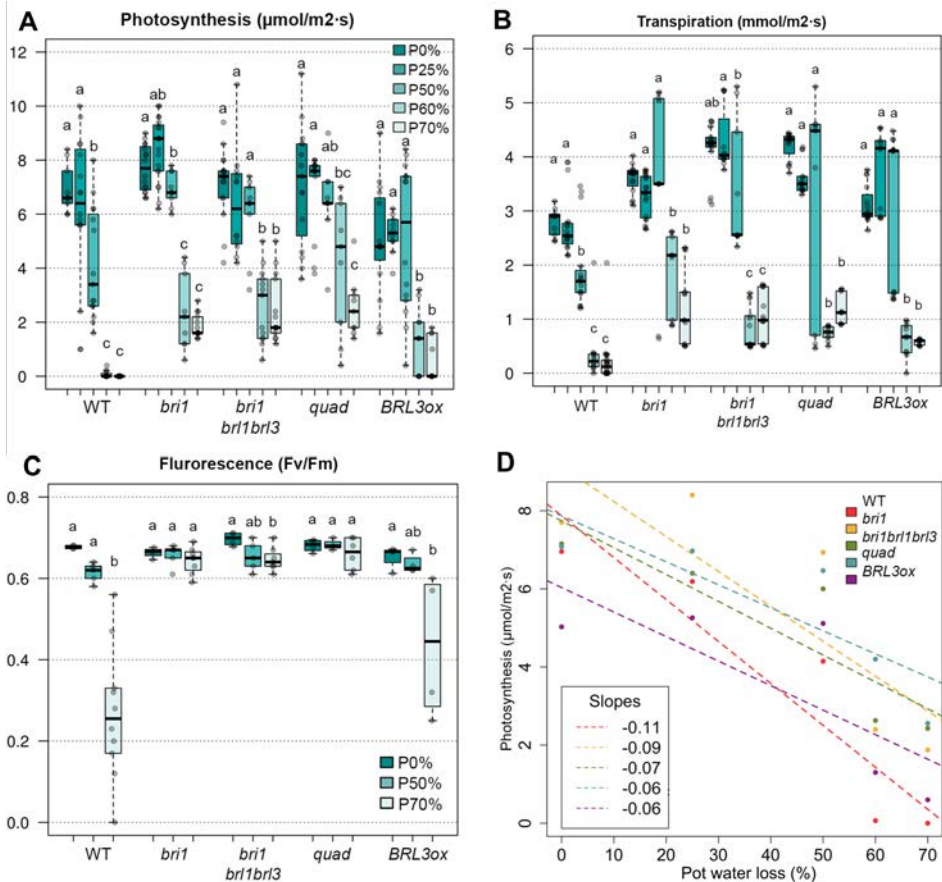


Figure 3.12: Physiological parameters of mature plants under comparable drought stress conditions

(A) Photosynthesis efficiency ($\mu\text{mol}/\text{m}^2\cdot\text{s}$) at different percentages of soil water loss. (B) Transpiration rates ($\text{mmol}/\text{m}^2\cdot\text{s}$) at different percentages of soil water loss. (C) Quantification of photosystem II (PSII) efficiency in mature rosettes at 0% (field capacity), 50% and 70% soil water loss. Points within boxplots represent experimental observations ($n=6$). Different letters depict significant differences within each genotype in a one-way ANOVA plus Tukey's pos hoc test. (D) Plot of photosynthesis efficiency versus soil water loss. It shows that the efficiency decays at different rates. Data was fitted to a lineal model and the slopes taken as indicators of drought-induced photosynthesis inhibition. Dots are the means for each genotype and dashed lines the fitted model.

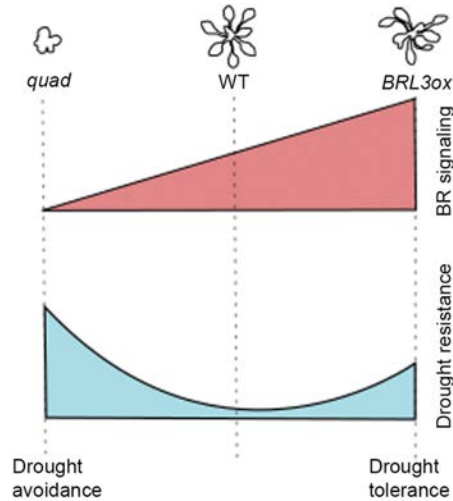


Figure 3.13: BR signaling, size and drought resistance balance

Schematic model representing BR signaling levels, adult plant size and drought resistance. Loss-of-function mutants passively avoid stress (drought avoidance), whereas plants with increased levels of BRL3 work actively to attenuate drought effects (drought tolerance).

glucose sensing (Tunc-Ozdemir and Jones, 2017), we wondered if the cause of the drought tolerance of *BRL3ox* plants might reside in the metabolism. To investigate this point, we performed a complete metabolite profiling of *BRL3ox* plants and compared it to the profile of WT and *quad* plants in a time course drought experiment spanning 6 days. Root were separated from shoots to address possible changes in metabolite accumulation from source to sink tissues. Complete metabolic fingerprints are deployed in Figure 3.14, Figure 3.15 and Figure 3.16.

Metabolite profiling of mature *BRL3ox* plants under control conditions (time 0) revealed an increment in the production of osmoprotectant metabolites. Both, shoots and roots of *BRL3ox* plants exhibited metabolic signatures enriched in proline and sugars (Figure 3.17). Proline has been extensively described to accumulate and protect plants during drought periods (Seki et al., 2007; Singh et al., 1972; Szabados and Savouré, 2010; Urano et al., 2009).

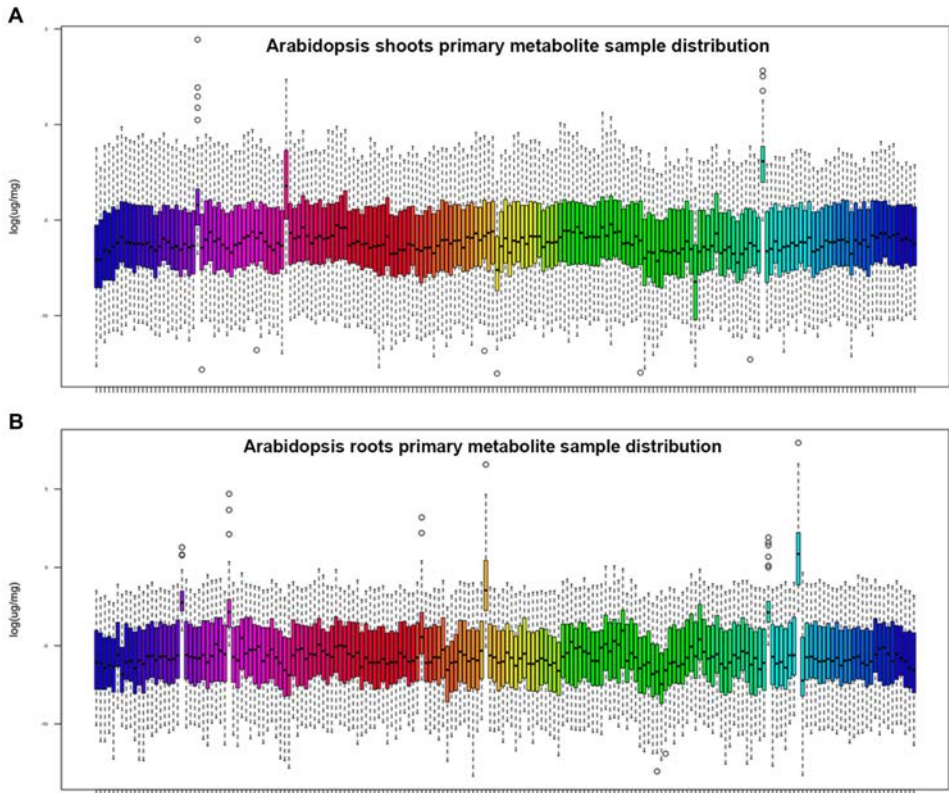


Figure 3.14: Distribution of metabolite levels per sample

Distribution of all quantified metabolites per sample. The complete set includes WT, *BRL3ox* and *quad* in shoots (A) and roots (B). Samples were collected daily during a drought time course of 6 days, including 5 biological replicates and watered controls (A total of 405 samples). Each boxplot represent a single sample. Data show a uniform distribution without normalization. Samples with the median value outside the average interquartile range were discarded.

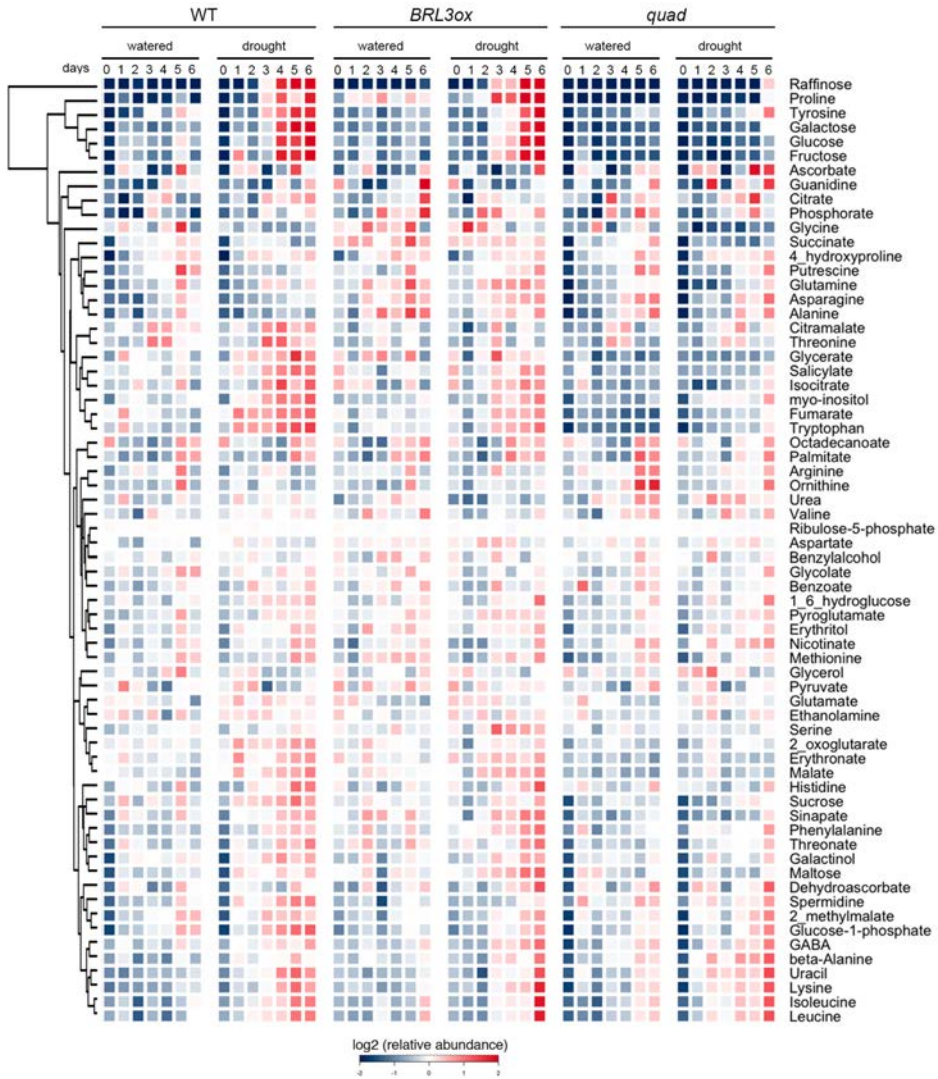


Figure 3.15: Metabolic fingerprint of WT, *BRL3ox* and *quad* shoots during drought time course

Heatmap represent the relative levels of shoot metabolites across all conditions tested. Color bar depicts row-scaled values for relative metabolite abundance.

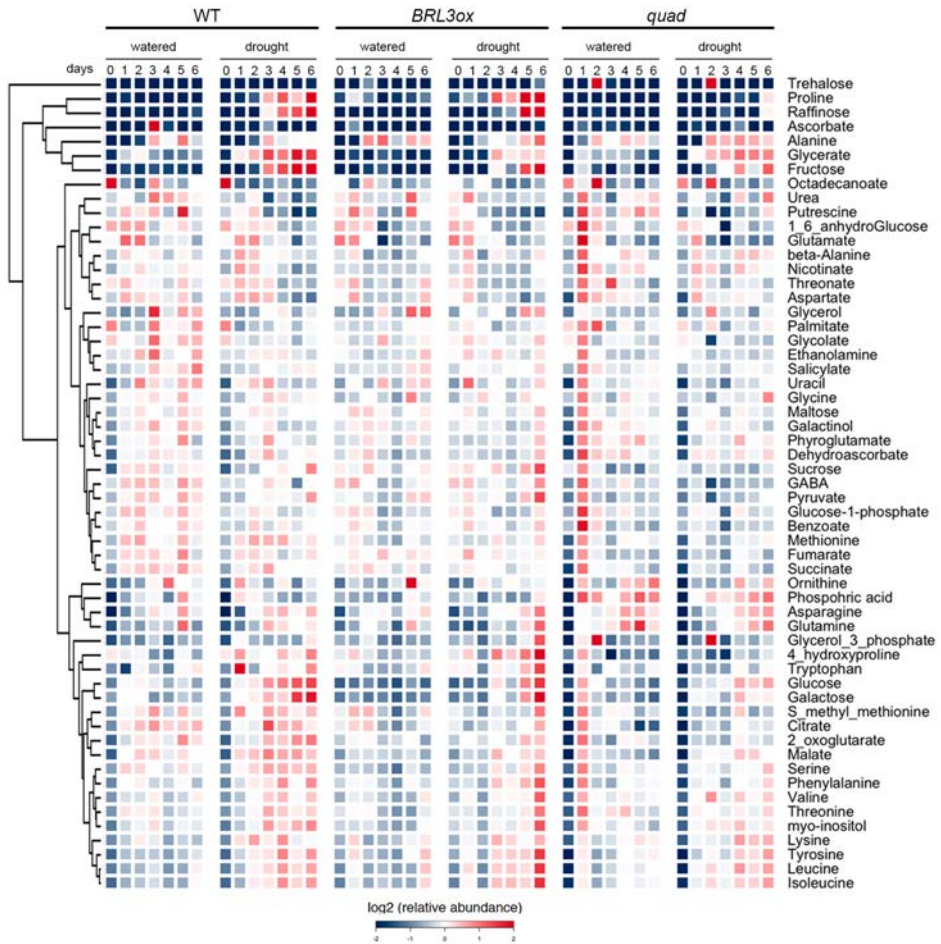


Figure 3.16: Metabolic fingerprint of WT, *BRL3ox* and *quad* roots during drought time course

Heatmap represent the relative levels of root metabolites across all conditions tested. Color bar depicts row-scaled values for relative metabolite abundance

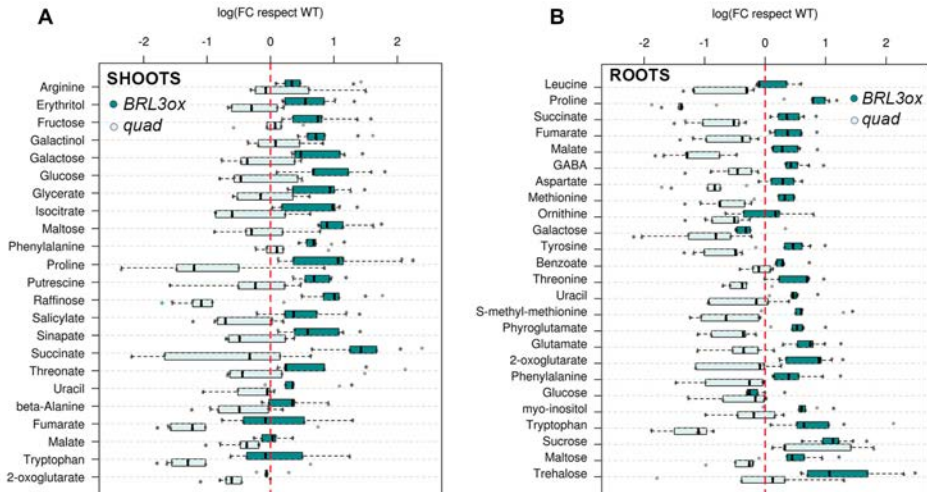


Figure 3.17: Differentially accumulated metabolites at basal conditions

Relative levels (respect WT mean) of differentially accumulated metabolites at basal conditions in *BRL3ox* (dark green) or *quad* (light green) shoots (A) and roots (B). Points in gray depict experimental observations ($n=5$). Asterisks denote statistical differences in a two-tailed t-test (p -value < 0.05) for raw data comparison *BRL3ox* vs. WT or *quad* vs. WT.

Similar observations have been made in the case of sugars (Durand et al., 2016; Seki et al., 2007; Urano et al., 2009). Especially, sugars like galactinol and raffinose, that belong to the Raffinose Family of Oligosaccharides (RFO), are known for their protective effects against stress (Nishizawa-Yokoi et al., 2008a; Seki et al., 2007; Urano et al., 2009). This result suggests that the BRL3 receptor promotes sugar accumulation of metabolites that alleviate the effects of drought, effect described as priming (Conrath et al., 2002). Importantly, the levels of these metabolites were lower in *quad* mutant plants (Figure 3.17). Compared to WT, sugars including fructose, glucose, galactinol, galactose, maltose and raffinose overaccumulated in the shoots of *BRL3ox* (Figure 3.17). Conversely, whereas glucose levels were lower in the roots, sucrose, trehalose, *myo*-inositol and maltose appeared to accumulate in roots (Figure 3.17) suggesting that the BRL3 pathway promotes sugar transport towards the roots.

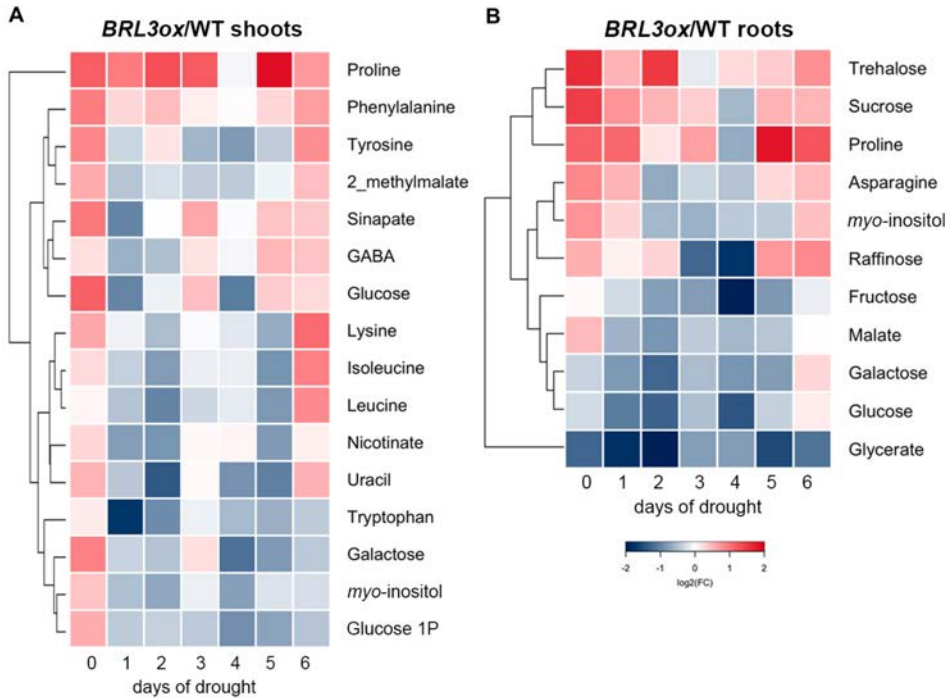


Figure 3.18: Metabolites following differential dynamics between *BRL3ox* and WT along the drought time course

Heatmaps represent the \log_2 of *BRL3ox*/WT averages ratio. A total of 16 metabolites follow differential dynamics in the shoot (A) and 11 in the roots (B). Dendrogram at the left of heatmaps represent the hierarchical clustering of the average metabolite profile.

Next we investigated the dynamics of each metabolite along the drought time course. Briefly, data for each genotype and metabolite was evaluated to find the best fit to a polynomial curve (maximum grade 3) function of time. The polynomial coefficients were compared, with WT coefficients as reference, in order to identify metabolites following different dynamics under drought (Conesa et al., 2006) (methods). In the time course, a total of 16 metabolites were identified to follow differential dynamics in the shoots of *BRL3ox* plants and 11 in the roots. A rapid accumulation of osmoprotectant metabolites was observed in both organs (Figure 3.18).

Then the dynamics of these metabolites were clustered. In the shoot of *BRL3ox*, glucose, *myo*-inositol and sinapate followed a linear increase along the drought time course but maintained decreased levels respect WT (Figure 3.19 A). In contrast, proline maintained higher levels along the entire drought time course and a steeper exponential increase in *BRL3ox* (Figure 3.19 B). The rest of differentially accumulated metabolites in the shoots grouped together in a cluster in which the average profile follow an exponential increase in *BRL3ox* while it was lineal in WT plants (Figure 3.19 C). In the roots, *BRL3ox* showed a rapid accumulation of osmoprotectant metabolites as trehalose, sucrose, proline and raffinose that followed a steeper exponential increase than in WT (Figure 3.19 D). Glycerate and malate kept lower levels in *BRL3ox* in all time course (Figure 3.19 E) while other osmoprotectant sugars followed a exponential dynamics in *BRL3ox* but lineal in WT (Figure 3.19 F).

Interestingly, throughout this time course the levels of these metabolites were lower in the *quad* mutants compared to WT (Figure 3.20). Altogether, these findings uncover a key role for BRL3 receptor in promoting sugar metabolism and support the idea that BRL3 triggers the accumulation of osmoprotectant metabolites to maintain growth during periods of drought.

3.5 Transcriptional control of metabolite production by BRL3

Because the prominent osmoprotectant metabolic signature in *BRL3ox* roots, we next investigated whether metabolic pathways are transcriptionally regulated in *BRL3ox* roots. The same material used for metabolite profiling was used for RNA sequencing, including root samples at control conditions (0 days drought) and after 5 days of drought, when metabolomic differences

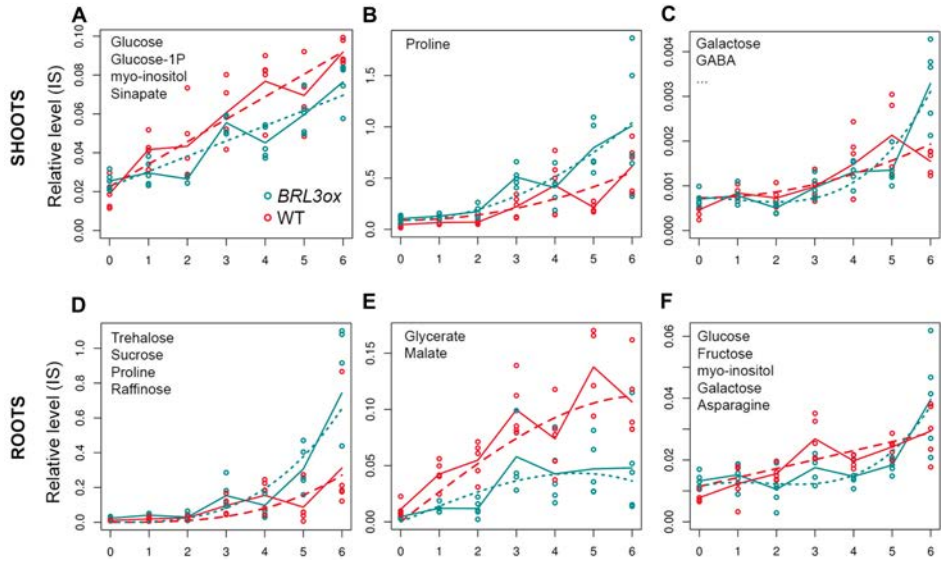


Figure 3.19: Clustering of the metabolite dynamics along the drought time course

(A-C) Metabolites following differential dynamics in BRL3ox shoots. (D-F) Metabolites following differential dynamics in BRL3ox roots. Metabolites falling in each cluster are annotated in the top left corner of the plots. Solid lines show the actual profile (average) of the representative metabolite of the cluster while dashed lines represent the polynomial curve that best fit with the profile.

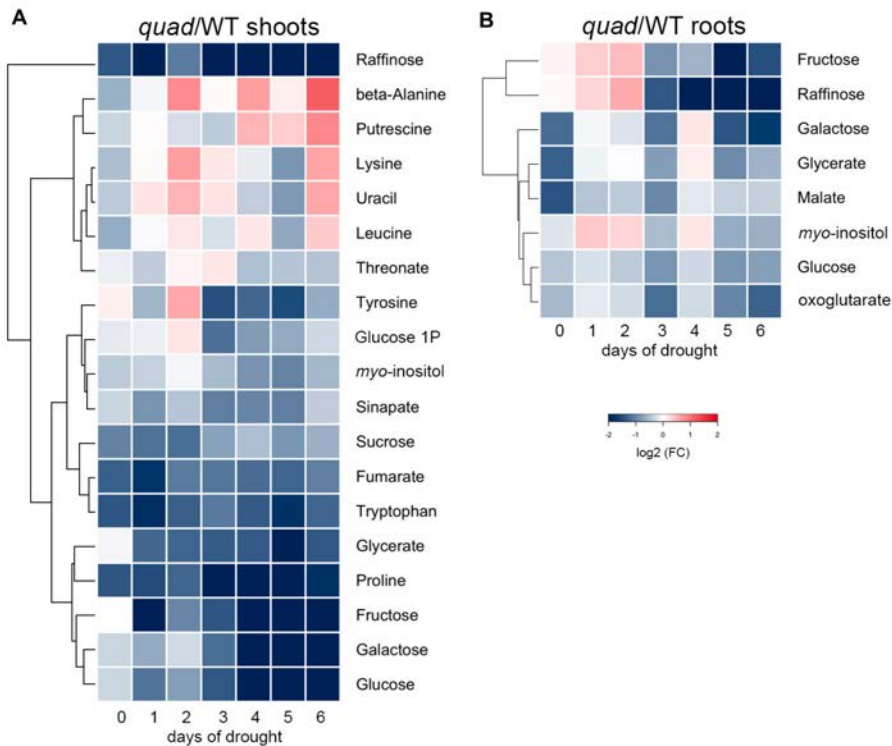


Figure 3.20: Metabolites following differential dynamics between *quad* and WT along the drought time course

Heatmaps represent the \log_2 of *quad*/WT averages ratio. A total of 19 metabolites follow differential dynamics in the shoot (A) and 9 in the roots (B). Note the general lack of metabolite accumulation in *quad* plants along the drought. Dendrogram at the left of heatmaps represent the hierarchical clustering of the average metabolite profile.

were clearly visible. RNAseq of *BRL3ox* roots revealed 759 differentially expressed genes at basal conditions (214 upregulated and 545 downregulated; $FC > 1.5$, $FDR < 0.05$) and 1068 differentially expressed genes in drought conditions (378 upregulated and 690 downregulated; $FC > 1.5$, $FDR < 0.05$). The Gene Ontology (GO) enrichment analysis of differentially expressed genes revealed a high proportion of the genes annotated in the response to water stress, response to oxygen-containing compounds and response to ABA categories, especially among upregulated genes in both, control conditions and under drought stress (Figure 3.21 A,B). In order to further investigate

the genes involved in stress response, we deployed the "Response to stress" category (GO:0006950) and classified the genes according their annotations in subcategories (Figure 3.22). We also intersect these genes with described list of high-confidence direct targets of the canonical transcription factors of the BR pathway, BES1 and BZR1 (Sun et al., 2010; Yu et al., 2011). Among differentially expressed stress genes, appeared classical drought stress markers, such as the Responsive to Dessication 22 (RD22) and Responsive to ABA 18 (RAB18), already upregulated in basal conditions (Figure 3.22). Interestingly, microarray analysis of *quad* adult plants submitted to 6 days drought period revealed a constitutive repression of response to stress categories in these plants (Figure 3.23).

Another prominent category in that appeared deregulated in *BRL3ox* RNAseq was response to hormone, indicating altered hormonal responses, mainly in *BRL3ox* plants under drought. Indeed responses to ABA and jasmonic acid (JA) stood out as the most affected (Figure 3.21). We also deployed genes annotated in "Response to hormone" (GO: 0009725) and classified them according subcategories (Figure 3.24). The ABA response genes was the widest category, with half of the genes upregulated at basal conditions, followed by JA response, which appeared almost totally repressed at basal conditions (Figure 3.24).

In order to further investigate the hormonal changes that might affects *BRL3ox* and *quad* plants we performed a complete hormonal analysis of the same shoot samples used for the metabolomic analysis, in control conditions and after 6 days of drought. According to what obtained in the GO analysis of differential expressed genes, ABA accumulated more in *BRL3ox* plants under drought whereas *quad* plants did not respond (Figure 3.25 A). Also in agreement with transcriptomics, JA levels were reduced in *BRL3ox* plants in basal conditions, whereas no differences with WT were found in drought. Repression of JA biosynthesis genes in *BRL3ox* is probably the cause of the JA decreased levels

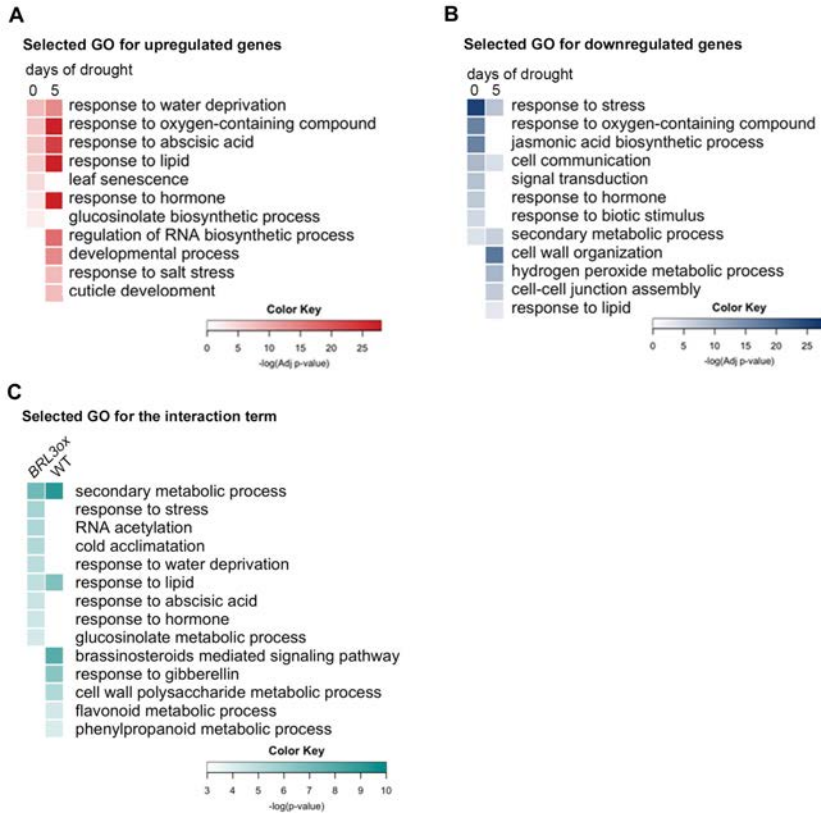


Figure 3.21: GO enrichment analysis of differentially expressed genes in *BRL3ox* roots

(A) Most representative enriched categories among the up-regulated genes in *BRL3ox* roots at basal conditions and after 5 days of drought stress. (B) Most representative enriched categories among the down-regulated genes in *BRL3ox* roots at basal conditions and after 5 days of drought stress. (C) GO categories enriched among genes affected by the interaction genotype-drought: Stronger activation in *BRL3ox* than WT upon drought or vice versa. Color bar: $-\log$ of the enrichment p-value (if denoted, adjusted by Benjamini-Hochberg method).

(Figure 3.24). The quad did not respond to drought, in agreement to the notion of their insensitivity (Figure 3.25 B). Another hormone with altered levels in *BRL3ox* was the cytokinin *trans*-Zeatin, that maintained higher levels in both, control and drought conditions (Figure 3.25 C). Other hormones did not show statistically significant changes, except for the increased levels of Salicylic acid (SA) in *BRL3ox* plants under drought (Figure 3.25 G). We also quantified the levels of the most active brassinosteroids, castasterone (CS) and

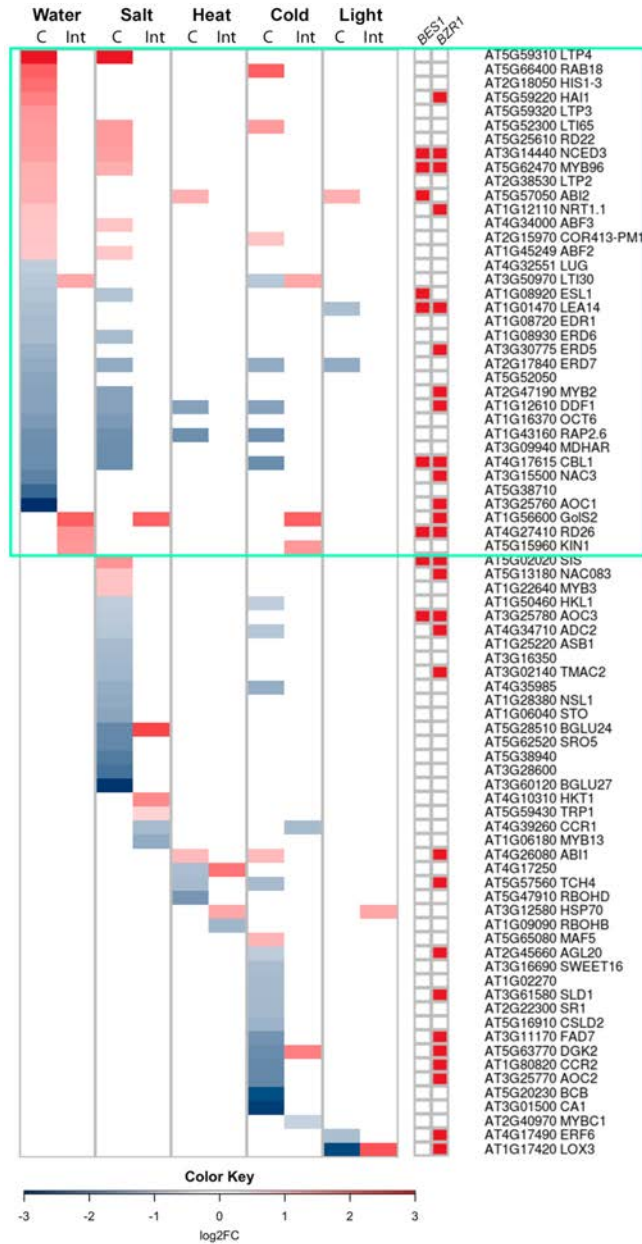


Figure 3.22: Response to stress genes differentially expressed in *BRL3ox* roots

Figure 3.22: Response to stress genes differentially expressed in *BRL3ox* roots

Deployment of genes within "Response to stress" (GO:0006950) term that are also annotated as responsive to water, salt, heat, cold and light stress. Colors in the heatmap represent the \log_2 fold change of *BRL3ox* vs. WT in control conditions (C) or the differential drought response ($\log_2(\text{FC drought}/\text{CTRL in } BRL3ox) - (\log_2(\text{FC drought}/\text{CTRL in WT}))$) if the gene is affected by the interaction genotype-drought. Red color in the squares on the right shows if a particular gene has previously identified as a direct target of BES1 or BZR1 transcription factors.

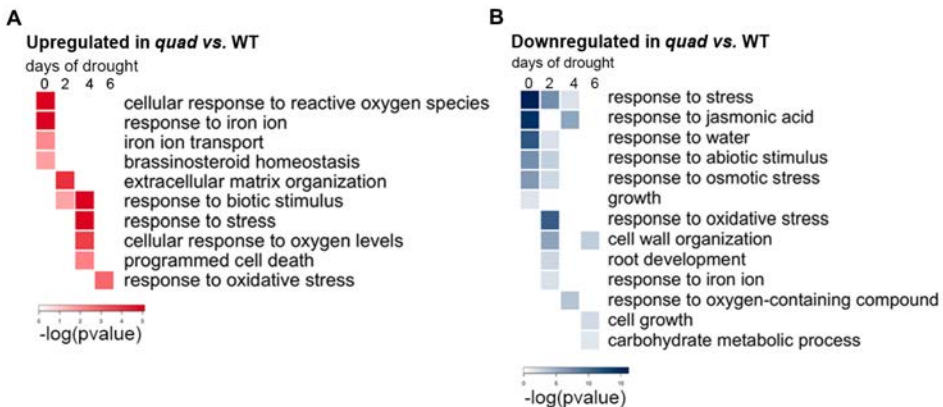


Figure 3.23: GO enrichment analysis of differentially expressed genes in *quad* plants along the drought time course

(A) Most representative enriched categories among the up-regulated genes in *quad* at 0, 2, 4 and 6 days of drought. (B) Most representative enriched categories among the down-regulated genes in *quad* at 0, 2, 4 and 6 days of drought. Color bar: $-\log$ of the enrichment p-value.

BL but unfortunately due to the high amount of material required (> 20g) we could only analyze one replica composed from a pool of plants grown separately, in either control or after 6-days of drought. Nevertheless results revealed an accumulation of CS in *quad* whereas *BRL3ox* showed decreased levels, both in control and drought conditions (Figure 3.25 H). In the case of BL, we could only detect the levels in *quad* plants, likely due to fairly high levels. Curiously the BL levels in *quad* increased during drought (Figure 3.25 I). These results are in agreement with what expected from plants with decreased (*quad*) or

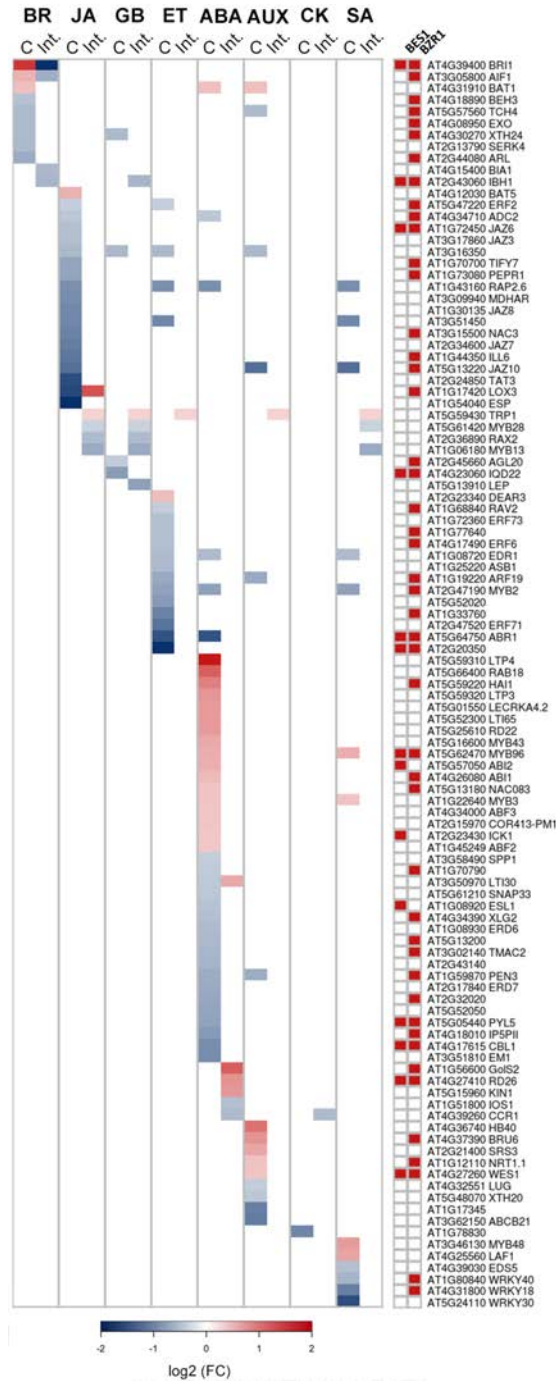


Figure 3.24: Response to hormone genes differentially expressed in *BRL3 α* roots

Figure 3.24: Response to hormone genes differentially expressed in *BRL3ox* roots

Deployment of genes within "Response to hormone" (GO:0009725) term that are also annotated as responsive to brassinosteroids (BR), jasmonic acid (JA), gibberellins (GB), ethylene (ET), abscisic acid (ABA), auxin (AUX), cytokinin (CK) or salicylic acid (SA). Colors in the heatmap represent the \log_2 fold change of *BRL3ox* vs. WT in control conditions (C) or the differential drought response ($\log_2(\text{FC drought}/\text{CTRL in } BRL3ox) - (\log_2(\text{FC drought}/\text{CTRL in WT}))$) if the gene is affected by the interaction genotype-drought. Red color in the squares on the right shows if a particular gene has previously identified as a direct target of BES1 or BZR1 transcription factors.

increased (*BRL3ox*) signaling levels.

We also monitored the expression levels of two key BR biosynthesis genes, Constitutive Photomorphogenic Dwarf (CPD) and DWARF4 (DWF4), along the drought time course in both root and shoots. Consistent with the hormone measurements, similar trend was observed in the transcript levels of *CPD* and *DWF4*. Transcript levels were increased levels in *quad* but reduced in *BRL3ox* compared to WT, however statistically significant levels were only obtained in shoots (Figure 3.26).

To specifically uncover the differences in transcriptional drought responses between WT and *BRL3ox* roots, we evaluated the RNAseq data with a linear model accounting for an interaction between the two factors tested in the experiment, genotype and drought (methods). Taking the 200 most significantly affected genes, we grouped them in (i) genes more activated in *BRL3ox* upon drought than in WT and (ii) genes more repressed in *BRL3ox* upon drought than in WT. GO-enrichment analysis of this genotype-drought interaction revealed secondary metabolism, response to stress and response to water deprivation in the first group and BR-mediated signaling pathway in the second group (Figure 3.21 C). The fact that *BRL3ox* plants showed decreased BR response upon drought respect WT is coherent with a constitutively

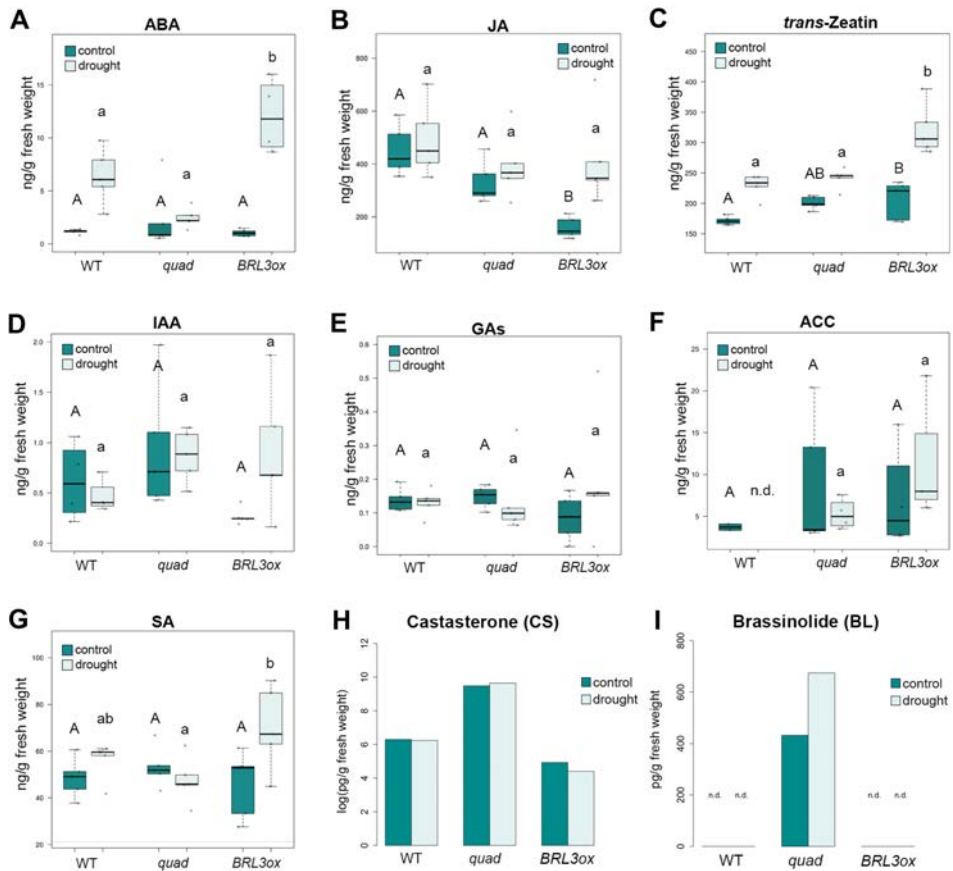


Figure 3.25: Hormone profiling on *BRL3ox* and *quad* shoots in control conditions and after 6 days drought

(A) Levels of abscisic acid (ABA). (B) Levels of jasmonic acid (JA). (C) Levels of the cytokinin *trans*-Zeatin. (D) Levels of the auxin indole-Acetic Acid (IAA). (E) Total levels of giberilic acids (GAs) in the plants. (F) Levels of 1-aminocyclopropane-1-carboxylic acid (ACC), a precursor of ethylene biosynthesis. (G) Levels of salicylic acid (SA). (A-G) Gray points are experimental observations (n=5). Different letters depict significant differences (p-value < 0.05) among genotypes in control (capital letters) or drought (lower-case letters) in a one-way ANOVA plus Tukey post-hoc test. (H,I) Hormone levels quantified from a pool of > 30 whole 28-days-old plants. n.d. means not detected.

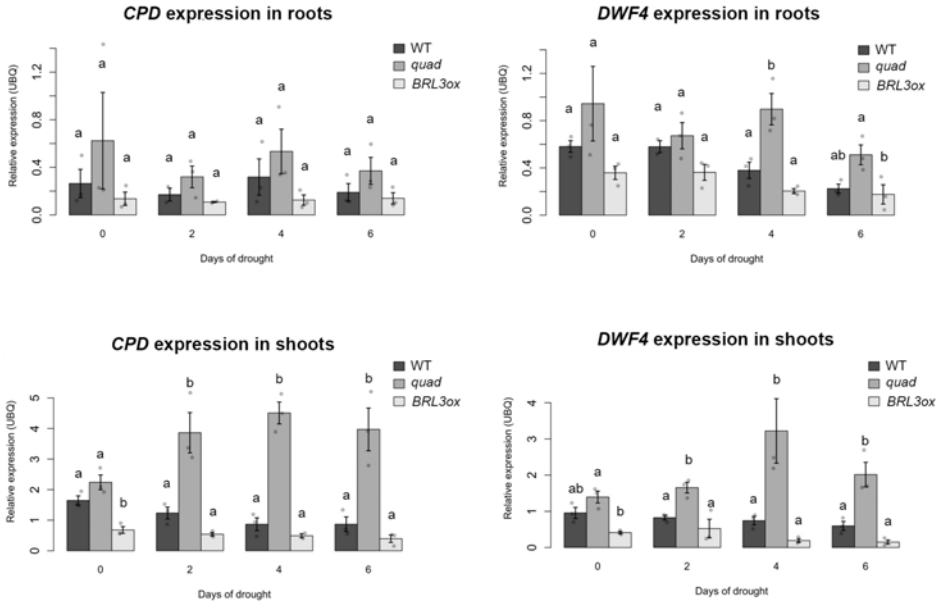


Figure 3.26: Transcript levels of two BR synthesis genes in *BRL3ox* and *quad* root and shoots during a 6 days drought time course

Transcript levels of *CPD* (left panels) and *DWF4* (right panels) in root (upper panels) and shoots (bottom panels). Barplots represent mean values \pm s.e.m. Gray points are experimental observations. Data from 3 independent biological replicates. Different letters man significant differences (p-value < 0.05) in one-way ANOVA test plus Tukey pos-thoc test.

activated BR signal due to BRL3. In agreement, these plants had reduced levels of CS and BL (Figure 3.25 H,I) and reduced expression of the biosynthesis genes CPD and DWF4 (Figure 3.26).

Given that the BRL3 is enriched in vascular tissues when overexpressed (Fàbregas et al., 2013), we aimed to further explore the spatial distribution of differentially expressed genes due to BRL3 overexpression and drought. For that, we used the Arabidopsis root spatiotemporal map as reference (Brady et al., 2007). We queried our deregulated genes set for enrichments in a particular root tissue, as tissue-specific gene lists were previously defined (Brady et al., 2007) (methods). Differentially expressed genes in basal conditions were enriched for genes that specifically express in vascular tissues. For the upregulated genes, enrichment was found in pericycle (J2261) and phloem pole pericycle (S17) but also in lateral root primordia (RM1000, which actually initiates from pericycle) and columella (PET111). In the case of the downregulated genes only enrichment in phloem pole pericycle was identified (S17) (Figure 3.27 A). Interestingly, the only tissue that had an over-representation of both upregulated and downregulated genes was the phloem pole pericycle, which is actually the native expression domain of BRL3 in vascular tissues (Fàbregas et al., 2013). Next we check for the any eventual tissue enrichment among the interaction-affected genes (genes behaving differentially between WT and *BRL3ox* in response to drought). Enrichment was found in the phloem companion cells (SUC2), pericycle (J2261) but also in root hairs (COBL9) and cortex (Figure 3.27 B).

We next deployed the *BRL3ox*-deregulated genes that are specific from pericycle (Figure 3.28 A) and phloem pole pericycle. Among the pericycle-enriched genes we found a Galactinol Synthase (GolS2) with an increased response to drought in *BRL3ox* compared to WT (Figure 3.28 A). And in the phloem enriched genes, we found two Trehalose-Phosphate Phosphatases (TPPs) that

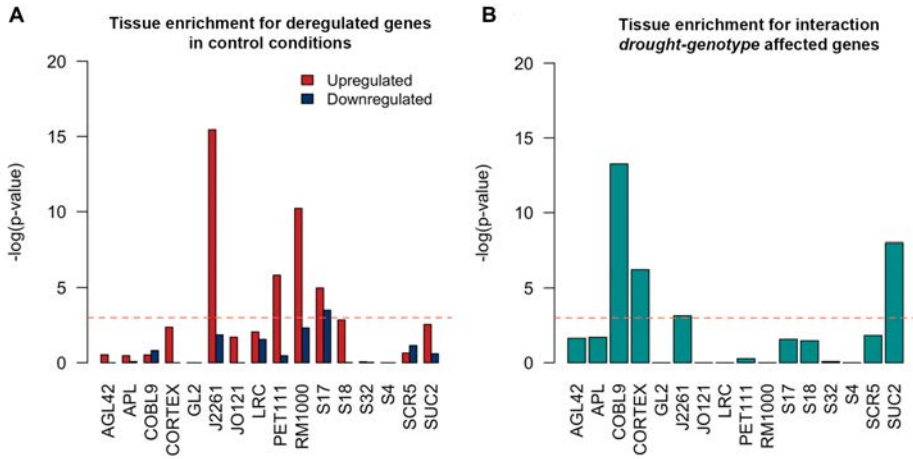


Figure 3.27: Deregulated genes in *BRL3ox* are enriched in root vascular tissues

(A) Arabidopsis root tissue enrichment for upregulated (red) or downregulated (blue) genes in control conditions. (B) Tissue enrichment for genes affected by the interaction genotype-drought. Bars trespassing the p-value threshold (0.05, dashed-red line) were considered enriched in the dataset. AGL42: Quiescent center, APL: Phloem + companion cells, COBL9: Root hair cells, CORTEX: Cortex, GL2: non-hair cells, J2261: Pericycle, JO121: Xylem pole pericycle, LRC: Laterac root cap, PET111: Columella, RM1000: Lateral root primordia, S17: Phloem pole pericycle, S18: Maturing xylem, S32: Protophloem, S4: Developing xylem, SCR5: Endodermis, SUC2: phloem companion cells. y-axis represent the negative logarithm of one-tailed Fisher's test.

show increased expression in *BRL3ox* roots at basal conditions along with a Beta-Glucosidase (BGLU24) and the Gols2 (Figure 3.28 B). These enzymes are directly involved in the synthesis of the osmoprotectant metabolites (trehalose, *myo*-inositol and raffinose) that overaccumulated in *BRL3ox* roots. Indeed these enzymes can provide drought tolerance when overexpressed or engineered (Ge et al., 2008; Himuro et al., 2014; Nuccio et al., 2015), precisely by increasing the pool of available osmoprotectants. Furthermore, apart from vascular-specific enzymes, other important enzymes for the metabolism of osmoprotectant were identified as deregulated. This is the case of a proline deshydrogenase gene, the early response to dehydration 5 (ERD5), which is involved in stress tolerance because it controls the proline degradation (Nanjo et al., 1999) and is strongly downregulated in *BRL3ox* plants (Figure 3.22).

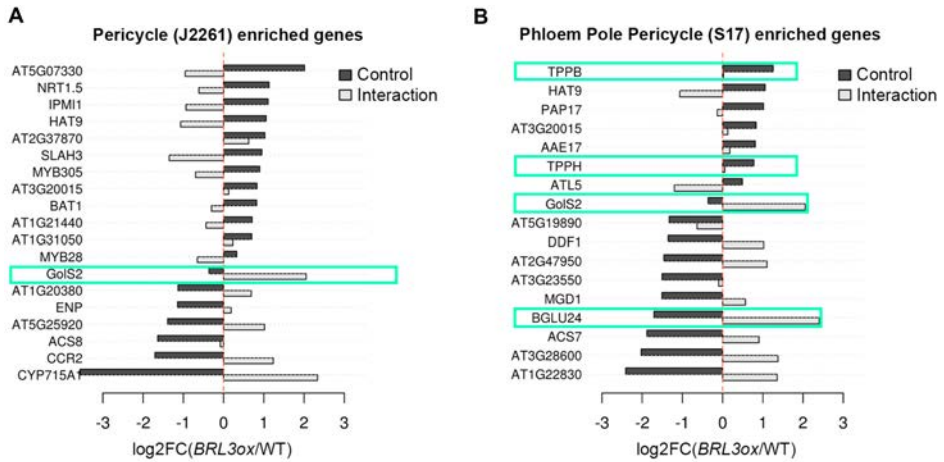


Figure 3.28: Pericycle and Phloem Pole Pericycle specific genes deregulated in *BRL3ox*

(A) Deregulated genes enriched in the pericycle (J2261 marker). (B). Deregulated genes enriched in the phloem pole pericycle (S17 marker). Bars represent the \log_2 -fold-change of *BRL3ox* vs. WT roots in control (black) or the difference of drought responses between *BRL3ox* and WT ($\log_2(\text{FC drought}/\text{CTRL in } BRL3ox) - (\log_2(\text{FC drought}/\text{CTRL in WT}))$) in the lineal model (gray). Enzymes involved in the metabolism of differentially accumulated metabolites are highlighted by greenish boxes.

Other non-vascular enzymes involved in sugar synthesis of transport include hexokinases, such as HXK3 and HKL1 (Figure 3.22) and the sucrose synthases SUS3 and SPS2F. Taken together, these results reveal the importance of change in expression of phloem-associated genes for sustaining metabolite production and drought resistance.

In order to identify potential regulators the drought response influenced by BRL3 overexpression, we isolated the transcription factors that were affected by the interaction genotype-drought in our lineal model. Analysis of transcription factors revealed 29 of them with differential responses to drought between *BRL3ox* and WT roots (Figure 3.29). We then plotted these TFs in a bidimensional space, where drought responses in WT and *BRL3ox* are in X and Y axis respectively. Genes falling near the diagonal are those not affected by the

interaction, whereas the further from the diagonal, the strongest is the influence of the interaction (in any direction). From these we also identify transcription factors that are specifically expressed in vascular tissues or in tissues where we found high enrichment in our differentially expressed genes (Brady et al., 2007) (Figure 3.29). As an example validating our approach, AGL12 has been already identified to have phloem-specific expression, to control root meristem cell proliferation and control QC division, processes in which BRs have a major role (Tapia-López et al., 2008). Strikingly, the drought-responsive transcription factor RD26 showed a strongly enhanced response in *BRL3ox* roots during stress (Figure 3.29). RD26 has been shown to antagonize the BR canonical transcription factor BES1 (Ye et al., 2017) and actually the gain-of-function *bes1-D* exhibits drought hypersensitivity (Ye et al., 2017). In light of these unexpected result, we propose that overexpression of the vascular may activate pathways that are independent from the canonical BRI1 pathway.

Finally we looked forward to link the transcriptomic changes observed in *BRL3ox* plants with its metabolomic profile. Statistical analysis revealed a significant link between the whole transcriptomic and metabolomic signatures, both in basal conditions and under drought (p-value = 0.017 and p-value = 0.001 respectively; see [methods](#)), suggesting that the metabolic signature of *BRL3ox* plants is transcriptionally controlled. We combined the metabolic and transcriptomic signatures to identify deregulated metabolic pathways, according to the annotations of the Kyoto Encyclopedia of Gene and Genomes (KEGG). For that purpose we used *Paintomics* software (Garcia-Alcalde et al., 2011). The analysis indicated a constitutive deregulation of sucrose metabolism in *BRL3ox* plants, deregulation that was enhanced during drought stress (Figure 3.30). Importantly we also found that BRL3 overexpression affects galactose metabolism under periods of drought. The galactose pathway includes the RFO synthesis pathway, which are recognized osmoprotectant metabolites (Figure 3.30) (Nishizawa-Yokoi et al., 2008a,b). Collectively, our

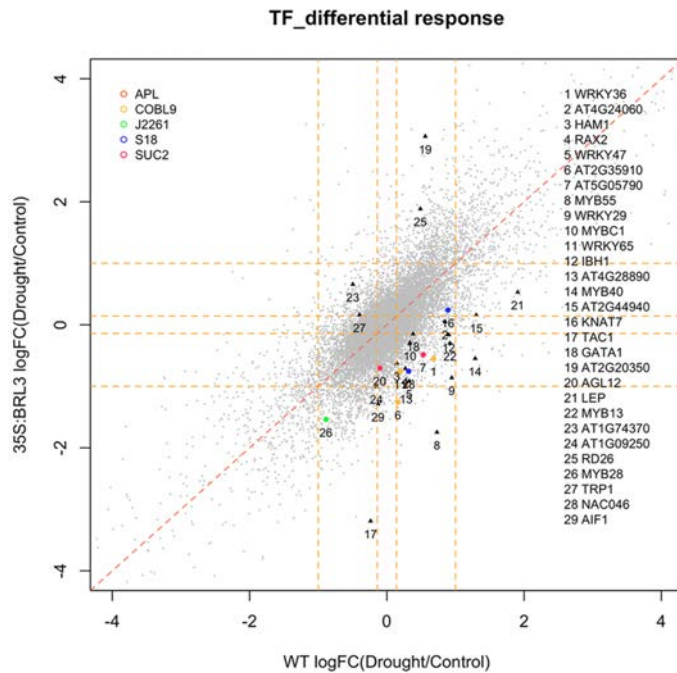


Figure 3.29: Transcription factors with a differential drought response between *BRL3ox* and WT

Transcription factors with a differential response to drought in *BRL3ox* and WT roots (lineal model accounting for interaction). Root tissue-specific transcription factors are denoted in colors: APL: Phloem and companion cells, COBL9: Root hair cells, J2261: Pericycle, S18: Maturing xylem, SUC2: Phloem companion cells. The further from the diagonal line, more differential response.

results suggest that BRL3 overexpression promotes drought tolerance, mainly by controlling sugar metabolism from vascular tissues.

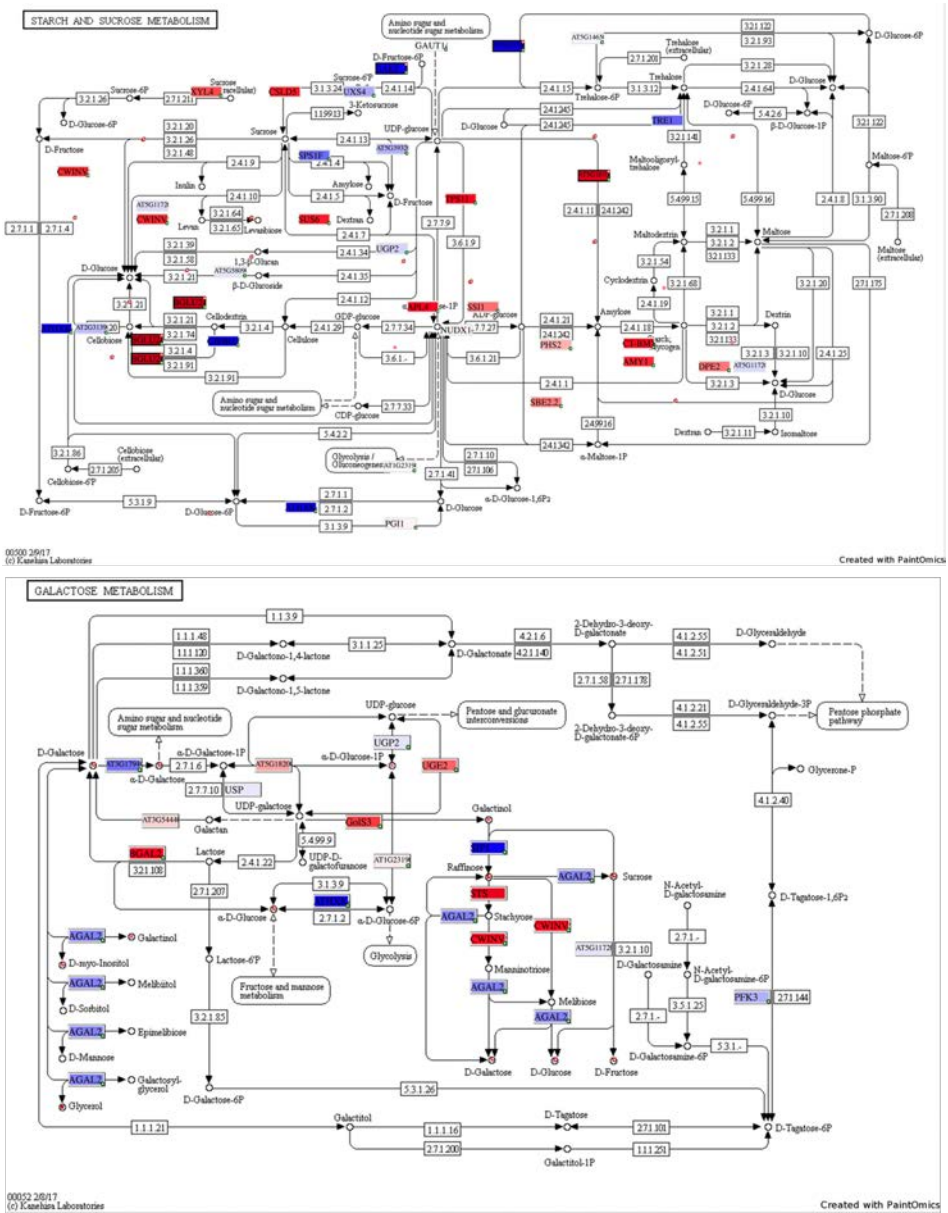


Figure 3.30: Deregulated metabolic pathways in *BRL3ox* under control conditions and drought

(Top) Starch and sucrose metabolism (KEGG ath00500). (Bottom) Galactose metabolism (KEGG ath00052). Deregulated genes in *BRL3ox* roots are depicted in colored boxes between metabolites, red for upregulated and blue for downregulated. The pathways with the deregulated enzymes colored were generated with *PainOmics*.

Chapter 4

TOTEM: A web Tool for Tissue-Enrichment analysis on gene lists

Part of this chapter will be published as:

TOTEM: A web tool for tissue-enrichment analysis on gene lists

Lozano-Elena, F., Vera, G. and Caño-Delgado, AI. (2019). Manuscript in preparation

TOTEM: A web Tool for Tissue-Enrichment analysis on gene lists

4.1 Introduction

The availability of massive gene expression data has boosted biological research. Currently it is common at some point to perform a high-throughput sequencing to find responses or effects derived from a particular model under study. More unbiased use of these expression profiling tools have yielded detailed expression maps at organ or tissue levels. These large datasets constitute valuable reference expression atlas that integrate spatial and/or temporal information of the organ or organism under study (Brady et al., 2007; Shinozaki et al., 2018; Zhang et al., 2004). The manipulation of such large datasets can be complicated, specially for non-experienced users. Indeed tools facilitating visualization of gene expression in a spatial context are available and widely used. Such is the case of the multipurpose tool *Genevestigator* or the *eFP* browser for Arabidopsis (Hruz et al., 2008; Winter et al., 2007). Although the available tools have their own strengths, regarding gene expression topology, these tools either lack high spatial resolution or only allow for single gene query or gene pair comparisons.

These limitations reduce their utility when users seek for high-resolution spatiotemporal information on a set of genes.

Specifically in our laboratory we have found very useful the comparison of gene lists (in our case derived from differential expression analysis) with the Arabidopsis root expression map (Brady et al., 2007). We routinely query our gene lists for any eventual enrichments in a defined set of tissue-specific genes, which recently have lead to the identification of vascular-specific genes involved in osmoprotectant production (Fàbregas et al., 2018) (chapter 3; Figure 3.26 and Figure 3.27).

With TOTEM (*Tool for Tissue-Enrichment analysis on gene lists*) we implement this approach in a simple and user-friendly web tool that do not require any previous programming or informatics skills and return easily interpretable representations and sorted gene lists. We have also followed a modular design on the reference datasets integration, so the incorporation of new or custom experiments is easy and does not require major code changes. TOTEM can be accessed in the following URL: <https://bioinformatics.cragenomica.es/totem>. The source code is deposited in <https://github.com/CRAGENOMICA/svg2-browser>¹ and can be freely accessed, reused and modified according the GNU-LGPL v2.1 license.

4.2 Basic usage and implementation

The development of TOTEM was motivated by the necessity of further exploiting published spatio-temporal expression datasets. The approach implemented in TOTEM resulted very fruitful for us in order to narrow down vascular-specific responses of Arabidopsis roots exposed to drought (chapter 3) (Fàbregas et al., 2018). TOTEM basically takes two inputs, with which it performs three basic operations. The inputs needed are (i) the selection of a reference experiment

¹The name of the repository will predictably be changed to **/totem*

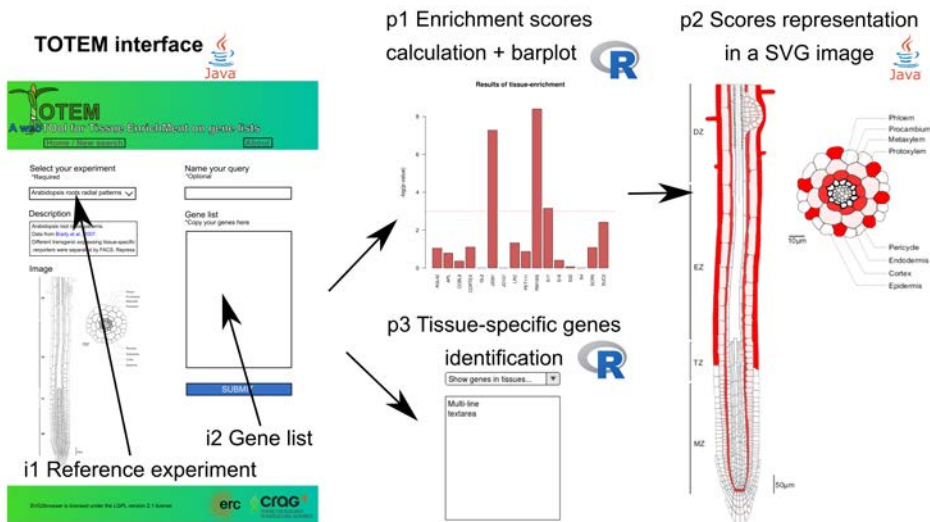


Figure 4.1: Summary of TOTEM workflow and its basic inputs, processes and outputs

First, in the home page, users choose the desired experiment as reference dataset by deploying the drop-down tab (i1). Its corresponding description and blank SVG image are prompted to the user. Then the users paste their genes in the text area (i2) and click submit. Upon submission the program calculate enrichment scores across tissues and represent them in form of barplot (p1). The returned p-values are then scaled and used to color the vectorial image of the organ/experiment selected (p2). Finally intersections are performed between user gene list (i2) and a list of tissue-enriched genes determined in the experiment (i1). The results are shown in a deployable box, in which each tab show which genes from the user input are specific of a particular tissue (p3).

and (ii) a gene list. The basic operations performed are: (i) The calculation of enrichment score per tissue and its representation as barplot; (ii) The representation of scaled enrichment scores over a organ/organism diagram and (iii) The classification of the introduced genes in tissue-specific genes. A summary of TOTEM workflow is presented in Figure 4.1.

TOTEM interface is written in JAVA, which allows an easy establishment of a web server. The function that represent scores over the organ diagram is also written in JAVA, partially based in the source code of a previous program from collaborators, SVGMap (Rafael-Palou et al., 2012). It maintains the same core function of translating numeric values into color intensities for the graph objects

of a Scalable Vector Graph (SVG) file. The rest of operations are performed in R, which is connected with TOTEM interface. We decided to use R because it is probably the most extended language among biologists and includes a large amount of statistical functions. Furthermore the connection with R allows to keep each dataset in a separate R-data file that is loaded into R when the experiment is selected by the user. Each Rdata include:

- A R *list* in which each entry is a vector (*tissue*) of genes specifically expressed in a single tissue.
- The gene universe of the experiment (expressed genes in RNAseq or probes in microarrays). It will serve as background for the enrichment function.
- An enrichment function that loops over the tissue list, calculating the enrichment value per tissue. It uses a Fisher's exact test and returns a vector with the (-)log-transformed p-value per tissue.
- A custom function for each experiment that represents the enrichment values in a barplot.
- A custom function for each experiment that fix any eventual incompatibility with the representation of the values (i.e. tissues that overlaps in the SVG file)
- A function that intersects the user's gene list with the tissue-specific genes of a selected tissue. It also identifies which genes of the input are either not found in the gene universe or not enriched in any tissue.

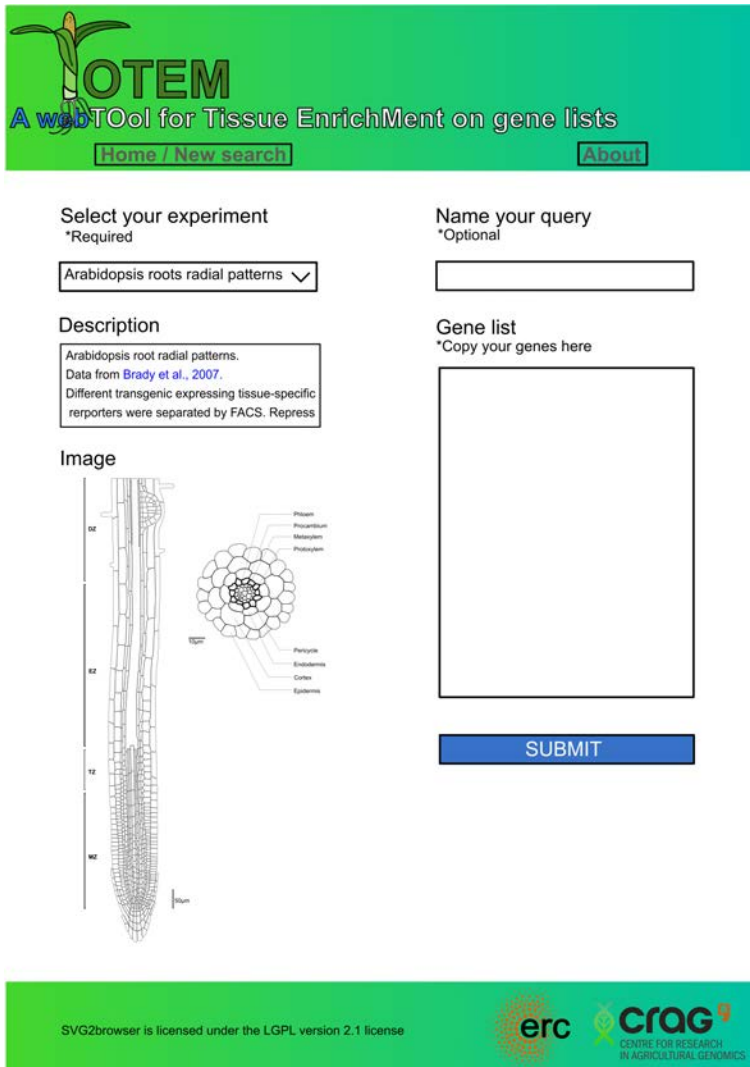
Because it is first needed to define which genes are tissue-specific, we prefer when possible, to respect the criteria of the authors that generated the dataset. If no tissue-specific genes are defined in the publication, as default approach, we consider a gene as tissue-specific when its normalized expression value in a tissue is over the 175% of the mean expression across all tissues. All the information about the experiment and the criteria followed to define a gene as

tissue-specific is prompted to the user in a description text box at the home page, once the experiment is selected. Furthermore for experiments involving more than 100 different zones or tissues, a multiple testing correction by the Benjamini-Hochberg procedure is applied to the enrichment p-values. The home page of TOTEM is composed by a drop-down tab where the available experiments are listed, a description box where experiment information is displayed once the experiment is selected, a text field where users can paste their genes of interest, a preview of the uncolored SVG for the selected experiment and a “submit” button (Figure 4.2).

When the data is submitted, TOTEM connects with R in the backend and calculate the enrichment scores. Then the results page is shown with the colored SVG together with a barplot depicting the actual enrichment scores. Also a drop-down tab allow users to explore which genes of their list are specifically expressed in a particular tissue. The colored SVG and barplot images can be redrawn in another color if desired and downloaded in PNG format (Figure 4.3).

Nevertheless, the generated SVG image is merely a visual representation and it may not depict all tissues examined in the experiment. The barplot is the representation which contains the actual enrichment scores for all tissues of the experiment. Additionally it should be considered that the threshold taken for defining a tissue as enriched is an arbitrary decision (as default when p-value < 0.05) and some tissues may pass the threshold just because random sampling (Figure 4.4). Therefore users may want to be more stringent or leaky with their threshold depending on their purposes. The only purpose of TOTEM is to facilitate the comparison with published spatio-temporal expression data and our criteria to define tissue-enriched genes may not satisfy all necessities. Thus, conclusions should be drawn at the risk of the users.

Finally, TOTEM has been designed with a modular structure, so new experiments (reference datasets) can be easily added without major code changes. New experiments can be included by adding a separate folder containing:



TOTEM
A webTOol for Tissue EnrichMent on gene lists

[Home / New search](#) [About](#)

Select your experiment
*Required

Arabidopsis roots radial patterns ▾

Description

Arabidopsis root radial patterns.
Data from Brady et al., 2007.
Different transgenic expressing tissue-specific reporters were separated by FACS. Repr

Image

Diagram illustrating the radial patterns of an Arabidopsis root, showing various tissue layers: Pteridium, Procambium, Metaxylem, Phloylem, Pterocyte, Endodermis, Cortex, and Epidermis.

Name your query
*Optional

Gene list
*Copy your genes here

SUBMIT

SVG2browser is licensed under the LGPL version 2.1 license

erc CRAG
CENTRE FOR RESEARCH
IN AGRICULTURAL GENOMICS

Figure 4.2: TOTEM homepage

The home page is composed by a drop-down tab where the experiment is chosen, a description box and the blank SVG of the experiment and a text field where the users can copy/paste their genes of interest.

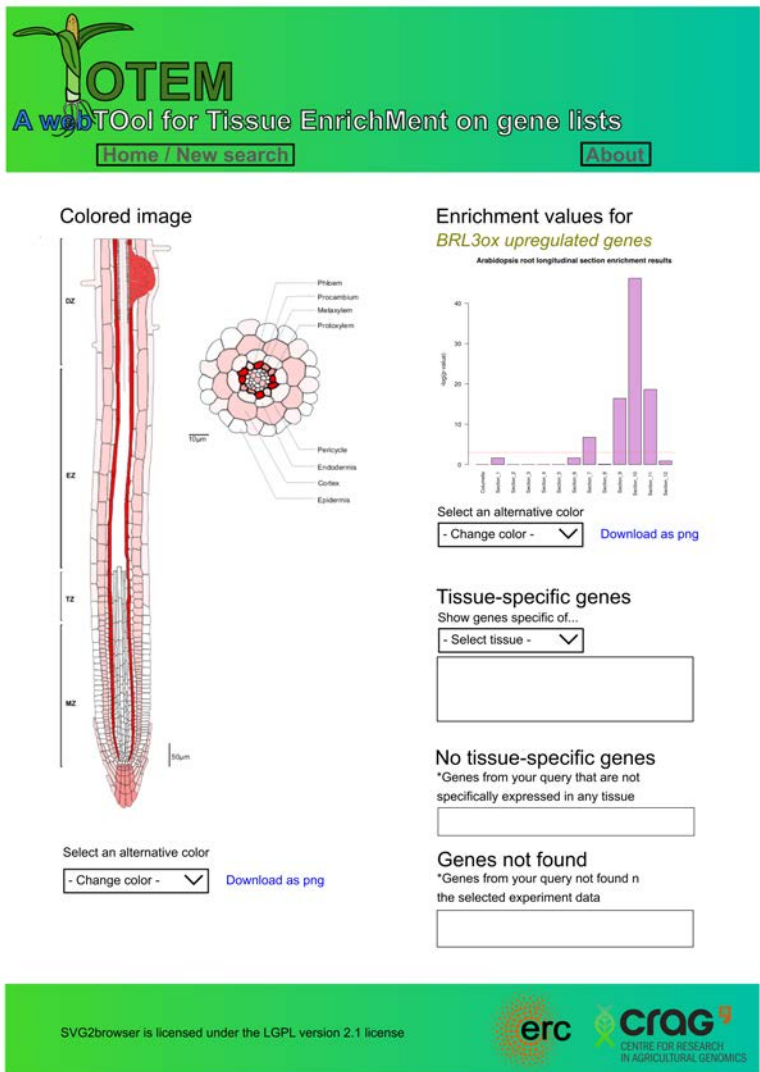


Figure 4.3: TOTEM result page

In the results page, the colored SVG is displayed along with the barplot with the actual enrichment scores and a drop-down tab in which the users genes are classified in tissues.

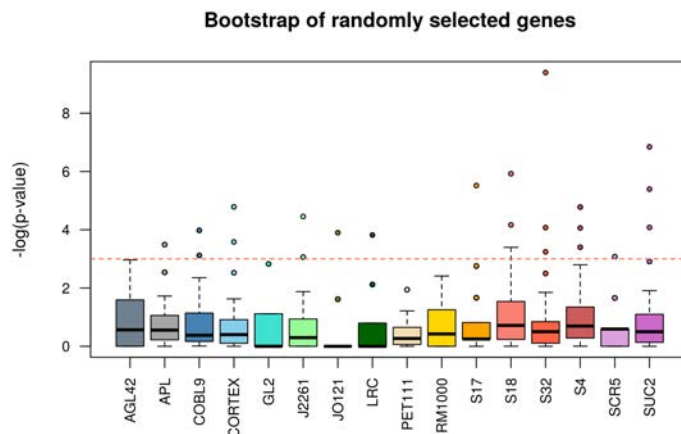


Figure 4.4: Enrichment values upon random sampling

To ensure that the enrichment function is returning significant results, we compared the enrichment values of upregulated genes in *BRL3ox* roots (Figure 3.27 A) with random sampling of the same number of genes among the gene universe. The enrichment function was run 100 times and results plotted in form of boxplot. Most of the enrichment values distributed between 0 and 1, but some observations are over the threshold ($-\log(\text{p-value}) > 3$), as it would be expected just by chance at that threshold. Colors of the boxplots are examples of available colors for the SVG and barplot.

- A SVG drawing with assigned IDs (i.e. tissue names)
- A Rdata file including the functions mentioned above
- A configuration text file with the experiment descriptions and file names

4.3 Tissue-enrichment analysis of deregulated genes in *BRL3ox* roots

In the current version of TOTEM we have added so far the spatio-temporal Arabidopsis root map from Brady et al. (2007) and the developmental map of tomato fruits from (Shinozaki et al., 2018). But in the case of Arabidopsis, we have split the data set in three. One including the radial dataset, that correspond to specific tissue markers that were separated by Fluorescence-Activated Cell Sorting (FACS). The second set is the longitudinal dataset that correspond

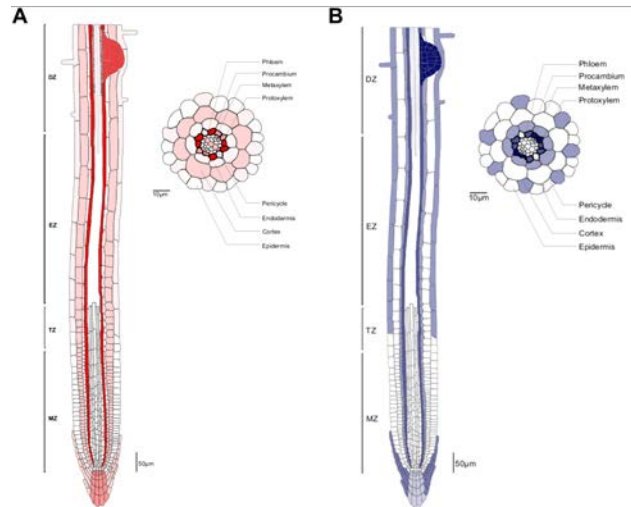


Figure 4.5: Arabidopsis root radial patterns of deregulated genes in *BRL3ox* at basal conditions

(A) Image generated by TOTEM with the upregulated genes in *BRL3ox* as input. (B) Image generated by TOTEM with the downregulated genes in *BRL3ox* as input. Enrichment values used for coloring the SVG file are the same than represented in Figure 3.27 A. Note that because visualization purposes, the color scale is relative, it adjusts the maximum value to the maximum enrichment score

to sections of the Arabidopsis root that correlate with developmental stages. And the third one is the combined (intersected) data of radial and longitudinal sets. We used these custom-defined datasets to narrow down to *BRL3ox* deregulated genes acting in very specific root zones. When our deregulated genes were queried against the Arabidopsis radial pattern we obtained a clear enrichment in pericycle, as described in Figure 3.27. Accordingly, when the *BRL3ox* upregulated genes (in basal conditions) are queried, the colored SVG images depict the highest color intensity in pericycle and lateral root primordia tissues (Figure 4.5 A). Among the downregulated genes, there was an enrichment in pericycle, lateral root primordia and phloem pole pericycle (Figure 4.5 B).

We also applied the same gene lists (deregulated in *BRL3ox* root at basal conditions) to the Arabidopsis longitudinal dataset, in order to situate transcriptional changes in the root developmental time line. Upregulated genes were enriched mostly in genes that are specific of mature tissues but there was also a marginal enrichment in the elongation zone and QC-surroundings (Figure 4.6 A). The downregulated genes were mainly enriched in genes specific of recently matured tissues (Figure 4.6 B). Along with the colored SVG images, TOTEM return lists of tissue-specific genes from the user's input (expandable tab in the results page). We checked which upregulated genes are specific from QC and stem cell niche sections and we obtained three unknown genes: AT1G23040, AT3G11600 and AT5G06330, the later one being a LEA protein, family that is involved in osmotic stress responses.

To further identify specific root zones affected by the *BRL3* overexpression, we intersected the radial and longitudinal datasets (Brady et al., 2007), creating a matrix of 208 possible "tissues". We queried the *BRL3ox* deregulated genes for enrichment in tissue-specific genes. Results revealed that among our upregulated genes there was an enrichment of genes specific of mature phloem tissues (Figure 4.7 A,C). Among downregulated genes, there clearly was an enrichment in genes specific of lateral root primordia (obviously this is only possible in root mature tissues) (Figure 4.7 B,D). If we deploy which genes are upregulated by *BRL3ox* and are phloem-specific, interestingly we get Centroradialis (ATC; AT2G27550), Early Flowering-Like protein 4 (ELF4; AT2G40080) and an unknown protein, AT3G10910.

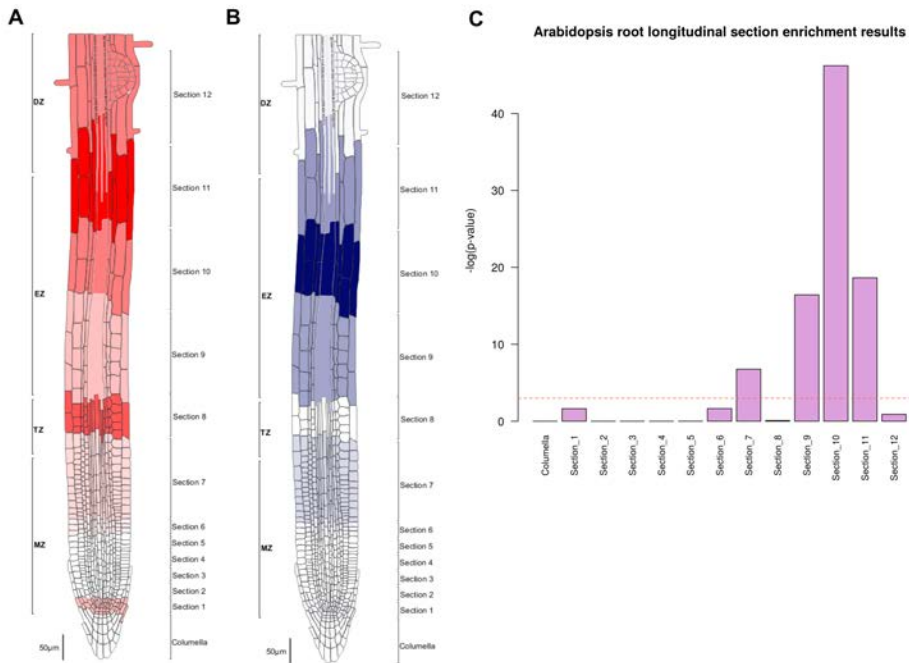


Figure 4.6: Arabidopsis root longitudinal patterns of deregulated genes in *BRL3ox* at basal conditions

(A) Image generated by TOTEM with the upregulated genes in *BRL3ox* as input. (B) Image generated by TOTEM with the downregulated genes in *BRL3ox* as input. Note that because visualization purposes, the color scale is relative, it adjusts the maximum value to the maximum enrichment score. (C) Actual enrichment values.

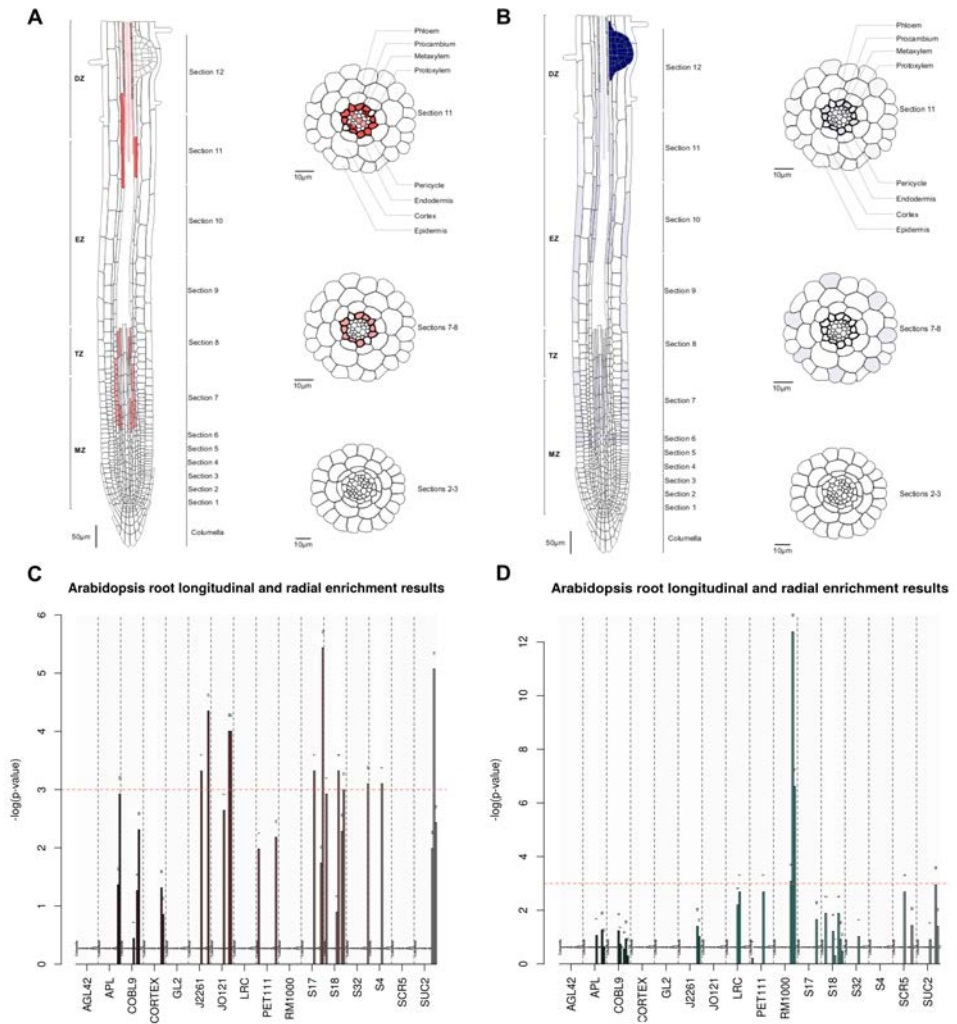


Figure 4.7: Intersection of Arabidopsis root radial and longitudinal patterns of deregulated genes in *BRL3ox* at basal conditions

(A) Image generated by TOTEM with the upregulated genes in *BRL3ox* as input. (B) Image generated by TOTEM with the downregulated genes in *BRL3ox* as input. Note that because visualization purposes, the color scale is relative and it adjusts the maximum value to the maximum enrichment score. (C, D) Barplot with actual enrichment scores.

4.4 Tissue-enrichment analysis of BR-regulated drought stress genes in maturing tomato fruits

In order to exemplify the use of TOTEM in another plant specie, we used a list of selected drought stress genes that correlated with developmental effects in tomato (*Solanum Lycopersicum*) (Lee et al., 2018). This study compares the Micro-Tom (MT) cultivar against the WT tomato. The MT cultivar is a dwarf tomato variety that carries a mutation in the BR biosynthesis gene DWF4 and it has been shown to be BR-defective (Marti et al., 2006). Using the provided 57 drought stress genes (Lee et al., 2018), we checked if there was any enrichment in specific tomato fruit tissues. We found that the only tissue overrepresented among these genes was the tomato fruit columella at early stages of fruit maturation (Figure 4.8), which is in coherence with the BR role in development.

4.5 Future perspectives

In the first version of TOTEM we included Arabidopsis roots and tomato fruits spatio-temporal gene expression datasets (Brady et al., 2007; Shinozaki et al., 2018), but we plan to progressively include many more experiments. Potentially any transcriptomic study that can be used to define region or phase-specific genes could be incorporated. The major current limitation could be found perhaps in the lack of high-resolution and coherent experiments, such as the Arabidopsis roots (Brady et al., 2007), in other crops. Although any experiment can be potentially included even if it refers to a specific study on an specific process. For this very same reason, we largely depend on the community to receive proposals and pre-drawn SVGs. In our particular case we are already working to include a sorghum expression dataset on specific tissues (Davidson

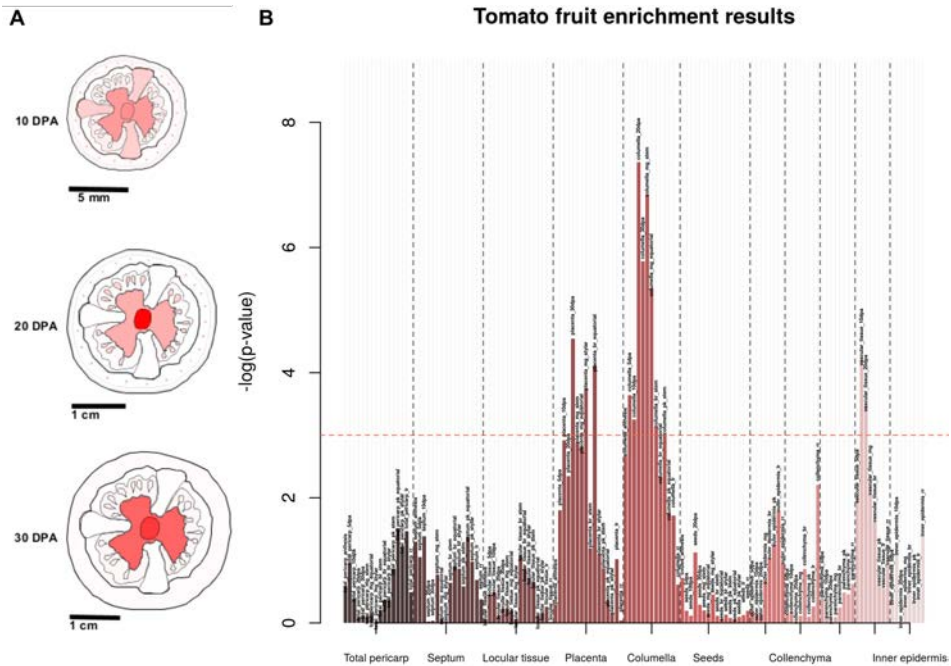


Figure 4.8: Tomato fruit enrichment pattern of drought stress genes deregulated in Micro-Tome cultivar

(A) Image generated by TOTEM with deregulated drought stress genes (Lee et al., 2018). Note that because visualization purposes, the color scale is relative and it adjusts the maximum value to the maximum enrichment score. (B) Barplot for the actual enrichment scores. Each chunk (separated by gray vertical dashed lines) represent a tissue, and the successive bars within the chunk are the tomato fruit ripening stages.

et al., 2012). In addition, the recent implementation of single-cell sequencing to *Arabidopsis* roots have yielded gene expression maps with unprecedented resolution (Denyer et al., 2019; Ryu et al., 2019; Shulse et al., 2019). However TOTEM focuses at tissue level and such resolution is useless if it is not possible to robustly reconstruct clusters and associate them with tissues at better resolution than what provided by FACS. Future integration of these datasets would pass through the reconstruction of a robust co-expression network and implementing a selectable threshold, in which the user decides the limits to consider a set of genes as tissue-specific.

Future versions of TOTEM could be improved in several aspects. Important points that we already identified and that will probably be implemented in coming versions are:

- Include functional annotations of genes (returned by the finder function as tissue-specific). These annotations could be implemented by including the complete annotation file into the R-data files or by including an hyperlink to a database harboring this information.
- Implementing GO enrichment analysis tools within TOTEM. Either using the same input used for the tissue-enrichment analysis or using the genes identified as tissue-specific by the finder function.
- Implementation of different algorithms for creating the color scale for the SVG. For example avoid the coloring of a tissue if its p-value is below a threshold or do not set the maximum of the color scale to highest value if this is a clear out-lier.
- Implement a function in which the user can set the threshold (astringency) used for defining a gene as tissue-specific within the dataset.

Chapter 5

Computational modeling of BRL3 interactors

Work described in this chapter in collaboration with:

Prof. Baldo Oliva, from Structural Biology department of University Pompeu Fabra, Barcelona.

Computational modeling of BRL3 interactors

5.1 Introduction

Computational biology is an emerging field in biology that greatly boosts and supports experimental efforts in basic research. Data generation in laboratories has ceased to be the bottleneck in regards to knowledge production. Rather, data mining, comprehensive annotation and massive data processing stand out as current challenges. Accordingly, more and more attention is being given to this field, which together with the constantly increasing computing power and more efficient algorithms are already yielding very fruitful results.

Within the computational biology, structural bioinformatics combines statistics and computation to predict, analyze and model protein structures without the necessity of crystallographic experiments. The processing of already available structural data in a massive way has brought an unforeseen insight of specific cellular processes ([Samish et al., 2015](#)). The great impact of the structural approach can be seen, for example, in cancer research ([Valls-Comamala et al., 2017](#)), however it remains largely unexploited in agriculture despite its huge

potential.

The aminoacid sequence determines the tertiary structure of a protein; that is its 3D structure. Due to physical constraints introduced by the residues' chemical properties, proteins do not fold randomly and proteins with similar sequences adopt similar structures (Sander and Schneider, 1991). Modeling algorithms use this principle to predict the 3D structures of proteins based on sequence alignments. For example Modeller¹, a widely used modeling program, looks for the most probable structure through optimally satisfying spatial restraints derived from the alignment with a known structure (Šali and Blundell, 1993). The determination of a protein structure based on another protein with known structure is, obviously, very dependent on the alignment similarity scores. Additionally it is also extremely dependent on the alignment length (Rost, 1999). These two parameters define a zone where the sequence alignment unambiguously identifies protein pairs with similar structures (long alignments with a pairwise identity >40%). For alignments identities between 20-30% there is a huge increment of false negatives when trying to identify sequences with similar structures. This zone of uncertainty has been denominated twilight zone (Rost, 1999). Below the minimum identity of the twilight zone or for very short alignments, it is nearly impossible to determine with confidence the structure of a protein based on an alignment with a known structure. This is called the midnight zone (Rost, 1999).

Over the years, structural studies have been yielding increasing amounts of resolved protein structures. These structures are collected and made available to everyone in large databases such as the Protein Data Bank (PDB) (Burley et al., 2019). Such abundance of known protein structures extends the capability of predicting the structure to potentially any protein of any organism, just by sequence comparison. And these structures not only include single proteins

¹<https://salilab.org/modeller/>

or small ligands bound to a single protein but also protein complexes. This last point allows the application of modeling approaches on protein complexes (mostly protein pairs), by performing alignments over both chains of the same crystal and then modeling the overall structure. Resolved structures of protein pairs also allowed the optimization of docking algorithms and scoring functions, improving the accuracy of the predictions of the final conformation for an interaction (Cockell et al., 2007; Pierce and Weng, 2007). Additionally, information from other databases can be included on top of the structural information provided by the crystal in order to improve the modeling accuracy of protein loops, which are normally the catalytically active (and flexible) zones of the protein but the less structurally conserved stretches in the sequence (Bonet et al., 2014).

Structural studies on BR signaling (i.e. crystallography of BRI1 receptor) have revealed the detailed mechanisms of BR ligand perception and signaling and have rationalized all previous knowledge derived from genetic and biochemical approaches (Bojar et al., 2014; Hothorn et al., 2011; She et al., 2011). Not only BRI1 receptor has been crystallized alone itself but also in complex with BL as ligand and its co-receptor BAK1 (Sun et al., 2013a), revealing that the BL-BRI1 complex acts as docking platform for the BAK1 binding (Figure 5.1). Further studies provided the structural evidence for the BRI1 ability to interact with other SERKs, as SERK1 (Santiago et al., 2013) and revealed that BAK1 (along with other SERKs) can also serve as co-receptor for other LRR-RLKs with radically different functions (Hohmann et al., 2018b; Sun et al., 2013b). The BRI1 kinase domain has been crystallized as well, alone (Bojar et al., 2014) and in complex with the BKI1 domain involved in its inhibition (Jaillais et al., 2011; Wang et al., 2014) (Figure 5.2).

In Fàbregas et al. (2013), the BRL3 signalosome was elucidated. It revealed several interactors closely related with drought, apart from the classical components of the BR pathways, such as BSKs. More recently we have

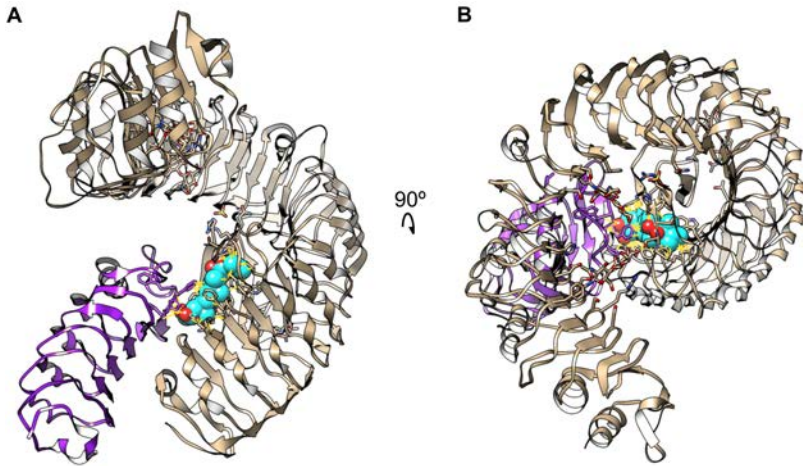


Figure 5.1: Crystal structure of the complex BRI1-BAK1 (extracellular parts) with BL bound

(A) Side view of the crystal structure of BRI1-BAK1 complex at the extracellular part with BL (PDB: 4M7E; Sun et al. (2013a)). The extracellular part of the BRI1 receptor is depicted in gold, BAK1 extracellular part is colored in purple and BL is represented as spheres in cyan. Contacts between BL and either BRI1 or BAK1 are represented as yellow lines. (B) Top view of the same crystal, upon a 90° rotation in the x-axis.

demonstrated that the BRL3 overexpression, preferentially in root vascular tissues, yielded drought resistant plants without an impaired growth. We also showed an unprecedented impact of a plant steroid receptor in the plant transcription and metabolic status, which is already “drought-activated” in basal conditions (Fàbregas et al., 2018) (chapter 3). Nevertheless, attributing this protective effect to BRL3 itself is a rather naive idea, especially because it is extremely similar to BRI1. Instead, we hypothesize that an important part of the drought-protective effects rely on a combination of spatial specificity and cross-signaling with membrane partners (interactors). Indeed, the cross-signaling is emerging as a new paradigm for fast and robust plant responses in front of external stimuli, phenomena that specifically involves membrane kinases (Ahmed et al., 2018; Smakowska-Luzan et al., 2018).

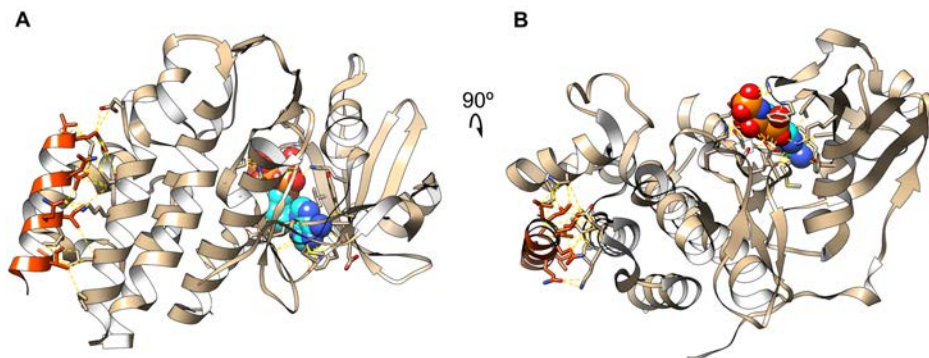


Figure 5.2: Crystal structure of the kinase domain of BRI1 in complex with BKI1 and with ATP bound

(A) Side view of the crystal structure of BRI1-BAK1 complex at the extracellular part with BL (PDB: 4OH4; Wang et al. (2014)). The kinase domain BRI1 is depicted in gold. The BKI1 peptide involved in BR signaling inhibition is colored in orange. ATP bound to the kinase is represented as spheres (carbon atoms in cyan and phosphorous in orange). Contacts between BRI1 kinase and either ATP or BKI1 are represented as yellow lines. (B) Top view of the same crystal, upon a 90° rotation in the x-axis.

In this chapter we apply a structural bioinformatics approach to explore the relevance of the components identified in the BRL3 signalosome (Fàbregas et al., 2013). We generated a large set of protein-protein interaction (PPI) models for high-confidence interactors of BRL3. We also included the resolved signalosomes of BRI1 and BRL1 receptor (Fàbregas, 2013), following a high-throughput homology-based modeling pipeline. After the generation of the models, the global affinities per interaction were calculated and the different models for the same PPI were ranked. The different interactors for the same BR receptor were compared. Interestingly we found that BAK1 is not the favorite co-receptor for BRL3 in terms of interaction affinity, and that some intracellular kinases have higher affinities for the kinase domains of BR receptors than the classical BR-pathway components. Future experimental validation of these computational predictions will be crucial in order to uncouple the pathways of the vascular-specific BR receptors, BRL1 and BRL3, from BRI1.

5.2 High-throughput modeling of protein-protein interactions with BR-receptors

In order to computationally analyze the PPI of the BR receptors with identified proteins in the signalosomes (Fàbregas, 2013; Fàbregas et al., 2013), we tried to model every interaction pair following a high-throughput approach. We used as input all proteins identified in the Co-Immuno Precipitation (CoIP) experiments that had a fold-change in IP/background > 100 (Fàbregas et al., 2013). Interacting pairs (BR receptor and interactor) were split and its sequences queried for significant alignments in the PDB (only structures involving PPIs) and the domain-domain structural database 3DiD (Mosca et al., 2014). Pair alignments not reaching a threshold in homology and alignment length were removed out and the interaction considered as impossible to model with confidence (See [methods](#)). For hits above the threshold, these structures were used as templates for the modeling of a specific interface of the PPI. Only about the 25% of the interactions identified by CoIP could be modeled with enough confidence. Almost all of these interactors were kinases, either intracellular (or membrane-bound but without transmembrane domain) or RLKs of several types ([Figure 5.3](#)).

The multiple models obtained per each protein pair were clustered according their sequence overlap, considering that they belongs to the same interface if their sequence overlap is > 5 aminoacids. Then the clusters were ranked based on their size, being the cluster 1 the largest (accounting for the largest PPI interface). For the PPI affinity estimation, the change in Gibbs' free energy (ddG) was calculated for each model using Rossetta (See [methods](#)). In order to obtain the global energy shift of an interaction, each model within the same cluster and similarly, each cluster within a particular PPI, were considered as subsystem states with an associated probability. The global PPI energy was calculated summing up the estimated ddGs for each subsystem, according the

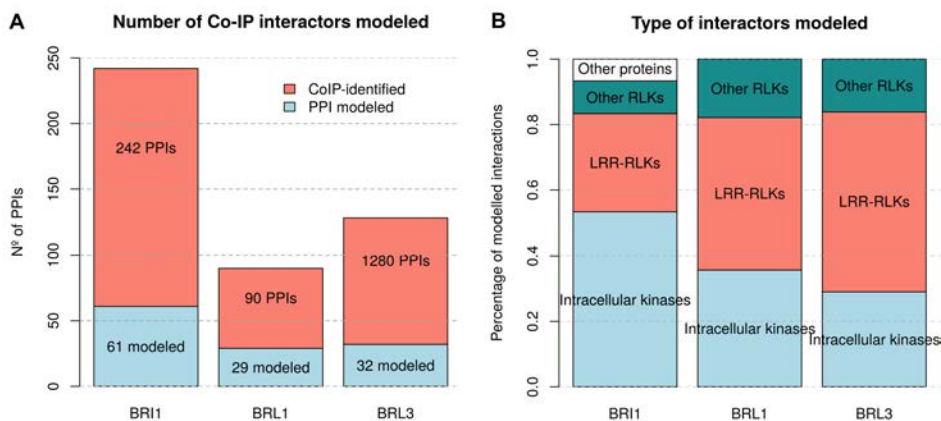


Figure 5.3: Number of interactions identified in CoIP experiments, PPIs modeled with confidence and type of interactor

(A) Barplot shows the total number of proteins identified in the complexes (passing the confidence threshold) and number of interactions that could be modeled. (B) From modeled interactions, the type of protein found to interact with the BR receptors.

Boltzmann distribution (See [methods](#)). The global energies for the different interactions and total cluster energies within the same interactions were compared. The interactions were ordered from energetically most favorable to less favorable.

Interestingly, for BRL3 we found a small LRR-RLK that has better binding energy (affinity) than the canonical BRI1-coreceptor BAK1 ([Figure 5.4](#)). The second best interaction was indeed with BAK1. The same approach was used for the BRI1 and BRL1 signalosomes. In the case of BRL1 the most favorable interaction was with an unknown RLK (AT4G23180) followed by the Brassinosteroid Signaling Kinase 1 (BSK1, [Figure 5.5](#)). In the modeling of BRL1 interactors, BAK1 was not included because it was not found in the protein complex. For the case of BRI1, a larger number of interactors were identified ([Fàbregas, 2013](#)) so more PPIs could be modeled. When the energies shifts were calculated and ranked, we found that BAK1 was not among the best interactors. Instead, the most energetically favorable interaction was with a cytoplasmatic protein kinase that curiously is targeted by a pathogen virulence factor, the *avrPphB* Susceptible 1 (PBS1) ([Figure 5.6](#)). After PBS1 kinase,

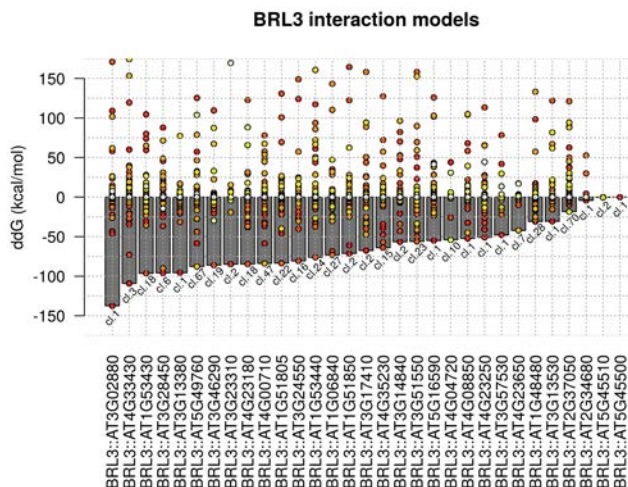


Figure 5.4: Overall energy calculation for the BRL3 interactions modeled

Bars represent the estimated global interaction energies for BRL3 interactors. Points are the calculated energies for each cluster of models per each interaction. Red depicts the 1st cluster of models (largest) and white the nth cluster. The second most favorable interaction energy (AT4G33430) is BAK1.

other kinases also showed better affinity for BRI1 than BAK1. These included cytoplasmic kinases such as BSK1, 3 and 7 and other membrane LRR-RLKs kinases as *Feronia* (FER) or *Hercules1* (HERK1). Interestingly many of the BRI1-interacting RLKs identified with more favorable interaction energy than BAK1 have already been identified as BSK3 interactors (Xu et al., 2014).

We also tested another way to rank the obtained models for each interaction. For these calculations we employed a scoring function originally used to refine the first predictions on a protein-protein docking, ZRANK (Pierce and Weng, 2007). ZRANK function takes into account detailed electrostatic, Van der Waals and desolvation energy terms and has been shown to significantly improve initial docking predictions (Pierce and Weng, 2007). Having a second ranking method allowed us to assess any eventual incoherence in the models automatically generated by the pipeline. We compared the calculated ddG

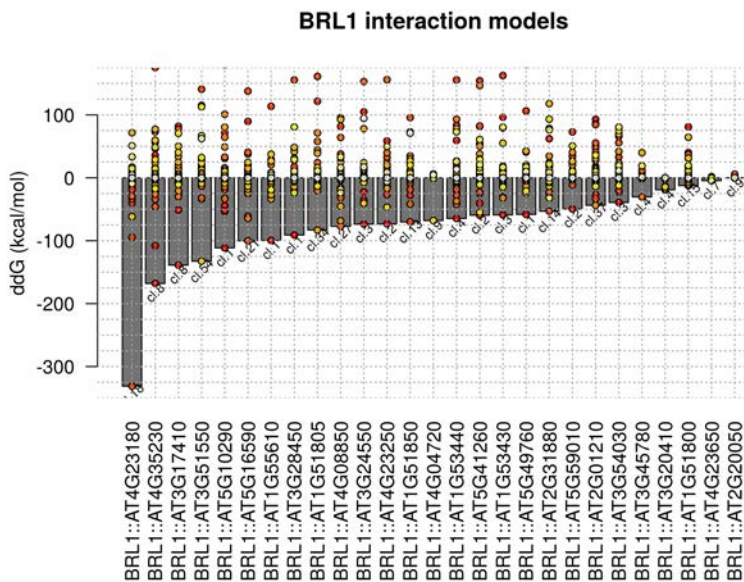


Figure 5.5: Overall energy calculation for the BRL1 interactions modeled

Bars represent the estimated global interaction energies for BRL1 interactors. Points are the calculated energies for each cluster of models per each interaction. Red depicts the 1st cluster of models (largest) and white the nth cluster.

and the ZRANK scores for each model and we did not find a global correlation between both scores (Figure 5.7). However, the largest clusters tend to fall together in the same zone of the plot, showing consistency in how favorable a specific interface is for the PPI. We decided to prioritize the ddG calculations because it is supposed to be a more quantitative measure and because only few models clearly stand out with very favorable energies. Additionally, all the very favorable models in terms of negative ddG had very negative ZRANK scores as well, although they are not necessarily the best ones. In the case of the AT3G02880 RLK (best BRL3 interactor), the model chosen as the nearest native conformation clearly stands out as very favorable energetically (Figure 5.7 A). Conversely, in the case of the BRL3-BAK1 interaction, the model chosen is the one with most negative ddG, but there is another one that also presents very low energy and better ZRANK score and could suppose

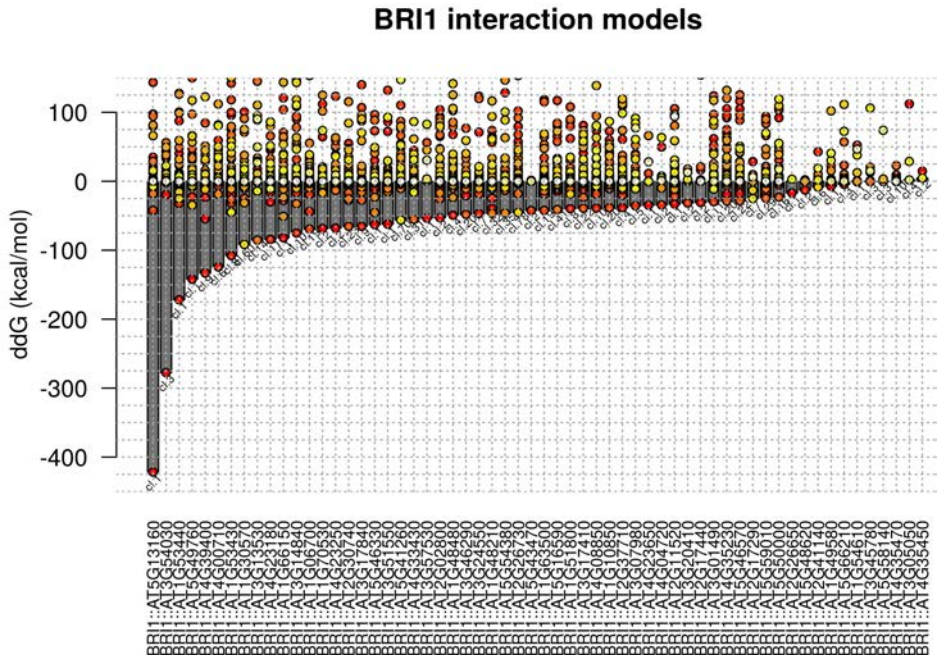


Figure 5.6: Overall energy calculation for the BRI1 interactions modeled

Bars represent the estimated global interaction energies for BRI1 interactors. Points are the calculated energies for each cluster of models per each interaction. Red depicts the 1st cluster of models (largest) and white the nth cluster. The most favorable interaction energy (AT4G33430) is PBS1 and the second most favorable is BSK7.

another near-native conformation (Figure 5.7).

In order to summarize all the results from the modeling experiment, we depicted all PPI interactions in form of a network. This network includes information on which proteins are shared interactors of the different BR receptor complexes (Fàbregas, 2013; Fàbregas et al., 2013) and how is the calculated strength of the interaction (Figure 5.8). Furthermore we included information about the drought regulation, through the incorporation of the RNAseq results from chapter 3. In the network, proteins are represented as nodes and CoIP-confirmed interactions as edges. The width of the edges represent the calculated affinities of the interactions ($-\Delta\Delta G$), the node size is

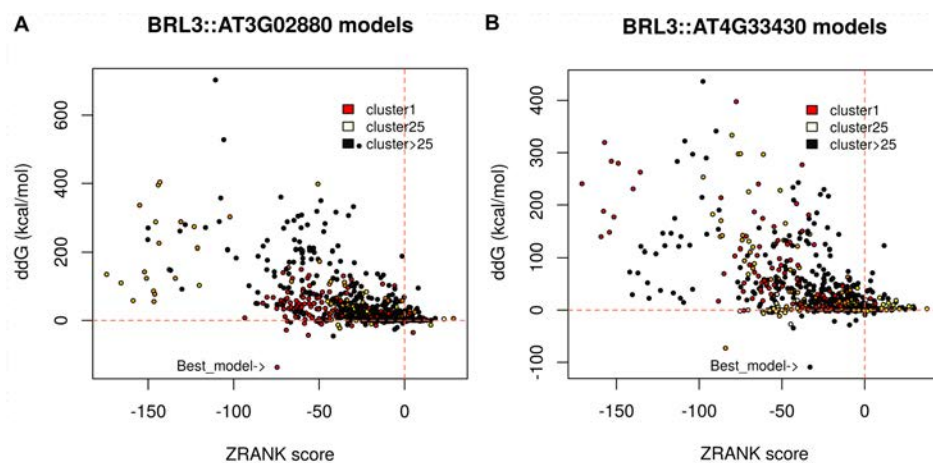


Figure 5.7: Comparison between calculated ddG and ZRANK scores per model

(A) ddG and ZRANK scores calculated for models of the BRL3-AT3G02880 interaction. (B) ddG and ZRANK scores calculated for models of the BRL3-BAK1 interaction. Points are the different models for the interaction and color represent the cluster they belong, being red the 1st (the largest) the cluster and white the 25th cluster. Clusters above the 25th were not considered for clarity reasons. Note that we chose as the most representative model the one with the lowest ddG.

the absolute fold change after 5 days of drought (in WT background) and the node color depicts if the gene was upregulated (red) or downregulated (blue) (Figure 5.8).

Given the role of BRL3 triggering drought responses (chapter 3) we decided to further investigate the BRL3 exclusive interactors. Strikingly, the protein with the most favorable binding energy to BRL3 (LRR-RLK AT3G02280, Figure 5.4), apart of being exclusively found in the BRL3 signalosome (CoIP experiment), showed a significant transcript upregulation upon 5 days on drought (Figure 5.8, left-most node).

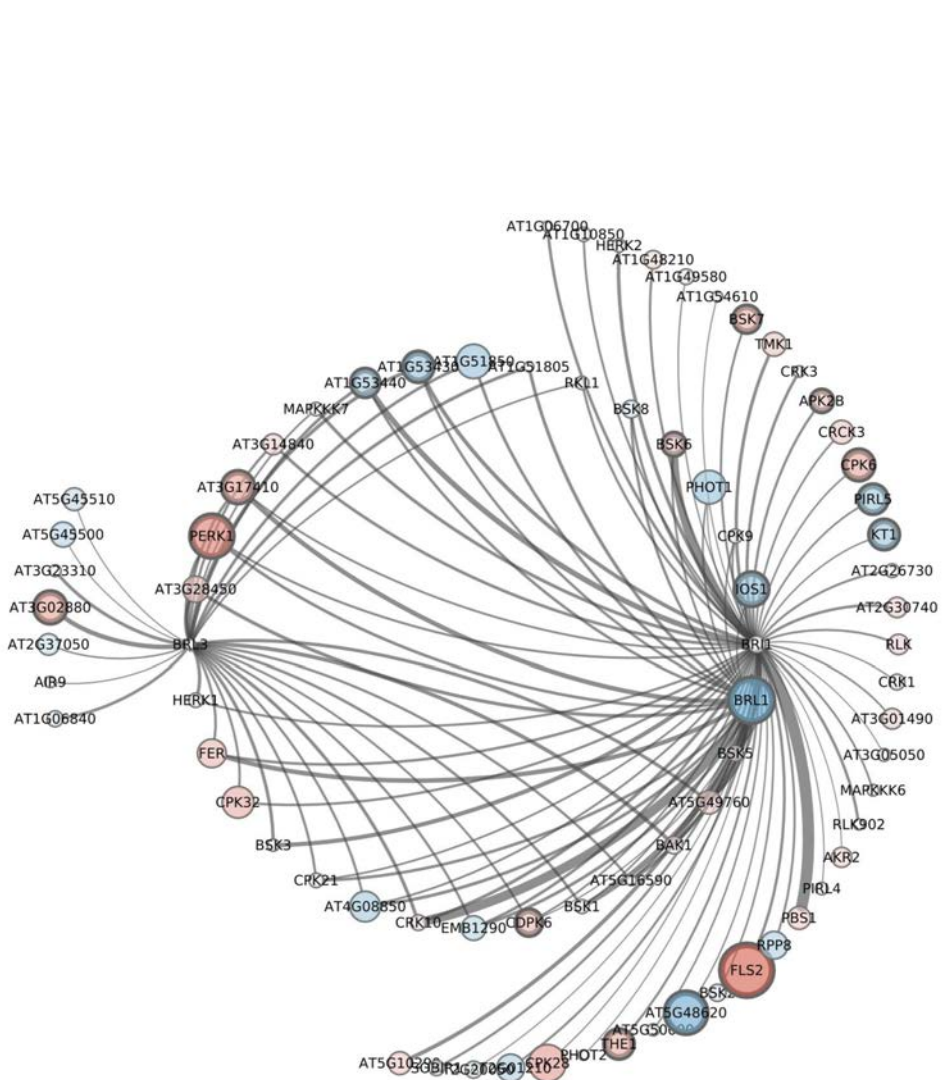


Figure 5.8: Modeled interactions network

Network representation of all modeled interactions. Nodes represent proteins and edges depict if the interaction has been detected by CoIP. The width of the edge is the (-) calculated ddG for the interaction. Node size is the absolute fold change of the transcript upon drought (chapter 3), red and blue depict up and downregulation, respectively. Only deregulated genes passing the statistical threshold show a wide outline in the node.

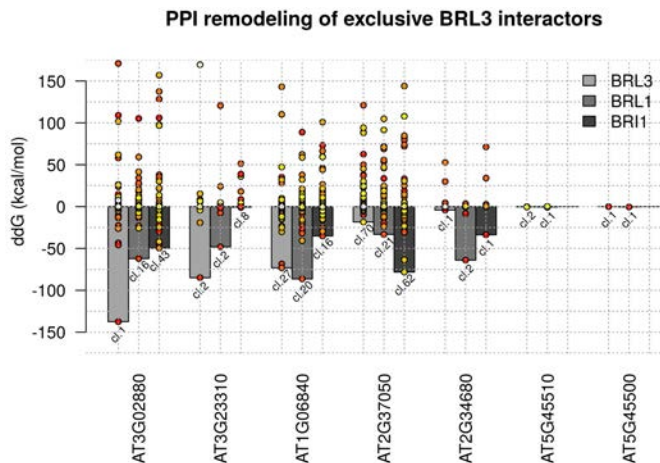


Figure 5.9: Remodeling of exclusive BRL3 interactors with the other BR receptors

Bars represent the estimated global interaction energies for the exclusive BRL3 interactors identified by CoIP that could be modeled (Figure 5.8) calculated for BRL3, BRL1 and BRI1. Points are the calculated energies for each cluster of models per each interaction. Red depicts the 1st cluster of models (largest) and white the nth cluster. Note the increased interaction affinity of AT3G02880 with BRL3 respect BRL1 or BRI1. This does not happen for all interactions, even though they were exclusively identified in the BRL3 signalosome.

5.3 BRL3 has a more favorable LRR-RLK interactor than BAK1

We next applied the same modeling pipeline to the exclusive BRL3 interactors (Figure 5.8) but forcing the interaction with either BRI1 or BRL1, even if these were not identified by CoIP experiments. Then the same procedure for estimating the interaction affinity was applied and the energies compared against the calculated for the interaction with BRL3. The AT3G02880 RLK, the best candidate for BRL3, maintains higher affinity with BRL3 than with BRL1 or BRI1 (Figure 5.9). This fact supports that this RLK has preference for BRL3 rather than for the other BR receptors. The same occurs for the second best candidate but not with the rest, they show better affinity with BRI1 or BRL1 if the interaction is computationally forced (Figure 5.9).

For a given PPI to take place, it is needed the presence of both proteins. Additionally, the amount of available protein determines the rate at which the PPI occurs, so large amounts of available protein could eventually overcome the bad affinity of a specific pair and trigger the interaction. Accordingly, we utilized transcript levels as an indirect indicator of the protein levels. We used a normalized measured, such as Reads Per Kilobase Million (RPKM), of our RNAseqs ([chapter 3](#)) for comparing transcript levels of the exclusive BRL3 interactors in WT roots. We calculated the ratio between transcript levels of our favorite interactors respect BRL3 and respect BAK1 ([Figure 5.10](#)), in both control conditions and drought. We found that the levels of AT3G02280 transcript are 6-fold higher than BRL3 levels, and it increases until 9-fold under drought conditions. The other kinases interacting exclusively with BRL3 also showed increased transcript levels respect BRL3 in most of the cases ([Figure 5.10 A](#)). When compared to BAK1, the AT3G02280 LRR-RLK also showed increased transcript levels respect BAK1, with around a 50% more transcript in normal conditions and doubling the levels of BAK1 under drought ([Figure 5.10 B](#)). These results show that, in general, the RLKs identified as exclusive BRL3 interactors (through CoIP) are more abundant than BRL3 itself.

In order to further explore the transcript abundance of AT3G02880 respect BAK1, we used the same transcriptional dataset of Arabidopsis roots used for analyzing the spatial distribution of our deregulated genes in *BRL3ox* and for TOTEM development ([chapter 3](#); [chapter 4](#); [Brady et al. \(2007\)](#)). The ratio of AT3G02880 between BAK1 transcript levels reveals an increased amount of transcript across all Arabidopsis root tissues but especially into the pericycle, where the increase is around 3-folds respect BAK1 ([Figure 5.11](#)). Interestingly, the pericycle is the most enriched tissue in upregulated genes due to BRL3 overexpression ([Figure 3.27 A](#)). The increased affinity of AT3G02880 (respect BAK1) for BRL3 together with higher transcript levels, especially in drought conditions, suggest that AT3G02280 is better BRL3 co-receptor than BAK1.

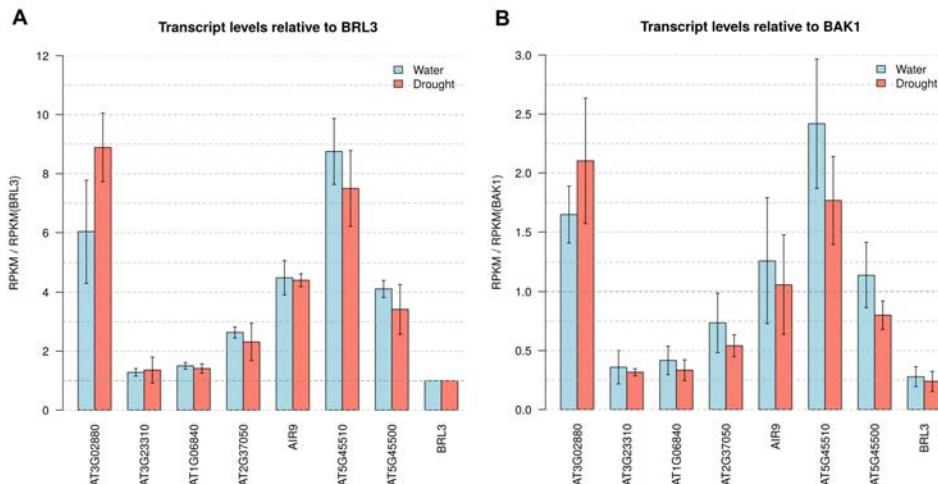


Figure 5.10: Relative transcript levels of the BRL3 exclusive interactors

(A) Relative transcript levels (RPKM) of the exclusive BRL3 interactors respect BRL3, in control conditions (blue) and after 5 days of drought (red). (B) Relative transcript levels (RPKM) of the exclusive BRL3 interactors respect BAK1, in control conditions (blue) and after drought (red).

We then took a close look at the best-ranked models for the interactions BRL3-AT3G02880 and BRL3-BAK1 (Figure 5.12). In order to check if BRL3 share the same interface for the binding of both RLKs, models were superimposed over the BRL3 kinase domain. We also included the crystal structure of BRI1-BKI1 interaction (Wang et al., 2014) and superimposed the BRI1 kinase with the BRL3 kinase. Interestingly both, BAK1 and AT3G02880, bind BRL3 through the same (BRL3) interface, which is different from the one binding BKI1 (Figure 5.12). This result suggests that BAK1 and AT3G02880 compete for the binding of BRL3.

Taken together, all evidences suggest that BRL3 can bind another RLK with more affinity than BAK1. The BRL3 interaction with BAK1 is energetically favorable, but given that AT3G02880 RLK compete with BAK1 for the same binding interface and it has increased affinity and transcript abundance,

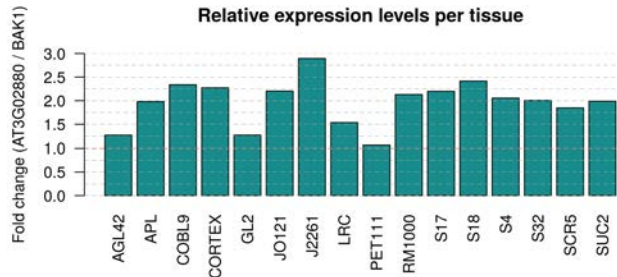


Figure 5.11: AT3G02880 RLK is more expressed than BAK1 across all Arabidopsis root tissues

Barplot showing the expression level ratio of AT3G02880 by BAK1. Expression levels from spatio-temporal Arabidopsis root expression data set (Brady et al., 2007). AGL42: Quiescent center, APL: Phloem + companion cells, COBL9: Root hair cells, CORTEX: Cortex, GL2: non-hair cells, J2261: Pericycle, JO121: Xylem pole pericycle, LRC: Laterac root cap, PET111: Columella, RM1000: Lateral root primordia, S17: Phloem pole pericycle, S18: Maturing xylem, S32: Protophloem, S4: Developing xylem, SCR5: Endodermis, SUC2: phloem companion cells

we hypothesize that AT3G02880 acts as BRL3 co-receptor instead BAK1, especially under stress conditions. Based on the best interaction models obtained (Figure 5.12), we next screened the structures in order to identify key residues (hot spots) for the interaction between BRL3 and AT3G02880 kinase domains.

5.4 Identification of critical residues for the interaction

A major part of the bases for protein-protein interactions resides into the stabilization of residues from different chains that are in physical contact. However only a small subset of these interface residues is actually crucial for recognition and binding. These residues are commonly referred as "hotspots" (Bogan and Thorn, 1998). For example, key residues for BRI1-BAK1 interaction are already identified, so when mutated the interaction is destabilized with

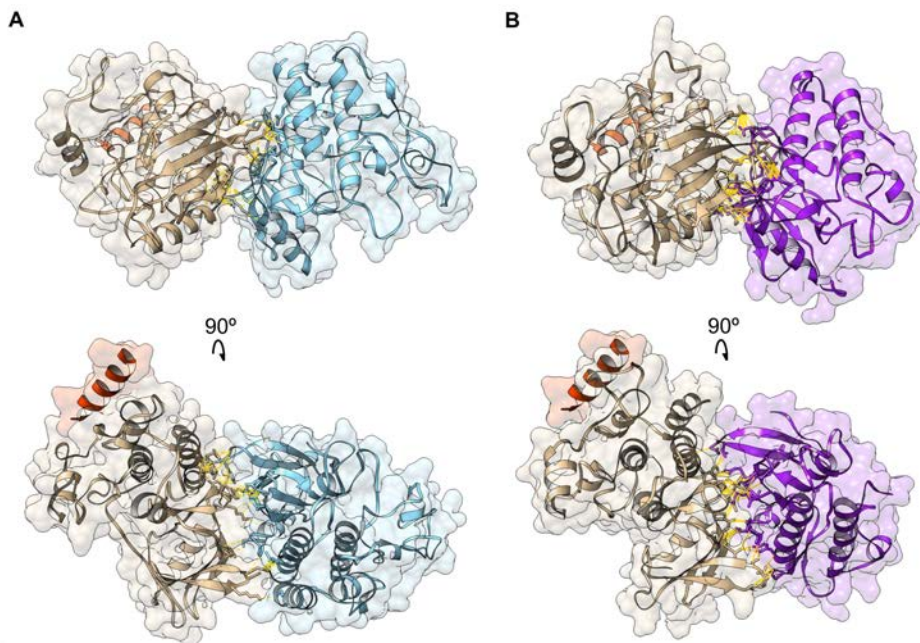


Figure 5.12: Interaction models of BRL3-AT3G02880 and BRL3-BAK1 kinase domains

(A) Interaction model of BRL3 (gold) and AT3G02880 (blue) kinase domains. (B) Interaction model of BRL3 (gold) and BAK1 (purple) kinase domains. Orange helix denotes an eventual interaction of BKI1, based on BRI1-BKI1 crystal (PDB: 40H4). Yellow lines are residues establishing contacts between both proteins. Note that AT3G02280 share approximately the same interface with BRL3 kinase domain. In top views the plasma membrane would be approximately upwards the models. Bottom views, are approximately perspectives from plasma mebrane. Structural alignments of the models, using BRL3 kinase as reference, were performed with *MatchMaker* function on UCSF Quimera.

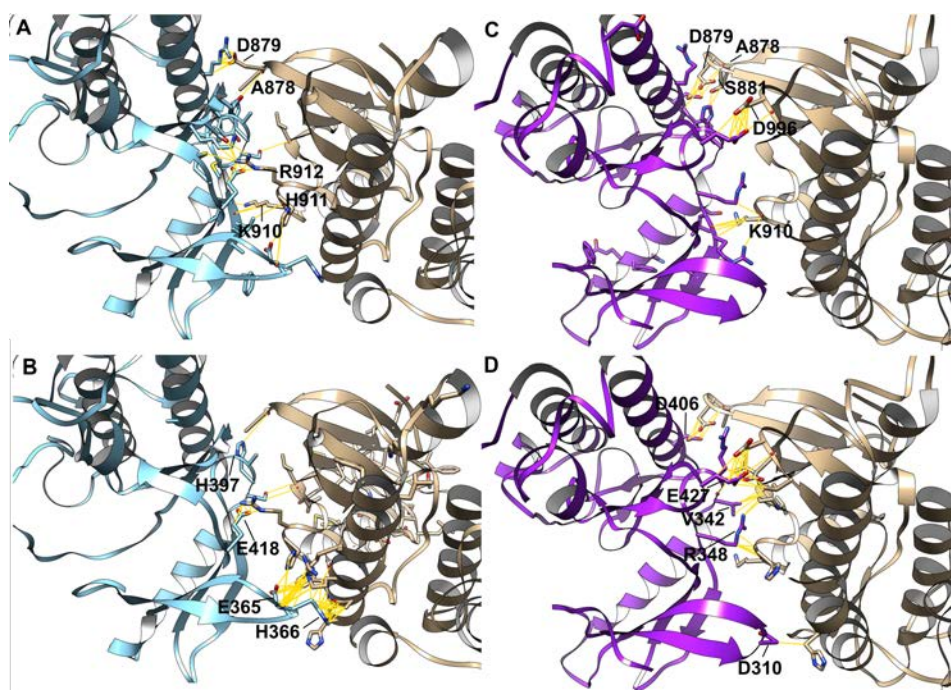
a consequent impact in brassionsteroid signaling transduction. Accordingly these single-point mutations yield *bri1*-like phenotypes (Hohmann et al., 2018b).

To predict hotspots for the BRL3-AT3G02880 interaction we used the PCRPI Server (Assi et al., 2010) (See [methods](#)) and we introduced the best-ranked model for the BRL3-AT3G02880 interaction. Briefly, the program integrates structural and energetic variables with evolutionary information through the use of Bayesian networks. As output, the it returns a list of residues for each protein ranked by their probability of being critical for the interaction. The first eight residues in the ranking for the interactions BRL3-BAK1 and BRL3-AT3G02880 are provided in [Table 5.1](#). Approximately from the fifth residue in the ranking, the scaled probability (The relative contribution of an specific residue compared to the most critical residue) are below the 50%. Interestingly the most critical residues are distributed in small patches mapping into protein loops that face towards the PPI interface. For example, the ALA878-ASP879-GLY880-SER881 and the LYS9210-HIS911-ARG912 patches in the BRL3 kinase domain or the GLU365-HIS366-GLY367 and SER396-HIS397-ALA398 patches in the AT3G02880 kinase domain ([Table 5.1](#)). Indeed, many hotspots of BRL3 kinase domain are shared between BAK1 and AT3G02880 interfaces, which is in agreement with a putative competition between BAK1 and AT3G02880 for the binding of BRL3. But not all critical residues of BRL3 are shared, fact that would account for the differences in the calculated binding affinities for both complexes ([Figure 5.5](#)). A close view of the BRL3-BAK1 and BRL3-AT3G02880 interaction models at their interfaces with the hotspots highlighted is presented in [Figure 5.13](#)).

Overall the analysis of the hotspots revealed that both, BAK1 and AT3G02880 largely use the same residues patches on the BRL3 surface for establishing contact, which supports the hypothesis of the competition for BRL3 binding. Critical residues found are mostly charged aminoacids, as histidine, arginine

Table 5.1: Identification of hotspots for the BRL3-AT3G02880 and BRL3-BAK1 interactions

Ranking	BRL3-AT3G02880		BRL3-BAK1	
	AT3G02880	BRL3	BAK1	BRL3
1 st	HIS366	ALA878	ASP406	GLY880
2 nd	GLY367	ARG912	GLU427	ASP879
3 rd	GLU418	LYS910	GLY311	LYS910
4 th	ALA398	ASP879	ASP310	ASP996
5 th	SER396	HIS911	ARG348	ALA878
6 th	GLU365	ALA971	ARG344	ASP994
7 th	HIS397	ARG968	ALA402	SER881
8 th	SER479	LEU918	VAL342	ALA971

**Figure 5.13: Representation of identified hotspots over the BRL3-BAK1 and BRL3-AT3G02880 interaction models**

(A) Identification of BRL3 critical residues for the interaction with the RLK AT3G02880. (B) Identification of AT3G02880 residues that are critical for the interaction with BRL3. (C) Identification of BRL3 residues that are critical for the interaction with BAK1. (D) Identification of BAK1 residues that are critical for the interaction with BRL3. The BRL3 kinase domain is depicted in gold, AT3G02880 kinase domain is depicted in blue and BAK1 kinase domain is depicted in purple.

or aspartic acid (Table 5.1). These likely stabilize the PPI by establishing ionic interactions with oppositely charged residues in the partner protein, for example the R912 in BRL3 with the E418 in AT3G02880 (Figure 5.13 A,B). Nevertheless these bulky and charged aminoacid could also be detrimental for the interaction because they can generate clashes with other residues. The software used do not specify if a residue is critical for the interaction because it establishes contact or generates clashes with the interacting protein, so further analysis should be performed on these hotspots. How mutations on these hotspots disrupt or stabilize the interaction could be estimated computationally through the ddG calculation on PPIs models remodeled with the mutant versions, although definitive evidence can only be obtained experimentally.

The best ranked models for the BRL3 interaction with either BAK1 or AT3G02880 (analyzed above) are restricted to the kinase domains. However what firstly allows the interaction between BRI1 and SERKs co-receptors is the interaction of the extracellular domains, which allows subsequent signal transduction (Hohmann et al., 2017, 2018b). Therefore, we next focused on the analysis of interaction models for the extracellular parts of BRL3, BAK1 and AT3G02880.

5.5 Modeling of ligand-mediated interaction at extracellular part

Among the hundreds of generated models for each PPI there was also models based on the extracellular part but these appear ranked from the 100th best model and further, even though they present also negative interaction energies (i.e. -0.13 kcal/mol for the BRL3-AT3G02880 interaction). These moderate

affinities obtained in the extracellular part could be explained by the fact that the dimerization of BRI1-SERKs depends on the BL binding to the extracellular part of BRI1. Indeed, the BRI1-BL complex act as docking platform for the binding of BAK1/SERK1 extracellular part, which in turn approximates the kinases domains under the plasma membrane (Hothorn et al., 2011; She et al., 2011, 2013).

We reasoned that the interaction between extracellular domains is probably critical for further interaction between kinase domains, so we specifically remodeled the BRL3-BAK1 and BRL3-AT3G02880 interactions at the extracellular domains in both scenarios, including a BL molecule bound to BRL3 and without including it. We used as templates for the modeling two crystals that include the BL molecule, the BRI1-BL-BAK1 complex (PDB: 4M7E; Sun et al. (2013a); Figure 5.14 A) and the BRI1-BL-SERK1 complex (PDB: 4LSX; Santiago et al. (2013); Figure 5.14 B). In order to check the if our energy calculation approach was coherent with what described into the bibliography, we calculated the ddG over the crystal structures, removing the BL molecule (*apo* form) or including it (*holo* form). In agreement with literature, both complexes (BRI1-BAK1 and BRI1-SERK1) show more favorable binding energies when BL is present (ddG shift from apo to holo forms is -10.635 and -3.478 kcal/mol, respectively; Figure 5.14 C).

We next modeled the same interaction BRI1-BAK1 using its own crystals as templates, in order to calibrate how the modeling process (with the inclusion of the BL and the optimization process) might alter the calculated energy shift (holo - apo) over the crystals. Unfortunately, when the interaction is modeled, the values of ddG greatly differ from those calculated directly over the crystals. Even for the case of BRI1-BAK1 interaction the energy shift is positive when BL is added, arguing with values obtained directly over the crystal and what described in bibliography (Figure 5.14 D). We used the discrepancy between

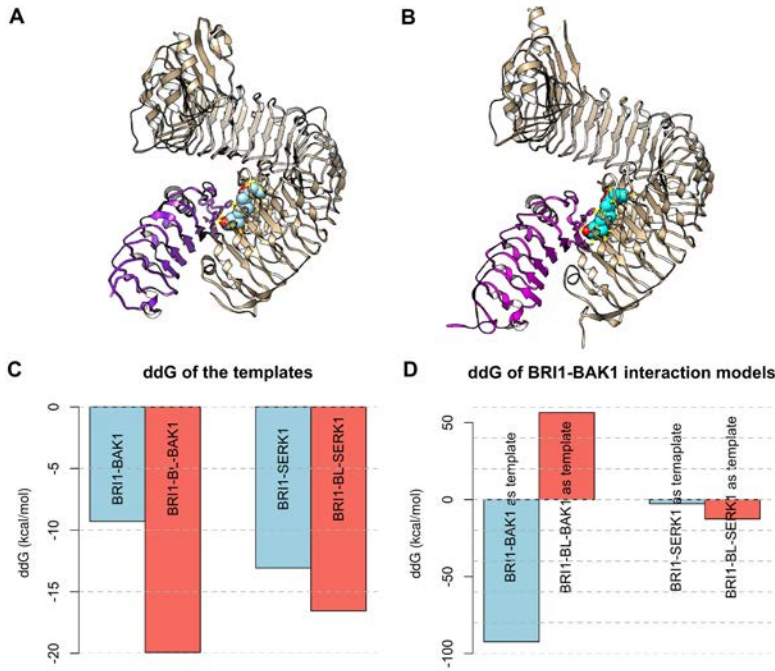


Figure 5.14: Modeling of extracellular part of BR receptors bound to BL

(A) Crystal structure of the interaction between BRI1, BL and BAK1 (PDB: 4M7E). (B) Crystal structure of the interaction between BRI1, BL and SERK1 (PDB: 4LSX). BRI1 receptor is depicted in gold, BAK1 and SERK1 coreceptors are depicted in purple and pink, respectively. BL is represented as cyan spheres. Yellow lines represent the interactions between the BL molecule and the receptors. (C) Energies (ddG) calculated for the interactions of the crystals in A and B, without the BL (blue) and including the BL (red). (D) Energies (ddG) calculated over the models of the BRI1-BAK1 interaction, using the same crystals in A and B as templates. Note the big discrepancies found between the calculated ddGs over the crystals and the models.

energies calculated over the crystals and the models as an offset value (for each template) for further correction of energy calculations. These values will be subtracted from the energy shifts (holo - apo) calculated directly over the models.

Then we modeled the interaction of BRL3 with AT3G02880 and BAK1. Despite both crystals are very similar, we focused in the BAK1-BL-BRI1 template because AT3G02880 shows more homology for BAK1 than for SERK1 and because practical reasons. When the ddG shift was calculated and corrected, we found that the interaction between BRL3 and AT3G02880 mediated by BL is more favorable than the interaction BRL3-BAK1 (Figure 5.15 A). Interestingly the interaction of BRI1 with AT3G02880 is also more favorable than the interaction BRI1-BAK1. However if we compare the overall affinity, the complex BRL3-BL-AT3G02880 shows better affinity than the BRI1-BL-AT3G02880 (Figure 5.15 A). Taken together, the AT3G02880 RLK shows better affinity than BAK1 in the interaction with BRL3 in both, kinase and extracellular domains.

Strikingly the models generated for the interaction BRL3-BL-AT3G02880 showed fairly evident differences respect the crystals of BRI1-BL-BAK1 complex. First, BRL3 shows a closer conformation than BRI1 in the horseshoe structure formed by the LRR repeats (Figure 5.15 B, C). Indeed, compared to BRI1, BRL3 protein lacks a stretch of 20 aminoacids between positions 208 and 209, where BRI1 shows an additional LRR repeat and it is precisely in this position where the LRRs of BRL3 take a closer turn towards the interior of the helicoid. And second, strikingly the BRL3-BL-AT3G02880 model present a different positioning of the BL molecule and the co-receptor AT3G02880 respect the crystals structures of BRI1-BL-BAK1. In our models, the BL binding is not taking place in the pocket formed by the island domain and the last LRRs of the extracellular part. Instead, the BL molecule is placed behind the

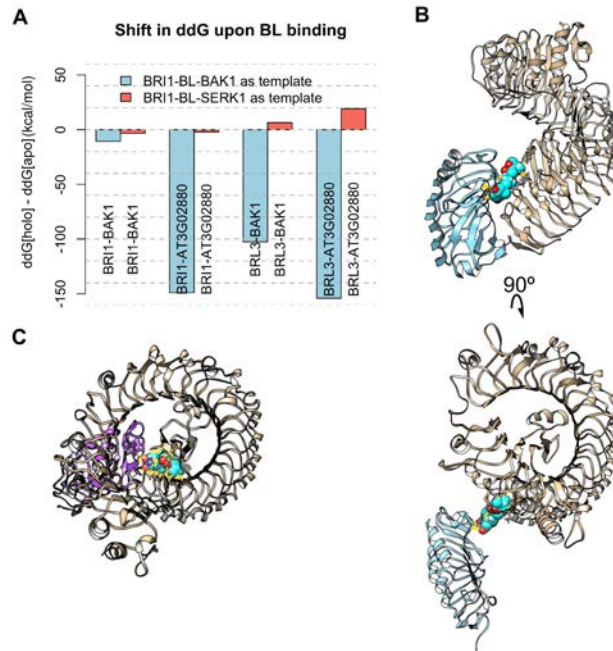


Figure 5.15: The BRL3-AT3G02880 interaction in the extracellular part is also more favorable than the BRL3-BAK1 interaction

(A) Calculation of the energy shift when BL is added to the BRI1-BAK1, BRI1-AT3G02880, BRL3-BAK1 and BRL3-AT3G02880 interaction models. Different models were generated with two different templates, the BRI1-BL-BAK1 (PDB: 4M7E, blue) and the BRI1-BL-SERK1 (PDB: 4LSX, red). (B) Model of the interaction BRL3-AT3G02880 in apo form (with BL) at the extracellular part. BRL3 is depicted in gold and AT3G02880 depicted in blue. (C) Structure of the BRI1-BL-BAK1 complex at the extracellular part (DB: 4M7E). BRL3 is depicted in gold and BAK1 depicted in purple. BL molecule are depicted as spheres in cyan. Yellow lines represent the interactions established between the BL and the receptors. Note the different conformations taken by the co-receptor AT3G02880 and BAK1 when bound to the BR receptor.

island domain, although it establishes contacts with LRR near the plasmatic membrane (Figure 5.15 B). With such positioning of the BL molecule, half of the surface of the BL would be exposed to the solvent, requiring two histidines of the RLK in contact with the BL to stabilize the complex and would make the extracellular part of AT3G02880 positioning itself almost perpendicular to the BRL3-LRR structure (Figure 5.15 B).

According to this model the positioning of the BL molecule and the AT3G02880 co-receptor would be completely different from the conformation taken in the BRI1-BAK1 interaction. In fact, both conformations could be superposed on the same BRL3 molecule without major spatial impediments (Figure 5.15 B,C). Nevertheless, we consider this possibility very improbable and it is more likely an artifact from the model refining step, so our models in the extracellular part should be revised in detail and further reevaluated.

5.6 Future perspectives

Based on experimental data of the BR receptors complexes (Fàbregas, 2013; Fàbregas et al., 2013), we followed a high-throughput modeling pipeline with the aim of modeling putative pair interactions with the BR receptors and rank them. We focused on BRL3 because of the described role in drought (chapter 3, Fàbregas et al. (2018)). Based on the results from our analyses, there exists a small LRR-RLK that has more affinity for BRL3 than BAK1 has. This protein is also named KINase7, KIN7 (AT3G02880), which according to our models, can interact in both, kinase and extracellular domains with better affinity than BAK1 and has more affinity for BRL3 than for the other BR receptors.

More *in silico* analyses could be performed in order to refine and improve the models generated, however we consider that the major part of conclusions drawn in this chapter will not change significantly. The most unexpected result from the modeling was obtained on the interaction between BRL3 and KIN7 at the extracellular part when BL was included. Because its incoherence with the current model of brassinosteroid perception, this modeling experiment worth to be repeated and refined, for example forcing the BL molecule bind the pocked formed by the island domain as a previous step to the modeling and avoiding the (energetic) optimization step of the modeled structure. Also the modeling and the interaction energies calculation can be repeated using mutated versions (sequences) in the identified hot spots, as estimation on how critical is a specific mutation for the interaction. This analysis can be performed massively substituting a large number of residues by the relatively small and neutral aminoacid alanine in what is known as Ala-scanning. Another additional bioinformatic analysis that could be performed is the *in silico* substitution of described or putative phosphorylation sites (phosphosites) by aspartic acid, which largely mimic the physico-chemical properties of a phosphorylation. Then models for the interaction are recalculated and compared to the WT versions, so some clues on the next biochemical steps for signaling may be extracted. Finally, the same high-throughput approach we took could be expanded to all RLKs or to all vascular-expressed RLKs, performing it in an unbiased way so all possible PPIs are tested. Results would be collected it in an interaction matrix, so a network similar to the presented in [Figure 5.8](#) could be completed, offering a wide (and quantitative) view of membrane interactions.

We consider that we have enough information to be confident that we will be able to confirm the BRL3-KIN7 interaction experimentally. Future work will focus on biochemical analyses. In particular, quantitative techniques as Isothermal Titration Calorimetry (ITC) can empirically determine the binding affinity of KIN7 with BRL3 or with the other BR receptors so we can compare it with what estimated through modeling. Additionally, given that we have identified

specific residues critical for the interaction BRL3-KIN7, comparison of the binding affinities of point-mutated BRL3 or KIN7 against WT versions can provide deep understanding of the molecular bases for receptor activation. And finally, testing if KIN7 instead of BAK1 acts as BRL3 co-receptor through competition assays at the extracellular part, with or without the addition of BL, could open a new door in the BR signaling field. For this last purpose we consider that grating-coupled interferometry (GCI) would be suitable, as previously described in [Hohmann et al. \(2018b\)](#). Likely, the bottleneck of the biochemistry experiments proposed above resides on the effective production of the extracellular domains. This point is achievable ([Hohmann et al., 2018a,b](#)) although these are high cost and labor intense experiments. Prior to that, experimental evidences of direct interaction using a more straight forward system as yeast-two hybrid (Y2H) assays on the kinase domains should be obtained.

Chapter 6

General Discussion

General Discussion

Brassinosteroids have been classically linked to growth regulation but over the two past decades a clear link between BRs and plant stress responses have emerged. Yet the mechanisms remains largely unknown. The present PhD dissertation advances in the contribution of BR receptors to abiotic stress responses.

In [chapter 2](#), a systematic physiological analysis of root stem cells revealed that BRs are required for QC division upon DNA damage. Whereas BRI1 is required for QC division under normal conditions, results left an open door for a prominent role of BRLs under stress. In [chapter 3](#), multiomic analyses revealed that overexpressing BRL3 receptor in vascular tissues yields massive transcriptional and metabolomics rearrangements that improve drought stress tolerance while maintaining plant growth. These results highlighted the importance of tissue-specific signaling. In [chapter 4](#), a web tool was developed in order to facilitate analyses of tissue-specific responses. And finally, in [chapter 5](#), a computational approach was taken in order to narrow down which of the BR receptor interactors obtained by mass spectrometry could account for tissue and stress-specific responses. Indeed, a novel co-receptor candidate was found, which opens the bases for the molecular dissection of the BRL3 pathway in plants. As summary, this dissertation set the basis for the elucidation of brassinosteroid-driven and tissue-specific abiotic stress responses. It offers a renewed vision on BR roles in

plant adaptation to changing environment that in the future may contribute to improve agriculture production in the current global warming scenario.

6.1 Brassinosteroid perception at the stem cell niche is necessary for QC division and cellular regeneration

The slow-dividing nature of the cells in the QC enable it to act as a cell reservoir and organized for surrounding stem cells (Fulcher and Sablowski, 2009; Pi et al., 2015; Sarkar et al., 2007; van den Berg et al., 1997; Vilarrasa-Blasi et al., 2014). Nonetheless, rather than being completely static, the QC is in fact regulated by plant hormone signaling. For instance, while ABA reinforces the quiescence of this group of cells (Zhang et al., 2010), ethylene (Ortega-Martínez et al., 2007) and cytokinin (Zhang et al., 2013) disrupt their quiescence and promote division. With respect BRs, they promote QC division and maintain a regular cell cycle progression in the rest of the root meristem (González-García et al., 2011). The mechanisms underlying BR-mediated QC divisions are starting to emerge, for example with the identification of BR-regulated and QC-specific transcription factors such as ERF115 (Heyman et al., 2013) and BRAVO (Vilarrasa-Blasi et al., 2014). But how these signaling mechanisms are locally confined to the stem cell niche of the root is still controversial. Although it has been proposed that BR action at the epidermis (Hacham et al., 2011) and vascular tissues (Kang et al., 2017) can similarly regulate meristem size and plant growth, it is unknown whether these local signals are also capable of driving QC divisions. In chapter 2 we showed that QC division requires the presence of BR receptors in both, the QC cells themselves and nearby surrounding cells. Accordingly the presence of BRs molecules would be required too.

BES1 can divide the QC cell-autonomously

Physiological analysis of QC-specific overexpression of BES1 revealed that active BES1 has the potential to trigger QC division in a cell-autonomous manner. However, reduced QC division rates were observed when pWOX5:*bes1-D*-YFP transgene was introduced into the *bri1* background (Figure 2.3), which reveals that BRI1 is also required for this process. Components acting downstream BRI1 may explain the reduced division rates in *bri1* background, despite BES1 is overexpressed. Such is the case of BZR1, which has been shown to promote autonomous QC division when activated (Chaiwanon and Wang, 2015; Lee et al., 2015). Therefore BES1 can trigger QC division cell-autonomously but further activation of other components of the BR pathway may be required to keep the division at high rates. Interestingly, transgenic lines in *bri1* background showed an increase in QC division frequency upon BL application (Figure 2.3). This increase could be attributed to BRLs receptors compensating for the lack of BRI1 and activating other downstream components.

The hormone is the limiting factor in the root stem cell niche

Surprisingly, when the plants that overexpressed BRI1 in the QC (pWOX5:BRI1-YFP) were assessed in terms of QC division rates, we found only a limited increase in both the WT and *bri1* backgrounds (Figure 2.3). In the mutant background, roots showed partial recovery of the *bri1* phenotype (i.e. longer roots), which confirmed that BRI1 was still functional when fused to YFP (Figure 2.5). Upon BL treatment, the QC division frequency of pWOX5:BRI1-YFP plants increased to similar levels that in BL-treated WT roots (Figure 2.3), thus revealing that an excess of receptor has no effect until the ligand is added. Given that plants overexpressing BRI1 in the QC displayed

no dramatic phenotype until exogenous hormone was applied, we concluded that the stem cell niche microenvironment must be characterized by a limited amount of free hormone. We discounted a competition for the ligand between BRI1 and BRLs (Figure 2.6), and hypothesize that in the root stem cell niche, a threshold of available hormone has to be reached in order to promote QC divisions (Figure 6.1).

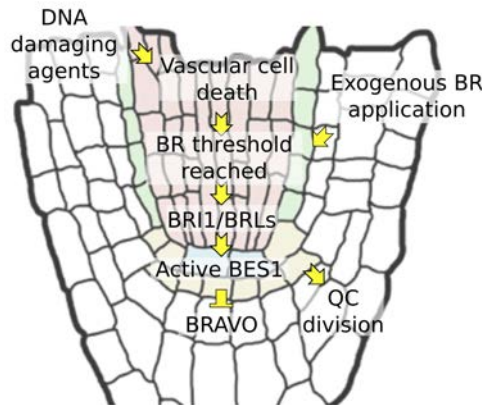


Figure 6.1: Working hypothesis: BR hormone concentration as a limiting factor for QC division

In order to promote QC divisions when needed, a threshold concentration of BRs has to be reached in the root apical meristem. Upon reaching this threshold, the signal is transduced via BRI1 with enough strength to promote BES1 dephosphorylation. Dephosphorylated BES1, in turn, inhibits BRAVO and triggers QC division.

BRI1 is necessary but not sufficient to promote QC division

According to our results, the presence of BRI1 in the QC is not the limiting factor for the QC division process. Indeed very low amounts of BRI1 receptor are normally present in these cell (Wilma van Esse et al., 2011). Moreover, BRL1 and BRL3, both of which bind the hormone with a higher affinity than BRI1, are also present in these cells (Caño-Delgado et al., 2004; Fàbregas et al., 2013), so we wondered whether BRI1 was absolutely necessary in this domain. Our results showed that WT lines expressing the amiRNA against BRI1 in the

stem cell niche (pWOX5:BRI1-amiR) are completely insensitive towards BL-induced QC divisions (Figure 2.12, Figure 2.13). But intriguingly, BRI1 acting exclusively in the QC (i.e. pWOX5:BRI1-YFP; *bri1-116* line) is not enough to recover BL-induced QC divisions to WT levels (Figure 2.3). Taken together, these results suggest that the effects of BRI1 are reinforced from surrounding cells. Thus, we concluded that BRI1 signaling in the QC is necessary but not sufficient to promote QC self-renewal. We could not uncover whether this signaling support required by BRI1 is given by BRLs because BRLs levels are also partially downregulated in pWOX5:BRI1-amiR lines, but in agreement with our data, previous results showed that *bri1bri3* double mutants have a normal BR-induced QC division (Fàbregas et al., 2013). On the other hand, *bri1-116* mutants, which have intact BRL1 and BRL3 genes, retain a quiescent QC even with the application of high BL doses (González-García et al., 2011) (Figure 2.3). All together, BRI1 stands out as the main driving factor for the QC division process, at least under normal conditions and BRLs are relegated to a supporting role for BRI1.

In addition, QC division frequency seems to have an impact on primary root growth, as the roots of pWOX5:BRI1-amiR lines are slightly shorter than those of the WT (Figure 2.14). Congruently, the *bri1-116* mutant lines that overexpressed BRI1 or BES1 in the QC not only partially recovered BR signaling in the QC, but also partially recovered overall seedling root length compared with that in the *bri1-116* mutant (Figure 2.5). This latter fact prompted us to hypothesize that some spontaneous QC divisions under basal conditions are required to sustain optimal root growth, presumably for replenishment the actively dividing stem cells (Rahni and Birnbaum, 2019).

Paracrine signaling of BRs to trigger QC division

It is known that the QC divides in response to environmental stresses such as the presence of DNA-damaging agents (Vilarrasa-Blasi et al., 2014) or changes in the homeostasis of reactive oxygen species (ROS) (Yu et al., 2016). In the root, DNA-damaging agents preferentially harm vascular and columella stem cells. Cells that are unable to repair this damage activate PCD and undergo apoptosis (Fulcher and Sablowski, 2009), which subsequently promotes QC divisions to replenish the stem cell niche and maintain meristematic activities (Heyman et al., 2016; Vilarrasa-Blasi et al., 2014). It has been demonstrated that downregulation of BRAVO is needed in this type of QC division (Vilarrasa-Blasi et al., 2014) but the exact nature of the signal from the damaged cells to the QC is still unclear. We used the amiRNA lines to analyze the receptor requirements for this kind of QC division. We discounted the idea that QC quiescence observed in the pWOX5:BRI1-amiR line after damage is due to a slower cell cycle (Figure 2.16), as is the case for the *bri1-116* mutant, so BRI1 receptor is necessary to trigger QC divisions after vascular cell death (Figure 2.18). Nevertheless, due to the off-targeting of the amiRNA we cannot discard a major contribution of BRLs under this stress scenario. In fact, a recent study has identified BRL3 as a direct target of SOG1, a transcription factors controlling responses to DNA damage. BRL3 expression is also strongly upregulated upon DNA damage (Ogita et al., 2018). If BRL3 takes over the control of QC division under genotoxic stress should be further investigated. Even if we cannot discern between BRI1 and the BRLs perceiving the signals that triggers QC divisions, results reveal that these signals are perceived by BR receptors acting in the stem cell niche. So the signal must be of a steroid nature acting in a paracrine manner. In contrast to other hormones that act over long distances, it is accepted that BRs act at a more local level (Fridman et al., 2014). In this scenario, BR biosynthesis genes as CPD or DWF4, become promising key factors: They might respond to stresses increasing their activity and subsequently transmitting signals to surrounding

tissues to, for example, regenerate the damaged stem cell niche. In the case of human stem cells it is known that stimulating paracrine signaling, cells can promote wound healing and cancer progression (Dittmer and Leyh, 2014) but in plants, the mechanisms behind autocrine and paracrine signaling are only just being uncovered (Qi et al., 2017; Vukašinović and Russinova, 2018). Measuring the dynamics of BR biosynthesis genes upon DNA damage is an easy experiment with a great potential to clarify plant stress responses at cellular level.

6.2 The vascular brassinosteroid receptor BRL3 confers drought resistance through metabolite production

The protective effects of BRs against abiotic stresses, including drought, have been known since time ago (Krishna, 2003). Indeed exogenous application of BR compounds has been widely used in agriculture to extend growth under stress (Kagale et al., 2007; Shakirova et al., 2016) but the precise mechanisms preserving growth in challenging conditions remains largely unknown. Analyses of BR signaling and BR synthesis mutants subjected to stress depicted a complex scenario for the role of BRs in abiotic stress. For instance, while the overexpression of the canonical BRI1 pathway and the BR biosynthesis gene DWF4 can both confer abiotic stress resistance (Eremina et al., 2016; Sahni et al., 2016), *bri1* loss-of-function mutants also show drought stress resistance (Feng et al., 2015; Ye et al., 2017). Moreover increased levels of BR-regulated transcription factors trigger deleterious effects in drought stress responses (Chen et al., 2017; Ye et al., 2017). These previous evidences depict a complex scenario for the role of BRs in abiotic stress, in which early signaling affects abiotic stress responses in multiple and is not necessarily connected with the

canonical BR transcription factors.

Our study shows that overexpression of the BRL3 receptor can prevent growth arrest during drought. We provide the first evidences that this drought tolerance is accomplished through the transcriptional control of metabolic pathways, which produce osmoprotectant metabolites that accumulate in the roots ([chapter 3](#)).

BR receptors control osmotic stress responses in the root

In agreement to recent reports, we found a resistance of *bri1* mutant to imposed osmotic stress ([Feng et al., 2015](#); [Ye et al., 2017](#)) ([Figure 3.1](#)). Accordingly, these plants show lesser degree of PCD upon the osmotic stress ([Figure 3.3](#)). This resistance is only visible in mutants with defective BRI1 and we consider that is linked to growth arrest and the decreased water necessities of these plants, that have indeed less exposure to osmotic stress. Interestingly we found no resistance to imposed osmotic stress in the *BRL3ox* plants, and these were indeed sensitive in terms of PCD levels ([Figure 3.3](#)). Despite of the apparent disadvantage of this sensitivity of *BRL3ox*, the osmotic-driven PCD has been described as an active process that modify root system architecture to better adapt the plant to the water content of the soil ([Cao and Li, 2010](#); [Duan et al., 2010](#); [Mira et al., 2017](#)).

In this line are the results obtained when the osmotic stress was applied but not imposed with the hydrotropism assay. The *BRL3ox* plants showed an increased hydrotropic sensitivity, triggering an exaggerated curvature compared to WT ([Figure 3.4](#)). Mutants for BRI1 showed, in general, less sensitivity but interestingly, the genotypes with the most defective hydrotropic responses included mutations in the BRLs ([Figure 3.4](#)). In support of our results, further connections between brassinosteroids and hydrotropic responses have been re-

cently found (Miao et al., 2018; Yuan et al., 2018). These involve the BR action together with H⁺-ATPases, however these reports only consider BRI1 receptor, whose mutants in fact show insensitivity to imposed osmotic stress and do not completely suppress the hydrotropic response (Miao et al., 2018; Yuan et al., 2018) (Figure 3.4). Similarly to BRI1, H⁺-ATPases have been also found in abundance in the BRL3 signalosome (Fàbregas et al., 2013). The specific localization of BRL3 in vascular tissues (Caño-Delgado et al., 2004; Fàbregas et al., 2013) likely also determines its role in hydrotropic responses, given that vascular tissues, especially the phloem, are crucial for the transmission of water availability signals (Shkolnik et al., 2018). Additionally the asymmetric root growth needed for hydrotropic response seems to be controlled from the cortex (Dietrich et al., 2017). This result would situate the role of BRL3 in hydrotropism in early signaling events in vascular tissues rather than in the response itself.

While the precise mechanism remains unknown, our results from *in vitro* osmotic stress experiments reveal an increased sensitivity of *BRL3ox* plants towards osmotic stress. We do not interpret this increased sensitivity as a detrimental trait but as a rapid response of the root system to adapt to decreased water potentials in the soil (Cao and Li, 2010; Iwata et al., 2013). Overall, these results supports a clear role of BR receptors in triggering osmotic stress responses. The precise sensing mechanism, downstream players and the exact contribution of BRI1 receptor and its vascular homologs remain subject of future studies.

Loss-of-function mutants show drought avoidance linked to growth arrest while *BRL3ox* plants actively promote drought tolerance

We found very high drought survival rates for plants with defective BR signaling, principally lacking BRI1 receptor (Figure 3.9). However these phenotypes are likely caused by a reduced exposure of these plants to the effects of

drought. Supporting this notion, loss-of-function mutants showed reduced water consumption and sustained RWC, photosynthesis and transpiration along the drought (Figure 3.10, Figure 3.11, Figure 3.12). Additionally *quad* plants showed constitutive repression of water stress-related genes and osmoprotectant metabolites during drought compared to WT (Figure 3.20, Figure 3.23). Interestingly this repression was already taking place in basal conditions (time 0), which indicates that BR receptors are directly involved in the activation water stress responses (Figure 3.17). The classical ABA accumulation upon drought stress was also very limited in *quad* plants compared to WT (Figure 3.25 A).

On the other hand, *BRL3ox* plants showed only slightly better water consumption and RWC, photosynthesis and transpiration decay compared to WT (Figure 3.10, Figure 3.11, Figure 3.12). However in this case the increased drought survival rates are not linked to growth arrest (Figure 3.9). In line with the increased sensitivity of these plants to osmotic stress, *BRL3ox* plants rapidly accumulated higher ABA levels than WT (Figure 3.25 A). Another interesting point is that *BRL3ox* showed decreased photosynthesis rates already at basal conditions, although it did not decay as fast as WT levels (Figure 3.12). Decreased photosynthesis levels could indicate a negative feedback mechanism due to the accumulation of photo-assimilates (Sheen, 1994). However the sucrose, the primary product of photosynthesis, was not accumulated in the shoots (Figure 3.17), fact that suggest a rapid mobilization towards the roots. In control conditions, *BRL3ox* plants exhibited a metabolic signature enriched in proline and sugars (Figure 3.17). Proline and sugar accumulation classically correlates with drought stress tolerance, osmolytes, ROS scavengers and chaperone functions (Durand et al., 2016; Krasensky and Jonak, 2012; Seki et al., 2007; Szabados and Savouré, 2010; Urano et al., 2009), suggesting that BRL3 overexpression "prepare" the plant for the drought, phenomenon known as priming (Conrath et al., 2002; Ding et al., 2012). Interestingly, the higher levels of sucrose in roots compared with the shoots and the higher levels of glucose and fructose in the shoots (Figure 3.17) suggest that the BRL3 pathway promotes

sugar mobilization from the leaves (source) to the roots (sink). In fact previous works reported that BRs promote the flow of assimilates in crops from source to sink via the vasculature (Wu et al., 2008) and via sucrose phloem unloading (Xu et al., 2015). Accordingly, trehalose, sucrose, *myo*-inositol, raffinose (together with proline) were rapidly accumulated in *BRL3ox* roots along the stress time course (Figure 3.19). Importantly raffinose and *myo*-inositol belong to RFO family and are involved in membrane protection and radical scavenging (Nishizawa-Yokoi et al., 2008b) and all these metabolites have previously been linked to drought resistance (Krasensky and Jonak, 2012; Szabados and Savouré, 2010). These data suggest that the increased production sugars in *BRL3ox* plants are rapidly mobilized towards the root once the drought is sensed. And subsequently the production rate of osmoprotectant sugars, such as trehalose or raffinose, is increased.

Overall these results unveil two opposing drought resistance mechanisms. One is linked to growth arrest, physiological changes and stress insensitivity and is referred as drought avoidance. This one is found in *quad* plants and involves extreme drought resistance but a dwarf plant size. Still, from a biotechnological point of view, this phenotype might be very promising in arid climates. In contrast, the moderate drought survival rates found in *BRL3ox* plants implies an active drought tolerance mechanism that do not penalize plant growth. It may be very promising strategy to increase cultivars yield with less water consumption. We summarized both concepts in Figure 3.13. These opposite mechanisms constitute different adaptation strategies that plants naturally follow in order to survive in diverse earth ecosystems (Bouzig et al., 2019; Kooyers, 2015)

Metabolite production in *BRL3ox* is transcriptionally regulated from vascular tissues

The roots of *BRL3ox* plants also showed a primed transcriptomic signature. Their constitutive activation of drought stress and ABA responsive genes sug-

gests that these plants are already "sensing" the stress and thus, activating the responses (Figure 3.21). These transcriptional changes enriched in stress genes have not been found in plants overexpressing BRI1 in different tissues, even with BL stimulation (Vragović et al., 2015). In addition, the tissue-specific BRI1 overexpression revealed opposing BL roles in the root inner/outer tissues (Vragović et al., 2015). These results, together with the native expression domain of BRL3 in root phloem cells (Fàbregas et al., 2013), support that BRL3-specific functions in stress responses are determined, at least partially, by its expression pattern.

Interestingly with the BRL3 overexpression, BRI1 was also upregulated. If we assume that their putative different functions reside in their confined expression domains, we can hypothesize a mutual exclusion from their respective domains. Then, if BRL3 expression is enhanced, BRI1 will also increase in order to keep BRL3 confined to its vascular domain. This hypothesis fits with the observed expression pattern in *BRL3ox* roots (BRL3 is under the constitutive promoter 35S) and with the unexpected upregulation of BRI1 transcript in *BRL3ox* background (Figure 3.2, Figure 3.24). This hypothesis worth to be further tested, for example with genetic crosses between mutants and reporters.

The metabolic signature found in *BRL3ox* plants suggested a possible role in phloem loading and unloading during drought. Indeed an enrichment in vascular-specific genes was detected among differentially expressed genes (Figure 3.27). These genes included enzymes implicated in trehalose and RFO metabolism that were either upregulated in basal conditions or strongly responding to drought (Figure 3.28) as the GolS2 or TTPs family, which are described to impact in drought responses (Ge et al., 2008; Himuro et al., 2014; Nuccio et al., 2015). But BRL3 overexpression also regulates non-vascular enzymes important for metabolism and drought responses. From example the hexokinases HXK3 and HKL1, the sucrose synthases SUS3 and SPS2F and proline dehydrogenase genes such as the Early Response to Dehydration 5 (ERD5) which is known to provide stress tolerance (Nanjo et al., 1999). Thus, BRL3

pathway may affect not only loading and unloading of the phloem, but may also controls directly metabolic pathways.

In light of our findings and given that *bes1-D* gain-of-function mutants exhibit drought hypersensitivity (Ye et al., 2017), we propose that overexpression of the vascular BRL3 receptors may act independently of the canonical growth-promoting BRI1 pathway. Our data further suggest that *BRL3ox* plants accumulate sugars in the sink tissues to enable plant roots to grow and escape drought by searching for water within the soil.

When we analyzed the differential drought response of the transcription factors, we found an enhanced expression of the drought-response transcription factor RD26 in *BRL3ox* roots subjected to drought (Figure 3.29). RD26 has been shown to antagonize the BR canonical transcription factor BES1 and in fact the *bes1-D* gain-of-function mutants exhibit drought hypersensitivity (Ye et al., 2017), thereby suggesting that BRL3 overexpression activates alternative pathways. Together with RD26, it appeared a set of transcription factors showing very different responses in *BRL3ox* in front of drought. Some of them are specifically-expressed in vascular tissues and could potentially be biotechnological targets (Figure 3.29). Especially those with enhanced repression on *BRL3ox* because they represent straight-forward targets for genome editing technologies.

Altogether these findings suggest that drought stress responses involving both, canonical drought genes activation and carbon metabolism adaptation towards osmoprotectants production, are correlated with BRL3 receptor levels in the root vasculature. These changes are also well correlated with the greater drought survival rates of *BRL3ox* plants and literature is rich in examples in which the increase of any of these osmoprotectants or in their synthesis enzymes yields improvement in drought tolerance. Our data further suggest that *BRL3ox* plants accumulate sugars in the sink tissues to enable plant roots to grow and escape drought by searching for water within the soil (Figure 6.2). In this scenario, vascular tissues become of special importance. Future cell type-specific engi-

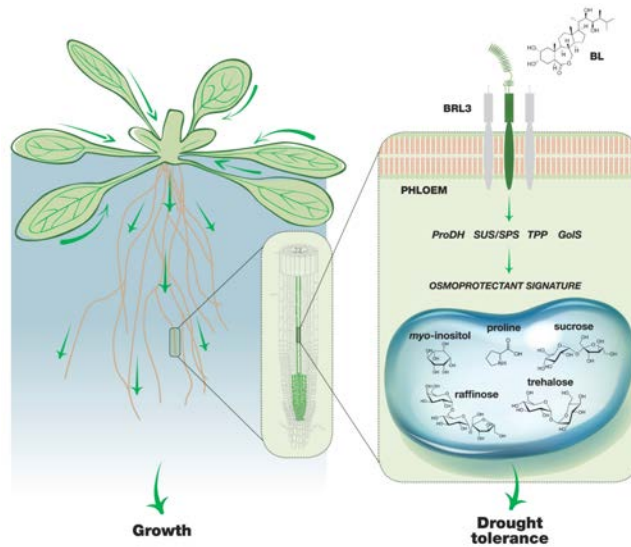


Figure 6.2: The vascular brassinosteroid receptor BRL3 confers drought resistance through osmoprotectant production

Drought resistance is generally associated to plant growth arrest. In [chapter 3](#), we uncover a role for vascular-enriched BRL3 receptors in conferring drought tolerance without penalizing overall plant growth. BRL3 receptors are enriched in the vascular (phloem) tissues where they control the division of stem cells. During drought, BRL3 signaling triggers the production of an osmoprotectant metabolic signature that is mobilized to the roots and prevents growth arrest during severe periods of drought.

neering of signaling cascades stands out as a promising strategy to circumvent growth arrest caused by drought stress.

6.3 Information on tissue-specific expression is a valuable resource to identify specific responses

In [chapter 4](#) we presented a simple web tool developed to help users to analyze their gene lists for eventual enrichments in any tissue. In our case this method has been of great utility to narrow down the differentially expressed genes until

specific enzymes that drive the production of osmoprotectant from vascular tissues (Figure 3.28). We firmly support that including topological information of the organism under study enhances the understanding of the responses at systemic level. Consistently, the contribution of tissue-specific responses (controlled by tissue-specific genes) to overall plant adaptation is increasingly becoming evident (Bernula et al., 2017; Dietrich et al., 2017; Georgii et al., 2019; Vragović et al., 2015).

In its conception, TOTEM was based on relatively old expression experiment in Arabidopsis roots (Brady et al., 2007), although it still is of extreme utility. Indeed other popular expression visualizer maintains this dataset as the core expression experiment for Arabidopsis roots (Winter et al., 2007). But differently to eFP browser, our tool allow for analyzing lists up to thousand genes and performs a statistical test over it and then it classifies the user input according the reference dataset. We also looked forward to make it easily expandable to other organs, species or experiments, so we followed a modular design. In summary, TOTEM is a very easy tool performing basic statistics on gene lists but it fills a gap by allowing not-experienced user to analyze their gene lists for topological enrichments and providing visual representations. It will be continuously updated with upcoming tissue-specific unbiased transcriptomic experiments that could serve as reference atlas for plant biologists.

6.4 KIN7 is a probable co-receptor of BRL3 implicated in abiotic stress responses

In sight of the large transcriptional and metabolic changes observed in the BRL3 overexpressor plants (chapter 3), we reasoned that it was very unlikely that they were provoked exclusively by BRL3. We hypothesized that some of the components implied in that response may be early signaling components

located already in the plasma membrane. So we took an unbiased approach in order to analyze and model direct interactions between the proteins found in the BR receptor complexes and the BR receptor themselves (Fàbregas, 2013; Fàbregas et al., 2013). For BRL3 we found a small LRR-RLK with 5 LRR (as BAK1), AT3G02880, that show better affinity for BRL3 than the co-receptor BAK1 (Figure 5.4) and also better affinity for BRL3 than for the other BR receptors (Figure 5.9). Actually this co-receptor-like RLK fulfilled our expectations because it shows increased transcript levels upon drought (Figure 5.10).

The AT3G02880 RLK has been already annotated as the probably inactive KINase 7 (KIN7) and its closest homologous is the Receptor-Like Kinase 1 (RLK1) with an identity of 52%. KIN7 has been previously shown to interact with BSK3 (Xu et al., 2014), which agrees with the presence of both, KIN7 and BSK3, in BR-receptor signalosomes (Fàbregas et al., 2013). Interestingly, phosphoproteomic studies have unveiled that KIN7 is phosphorylated and dephosphorylated in a sucrose-dependent way (Niittylä et al., 2007; Wu et al., 2013). In addition the KIN7 phosphorylation is also strongly induced by salt stress (Chang et al., 2012; Hsu et al., 2009; Vialaret et al., 2014). The phosphorylation of KIN7 upon salt stress or sucrose application were always reported to be accompanied by phosphorylations in proton exporters (H^+ ATPases) and aquaporines (Chang et al., 2012; Hsu et al., 2009; Niittylä et al., 2007; Vialaret et al., 2014; Wu et al., 2013), protein families from which some members appear in the BRL3 signalosome, i.e. HA1, HA3 and HA11 or PIP2E (Fàbregas et al., 2013). Unfortunately, putative PPI between these proteins and the BR receptors could not be modeled due to the lack of templates with acceptable homology. Further computational modeling for these putative interaction (aquaporines and proton exporters with either BRL3 or KIN7) should be tested through a protein-protein docking approach.

KIN7 has recently been shown to control stomatal closure. KIN7 translocates from plasma membrane to vacuole in response to ABA or CO₂, where it interacts and phosphorylates the vacuolar K⁺ transporter TPK1 (Isner et al., 2018). Accordingly, either *kin7* or *tpk1* mutants are defective in stomata closing in response to ABA or CO₂ (Isner et al., 2018). While KIN7 appears to play a role in transmitting signals to the effectors involved in the response, how KIN7 is activated in front of these external signals is still unknown. Another recent study, also showed the re-localization of KIN7 from plasma membrane to plasmodesmata in front of imposed osmotic stress (Grison et al., 2019). Importantly, *kin7* mutant shows reduced levels of callose deposition in plasmodesmata and a delay in lateral root development in response to osmotic stress (Grison et al., 2019). Another interesting revelation of this study is that the translocation of KIN7 to the plasmodesmata is dependent of its phosphorylation (Grison et al., 2019), which implies that the activation of KIN7 takes place in the plasma membrane. The exact mechanism of KIN7 activation (phosphorylation) is still unknown. The BR perception by BRL3 and subsequent BRL3-KIN7 mutual phosphorylations by their kinase domains could be one mechanism. According to this hypothesis, BR perception by BRL3 could bypass the classical ABA-signaling when transmitting osmotic stress signals to the effectors. Nevertheless, an opposite mechanism is also plausible: KIN7 could be activated by other components directly sensing the osmotic stress, such as aquaporines or Ca²⁺-activated kinases, and then the signal transmitted to other components as the TPK1 K⁺ transporter in the vacuole (Isner et al., 2018) and the BRL3 receptor in the plasma membrane, which in turn would trigger the BR-cascade (Figure 6.3). Our high-throughput approach to model these PPIs is too preliminary for pointing any of these mechanisms but the study of the interaction of BRL3-KIN7 at the extracellular domains and its ligand requirements offers some clues.

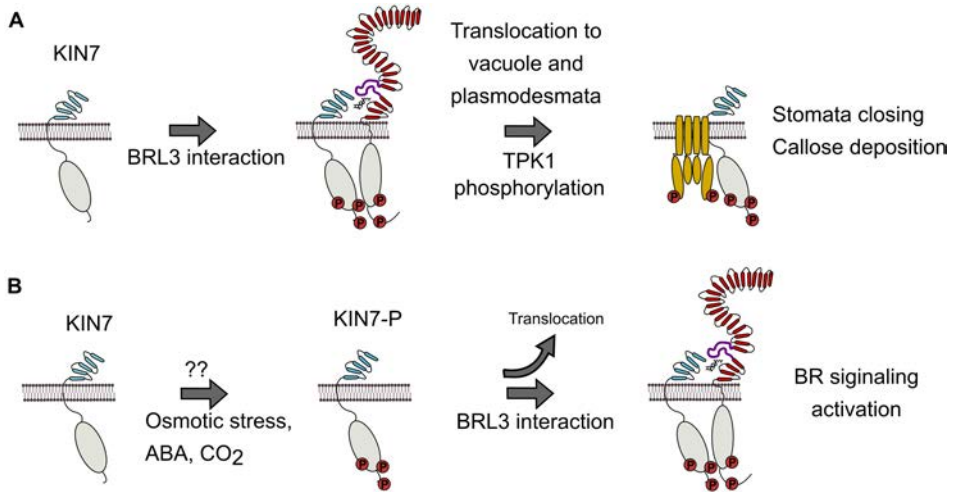


Figure 6.3: Plausible mechanisms of a putative BRL3-KIN7 cross-signaling upon abiotic stress

(A) Proposed mechanism for the BRL3 activation of stress responses: The perception of BL by BRL3 promotes the interaction with KIN7, which can then translocate to vacuole and plasmodesmata and activate downstream component. The phosphorylation of KIN7 by BRL3 would bypass the activation of KIN7 by stress, resulting in a constitutive activated stress response. (B) Inverse mechanism: The activation of KIN7 (phosphorylation by stress sensors) promotes the interaction with BRL3 and its phosphorylation, which would activate the brassinosteroid signaling pathway.

Our modeling pipeline is not designed to discriminate between intracellular part (kinase domain) and extracellular part (LRRs + island domain) but most of the models generated (and most energetically favorable) were limited to the kinase domains. This is probably due to the very few number of available crystals involving two proteins with LRRs domains and to the dependency of these interactions on a ligand (Sun et al., 2013a,b). So we specifically modeled the interaction between BRL3 and KIN7 at the extracellular part, with and without BL, based on the BRI1-BAK1 crystal (Sun et al., 2013a). The analysis of the interaction revealed a reduction in the energy when BL is present and the overall affinity of KIN7 for BRL3 is higher than for BAK1 (Figure 5.15). Nevertheless, this was only observed only after applying a correction for the discrepancies of calculated energies between the crystal itself and the model of the very same interaction (Figure 5.14). This discrepancy is probably caused

by the optimization protocol applied to the model, which relaxes energetically the structure and collapses the lateral chains when BL is not present, thus differing from the actual conformation taken by the receptor-coreceptor complex upon BL binding. Strikingly, when the best models of the interaction at the extracellular part are observed the binding of KIN7 happens in a different BRL3 interface than for BAK1, with the BL positioned in a different position (Figure 5.15). These are still very preliminary results for hypothesize that BRL3 can bind two co-receptor at once but if it would be possible, our modeling approach would suggest a trimer protein complex for BRL3 in which both, the canonical BR pathway and a stress-response pathway would be activated at the same time. Further computational modeling of the BRL3-KIN7 interaction in the extracellular part is required. The interaction should be re-evaluated trying softer (or without) relaxation protocols and forcing the BL binding to take place at the same pocket where takes place in the BRI1 receptor and then compare results.

In summary, the phosphorylation events reported in the literature suggest that KIN7 is a key signaling component for the response to abiotic stress. The results obtained from the modeling here support that BRL3 can activate KIN7. Although KIN7 is widely expressed across all tissues (Figure 5.11), if the BL-mediated KIN7 activation takes place uniquely through BRL3 as suggested by the models analyses (Figure 5.9), it would constitute a BR-dependent bypass to rapidly activate abiotic stress responses specifically in the vascular tissues. Next steps will require biochemical experiments in order to empirically confirm the *in silico* predictions.

6.5 Future perspectives

The role of BRs modulating plant stress responses is still controversial. The research presented in this thesis advances some functional principles of BR receptors in front of abiotic stress. For example, a prominent role of BRL3 under stress, the importance of tissue-specific responses and the possibility of new channels for stress signal transmission through specific membrane partners. However, direct evidences of specific molecular mechanisms are still needed. These remained somehow elusive, mostly because BRLs single and double mutants lack visible phenotypes and any secondary phenotype associated to *bri1* mutant is masked by its dwarfism. A key point would be to disentangle this BR receptor redundancy. In this direction, our transcriptomic data suggest a mutual regulation between BRI1 and BRL3, so its understanding is critical to uncouple putative differences between BRI1 and BRLs pathways. Crosses of the reporter lines used in [chapter 2](#) with BRLs single mutants, RT-qPCR or RNAseq experiments in *brls* mutant backgrounds may shed some light.

Regarding to BR signaling in the root stem cell niche, its involvement in QC division upon abiotic stress seems clear but the role of BRLs in this process should be addressed. The new single-cell sequencing techniques offer an unprecedented resolution to approach that. Indeed, recent evidences suggest a role for BRL3 in the stem cell responses under DNA damage ([Ogita et al., 2018](#)).

Respect the drought stress, it is a very complex stress in which several traits intervene in the response. Among these, BRs actually can promote changes in the transcriptomic and metabolic state that help to tolerate the drought. Because these effects were observed in a BRL3 overexpression that accumulated in vascular tissues, we propose that the investigation of tissue-specific responses stand as a promising starting point to pull apart the different plant mechanisms to drought adaptation. Accordingly, from the analysis of deregulated transcripts in *BRL3ox* plants exposed to drought, a set of tissue-specific transcription factors were selected as potential targets for improving drought tolerance ([Figure 3.29](#)).

A more applied approach will be taken on these to screen their potential effects in drought stress responses.

Finally, the membrane signalosomes of BRLs can offer insights to specific pathways that are jointly activated by BRs and stress. This idea resides behind our computational modeling approach. The bases of our structural work are solid and offer great accuracy and resolution. Nevertheless, even though our models can be still refined and further exploited, these predictions now urge of experimental demonstration. They suppose promising threads to elucidate specific molecular mechanisms that explain the protective effect of BRs in front of abiotic stresses.

Conclusions

Conclusions

1. **Brassinosteroids are required for cellular regeneration and quiescent center (QC) stem cell division upon cell death caused by DNA damage at root apex.**
 - i BRI1 is necessary but not sufficient to autonomously divide the QC.
 - ii Local steroid levels but not receptor levels in the root stem cell niche is the limiting factor the main limiting factor for QC division.
 - iii QC cell division activity can be promoted cell-autonomously by BES1 transcription factor but BR membrane signaling supports it.
 - iv BR receptors in the root stem cell niche are required to perceive the paracrine signals from neighboring damaged cells.

2. **Overexpression of BRL3 receptor in vascular tissues confers drought tolerance without penalizing plant growth.**
 - i BR receptors control osmotic stress sensitivity in the roots.
 - ii BRLs receptor complex plays a role in the sensing of osmotic gradients and promotes hydrotropic responses.
 - iii The *bri1* or *quad* mutant plants are very resistant to drought but have impaired growth, which indicates a drought-avoidance mechanism.

- iv BRL3 overexpression in vascular tissues yield a metabolic signature enriched in osmoprotectant metabolites, like proline and particularly sugars like raffinose or trehalose.
 - v The metabolic pathways synthesizing osmoprotectant metabolites are transcriptionally controlled by BRL3 from vascular tissues.
- 3. The use of published spatiotemporal expression maps is proven to be useful to test gene lists for eventual enrichments in a particular tissue and narrow down tissue-specific responses.**
- 4. BRL3 is predicted to have a co-receptor, KIN7, a LRR receptor kinase that is involved in osmotic stress responses.**
- i Computational modeling of protein-protein interaction (PPI) of BR receptors with co-immunoprecipitated proteins reveals KIN7 as the protein with more affinity for BRL3.
 - ii KIN7 expression levels are higher across root tissues than BAK1, especially in vascular tissues and under drought conditions.
 - iii The modeling predicts a competition between BAK1 and KIN7 for the binding of BRL3 kinase domain at the same interface and through nearly the same residues patches of the BRL3 kinase.

Materials and methods

Materials and methods

Plant material and growth conditions

Arabidopsis seeds were sterilized in the flow hood by applying 5 min wash with 35% (v/v) sodium hypochlorite solution (NaClO). Then the sterilization solution was removed with 5 successive washes with sterile distilled water. Then the seeds were stratified by keeping them in dark at 4°C for 2-3 days. Seeds were then sowed under sterility conditions in half-strength Murashige and Skoog media (MS) without sucrose and supplemented with vitamins poured over 120 mm x 120 mm square plates. Then the plates were sealed with Micropore tape (<https://www.3m.com>) to allow gas exchange. Plates with the Arabidopsis seeds were grown vertically in chambers with long day conditions (LD, cycles of 16h light and 8h dark), at 22°C with approximately 60% relative humidity. After 7 days of grow (or less if the seedlings were used at younger age), seedlings were transferred to soil-containing pot (mixture of soil:perlite:vermiculite at a proportion of 8:1:1) and grown until desired age in growing chambers with LD conditions at 22°C with approximately 60% relative humidity. The Arabidopsis lines used in this thesis are summarized in [Table 7.1](#).

Table 7.1: Arabidopsis plant lines used in this thesis

Line name	Affected gene(s)	Description	Reference	Chapter
Col-0 (WT)	-	Wild type, ecotype Columbia-0	-	chapter 2, chapter 3
<i>bri1-116</i>	BRI1	Knockout allele, Q583STOP	Li and Chory (1997)	chapter 2
<i>bes1-D</i>	BES1	Point mutation, P223L that causes a dominant gain-of-function	Yin et al. (2002)	chapter 2
pWOX5: <i>bes1-D</i> -GFP	BES1	Transgenic line with BES1 overexpression in the QC	Vilarrasa-Blasi et al. (2014)	chapter 2
pWOX5:BRI1-YFP	BRI1	Increased expression of BRI1 just in the QC	This work	chapter 2
pBRL1:BRL1-YFP	BRL1	Reporter line for BRL1 receptor	Fàbregas et al. (2013)	chapter 2
pBRL3:BRL3-YFP	BRL3	Reporter line for BRL3 receptor	Fàbregas et al. (2013)	chapter 2
pBRI1:BRI1-GFP	BRI1	Reporter line for BRI1 receptor	Geldner et al. (2007)	chapter 2
pSCR:BRI1-YFP	BRI1	Endodermis-specific BRI1 overexpression	Hacham et al. (2011)	chapter 2
pWOX5:BRI1-amiRNA	BRI1	QC-specific knockout of BRI1	This work	chapter 2
<i>bri1-301</i>	BRI1	G989I mutation in the kinase domain of BRI1 that inactivate it, yielding a weak BR-phenotype	Kang et al. (2010)	chapter 3
<i>bak1-3</i>	BAK1	T-DNA insertion mutant (SALK_034523)	Kemmerling et al. (2007)	chapter 3
<i>brl1brl3</i>	BRL1, BRL3	Double knockout mutants (T-DNA insertion)	Caño-Delgado et al. (2004)	chapter 3
<i>bak1-3br1brl3</i>	BAK1, BRL1, BRL3	Triple knockout mutant	Fàbregas et al. (2013)	chapter 3
<i>bri1-301brl1brl3</i>	BRI1, BRL1, BRL3	Triple knockout mutant	Fàbregas et al. (2013)	chapter 3
<i>bak1-3bri1-301brl1brl3</i> (<i>quad</i>)	BAK1, BRI1, BRL1, BRL3	Quadruple knockout mutant	Fàbregas (2013)	chapter 3
35S:BRL3-GFP (<i>BRL3ox</i>)	BRL3	Overexpression of BRL3 preferentially in vascular tissues	Fàbregas et al. (2013)	chapter 3

Plant physiology

Root length measurements

For root length measurements, images of seedlings grown in 120 mm x 120 mm square plates were taken with a Nikon D7000 camera, adding a small ruler at the bottom corner of the plates for calibration purposes. Roots from images were measured with ImageJ software (<http://imagej.nih.gov/ij/>).

Hormone and drug treatments

For brassinolide (BL) treatment, BL (Wako, Osaka, Japan) previously dissolved in DMSO and added to medium at a final concentration of either 4nM or 0.04nM. Seedlings were continuously grown in plates containing BL. For treatments with the brassinosteorid synthesis inhibitor brassinazole, BRZ (Asami et al., 2000), the BRZ (Sigma) was previously dissolved in DMSO and added to medium at a final concentration of 1 μ M. Seedlings were transferred to plates containing both BRZ and BRZ + sorbitol in the bottom part (for hydrotropism experiments) and let them grow for 24h. For bleomycin treatment, bleomycin (Calbiochem) was dissolved in the liquid media (previously tempered at < 45°C because bleomycin is thermolabile) at a final concentration of 0.6 μ g/ml. Seedlings were transferred to bleomycin plates 4 days after sowing. Seedlings were let grow 24h in bleomycin-supplemented plates and then transferred back (recovery experiment) to control medium for one day.

QC division quantification

For QC division quantification, 6-days-old seedlings were fixed, clarified and counterstained using modified pseudo Schiff-propidium iodine (mPS-PI) staining (Truernit and Haseloff, 2008). Briefly, seedlings were submerged into a 10%

acetic acid, 50% methanol solution in 6-well plates with cell strainers (100 μm pore, Corning). Samples were stored at 4°C overnight (up to a month). Using the cell strainers, samples were washed twice with H₂O and then submerged in a 1% periodic acid solution and incubated for 30 min. Samples were washed twice with H₂O, submerged in Schiff reagent (25 mg/ml of sodium bisulfite and 1.5% (v/v) pure HCl) supplemented with PI at a final concentration of 1 $\mu\text{g}/\text{ml}$ and incubated 1-2 h at room temperature with very gently shaking. Then seedlings were mounted into microscope slides with a drop of Hoyer's solution (0.6 g/ml gum arabic, 4 g/ml chloral hydrate and 0.4 g/ml glycerol). QCs were visualized with the confocal microscope with a 60x water-submerged objective. The scoring of the QC division was as follow: QC divided (D) if all QC cells showed a division plane; partially divide (PD) if not all QC cells presented division plant and non-divided (ND) if any of the QC cells showed a division plane.

Meristem cell number, length and vascular width quantification

For meristem cell counts, 6-day-old seedlings were stained with 10 $\mu\text{g}/\text{ml}$ PI and photographed under the confocal microscope using a 20x objective. Then cells were counted by tracking the cortex, starting from QC cells. The end of the meristem was considered when a cell had > 75% increase in cell length (longitudinally) respect the previous one. For meristem length, the distance between the QC cells and the end of the meristem was quantified following the central axis of the root. For root stele width, measures were taken at 50 μm above the QC. The separation between pericycle cell files (stele) was measured perpendicular to the root longitudinal axis. All measures were made with ImageJ (<http://imagej.nih.gov/ij/>).

In vitro osmotic stress assays

For the imposed osmotic stress assays, 3-days-old seedlings were transferred to media containing a final concentration of 270 mM sorbitol. A 2.7 M stock solution was prepared first (the required amount of sorbitol was first mixed with a little proportion of water and completely dissolved in a hot plate (<60°C) with stirring, the water was added until the final volume) and the solution sterilized thorough filtration with a 0.45 Whatman[®] μm filter (Sigma) and syringe. When performing the assay the stock solution was dissolved 10 times with the growing media under sterility conditions. After 4 additional days growing in sorbitol-containing plates, root length was measured. The root growth inhibition due to osmotic stress was calculated according the formula:

$$\text{Root growth inhibition} = 1 - \frac{\text{Root length}_{\text{sorbitol}}}{\text{Root length}_{\text{control}}}$$

For statistical comparisons, measurements of root length in sorbitol conditions were normalized with the mean of the same genotype grown in control conditions.

Hydrotropism assay

For the hydrotropism assay the protocol was adapted from [Takahashi et al. \(2002\)](#) and [Galvan-Ampudia et al. \(2013\)](#). Seedlings were grown for 6 days in normal media, then a diagonal with an offset of 2 cm towards the bottom was traced in the plate. The bottom half of the plate was carefully removed and replaced (under sterility conditions) with media containing 270 mM sorbitol. Plates were let 10 min in horizontal to allow the solidification of the media and diffusion of sorbitol, which creates an osmotic gradient. Then the seedlings were moved in such a way that the root tips are exactly at 5 mm from the edge separating the two medias and the root were vertically aligned. Plates were

closed again and grown vertically for 24 h more. The plates were photographed and the angle formed by the root tip and the vertical axis of each root was measured. Seedlings very close to either the top or the bottom of the plate were discarded. Further statistical treatment of the data was applied to avoid outliers: The percentiles 0.025 and 0.975 were calculated per each genotype and the data trimmed eliminating the data points below or over such percentiles.

In soil drought stress assays

The drought time course performed in [chapter 3](#) was done as follows: One-week-old seedlings grown in plates were transferred individually to pots containing 30 ± 1 g of substrate. For each biological replicate at least 40 plants of each genotype were grown in LD conditions. Irrigation was in a daily basis with a watering tray, so the bottom of the pots is always in contact with water. After 2 weeks of growth, the irrigation was stopped for 12 days (drought period) and followed by one week more of rewatering. After the 7 days of rewatering the surviving plants were manually counted. The total surviving proportions (adding all biological replicates) were statistically compared with two-sided chi-squared test and considered significative only if $p\text{-value} < 0.01$.

Relative Water Contents and photosynthesis parameters

All these experiments were performed by the team of Dr. Francisco Pérez-Alfocea in the Center of Edaphology and Applied Biology of the Segura (CE-BAS¹).

One-week-old seedlings were placed in individual pots and watered with a fixed volume of a modified Hoagland solution (1/5 strength). Pots were weighted daily during the experiment and the control was kept at 100% of field capacity. Time course drought experiments started withholding the nutrient solution un-

¹http://www.cebas.csic.es/dep_spain/nutricion/nutri_lineas.html

til reaching a 75%, 50%, 40% and 30% of field capacity (25%, 50%, 60% and 70% water loss). Relative water content (RWC) per genotype and water loss point was calculated as:

$$RWC = \frac{FW - DW}{TW - DW}$$

Where,

FW = Fresh weight,

DW = Dry weight,

TW = Turgor weight,

Photosynthesis (A) and transpiration (E) parameters were measured at these water loss levels. Measurements were repeated three times and at least four plants per genotype and treatment were analyzed.

Imaging

Confocal microscopy

Confocal images were obtained using a FV 1000 confocal microscope (Olympus, Tokyo, Japan) equipped with a multi argon laser (with excitation line at 488 nm for GFP and YFP, and at 514 nm for Alexa Fluor 555) and a Laser-Diode line (emission at 405 nm, used for PI and DAPI).

EdU staining

For EdU staining presented in [chapter 2](#), we used the Click-iT[®] EdU Alexa Fluor[®] 555 Imaging Kit (ThermoFisher). Five days after sowing, seedlings were transferred to vertical plates supplemented with 10 μ g/ml EdU. After 24 h, seedlings were fixed in a solution containing 3.7% (w/v) paraformaldehyde

and 1% (v/v) Triton X-100 in 1x PBS for 1 h in vacuum. After fixation, the seedlings were washed twice with 3% (w/v) BSA in 1x PBS and subsequently incubated in the Click-iT reaction cocktail (as described in the manufacturer's protocol) for 1 h in the dark. For counterstaining, seedlings were washed twice with 3% BSA in 1x PBS and incubated for 30 min with 1 $\mu\text{g}/\text{ml}$ DAPI in 1x PBS in the dark. Finally, the seedlings were washed a final time in 3% BSA in 1x PBS.

Fluorescence quantification

For fluorescence quantification, the mean pixel intensity/area of fluorescence in the green channel (to quantify GFP) or the red channel (to quantify EdU incorporation) were quantified over the confocal microscopy images using ImageJ (<http://imagej.nih.gov/ij/>). Quantification was performed either on the complete images for EdU-stained samples or restricted to the expression area of the BRLs.

Cell damage quantification

For quantifying stem cell damage due to bleomycin, 5-days-old seedlings were transferred to plates containing bleomycin for 24h. After 24h, roots were *in vivo* stained with 10 $\mu\text{g}/\text{ml}$ PI (Sigma) and observed into the confocal microscope with a 60x water-immersion objective. The PI stains the cell wall (control) but also the DNA in the nuclei upon cell death. The amount of damage take was qualitatively scored, depending on the amount of death cells in the vasculature (stained by the PI): No damage (ND) indicate that cells did not uptake PI; Mid damage (MD) indicates that some cells in the stem cell niche area were stained; Hard damage (HD) indicates that all cells in the stem cell niche and some cells in the vascular system were stained with PI.

For the cell damage caused by osmotic stress, 4-day-old seedlings were transferred to plates containing sorbitol for 24h. After 24h in sorbitol-containing media, roots were stained with 10 $\mu\text{g}/\text{ml}$ PI, and observed in the confocal microscope. Cell death damage in primary root tips was quantified in the middle longitudinal section of the roots, in a window of 500 μm from QC upwards. As an arbitrary setting to measure the stained area, the number of pixels within a color threshold window ranging from 160 to 255 in brightness in the red channel was quantified with ImageJ (<http://imagej.nih.gov/ij/>). Measurements were also done in control root tips (transferred 24h to normal media) in order to relativize measurements and correct for eventual differences in the cell wall staining due to the genotype.

Methods in molecular biology

amiRNA design and cloning

The artificial miRNA used in [chapter 2](#) was designed using the Web MicroRNA Designer (WMD2)² as previously described in [Ossowski et al. \(2008\)](#) and [Schwab et al. \(2006\)](#). Briefly, the nucleotides encoding the mature miRNA sequence (GCCCTATCTAAGTGTCAGTT) were engineered in the miR319a precursor as described in [Schwab et al. \(2006\)](#). The complete amiRNA fragment was then subcloned under the control of the 35SCaMV promoter or the WOX5 promoter (4.2 kb upstream of the WOX5 start codon) in the binary plasmid pH7m24GW,3 (<https://gateway.psb.ugent.be>) using the Gateway system (Invitrogen). An allelic series of amiRNAs against BRI1 transcript was generated and cloned under the 35S promoter, although results are not shown in this dissertation. The amiRNA showing the most dramatic phenotype was the only one used afterwards. For the generation of the pWOX5:BRI1-YFP

²Next version of WMD2 available in: <http://wmd3.weigelworld.org/cgi-bin/webapp.cgi>

transgene, the BRI1 coding sequence was amplified and introduced into the pDONR221 vector using Gateway system. Plasmids including the WOX5 promoter, BRI1 gene and the YFP (Vilarrasa-Blasi et al., 2014) were recombined into the binary plasmid pB7m34GW (<https://gateway.psb.ugent.be>). Binary plasmids were transformed into Arabidopsis Col-0 background using the floral dip method (Zhang et al., 2006).

DNA extraction

For genotyping purposes, DNA was extracted from plant leaves according the following rapid extraction protocol: A small piece of young leaves (approx. 10 mg) was collected per plant in a 2 mL microcentrifuge tubes containing two 5 mm glass beads and flash-frozen in liquid nitrogen. Frozen samples were converted into a fine powder through aggressive agitation in TissueLyser (Quiagen) at frequency of 1/30s for 30s. Then 400 μ l of extraction solution was added to each sample (0.4 M NaCl, 10 mM Tris-HCl pH8.0, 2 mM EDTA pH8.0 and 2% (v/v) SDS) and tubes agitated thoroughly. Samples were centrifuged for 5 min at 10000 g and the pellet discarded. To the supernatant, 1 volume of isopropanol was added, mixed gently and incubated for 1 min at room temperature. Then centrifuged at 10000 g for 1 min. The supernatant was discarded and the pellet was washed twice with 70% ethanol. Finally the pellet was resuspended in 100 μ l of sterile-distilled water. DNA concentration and purity was assessed with a Nanodrop[®] (ThermoFisher) spectrophotometer.

RNA extraction

Sample collection and RNA extraction for real time PCRs and RNAseqs was as follow: For seedlings roots, Arabidopsis seeds were sowed over an autoclaved nylon mesh with a pore < 100 μ m (Sefar). After 6 days of grown, plates were opened in a flow hood and roots separated from hypocotyls using a razor blade.

Roots were collected gently scraping the mesh with a tweezers and rapidly transferred to 2 mL microcentrifuge tubes with two 5 mm glass beads (previously baked at 200°C overnight) and flash-frozen in liquid nitrogen. Frozen samples were converted into a fine powder through aggressive agitation in TissueLyser[®] (Quiagen) at frequency of 30 s⁻¹ for 30 s, and then kept in liquid nitrogen until the RNA extraction. For mature roots, 21-days-old plants grown in soil were carefully washed in trays full of water (sequentially transferring from trays with the dirtiest water to the cleanest). Then the roots were gently dried with soft tissue paper and the root system detached from shoots with a razor blade. The root system were introduced in 2ml microcentrifuge tubes with two 5 mm glass beads and flash-frozen in liquid nitrogen. We tried to keep the times of clearing one root system below 2 min, to avoid significant transcriptomic changes. Frozen samples were converted into a fine powder with TissueLyser[®]. For plant aerial parts, mature rosettes were pooled, wrapped in aluminum foil and flash-frozen in liquid nitrogen. Rosettes were converted into fine powder with a liquid-nitrogen cooled mortar and pestle. Powder were collected in 1.5 ml microcentrifuge tubes and stored at -80°C until RNA extraction.

RNA extraction was performed with the RNAeasy[®] Plant Mini Kit (Quiagen) according the manufacturers' instructions and starting from 50 mg of tissue powder. Final elution was done in 40 μ l of RNase-free water. After the RNA extraction, a DNase treatment was applied with the DNA-free[™] Kit (Ambion) according manufacturer's instructions. The quality of the RNA was checked using Bioanalyzer (Agilent).

Real Time quantitative PCRs

For RT-qPCRs described in [chapter 3](#), cDNA was obtained from RNA samples using the Transcription First Strand cDNA Synthesis Kit (Roche) with oligo dT primers. The qPCR amplifications were performed from 10 ng of cDNA

using LightCycler® 480 SYBR Green I Master (Roche) in 96-well plates according to the manufacturer's recommendations. Arabidopsis ubiquitin 30 gene (AT5G56150) was used as housekeeping gene for relativizing expression, according to the formula:

$$Relative\ expression = 2^{(C_{P_{housekeeping}} - C_{P_{transcript}})}$$

Where,

C_p (*Crossing point*) is the double derivative of the logistic function best fitted to the amplification curve (fluorescence vs. cycles).

Primers used for RT-qPCR are described in [Table 7.2](#):

Table 7.2: Primers used for Real-Time qPCR

Primer Name	Transcript	Sequence
CPD Fwd	CPD	AGAGCGGTTTCATTTAGACCCA
CPD Rev	CPD	TACCGAGTTGCTCTGCCATC
DWF4 Fwd	DWF4	CTCAGCCGTGGAACATTTGG
DWF4 Rev	DWF4	AACAACGGAGCGTCATCCTC
BRL1 Fwd	BRL1	CTTGAACAAGGAGTTGAGCAC
BRL1 Rev	BRL1	GCTTCATTTGGCACAGCAAGA
BRL3 Fwd	BRL3	TCCGGATCCGACCATCTCTG
BRL3 Rev	BRL3	GCTTGGAACGATGTATATGTG
UBQ30 Rev	UBQ30	GGTCCGGAAGGCAACCTTT
UBQ30 Rev	UBQ30	CATGGGTCCAGCAGATAGCC

Methods in biochemistry

Metabolite extraction, gas chromatography (GC) and metabolite detection were performed by Dr. Norma Fábregas in the laboratory of Prof. Alisdair Fernie in the Max Planck Institute of Molecular Plant Physiology, Postdam-Golm, Germany³.

³<https://www.mpimp-golm.mpg.de/5858/4fernie>

Metabolite extraction

A total of five biological replicates were collected every 24 h during the time course (from day 0 to day 6) both in drought and watered conditions, and for each genotype (WT, *quad*, and *BRL3ox*). Four independent plants were bulked in each biological replicate. Roots were manually separated from shoots. Four entire shoots were grind using the Frosty Cryogenic grinder system (Labman). Four entire root samples were grind in the Tissue Lyser Mixer- Mill (Qiagen). Roots were aliquoted into 20 mg samples and shoot into 50 mg samples (the exact weight was annotated for data normalization). Primary metabolite extraction was carried as described in [Lisec et al. \(2006\)](#): One zirconia and 500 μl of 100% methanol premixed with ribitol (20:1) were added and samples were subsequently homogenized in the Tissue Lyser[®] (Qiagen) 3 min at 25 Hz. Samples were centrifuged 10 min at 14,000 rpm (10°C) and the resulting supernatant was transferred into fresh tubes, followed by the addition of 200 μl of CHCl_3 and then vortex ensuring one single phase. It was followed by the addition of 600 μl of H_2O and vortex 15 s. Samples were centrifuged 10 min at 14000 rpm (10°C). 100 μl from the upper phase (polar phase) were transferred into fresh microcentrifuge tubes (1.5 ml) and dried in a speed vacuum for at least 3 h without heating. 40 μl of derivatization agent (methoxyaminhy-drochloride in pyridine) were added to each sample (20 mg/ml). Samples were shaken for 3 h at 900 rpm at 37°C. Drops on the cover were shortly spun down. One sample vial with 1 ml MSTFA + 20 μl FAME mix was prepared. Addition of 70 μl MSTFA+FAMEs in each sample was done followed by shaking 30 min at 37°C. Drops on the cover were shortly spun down.

Gas chromatography

Samples were transferred into glass vials specific for injection in GC-TOF-MS. The GC-TOF-MS system comprised of a CTC CombiPAL autosampler, an

Agilent 6890N gas chromatograph, and a LECO Pegasus III TOF-MS running in EI+ mode. Metabolites were identified by comparing to database entries of authentic standards (Kopka et al., 2005). Chromatograms were evaluated using Chroma TOF 1.0 (Leco). Pegasus software was used for peak identification and correction of RT. Mass spectra were evaluated using the TagFinder 4.0 software (Luedemann et al., 2008) for metabolite annotation and quantification (peak area measurements).

Hormone levels measurements

Hormones extraction and measurements were carried out by Dr. Alfonso Albacete in the Center of Edaphology and Applied Biology of the Segura, Murcia, Spain (CEBAS⁴) except for BRs. Brassinolide (BL) and Castasterona (CS) were extracted and measured by Dr. Takahito Nomura and Prof. Takao Yokota in the Department of Biosciences, Teikyo University, Toyosatodai Utsunomiya, Japan.

Plant hormones cytokinins (trans-zeatin), gibberellins (GA1, GA4, and GA3), indole-3-acetic acid (IAA), ABA, salicylic acid (SA), JA, and the ethylene precursor 1-aminocyclopropane-1-carboxylic acid (ACC) were analyzed as follows: 10 μ l of extracted sample were injected in a UHPLC-MS system consisting of an Accela Series U-HPLC coupled to an exactive mass spectrometer (ThermoFisher Scientific, Waltham, MA, USA) using a heated electrospray ionization (HESI) interface. Mass spectra were obtained using the Xcalibur software version 2.2 (ThermoFisher Scientific, Waltham, MA, USA). For quantification, calibration curves were constructed for each analyzed hormone (1, 10, 50, and 100 μ g/l) and corrected for 10 μ g/l deuterated internal

⁴http://www.cebas.csic.es/dep_english/nutrition/plant_nutrition/nutri_lineas_en.html

standards. Recovery percentages ranged between 92% and 95%.

For endogenous BR analysis plant materials (4 g fresh weight) were grinded and lyophilized. BL and CS were extracted with methanol and purified by solvent partitions by using a silica gel column and ODS-HPLC as follows: The endogenous levels of BL and CS were quantified by LC-MS/MS using their deuterated internal standards (2 ng). LC-MS/MS analysis was performed with a triple quadrupole/linear ion trap instrument (QTRAP5500; AB Sciex, USA) with an electrospray source. Ion source was maintained at 300°C. Ion spray voltage was set at 4500 V in positive ion mode. MRM analysis were performed at the transitions of m/z 487–433 (collision energy (CE) 30 V) and 487–451 (CE 21 V) for 2H 6 -BL, m/z 481 to 427 (CE 30 V) and 481–445 (CE 30 V) for BL, m/z 471–435 (CE 23 V) and 471–453 (CE 25 V) for 2 H 6 -CS and m/z 465–429 (CE 23 V) and 465–447 (CE 25 V) for CS. Enhanced product ion scan was carried out at CE 21 V. HPLC separation was performed using a UHPLC (Nexera X2; Shimadzu, Japan) equipped with an ODS column (Kinetex C18, f2.1 150 mm, 1.7 μ m; Phenomenex, USA). The column oven temperature was maintained at 30°C. The mobile phase consisted of acetonitrile (solvent A) and water (solvent B), both of which contained 0.1% (v/v) acetic acid. HPLC separation was conducted with the following gradient at flow rate of 0.2 ml/min: 0–12 min, 20% A–80% A; 12–13 min, 80% A–100% A; 13–16 min, 100% A.

Bioinformatics and statistics

Microarray analysis

For microarray analysis presented in [chapter 3](#), a drought stress time course was carried out in WT and *quad* mutant 3-week-old plants. Entire plants grown un-

der drought stress and control conditions were collected every 48 h during the time course (Day 0, Day 2 and Day 4). Two biological replicates composed of five plant rosettes each were collected. RNA was extracted as described above. A Genome-Wide Microarray platform (Dual color, Agilent) was used by swapping the color hybridization of each biological replicate (Cy3 and Cy5). Statistical analysis was performed with the package "limma". The background was corrected with the "mle2/normexpr" function. Then the different microarrays were quantile-normalized and a Bayes test was used to identify differentially expressed probes. The results were filtered for adjusted p-value < 0.05 (after Benjamini-Hochberg correction) and $\text{Log}_2 \text{FC} > |1.5|$. Raw microarray data was deposited on Gene Expression Omnibus (GEO) under the accession [GSE119383](#).

RNAseq analysis

For RNAseq analysis presented in [chapter 3](#), 3-week-old roots were detached from mature plants grown in soil under control conditions and 5 days of drought. RNA was extracted as described above. Stranded cDNA libraries were prepared with TruSeq[®] Stranded mRNA Kit (Illumina). Single-end sequencing with 50-bp reads was performed in an Illumina HiSeq[®] 500 sequencer at a minimum sequencing depth of 21 M. Reads were firstly trimmed 5 bp at their 3' end, quality filtered and then mapped against the TAIR10 genome with "HISAT2" aligner. Mapped reads were quantified at the gene level with "HtSeq". For differential expression analysis, samples were TMM-normalized and statistical values calculated with the "EdgeR" package in R. Results were filtered for adjusted p-value (FDR) < 0.05 and $\text{FC} > |2|$ in the pairwise comparisons. For the evaluation of differential drought response between WT and *BRL3ox* roots, a lineal model accounting for the interaction genotype and drought was constructed with "EdgeR" package and then the interaction term was evaluated. A gene was considered to be affected by the interaction if its p-value (uncorrected) $<$

0.0025. Raw RNAseq data was deposited on Gene Expression Omnibus (GEO) under the accession [GSE119382](#).

Time course metabolite analysis

The data matrix resulting from metabolite identification and peak area quantification was first normalized using the internal standard, Ribitol, followed by a normalization with the fresh weight of each sample. Metabolomics data from control (well-watered) conditions at day 0 were analyzed with a two-tailed t-test, p -value < 0.05 (no multiple testing correction). Data from the time course was analyzed with R software using the "maSigPro" package ([Conesa et al., 2006](#)). Briefly, the profile of each metabolite under each condition was fitted to a polynomial model of maximum degree 3. The best fitted curves per each metabolite were filtered for the fitting. If the fitting coefficient was < 0.45 , the metabolite changes were not considered to be time-dependent and were not further considered. The curves of each metabolite were statistically compared across genotypes. Significant metabolites (p -value ≤ 0.05 , corrected with Benjamini-Hochberg method) having a differential profile between genotypes were plotted to visualize their behavior under the drought time course. The best fitted polynomial curve was plotted too. Clustering analysis was performed using the "maSigPro" package and the `hclust` R core function.

Root tissue enrichment analysis

For tissue-enrichment analysis on gene lists used in [chapter 3](#) (and further implemented in TOTEM, the web tool presented in [chapter 4](#)), deregulated genes were queried against available lists of tissue-enriched genes ([Brady et al., 2007](#)). For each tissue, a 2x2 contingency table was constructed, counting the number deregulated genes in the tissues that were enriched and non-enriched and also the number of non-deregulated genes (for either $FDR > 0.05$ or $|\log FC| < 2$ in

the RNAseq gene universe) that were enriched and non-enriched in the tissue. Statistical values of the enrichment were obtained using a one-sided Fisher's exact test for each tissue. This approach was implemented in a R function that loops over a list: Specific genes for each tissue were saved as a vector entry of a list containing all tissues dissected in [Brady et al. \(2007\)](#).

Match of metabolomic and transcriptomic changes

To statistically evaluate the influence of transcriptomic changes on the metabolic signature described in [chapter 3](#), both the deregulated enzymes and metabolites were queried in an annotation file containing all metabolic pathways of *Arabidopsis thaliana*, which integrates enzymes and metabolites involved in each particular reaction. The annotation file included merged data from the KEGG (<http://www.genome.jp/kegg/>) and BRENDA (www.brenda-enzymes.org) databases. For the global association between metabolic and transcriptomic changes, a 2x2 contingency table was constructed, including significant and non-significant metabolites annotated in the database and the matched differentially and non-differentially expressed genes.. The statistical value of the association between regulated metabolites and genes was obtained through a two-sided Fisher's exact test. Genes and metabolites were mapped onto the KEGG pathways using PaintOmics3 (<http://www.paintomics.org>) and the significance of each particular metabolic pathway was evaluated according to the developer's instructions ([Garcia-Alcalde et al., 2011](#)).

TOTEM implementation

We implemented the approach for detect and classify deregulated genes in different tissues ([chapter 4](#)) in form of a web tool. The web tool is mainly written in JAVA, modifying the source code of a previous tool developed in collaboration with our lab ([Rafael-Palou et al., 2012](#)). TOTEM translates numeric

values (enrichment p-values) into color intensity of the graph objects in a Scalable Vector Graph (SVG) file. This is achieved by assigning IDs to objects within the SVG file, which allows the program to sweep the SVG file for IDs coincidences with tissue names that have score associated. For the calculation of enrichment scores we connected TOTEM interface with R. The use of R allows to keep each dataset (each experiment) in a separate Rdata file that is loaded into R when the experiment is selected by the user. Each Rdata include: (i) a list in which each entry represents a tissue with a vector of genes specifically expressed. (ii) The gene universe of the experiment (i.e. detected genes in RNAseq or probes in microarrays). It will serve as background for the enrichment function. (iii) A enrichment function that calculates the enrichment values per tissue. It uses a Fisher's exact test and returns a vector with the -log transformed p-value per tissue. (iv) A custom function per experiment that represent the enrichment values in a barplot. (v) A custom function for each experiment that fix any incompatibility with the representation of the values (i.e. tissues that overlaps in the SVG file) and normalizes the enrichment values between 0 and 1. (vi) A set of functions that identify user's genes that are not enriched in any tissue, not detected in the gene universe and intersects the list with the tissue-specific genes of a selected tissue. For experiments involving more than 100 different zones or tissues, a multiple testing correction by the Benjamini-Hochberg procedure is applied to the enrichment p-values The tool was finally mounted in the server allocating the web of our institute and can be accessed though this url: <https://bioinformatics.cragenomica.es/totem>. The source code is under the open source license and can be freely downloaded, reused and modified. The source code can be accessed here: <https://github.com/CRAGENOMICA/svg2-browser>⁵.

⁵The repository will be shortly renamed as */totem*

Structural bioinformatics

The modeling and analysis of protein-protein interactions ([chapter 5](#)) was performed in collaboration and under the supervision of Prof. Baldomero Oliva from University Pompeu Fabra, Barcelona⁶ (Head of the Structural Bioinformatics group at GRIB⁷).

Homology modeling of protein-protein interactions

For the modeling of PPIs involving BR receptors and proteins that co-immunoprecipitated with them ([Fàbregas, 2013](#); [Fàbregas et al., 2013](#)) a fully automatized modeling pipeline was used in a high-throughput manner. A list including all pairs of protein identifiers to be modeled and their FASTA protein sequences were provided to the pipeline as inputs.

In general terms, the pipeline runs as it follows:

First it performs homologous searches for a protein pair (query) within a complete set of PPI resolved structures extracted from PDB (<https://www.rcsb.org/>) and 3DiD (<https://3did.irbbarcelona.org/>) databases. Sequence redundancy in the combined database was reduced through clustering them with a 90% identity threshold, using CD-HIT program (<http://weizhongli-lab.org/cd-hit/>). Alignments of both sequences (BR receptor and interactor) were performed separately against the clustered databases with BLAST (<https://blast.ncbi.nlm.nih.gov/Blast.cgi>), using *gapped blastp* searches. The hits are filtered according Rost's identity curve, discarding hits falling in the twilight zone ([Rost, 1999](#)). Then for each hit a template is searched in the database. Only if two hits (corresponding to both protein sequences of a queried protein pair) are

⁶<https://www.upf.edu/web/bioinformatics/entry/-/-/19278/adscricpion/baldomero-oliva>

⁷<http://sbi.imim.es/web/index.php/members>

found in the same template, the interaction is considered. The generated alignment files and their corresponding template structures are used to model the tridimensional conformation of the queried PPI using Modeller (<https://salilab.org/modeller/>). Further refinement of modeled structures was performed through the addition of hydrogen atoms with Reduce software (<http://kinemage.biochem.duke.edu/software/reduce.php>) and the relaxation of the resulting conformation with Rosetta program (<https://www.rosettacommons.org/software>).

For the modeling of the extracellular parts, a particular modeling was performed using as templates either BRI1-BL-BAK1 crystal (PDB: 4M7E; Sun et al. (2013a)) and BRI1-BL-SERK1 crystal (PDB: 4LSX; Santiago et al. (2013)). The modeling process basically followed the same steps than the automatized pipeline except for the modification of the generated alignment files, which included the BL molecule.

Then the set of models generated for the same PPI were clustered according the interaction interfaces. Models with more than 5 common residues in their interface were grouped together. The biggest cluster (the largest interface) was ranked as first cluster and the smallest as the last. List containing the models included in each cluster were also generated.

ZRANK scoring

In order to rank the obtained models for the same PPI and have an estimation of the best structural prediction, the ZRANK algorithm was applied (Pierce and Weng, 2007). Models for the same PPI were treated as rigid-body protein-protein docking prediction and scored with the ZRANK

(<http://zdock.umassmed.edu/software/>).

Affinity calculation

For the prediction of binding affinities between the protein chains of each model, we used the interface analyzer of Rosetta (<https://www.rosettacommons.org/software>). Binding affinities calculated by Rosetta are returned in Rosetta's own units, however they can be safely approximated to changes in Gibb's free energy (ddG, expressed in kcal/mol).

To obtain the global interaction affinity for a particular cluster (specific interface of the PPI) or for the overall interaction, models being part of a cluster of PPI were considered as possible states of the system with an associated probability (the calculated affinity). Then the global energy of the cluster or the PPI was calculated averaging the relative contribution of each state according the Boltzmann distribution. Thus the global energies were calculated as:

$$ddG_i = \sum_{n=1}^n ddG_n \cdot \exp\left(\frac{-ddG_n}{k_B T Z}\right)$$

Where,

i is a particular cluster or PPI,

n is the model number within cluster _{i} or PPI _{i} ,

T is temperature = 300K,

k_B is the Boltzmann constant = $1.987 \cdot 10^{-3}$ kcal/mol·K,

Z is the canonical partition function of the system

Z is defined as:

$$Z_i = \sum_{n=1}^n \exp\left(\frac{-ddG_n}{k_B T}\right)$$

Protein structure representations

Graphical representations of protein structures (PDB files) were done with UCSF Chimera software (<https://www.cgl.ucsf.edu/chimera/>). Alignments of different structures were done with the MatchMaker function implemented in UCSF Chimera (Meng et al., 2006). For identifying contacts between protein chains or with BL, the default contact criterion was used in the Find Clashes/-Contacts function of UCSF Chimera (Meng et al., 2006).

Bibliography

- Ahmed, H., Howton, T. C., Sun, Y., Weinberger, N., Belkhadir, Y., and Mukhtar, M. S. (2018). Network biology discovers pathogen contact points in host protein-protein interactomes. *Nature Communications*, 9(1):2312.
- Anne, P., Azzopardi, M., Gissot, L., Beaubiat, S., Hématy, K., and Palauqui, J.-C. (2015). OCTOPUS Negatively Regulates BIN2 to Control Phloem Differentiation in *Arabidopsis thaliana*. *Current Biology*, 25(19):2584–2590.
- Aranda, A. and Pascual, A. (2001). Nuclear Hormone Receptors and Gene Expression. *Physiological Reviews*, 81(3):1269–1304.
- Asami, T., Min, Y. K., Nagata, N., Yamagishi, K., Takatsuto, S., Fujioka, S., Murofushi, N., Yamaguchi, I., and Yoshida, S. (2000). Characterization of brassinazole, a triazole-type brassinosteroid biosynthesis inhibitor. *Plant physiology*, 123(1):93–100.
- Assi, S. A., Tanaka, T., Rabbitts, T. H., and Fernandez-Fuentes, N. (2010). PCRPi: Presaging Critical Residues in Protein interfaces, a new computational tool to chart hot spots in protein interfaces. *Nucleic acids research*, 38(6):e86.
- Azhar, N., Su, N., Shabala, L., and Shabala, S. (2017). Exogenously Applied 24-Epibrassinolide (EBL) Ameliorates Detrimental Effects of Salinity by Reducing K⁺ Efflux via Depolarization-Activated K⁺ Channels. *Plant and Cell Physiology*, 58(4):802–810.
- Belkhadir, Y. and Jaillais, Y. (2015). The molecular circuitry of brassinosteroid signaling. *New Phytologist*, 206(2):522–540.

- Bell, E. M., Lin, W.-c., Husbands, A. Y., Yu, L., Jaganatha, V., Jablonska, B., Mangen, A., Neff, M. M., Girke, T., and Springer, P. S. (2012). Arabidopsis LATERAL ORGAN BOUNDARIES negatively regulates brassinosteroid accumulation to limit growth in organ boundaries. *Proceedings of the National Academy of Sciences*, 109(51):21146–21151.
- Bernula, P., Crocco, C. D., Arongaus, A. B., Ulm, R., Nagy, F., and Viczián, A. (2017). Expression of the UVR8 photoreceptor in different tissues reveals tissue-autonomous features of UV-B signalling. *Plant, Cell & Environment*, 40(7):1104–1114.
- Bogan, A. A. and Thorn, K. S. (1998). Anatomy of hot spots in protein interfaces. *Journal of Molecular Biology*, 280(1):1–9.
- Bojar, D., Martinez, J., Santiago, J., Rybin, V., Bayliss, R., and Hothorn, M. (2014). Crystal structures of the phosphorylated BRI1 kinase domain and implications for brassinosteroid signal initiation. *The Plant Journal*, 78(1):31–43.
- Bonet, J., Planas-Iglesias, J., Garcia-Garcia, J., Marín-López, M. A., Fernandez-Fuentes, N., and Oliva, B. (2014). ArchDB 2014: structural classification of loops in proteins. *Nucleic Acids Research*, 42(D1):D315–D319.
- Bouzig, M., He, F., Schmitz, G., Häusler, R. E., Weber, A. P. M., Mettler-Altmann, T., and De Meaux, J. (2019). Arabidopsis species deploy distinct strategies to cope with drought stress. *Annals of Botany*.
- Boyer, J. S. (1982). Plant productivity and environment. *Science*, 218(4571):443–8.
- Brady, S. M., Orlando, D. A., Lee, J.-Y., Wang, J. Y., Koch, J., Dinneny, J. R., Mace, D., Ohler, U., and Benfey, P. N. (2007). A high-resolution root spatiotemporal map reveals dominant expression patterns. *Science*, 318(5851):801–6.
- Burley, S. K., Berman, H. M., Bhikadiya, C., Bi, C., Chen, L., Di Costanzo, L., Christie, C., Dalenberg, K., Duarte, J. M., Dutta, S., Feng, Z., Ghosh, S., Goodsell, D. S., Green, R. K., Guranović, V., Guzenko, D., Hudson, B. P., Kalro, T., Liang, Y., Lowe, R., Namkoong, H., Peisach, E., Periskova, I., Prlić, A., Randle, C., Rose, A., Rose, P., Sala, R., Sekharan, M., Shao, C., Tan, L., Tao, Y.-P., Valasatava, Y., Voigt, M., Westbrook, J., Woo, J., Yang, H., Young, J., Zhuravleva, M., and Zardecki, C. (2019). RCSB Protein Data Bank: biological macromolecular

- structures enabling research and education in fundamental biology, biomedicine, biotechnology and energy. *Nucleic Acids Research*, 47(D1):D464–D474.
- Caño-Delgado, A., Yin, Y., Yu, C., Vafeados, D., Mora-García, S., Cheng, J.-C., Nam, K. H., Li, J., and Chory, J. (2004). BRL1 and BRL3 are novel brassinosteroid receptors that function in vascular differentiation in Arabidopsis. *Development*, 131(21):5341–51.
- Cao, M. and Li, X. (2010). Die for living better: plants modify root system architecture through inducing PCD in root meristem under severe water stress. *Plant signaling & behavior*, 5(12):1645–6.
- Ceserani, T., Trofka, A., Gandotra, N., and Nelson, T. (2009). VH1/BRL2 receptor-like kinase interacts with vascular-specific adaptor proteins VIT and VIK to influence leaf venation. *Plant Journal*, 57(6):1000–1014.
- Chaiwanon, J. and Wang, Z.-Y. (2015). Spatiotemporal Brassinosteroid Signaling and Antagonism with Auxin Pattern Stem Cell Dynamics in Arabidopsis Roots. *Current Biology*, 25(8):1031–1042.
- Chang, I.-F., Hsu, J.-L., Hsu, P.-H., Sheng, W.-A., Lai, S.-J., Lee, C., Chen, C.-W., Hsu, J.-C., Wang, S.-Y., Wang, L.-Y., and Chen, C.-C. (2012). Comparative phosphoproteomic analysis of microsomal fractions of Arabidopsis thaliana and Oryza sativa subjected to high salinity. *Plant Science*, 185-186:131–142.
- Chaves, M. M., Pereira, J. S., Maroco, J., Rodrigues, M. L., Ricardo, C. P. P., Osório, M. L., Carvalho, I., Faria, T., and Pinheiro, C. (2002). How plants cope with water stress in the field. Photosynthesis and growth. *Annals of botany*, 89 Spec No(7):907–16.
- Chen, J., Nolan, T. M., Ye, H., Zhang, M., Tong, H., Xin, P., Chu, J., Chu, C., Li, Z., and Yin, Y. (2017). Arabidopsis WRKY46, WRKY54, and WRKY70 Transcription Factors Are Involved in Brassinosteroid-Regulated Plant Growth and Drought Responses. *The Plant cell*, 29(6):1425–1439.
- Cheon, J., Park, S.-Y., Schulz, B., and Choe, S. (2010). Arabidopsis brassinosteroid biosynthetic mutant dwarf7-1 exhibits slower rates of cell division and shoot induction. *BMC Plant Biology*, 10(1):270.

- Choudhary, S. P., Yu, J.-Q., Yamaguchi-Shinozaki, K., Shinozaki, K., and Tran, L.-S. P. (2012). Benefits of brassinosteroid crosstalk. *Trends in Plant Science*, 17(10):594–605.
- Chung, Y., Kwon, S. I., and Choe, S. (2014). Antagonistic Regulation of Arabidopsis Growth by Brassinosteroids and Abiotic Stresses. *Molecules and Cells*, 37(11):795–803.
- Clay, N. K. and Nelson, T. (2002). VH1, a provascular cell-specific receptor kinase that influences leaf cell patterns in Arabidopsis. *The Plant cell*, 14(11):2707–22.
- Clouse, S. D., Langford, M., and McMorris, T. C. (1996). A brassinosteroid-insensitive mutant in Arabidopsis thaliana exhibits multiple defects in growth and development. *Plant physiology*, 111(3):671–8.
- Cockell, S. J., Oliva, B., and Jackson, R. M. (2007). Structure-based evaluation of in silico predictions of protein–protein interactions using Comparative Docking. *Bioinformatics*, 23(5):573–581.
- Conesa, A., Nueda, M. J., Ferrer, A., and Talon, M. (2006). maSigPro: a method to identify significantly differential expression profiles in time-course microarray experiments. *Bioinformatics*, 22(9):1096–1102.
- Conrath, U., Pieterse, C. M., and Mauch-Mani, B. (2002). Priming in plant–pathogen interactions. *Trends in Plant Science*, 7(5):210–216.
- Cruz-Ramírez, A., Díaz-Triviño, S., Wachsman, G., Du, Y., Arteága-Vázquez, M., Zhang, H., Benjamins, R., Blilou, I., Neef, A. B., Chandler, V., and Scheres, B. (2013). A SCARECROW-RETINOBLASTOMA protein network controls protective quiescence in the Arabidopsis root stem cell organizer. *PLoS biology*, 11(11):e1001724.
- Davidson, R. M., Gowda, M., Moghe, G., Lin, H., Vaillancourt, B., Shiu, S.-H., Jiang, N., and Robin Buell, C. (2012). Comparative transcriptomics of three Poaceae species reveals patterns of gene expression evolution. *The Plant Journal*, 71(3):no–no.

- Denyer, T., Ma, X., Klesen, S., Scacchi, E., Nieselt, K., and Timmermans, M. C. (2019). Spatiotemporal Developmental Trajectories in the Arabidopsis Root Revealed Using High-Throughput Single-Cell RNA Sequencing. *Developmental Cell*, 48(6):840–852.e5.
- Dhaubhadel, S., Browning, K. S., Gallie, D. R., and Krishna, P. (2002). Brassinosteroid functions to protect the translational machinery and heat-shock protein synthesis following thermal stress. *The Plant Journal*, 29(6):681–691.
- Dietrich, D., Pang, L., Kobayashi, A., Fozard, J. A., Boudolf, V., Bhosale, R., Antoni, R., Nguyen, T., Hiratsuka, S., Fujii, N., Miyazawa, Y., Bae, T.-W., Wells, D. M., Owen, M. R., Band, L. R., Dyson, R. J., Jensen, O. E., King, J. R., Tracy, S. R., Sturrock, C. J., Mooney, S. J., Roberts, J. A., Bhalerao, R. P., Dinneny, J. R., Rodriguez, P. L., Nagatani, A., Hosokawa, Y., Baskin, T. I., Pridmore, T. P., De Veylder, L., Takahashi, H., and Bennett, M. J. (2017). Root hydrotropism is controlled via a cortex-specific growth mechanism. *Nature Plants*, 3(6):17057.
- Ding, Y., Fromm, M., and Avramova, Z. (2012). Multiple exposures to drought 'train' transcriptional responses in Arabidopsis. *Nature Communications*, 3(1):740.
- Dittmer, J. and Leyh, B. (2014). Paracrine effects of stem cells in wound healing and cancer progression (Review). *International journal of oncology*, 44(6):1789–98.
- Dolan, L., Janmaat, K., Willemsen, V., Linstead, P., Poethig, S., Roberts, K., and Scheres, B. (1993). Cellular organisation of the Arabidopsis thaliana root. *Development*, 119(1):71–84.
- Domagalska, M. A., Schomburg, F. M., Amasino, R. M., Vierstra, R. D., Nagy, F., and Davis, S. J. (2007). Attenuation of brassinosteroid signaling enhances FLC expression and delays flowering. *Development*, 134(15):2841–50.
- Duan, Y., Zhang, W., Li, B., Wang, Y., Li, K., Sodmergen, Han, C., Zhang, Y., and Li, X. (2010). An endoplasmic reticulum response pathway mediates programmed cell death of root tip induced by water stress in Arabidopsis. *New Phytologist*, 186(3):681–695.
- Durand, M., Porcheron, B., Hennion, N., Maurousset, L., Lemoine, R., and Pourtau, N. (2016). Water Deficit Enhances C Export to the Roots in Arabidopsis thaliana

- Plants with Contribution of Sucrose Transporters in Both Shoot and Roots. *Plant physiology*, 170(3):1460–79.
- Enkhbayar, P., Kamiya, M., Osaki, M., Matsumoto, T., and Matsushima, N. (2003). Structural principles of leucine-rich repeat (LRR) proteins. *Proteins: Structure, Function, and Bioinformatics*, 54(3):394–403.
- Eremina, M., Unterholzner, S. J., Rathnayake, A. I., Castellanos, M., Khan, M., Kugler, K. G., May, S. T., Mayer, K. F. X., Rozhon, W., and Poppenberger, B. (2016). Brassinosteroids participate in the control of basal and acquired freezing tolerance of plants. *Proceedings of the National Academy of Sciences of the United States of America*, 113(40):E5982–E5991.
- Espinosa-Ruiz, A., Martínez, C., de Lucas, M., Fàbregas, N., Bosch, N., Caño-Delgado, A. I., and Prat, S. (2017). TOPLESS mediates brassinosteroid control of shoot boundaries and root meristem development in *Arabidopsis thaliana*. *Development*, 144(9):1619–1628.
- Fàbregas, N. (2013). *Novel functions and interactors for Brassinosteroid receptors In Arabidopsis thaliana*. PhD thesis, Universitat de Barcelona.
- Fàbregas, N., Li, N., Boeren, S., Nash, T. E., Goshe, M. B., Clouse, S. D., de Vries, S., and Caño-Delgado, A. I. (2013). The brassinosteroid insensitive1-like3 signalosome complex regulates *Arabidopsis* root development. *The Plant cell*, 25(9):3377–88.
- Fàbregas, N., Lozano-Elena, F., Blasco-Escámez, D., Tohge, T., Martínez-Andújar, C., Albacete, A., Osorio, S., Bustamante, M., Riechmann, J., Nomura, T., Yokota, T., Conesa, A., Alfocea, F., Fernie, A., and Caño-Delgado, A. (2018). Overexpression of the vascular brassinosteroid receptor BRL3 confers drought resistance without penalizing plant growth. *Nature Communications*, 9(1).
- Feng, Y., Yin, Y., and Fei, S. (2015). Down-regulation of BdBRI1, a putative brassinosteroid receptor gene produces a dwarf phenotype with enhanced drought tolerance in *Brachypodium distachyon*. *Plant Science*, 234:163–173.
- Filek, M., Rudolphi-Skórska, E., Sieprawska, A., Kvasnica, M., and Janeczko, A. (2017). Regulation of the membrane structure by brassinosteroids and progesterone in winter wheat seedlings exposed to low temperature. *Steroids*, 128:37–45.

- Fridman, Y., Elkouby, L., Holland, N., Vragović, K., Elbaum, R., and Savaldi-Goldstein, S. (2014). Root growth is modulated by differential hormonal sensitivity in neighboring cells. *Genes & development*, 28(8):912–20.
- Friedrichsen, D. M., Joazeiro, C. A. P., Li, J., Hunter, T., and Chory, J. (2000). Brassinosteroid-Insensitive-1 Is a Ubiquitously Expressed Leucine-Rich Repeat Receptor Serine/Threonine Kinase. *Plant Physiology*, 123(4):1247 LP – 1256.
- Fukuda, H. (2004). Signals that control plant vascular cell differentiation. *Nature Reviews Molecular Cell Biology*, 5(5):379–391.
- Fulcher, N. and Sablowski, R. (2009). Hypersensitivity to DNA damage in plant stem cell niches. *Proceedings of the National Academy of Sciences of the United States of America*, 106(49):20984–8.
- Galvan-Ampudia, C., Julkowska, M., Darwish, E., Gandullo, J., Korver, R., Brunoud, G., Haring, M., Munnik, T., Vernoux, T., and Testerink, C. (2013). Halotropism Is a Response of Plant Roots to Avoid a Saline Environment. *Current Biology*, 23(20):2044–2050.
- Gampala, S. S., Kim, T.-W., He, J.-X., Tang, W., Deng, Z., Bai, M.-Y., Guan, S., Lalonde, S., Sun, Y., Gendron, J. M., Chen, H., Shibagaki, N., Ferl, R. J., Ehrhardt, D., Chong, K., Burlingame, A. L., and Wang, Z.-Y. (2007). An Essential Role for 14-3-3 Proteins in Brassinosteroid Signal Transduction in Arabidopsis. *Developmental Cell*, 13(2):177–189.
- Garcia-Alcalde, F., Garcia-Lopez, F., Dopazo, J., and Conesa, A. (2011). Paintomics: a web based tool for the joint visualization of transcriptomics and metabolomics data. *Bioinformatics*, 27(1):137–139.
- Ge, L.-F., Chao, D.-Y., Shi, M., Zhu, M.-Z., Gao, J.-P., and Lin, H.-X. (2008). Over-expression of the trehalose-6-phosphate phosphatase gene OsTPP1 confers stress tolerance in rice and results in the activation of stress responsive genes. *Planta*, 228(1):191–201.
- Geldner, N., Hyman, D. L., Wang, X., Schumacher, K., and Chory, J. (2007). Endosomal signaling of plant steroid receptor kinase BRI1. *Genes & Development*, 21(13):1598–1602.

- Gendron, J. M., Liu, J.-S., Fan, M., Bai, M.-Y., Wenkel, S., Springer, P. S., Barton, M. K., and Wang, Z.-Y. (2012). Brassinosteroids regulate organ boundary formation in the shoot apical meristem of Arabidopsis. *Proceedings of the National Academy of Sciences*, 109(51):21152–21157.
- Georgii, E., Kugler, K., Pfeifer, M., Vanzo, E., Block, K., Domagalska, M. A., Jud, W., AbdElgawad, H., Asard, H., Reinhardt, R., Hansel, A., Spannagl, M., Schäffner, A. R., Palme, K., Mayer, K. F. X., and Schnitzler, J.-P. (2019). The Systems Architecture of Molecular Memory in Poplar after Abiotic Stress. *The Plant cell*, 31(2):346–367.
- González-García, M.-P., Vilarrasa-Blasi, J., Zhiponova, M., Divol, F., Mora-García, S., Russinova, E., and Caño-Delgado, A. I. (2011). Brassinosteroids control meristem size by promoting cell cycle progression in Arabidopsis roots. *Development*, 138(5):849 – 859.
- Gou, X., Yin, H., He, K., Du, J., Yi, J., Xu, S., Lin, H., Clouse, S. D., and Li, J. (2012). Genetic Evidence for an Indispensable Role of Somatic Embryogenesis Receptor Kinases in Brassinosteroid Signaling. *PLoS Genetics*, 8(1):e1002452.
- Graether, S. P. and Boddington, K. F. (2014). Disorder and function: a review of the dehydrin protein family. *Frontiers in Plant Science*, 5:576.
- Grisson, M. S., Kirk, P., Brault, M., Wu, X. N., Schulze, W. X., Benitez-Alfonso, Y., Immel, F., and Bayer, E. M. (2019). Plasma membrane associated Receptor Like Kinases relocate to plasmodesmata in response to osmotic stress. *bioRxiv*, page 610881.
- Gui, J., Zheng, S., Liu, C., Shen, J., Li, J., and Li, L. (2016). OsREM4.1 Interacts with OsSERK1 to Coordinate the Interlinking between Abscisic Acid and Brassinosteroid Signaling in Rice. *Developmental Cell*, 38(2):201–213.
- Guo, H., Li, L., Ye, H., Yu, X., Algreen, A., and Yin, Y. (2009). Three related receptor-like kinases are required for optimal cell elongation in Arabidopsis thaliana. *Proceedings of the National Academy of Sciences of the United States of America*, 106(18):7648–53.
- Ha, Y., Shang, Y., and Nam, K. H. (2016). Brassinosteroids modulate ABA-induced stomatal closure in Arabidopsis. *Journal of Experimental Botany*, 67(22):6297.

- Hacham, Y., Holland, N., Butterfield, C., Ubeda-Tomas, S., Bennett, M. J., Chory, J., and Savaldi-Goldstein, S. (2011). Brassinosteroid perception in the epidermis controls root meristem size. *Development*, 138(5):839–48.
- Hartwig, T., Chuck, G. S., Fujioka, S., Klempien, A., Weizbauer, R., Potluri, D. P. V., Choe, S., Johal, G. S., and Schulz, B. (2011). Brassinosteroid control of sex determination in maize. *Proceedings of the National Academy of Sciences*, 108(49):19814–19819.
- Hategan, L., Godza, B., Kozma-Bognar, L., Bishop, G. J., and Szekeres, M. (2014). Differential expression of the brassinosteroid receptor-encoding BRI1 gene in Arabidopsis. *Planta*, 239(5):989–1001.
- He, J.-X., Gendron, J. M., Sun, Y., Gampala, S. S. L., Gendron, N., Sun, C. Q., and Wang, Z.-Y. (2005). BZR1 is a transcriptional repressor with dual roles in brassinosteroid homeostasis and growth responses. *Science*, 307(5715):1634–8.
- He, K., Gou, X., Yuan, T., Lin, H., Asami, T., Yoshida, S., Russell, S. D., and Li, J. (2007). BAK1 and BKK1 Regulate Brassinosteroid-Dependent Growth and Brassinosteroid-Independent Cell-Death Pathways. *Current Biology*, 17(13):1109–1115.
- Heyman, J., Cools, T., Canher, B., Shavialenka, S., Traas, J., Vercauteren, I., Van den Daele, H., Persiau, G., De Jaeger, G., Sugimoto, K., and De Veylder, L. (2016). The heterodimeric transcription factor complex ERF115–PAT1 grants regeneration competence. *Nature Plants*, 2(11):16165.
- Heyman, J., Cools, T., Vandenbussche, F., Heyndrickx, K. S., Van Leene, J., Vercauteren, I., Vanderauwera, S., Vandepoele, K., De Jaeger, G., Van Der Straeten, D., and De Veylder, L. (2013). ERF115 controls root quiescent center cell division and stem cell replenishment. *Science*, 342(6160):860–3.
- Himuro, Y., Ishiyama, K., Mori, F., Gondo, T., Takahashi, F., Shinozaki, K., Kobayashi, M., and Akashi, R. (2014). Arabidopsis galactinol synthase AtGolS2 improves drought tolerance in the monocot model Brachypodium distachyon. *Journal of Plant Physiology*, 171(13):1127–1131.

- Hink, M. A., Shah, K., Russinova, E., de Vries, S. C., and Visser, A. J. W. G. (2008). Fluorescence fluctuation analysis of *Arabidopsis thaliana* somatic embryogenesis receptor-like kinase and brassinosteroid insensitive 1 receptor oligomerization. *Biophysical journal*, 94(3):1052–62.
- Hohmann, U., Lau, K., and Hothorn, M. (2017). The Structural Basis of Ligand Perception and Signal Activation by Receptor Kinases. *Annual Review of Plant Biology*, 68(1):109–137.
- Hohmann, U., Nicolet, J., Moretti, A., Hothorn, L. A., and Hothorn, M. (2018a). The SERK3 elongated allele defines a role for BIR ectodomains in brassinosteroid signalling. *Nature Plants*, 4(6):345–351.
- Hohmann, U., Santiago, J., Nicolet, J., Olsson, V., Spiga, F. M., Hothorn, L. A., Butenko, M. A., and Hothorn, M. (2018b). Mechanistic basis for the activation of plant membrane receptor kinases by SERK-family coreceptors. *Proceedings of the National Academy of Sciences of the United States of America*, 115(13):3488–3493.
- Holzwardt, E., Huerta, A. I., Glöckner, N., Garnelo Gómez, B., Wanke, F., Augustin, S., Askani, J. C., Schürholz, A.-K., Harter, K., and Wolf, S. (2018). BRI1 controls vascular cell fate in the *Arabidopsis* root through RLP44 and phyto-sulfokine signaling. *Proceedings of the National Academy of Sciences of the United States of America*, 115(46):11838–11843.
- Hossain, Z., McGarvey, B., Amyot, L., Gruber, M., Jung, J., and Hannoufa, A. (2012). DIMINUTO 1 affects the lignin profile and secondary cell wall formation in *Arabidopsis*. *Planta*, 235(3):485–498.
- Hothorn, M., Belkhadir, Y., Dreux, M., Dabi, T., Noel, J. P., Wilson, I. A., and Chory, J. (2011). Structural basis of steroid hormone perception by the receptor kinase BRI1. *Nature*, 474(7352):467–71.
- Hruz, T., Laule, O., Szabo, G., Wessendorp, F., Bleuler, S., Oertle, L., Widmayer, P., Gruissem, W., and Zimmermann, P. (2008). Genevestigator v3: a reference expression database for the meta-analysis of transcriptomes. *Advances in bioinformatics*, 2008:420747.

- Hsu, J.-L., Wang, L.-Y., Wang, S.-Y., Lin, C.-H., Ho, K.-C., Shi, F.-K., and Chang, I.-F. (2009). Functional phosphoproteomic profiling of phosphorylation sites in membrane fractions of salt-stressed *Arabidopsis thaliana*. *Proteome science*, 7:42.
- Hu, Y. and Yu, D. (2014). BRASSINOSTEROID INSENSITIVE2 interacts with ABSCISIC ACID INSENSITIVE5 to mediate the antagonism of brassinosteroids to abscisic acid during seed germination in *Arabidopsis*. *The Plant cell*, 26(11):4394–408.
- Huang, D., Wu, W., Abrams, S. R., and Cutler, A. J. (2008). The relationship of drought-related gene expression in *Arabidopsis thaliana* to hormonal and environmental factors. *Journal of Experimental Botany*, 59(11):2991–3007.
- Ibañez, M., Fàbregas, N., Chory, J., and Caño-Delgado, A. I. (2009). Brassinosteroid signaling and auxin transport are required to establish the periodic pattern of *Arabidopsis* shoot vascular bundles. *Proceedings of the National Academy of Sciences of the United States of America*, 106(32):13630–13635.
- Inoue, S.-i., Iwashita, N., Takahashi, Y., Gotoh, E., Okuma, E., Hayashi, M., Tabata, R., Takemiya, A., Murata, Y., Doi, M., Kinoshita, T., and Shimazaki, K.-i. (2017). Brassinosteroid Involvement in *Arabidopsis thaliana* Stomatal Opening. *Plant and Cell Physiology*, 58(6):1048–1058.
- Isayenkov, S. V. and Maathuis, F. J. M. (2019). Plant Salinity Stress: Many Unanswered Questions Remain. *Frontiers in Plant Science*, 10:80.
- Isner, J. C., Begum, A., Nuehse, T., Hetherington, A. M., and Maathuis, F. J. M. (2018). KIN7 Kinase Regulates the Vacuolar TPK1 K⁺ Channel during Stomatal Closure. *Current biology : CB*, 28(3):466–472.e4.
- Iwata, S., Miyazawa, Y., Fujii, N., and Takahashi, H. (2013). MIZ1-regulated hydrotropism functions in the growth and survival of *Arabidopsis thaliana* under natural conditions. *Annals of Botany*, 112(1):103–114.
- Jaillais, Y., Hothorn, M., Belkhadir, Y., Dabi, T., Nimchuk, Z. L., Meyerowitz, E. M., and Chory, J. (2011). Tyrosine phosphorylation controls brassinosteroid receptor activation by triggering membrane release of its kinase inhibitor. *Genes & development*, 25(3):232–7.

- Kagale, S., Divi, U. K., Krochko, J. E., Keller, W. A., and Krishna, P. (2007). Brassinosteroid confers tolerance in *Arabidopsis thaliana* and *Brassica napus* to a range of abiotic stresses. *Planta*, 225(2):353–364.
- Kang, B., Wang, H., Nam, K. H., Li, J., and Li, J. (2010). Activation-Tagged Suppressors of a Weak Brassinosteroid Receptor Mutant. *Molecular Plant*, 3(1):260–268.
- Kang, Y. H., Breda, A., and Hardtke, C. S. (2017). Brassinosteroid signaling directs formative cell divisions and protophloem differentiation in *Arabidopsis* root meristems. *Development*, 144(2):272–280.
- Karlova, R., Boeren, S., Russinova, E., Aker, J., Vervoort, J., and de Vries, S. (2006). The *Arabidopsis* SOMATIC EMBRYOGENESIS RECEPTOR-LIKE KINASE1 Protein Complex Includes BRASSINOSTEROID-INSENSITIVE1. *The Plant Cell*, 18(3):626 LP – 638.
- Kauschmann, A., Jessop, A., Koncz, C., Szekeres, M., Willmitzer, L., and Altmann, T. (1996). Genetic evidence for an essential role of brassinosteroids in plant development. *The Plant Journal*, 9(5):701–713.
- Kemmerling, B., Schwedt, A., Rodriguez, P., Mazzotta, S., Frank, M., Qamar, S. A., Mengiste, T., Betsuyaku, S., Parker, J. E., Müssig, C., Thomma, B. P., Albrecht, C., de Vries, S. C., Hirt, H., and Nürnberger, T. (2007). The BRI1-Associated Kinase 1, BAK1, Has a Brassinolide-Independent Role in Plant Cell-Death Control. *Current Biology*, 17(13):1116–1122.
- Khripach, V., Zhabinskii, V., and de Groot, A. (2000). Twenty Years of Brassinosteroids: Steroidal Plant Hormones Warrant Better Crops for the XXI Century. *Annals of Botany*, 86(3):441–447.
- Kim, T.-W., Guan, S., Burlingame, A., and Wang, Z.-Y. (2011). The CDG1 Kinase Mediates Brassinosteroid Signal Transduction from BRI1 Receptor Kinase to BSU1 Phosphatase and GSK3-like Kinase BIN2. *Molecular Cell*, 43(4):561–571.
- Kinoshita, T., Caño-Delgado, A., Seto, H., Hiranuma, S., Fujioka, S., Yoshida, S., and Chory, J. (2005). Binding of brassinosteroids to the extracellular domain of plant receptor kinase BRI1. *Nature*, 433(7022):167–171.

- Klok, E. J., Wilson, I. W., Wilson, D., Chapman, S. C., Ewing, R. M., Somerville, S. C., Peacock, W. J., Dolferus, R., and Dennis, E. S. (2002). Expression profile analysis of the low-oxygen response in *Arabidopsis* root cultures. *The Plant cell*, 14(10):2481–94.
- Kooyers, N. J. (2015). The evolution of drought escape and avoidance in natural herbaceous populations. *Plant Science*, 234:155–162.
- Kopka, J., Schauer, N., Krueger, S., Birkemeyer, C., Usadel, B., Bergmuller, E., Dormann, P., Weckwerth, W., Gibon, Y., Stitt, M., Willmitzer, L., Fernie, A. R., and Steinhauser, D. (2005). GMD@CSB.DB: the Golm Metabolome Database. *Bioinformatics*, 21(8):1635–1638.
- Krasensky, J. and Jonak, C. (2012). Drought, salt, and temperature stress-induced metabolic rearrangements and regulatory networks. *Journal of Experimental Botany*, 63(4):1593–1608.
- Krishna, P. (2003). Brassinosteroid-Mediated Stress Responses. *Journal of Plant Growth Regulation*, 22(4):289–297.
- Kuromori, T., Seo, M., and Shinozaki, K. (2018). ABA Transport and Plant Water Stress Responses. *Trends in Plant Science*, 23(6):513–522.
- Lee, H.-S., Kim, Y., Pham, G., Kim, J. W., Song, J.-H., Lee, Y., Hwang, Y.-S., Roux, S. J., and Kim, S.-H. (2015). Brassinazole resistant 1 (BZR1)-dependent brassinosteroid signalling pathway leads to ectopic activation of quiescent cell division and suppresses columella stem cell differentiation. *Journal of experimental botany*, 66(15):4835–49.
- Lee, J., Shim, D., Moon, S., Kim, H., Bae, W., Kim, K., Kim, Y.-H., Rhee, S.-K., Hong, C. P., Hong, S.-Y., Lee, Y.-J., Sung, J., and Ryu, H. (2018). Genome-wide transcriptomic analysis of BR-deficient Micro-Tom reveals correlations between drought stress tolerance and brassinosteroid signaling in tomato. *Plant Physiology and Biochemistry*, 127:553–560.
- Lesk, C., Rowhani, P., and Ramankutty, N. (2016). Influence of extreme weather disasters on global crop production. *Nature*, 529(7584):84–87.

- Li, J. and Chory, J. (1997). A Putative Leucine-Rich Repeat Receptor Kinase Involved in Brassinosteroid Signal Transduction. *Cell*, 90(5):929–938.
- Li, J., Nagpal, P., Vitart, V., McMorris, T. C., and Chory, J. (1996). A role for brassinosteroids in light-dependent development of Arabidopsis. *Science*, 272(5260):398–401.
- Li, J., Nam, K. H., Vitart, V., McMorris, T. C., and Chory, J. (2002a). Regulation of brassinosteroid signaling by a GSK3/SHAGGY-like kinase. *Science*, 295(5558):1299–301.
- Li, J., Wen, J., Lease, K. A., Doke, J. T., Tax, F. E., and Walker, J. C. (2002b). BAK1, an Arabidopsis LRR Receptor-like Protein Kinase, Interacts with BRI1 and Modulates Brassinosteroid Signaling. *Cell*, 110(2):213–222.
- Lisec, J., Schauer, N., Kopka, J., Willmitzer, L., and Fernie, A. R. (2006). Gas chromatography mass spectrometry-based metabolite profiling in plants. *Nature Protocols*, 1(1):387–396.
- Lozano-Durán, R. and Zipfel, C. (2015). Trade-off between growth and immunity: role of brassinosteroids. *Trends in Plant Science*, 20(1):12–19.
- Lozano-Elena, F., Planas-Riverola, A., Vilarrasa-Blasi, J., Schwab, R., and Caño-Delgado, A. I. (2018). Paracrine brassinosteroid signaling at the stem cell niche controls cellular regeneration. *Journal of Cell Science*, 131(2):jcs204065.
- Luedemann, A., Strassburg, K., Erban, A., and Kopka, J. (2008). TagFinder for the quantitative analysis of gas chromatography—mass spectrometry (GC-MS)-based metabolite profiling experiments. *Bioinformatics*, 24(5):732–737.
- Mandava, N. B. (1988). Plant Growth-Promoting Brassinosteroids. *Annual Review of Plant Physiology and Plant Molecular Biology*, 39(1):23–52.
- Marti, E., Gisbert, C., Bishop, G. J., Dixon, M. S., and García-Martínez, J. L. (2006). Genetic and physiological characterization of tomato cv. Micro-Tom. *Journal of Experimental Botany*, 57(9):2037–2047.
- Martins, S., Montiel-Jorda, A., Cayrel, A., Huguet, S., Roux, C. P.-L., Ljung, K., and Vert, G. (2017). Brassinosteroid signaling-dependent root responses to prolonged elevated ambient temperature. *Nature communications*, 8(1):309.

- Meng, E. C., Pettersen, E. F., Couch, G. S., Huang, C. C., and Ferrin, T. E. (2006). Tools for integrated sequence-structure analysis with UCSF Chimera. *BMC Bioinformatics*, 7(1):339.
- Miao, R., Wang, M., Yuan, W., Ren, Y., Li, Y., Zhang, N., Zhang, J., Kronzucker, H. J., and Xu, W. (2018). Comparative Analysis of Arabidopsis Ecotypes Reveals a Role for Brassinosteroids in Root Hydrotropism. *Plant physiology*, 176(4):2720–2736.
- Minami, A., Takahashi, K., Inoue, S.-i., Tada, Y., and Kinoshita, T. (2019). Brassinosteroid Induces Phosphorylation of the Plasma Membrane H⁺-ATPase during Hypocotyl Elongation in Arabidopsis thaliana. *Plant and Cell Physiology*.
- Mira, M. M., Huang, S., Kapoor, K., Hammond, C., Hill, R. D., and Stasolla, C. (2017). Expression of Arabidopsis class 1 phytoglobin (AtPgb1) delays death and degradation of the root apical meristem during severe PEG-induced water deficit. *Journal of experimental botany*, 68(20):5653–5668.
- Mitchell, J. W., Mandava, N., Worley, J. F., Plimmer, J. R., and Smith, M. V. (1970). Brassins—a New Family of Plant Hormones from Rape Pollen. *Nature*, 225(5237):1065–1066.
- Mittler, R. (2017). ROS Are Good. *Trends in Plant Science*, 22(1):11–19.
- Mora-García, S., Vert, G., Yin, Y., Caño-Delgado, A., Cheong, H., and Chory, J. (2004). Nuclear protein phosphatases with Kelch-repeat domains modulate the response to brassinosteroids in Arabidopsis. *Genes & development*, 18(4):448–60.
- Mosca, R., Céol, A., Stein, A., Olivella, R., and Aloy, P. (2014). 3did: a catalog of domain-based interactions of known three-dimensional structure. *Nucleic Acids Research*, 42(D1):D374–D379.
- Nagata, N., Asami, T., and Yoshida, S. (2001). Brassinazole, an Inhibitor of Brassinosteroid Biosynthesis, Inhibits Development of Secondary Xylem in Cress Plants (*Lepidium sativum*). *Plant and Cell Physiology*, 42(9):1006–1011.
- Nakamura, A., Fujioka, S., Sunohara, H., Kamiya, N., Hong, Z., Inukai, Y., Miura, K., Takatsuto, S., Yoshida, S., Ueguchi-Tanaka, M., Hasegawa, Y., Kitano, H., and

- Matsuoka, M. (2006). The role of OsBRI1 and its homologous genes, OsBRL1 and OsBRL3, in rice. *Plant physiology*, 140(2):580–90.
- Nam, K. H. and Li, J. (2002). BRI1/BAK1, a Receptor Kinase Pair Mediating Brassinosteroid Signaling. *Cell*, 110(2):203–212.
- Nanjo, T., Kobayashi, M., Yoshiba, Y., Kakubari, Y., Yamaguchi-Shinozaki, K., and Shinozaki, K. (1999). Antisense suppression of proline degradation improves tolerance to freezing and salinity in *Arabidopsis thaliana*. *FEBS Letters*, 461(3):205–210.
- Nie, S., Huang, S., Wang, S., Mao, Y., Liu, J., Ma, R., and Wang, X. (2019). Enhanced brassinosteroid signaling intensity via SIBRI1 overexpression negatively regulates drought resistance in a manner opposite of that via exogenous BR application in tomato. *Plant Physiology and Biochemistry*, 138:36–47.
- Nie, W.-F., Wang, M.-M., Xia, X.-J., Zhou, Y.-H., Shi, K., Chen, Z., and Yu, J. Q. (2013). Silencing of tomato RBOH1 and MPK2 abolishes brassinosteroid-induced H₂O₂ generation and stress tolerance. *Plant, Cell & Environment*, 36(4):789–803.
- Niittylä, T., Fuglsang, A. T., Palmgren, M. G., Frommer, W. B., and Schulze, W. X. (2007). Temporal analysis of sucrose-induced phosphorylation changes in plasma membrane proteins of *Arabidopsis*. *Molecular & cellular proteomics : MCP*, 6(10):1711–26.
- Nishizawa-Yokoi, A., Yabuta, Y., and Shigeoka, S. (2008a). Galactinol and raffinose constitute a novel function to protect plants from oxidative damage. *Plant physiology*, 147(3):1251–63.
- Nishizawa-Yokoi, A., Yabuta, Y., and Shigeoka, S. (2008b). The contribution of carbohydrates including raffinose family oligosaccharides and sugar alcohols to protection of plant cells from oxidative damage. *Plant signaling & behavior*, 3(11):1016–8.
- Nolan, T. M., Brennan, B., Yang, M., Chen, J., Zhang, M., Li, Z., Wang, X., Bassham, D. C., Walley, J., and Yin, Y. (2017). Selective Autophagy of BES1 Mediated by DSK2 Balances Plant Growth and Survival. *Developmental cell*, 41(1):33–46.e7.
- Nuccio, M. L., Wu, J., Mowers, R., Zhou, H.-P., Meghji, M., Primavesi, L. F., Paul, M. J., Chen, X., Gao, Y., Haque, E., Basu, S. S., and Lagrimini, L. M. (2015).

- Expression of trehalose-6-phosphate phosphatase in maize ears improves yield in well-watered and drought conditions. *Nature Biotechnology*, 33(8):862–869.
- Ogita, N., Okushima, Y., Tokizawa, M., Yamamoto, Y. Y., Tanaka, M., Seki, M., Makita, Y., Matsui, M., Okamoto-Yoshiyama, K., Sakamoto, T., Kurata, T., Hiruma, K., Saijo, Y., Takahashi, N., and Umeda, M. (2018). Identifying the target genes of SUPPRESSOR OF GAMMA RESPONSE 1, a master transcription factor controlling DNA damage response in Arabidopsis. *The Plant Journal*, 94(3):439–453.
- Oh, E., Zhu, J.-Y., and Wang, Z.-Y. (2012). Interaction between BZR1 and PIF4 integrates brassinosteroid and environmental responses. *Nature Cell Biology*, 14(8):802–809.
- Oh, M.-H., Bender, K. W., Kim, S. Y., Wu, X., Lee, S., Nou, I.-S., Zielinski, R. E., Clouse, S. D., and Huber, S. C. (2015). Functional analysis of the BRI1 receptor kinase by Thr-for-Ser substitution in a regulatory autophosphorylation site. *Frontiers in Plant Science*, 6:562.
- Oh, M.-H., Ray, W. K., Huber, S. C., Asara, J. M., Gage, D. A., and Clouse, S. D. (2000). Recombinant Brassinosteroid Insensitive 1 Receptor-Like Kinase Autophosphorylates on Serine and Threonine Residues and Phosphorylates a Conserved Peptide Motif in Vitro. *Plant Physiology*, 124(2):751 – 766.
- Ohashi-Ito, K., Kubo, M., Demura, T., and Fukuda, H. (2005). Class III Homeodomain Leucine-Zipper Proteins Regulate Xylem Cell Differentiation. *Plant and Cell Physiology*, 46(10):1646–1656.
- Ortega-Martínez, O., Pernas, M., Carol, R. J., and Dolan, L. (2007). Ethylene modulates stem cell division in the Arabidopsis thaliana root. *Science*, 317(5837):507–10.
- Ossowski, S., Schwab, R., and Weigel, D. (2008). Gene silencing in plants using artificial microRNAs and other small RNAs. *The Plant Journal*, 53(4):674–690.
- Peng, P., Yan, Z., Zhu, Y., and Li, J. (2008). Regulation of the Arabidopsis GSK3-like kinase BRASSINOSTEROID-INSENSITIVE 2 through proteasome-mediated protein degradation. *Molecular plant*, 1(2):338–46.

- Perraki, A., DeFalco, T. A., Derbyshire, P., Avila, J., Séré, D., Sklenar, J., Qi, X., Stransfeld, L., Schwessinger, B., Kadota, Y., Macho, A. P., Jiang, S., Couto, D., Torii, K. U., Menke, F. L. H., and Zipfel, C. (2018). Phosphocode-dependent functional dichotomy of a common co-receptor in plant signalling. *Nature*, 561(7722):248–252.
- Pi, L., Aichinger, E., van der Graaff, E., Llavata-Peris, C., Weijers, D., Hennig, L., Groot, E., and Laux, T. (2015). Organizer-Derived WOX5 Signal Maintains Root Columella Stem Cells through Chromatin-Mediated Repression of CDF4 Expression. *Developmental Cell*, 33(5):576–588.
- Pierce, B. and Weng, Z. (2007). ZRANK: Reranking protein docking predictions with an optimized energy function. *Proteins: Structure, Function, and Bioinformatics*, 67(4):1078–1086.
- Planas-Riverola, A., Gupta, A., Betegón-Putze, I., Bosch, N., Ibañes, M., and Caño-Delgado, A. I. (2019). Brassinosteroid signaling in plant development and adaptation to stress. *Development*, 146(5):dev151894.
- Qi, X., Han, S.-K., Dang, J. H., Garrick, J. M., Ito, M., Hofstetter, A. K., and Torii, K. U. (2017). Autocrine regulation of stomatal differentiation potential by EPF1 and ERECTA-LIKE1 ligand-receptor signaling. *eLife*, 6.
- Rafael-Palou, X., Schroeder, M. P., and Lopez-Bigas, N. (2012). SVGMap: configurable image browser for experimental data. *Bioinformatics*, 28(1):119–120.
- Rahni, R. and Birnbaum, K. D. (2019). Week-long imaging of cell divisions in the Arabidopsis root meristem. *Plant Methods*, 15(1):30.
- Rajewska, I., Talarek, M., and Bajguz, A. (2016). Brassinosteroids and Response of Plants to Heavy Metals Action. *Frontiers in Plant Science*, 7:629.
- Rao, X. and Dixon, R. A. (2017). Brassinosteroid Mediated Cell Wall Remodeling in Grasses under Abiotic Stress. *Frontiers in plant science*, 8:806.
- Ren, H., Willige, B. C., Jaillais, Y., Geng, S., Park, M. Y., Gray, W. M., and Chory, J. (2019). BRASSINOSTEROID-SIGNALING KINASE 3, a plasma membrane-associated scaffold protein involved in early brassinosteroid signaling. *PLOS Genetics*, 15(1):e1007904.

- Rost, B. (1999). Twilight zone of protein sequence alignments. *Protein Engineering, Design and Selection*, 12(2):85–94.
- Russinova, E., Borst, J.-W., Kwaaitaal, M., Caño-Delgado, A., Yin, Y., Chory, J., and de Vries, S. C. (2004). Heterodimerization and endocytosis of Arabidopsis brassinosteroid receptors BRI1 and AtSERK3 (BAK1). *The Plant cell*, 16(12):3216–29.
- Ryu, H., Kim, K., Cho, H., Park, J., Choe, S., and Hwang, I. (2007). Nucleocytoplasmic Shuttling of BZR1 Mediated by Phosphorylation Is Essential in Arabidopsis Brassinosteroid Signaling. *The Plant Cell*, 19(9):2749–2762.
- Ryu, K. H., Huang, L., Kang, H. M., and Schiefelbein, J. (2019). Single-Cell RNA Sequencing Resolves Molecular Relationships Among Individual Plant Cells. *Plant physiology*, 179(4):1444–1456.
- Sabatini, S., Heidstra, R., Wildwater, M., and Scheres, B. (2003). SCARECROW is involved in positioning the stem cell niche in the Arabidopsis root meristem. *Genes & development*, 17(3):354–8.
- Sablowski, R. (2004). Plant and animal stem cells: conceptually similar, molecularly distinct? *Trends in Cell Biology*, 14(11):605–611.
- Sahni, S., Prasad, B. D., Liu, Q., Grbic, V., Sharpe, A., Singh, S. P., and Krishna, P. (2016). Overexpression of the brassinosteroid biosynthetic gene DWF4 in Brassica napus simultaneously increases seed yield and stress tolerance. *Scientific Reports*, 6(1):28298.
- Saito, M., Kondo, Y., and Fukuda, H. (2018). BES1 and BZR1 Redundantly Promote Phloem and Xylem Differentiation. *Plant and Cell Physiology*, 59(3):590–600.
- Salazar-Henao, J. E., Lehner, R., Betegón-Putze, I., Vilarrasa-Blasi, J., and Caño-Delgado, A. I. (2016). BES1 regulates the localization of the brassinosteroid receptor BRL3 within the provascular tissue of the Arabidopsis primary root. *Journal of experimental botany*, 67(17):4951–61.
- Šali, A. and Blundell, T. L. (1993). Comparative Protein Modelling by Satisfaction of Spatial Restraints. *Journal of Molecular Biology*, 234(3):779–815.

- Salic, A. and Mitchison, T. J. (2008). A chemical method for fast and sensitive detection of DNA synthesis in vivo. *Proceedings of the National Academy of Sciences of the United States of America*, 105(7):2415–20.
- Samish, I., Bourne, P. E., and Najmanovich, R. J. (2015). Achievements and challenges in structural bioinformatics and computational biophysics. *Bioinformatics*, 31(1):146–150.
- Sánchez-Rodríguez, C., Ketelaar, K., Schneider, R., Villalobos, J. A., Somerville, C. R., Persson, S., and Wallace, I. S. (2017). BRASSINOSTEROID INSENSITIVE2 negatively regulates cellulose synthesis in Arabidopsis by phosphorylating cellulose synthase 1. *Proceedings of the National Academy of Sciences of the United States of America*, 114(13):3533–3538.
- Sander, C. and Schneider, R. (1991). Database of homology-derived protein structures and the structural meaning of sequence alignment. *Proteins: Structure, Function, and Genetics*, 9(1):56–68.
- Santiago, J., Henzler, C., and Hothorn, M. (2013). Molecular Mechanism for Plant Steroid Receptor Activation by Somatic Embryogenesis Co-Receptor Kinases. *Science*, 341(6148):889–892.
- Sarkar, A. K., Luijten, M., Miyashima, S., Lenhard, M., Hashimoto, T., Nakajima, K., Scheres, B., Heidstra, R., and Laux, T. (2007). Conserved factors regulate signalling in Arabidopsis thaliana shoot and root stem cell organizers. *Nature*, 446(7137):811–814.
- Savaldi-Goldstein, S., Peto, C., and Chory, J. (2007). The epidermis both drives and restricts plant shoot growth. *Nature*, 446(7132):199–202.
- Scheres, B. (2007). Stem-cell niches: nursery rhymes across kingdoms. *Nature Reviews Molecular Cell Biology*, 8(5):345–354.
- Schwab, R., Ossowski, S., Riester, M., Warthmann, N., and Weigel, D. (2006). Highly specific gene silencing by artificial microRNAs in Arabidopsis. *The Plant cell*, 18(5):1121–33.

- Seki, M., Umezawa, T., Urano, K., and Shinozaki, K. (2007). Regulatory metabolic networks in drought stress responses. *Current Opinion in Plant Biology*, 10(3):296–302.
- Shakirova, F., Allagulova, C., Maslennikova, D., Fedorova, K., Yuldashev, R., Lubyanova, A., Bezrukova, M., and Avalbaev, A. (2016). Involvement of dehydrins in 24-epibrassinolide-induced protection of wheat plants against drought stress. *Plant Physiology and Biochemistry*, 108:539–548.
- Shao, H.-B., Chu, L.-Y., Jaleel, C. A., and Zhao, C.-X. (2008). Water-deficit stress-induced anatomical changes in higher plants. *Comptes Rendus Biologies*, 331(3):215–225.
- She, J., Han, Z., Kim, T.-W., Wang, J. J., Cheng, W., Chang, J., Shi, S., Wang, J. J., Yang, M., Wang, Z.-Y., and Chai, J. (2011). Structural insight into brassinosteroid perception by BRI1. *Nature*, 474(7352):472–476.
- She, J., Han, Z., Zhou, B., and Chai, J. (2013). Structural basis for differential recognition of brassinolide by its receptors. *Protein & cell*, 4(6):475–82.
- Sheen, J. (1994). Feedback control of gene expression. *Photosynthesis Research*, 39(3):427–438.
- Shinozaki, Y., Nicolas, P., Fernandez-Pozo, N., Ma, Q., Evanich, D. J., Shi, Y., Xu, Y., Zheng, Y., Snyder, S. I., Martin, L. B. B., Ruiz-May, E., Thannhauser, T. W., Chen, K., Domozych, D. S., Catalá, C., Fei, Z., Mueller, L. A., Giovannoni, J. J., and Rose, J. K. C. (2018). High-resolution spatiotemporal transcriptome mapping of tomato fruit development and ripening. *Nature Communications*, 9(1):364.
- Shkolnik, D., Nuriel, R., Bonza, M. C., Costa, A., and Fromm, H. (2018). MIZ1 regulates ECA1 to generate a slow, long-distance phloem-transmitted Ca²⁺ signal essential for root water tracking in Arabidopsis. *Proceedings of the National Academy of Sciences of the United States of America*, 115(31):8031–8036.
- Shulse, C. N., Cole, B. J., Ciobanu, D., Lin, J., Yoshinaga, Y., Gouran, M., Turco, G. M., Zhu, Y., O’Malley, R. C., Brady, S. M., and Dickel, D. E. (2019). High-Throughput Single-Cell Transcriptome Profiling of Plant Cell Types. *Cell Reports*, 27(7):2241–2247.e4.

- Singh, T., Aspinall, D., and Paleg, L. (1972). Proline Accumulation and Varietal Adaptability to Drought in Barley: a Potential Metabolic Measure of Drought Resistance. *Nature New Biology*, 236(67):188–190.
- Smakowska-Luzan, E., Mott, G. A., Parys, K., Stegmann, M., Howton, T. C., Layeghifard, M., Neuhold, J., Lehner, A., Kong, J., Grünwald, K., Weinberger, N., Satbhai, S. B., Mayer, D., Busch, W., Madalinski, M., Stolt-Bergner, P., Provart, N. J., Mukhtar, M. S., Zipfel, C., Desveaux, D., Guttman, D. S., and Belkhadir, Y. (2018). An extracellular network of Arabidopsis leucine-rich repeat receptor kinases. *Nature*, 553(7688):342–346.
- Springmann, M., Clark, M., Mason-D’Croz, D., Wiebe, K., Bodirsky, B. L., Las-saletta, L., de Vries, W., Vermeulen, S. J., Herrero, M., Carlson, K. M., Jonell, M., Troell, M., DeClerck, F., Gordon, L. J., Zurayk, R., Scarborough, P., Rayner, M., Loken, B., Fanzo, J., Godfray, H. C. J., Tilman, D., Rockström, J., and Willett, W. (2018). Options for keeping the food system within environmental limits. *Nature*, 562(7728):519–525.
- Sreeramulu, S., Mostizky, Y., Sunitha, S., Shani, E., Nahum, H., Salomon, D., Hayun, L. B., Gruetter, C., Rauh, D., Ori, N., and Sessa, G. (2013). BSKs are partially redundant positive regulators of brassinosteroid signaling in Arabidopsis. *The Plant Journal*, 74(6):905–919.
- Sun, Y., Fan, X.-Y., Cao, D.-M., Tang, W., He, K., Zhu, J.-Y., He, J.-X., Bai, M.-Y., Zhu, S., Oh, E., Patil, S., Kim, T.-W., Ji, H., Wong, W. H., Rhee, S. Y., and Wang, Z.-Y. (2010). Integration of Brassinosteroid Signal Transduction with the Transcription Network for Plant Growth Regulation in Arabidopsis. *Developmental Cell*, 19(5):765–777.
- Sun, Y., Han, Z., Tang, J., Hu, Z., Chai, C., Zhou, B., and Chai, J. (2013a). Structure reveals that BAK1 as a co-receptor recognizes the BRI1-bound brassinolide. *Cell Research*, 23(11):1326–1329.
- Sun, Y., Li, L., Macho, A. P., Han, Z., Hu, Z., Zipfel, C., Zhou, J.-M., and Chai, J. (2013b). Structural Basis for flg22-Induced Activation of the Arabidopsis FLS2-BAK1 Immune Complex. *Science*, 342(6158):624–628.

- Szabados, L. and Saviouré, A. (2010). Proline: a multifunctional amino acid. *Trends in Plant Science*, 15(2):89–97.
- Szekeres, M., Németh, K., Koncz-Kálmán, Z., Mathur, J., Kauschmann, A., Altmann, T., Rédei, G. P., Nagy, F., Schell, J., and Koncz, C. (1996). Brassinosteroids Rescue the Deficiency of CYP90, a Cytochrome P450, Controlling Cell Elongation and Detiolation in Arabidopsis. *Cell*, 85(2):171–182.
- Takahashi, N., Goto, N., Okada, K., and Takahashi, H. (2002). Hydrotropism in abscisic acid, wavy, and gravitropic mutants of Arabidopsis thaliana. *Planta*, 216(2):203–211.
- Tang, W., Kim, T.-W., Osés-Prieto, J. A., Sun, Y., Deng, Z., Zhu, S., Wang, R., Burlingame, A. L., and Wang, Z.-Y. (2008). BSKs mediate signal transduction from the receptor kinase BRI1 in Arabidopsis. *Science*, 321(5888):557–60.
- Tang, W., Yuan, M., Wang, R., Yang, Y., Wang, C., Osés-Prieto, J. A., Kim, T.-W., Zhou, H.-W., Deng, Z., Gampala, S. S., Gendron, J. M., Jonassen, E. M., Lillo, C., DeLong, A., Burlingame, A. L., Sun, Y., and Wang, Z.-Y. (2011). PP2A activates brassinosteroid-responsive gene expression and plant growth by dephosphorylating BZR1. *Nature Cell Biology*, 13(2):124–131.
- Tanveer, M., Shahzad, B., Sharma, A., Biju, S., and Bhardwaj, R. (2018). 24-Epibrassinolide; an active brassinolide and its role in salt stress tolerance in plants: A review. *Plant Physiology and Biochemistry*, 130:69–79.
- Tanveer, M., Shahzad, B., Sharma, A., and Khan, E. A. (2019). 24-Epibrassinolide application in plants: An implication for improving drought stress tolerance in plants. *Plant Physiology and Biochemistry*, 135:295–303.
- Tapia-López, R., García-Ponce, B., Dubrovsky, J. G., Garay-Arroyo, A., Pérez-Ruíz, R. V., Kim, S.-H., Acevedo, F., Pelaz, S., and Alvarez-Buylla, E. R. (2008). An AGAMOUS-related MADS-box gene, XAL1 (AGL12), regulates root meristem cell proliferation and flowering transition in Arabidopsis. *Plant physiology*, 146(3):1182–92.
- Tardieu, F. (2012). Any trait or trait-related allele can confer drought tolerance: just design the right drought scenario. *Journal of Experimental Botany*, 63(1):25–31.

- Tenhaken, R. (2015). Cell wall remodeling under abiotic stress. *Frontiers in Plant Science*, 5:771.
- Thummel, C. S. and Chory, J. (2002). Steroid signaling in plants and insects—common themes, different pathways. *Genes & development*, 16(24):3113–29.
- Tian, Y., Fan, M., Qin, Z., Lv, H., Wang, M., Zhang, Z., Zhou, W., Zhao, N., Li, X., Han, C., Ding, Z., Wang, W., Wang, Z.-Y., and Bai, M.-Y. (2018). Hydrogen peroxide positively regulates brassinosteroid signaling through oxidation of the BRASSINAZOLE-RESISTANT1 transcription factor. *Nature Communications*, 9(1):1063.
- Todaka, D., Shinozaki, K., and Yamaguchi-Shinozaki, K. (2015). Recent advances in the dissection of drought-stress regulatory networks and strategies for development of drought-tolerant transgenic rice plants. *Frontiers in Plant Science*, 6:84.
- Truernit, E. and Haseloff, J. (2008). A simple way to identify non-viable cells within living plant tissue using confocal microscopy. *Plant Methods*, 4(1):15.
- Tunc-Ozdemir, M. and Jones, A. M. (2017). BRL3 and AtRGS1 cooperate to fine tune growth inhibition and ROS activation. *PloS one*, 12(5):e0177400–e0177400.
- Tunc-Ozdemir, M., Li, B., Jaiswal, D. K., Urano, D., Jones, A. M., and Torres, M. P. (2017). Predicted Functional Implications of Phosphorylation of Regulator of G Protein Signaling Protein in Plants. *Frontiers in plant science*, 8:1456.
- Ullah, H., Chen, J. G., Young, J. C., Im, K. H., Sussman, M. R., Jones, A. M., and Siderovski, D. P. (2001). Modulation of cell proliferation by heterotrimeric G protein in Arabidopsis. *Science*, 292(5524):2066–9.
- Urano, K., Maruyama, K., Ogata, Y., Morishita, Y., Takeda, M., Sakurai, N., Suzuki, H., Saito, K., Shibata, D., Kobayashi, M., Yamaguchi-Shinozaki, K., and Shinozaki, K. (2009). Characterization of the ABA-regulated global responses to dehydration in Arabidopsis by metabolomics. *The Plant Journal*, 57(6):1065–1078.
- Valls-Comamala, V., Guivernau, B., Bonet, J., Puig, M., Perálvarez-Marín, A., Palomer, E., Fernández-Busquets, X., Altafaj, X., Tajés, M., Puig-Pijoan, A., Vicente, R., Oliva, B., and Muñoz, F. J. (2017). The antigen-binding fragment of

- human gamma immunoglobulin prevents amyloid beta-peptide folding into beta-sheet to form oligomers. *Oncotarget*, 8(25):41154–41165.
- van den Berg, C., Willemsen, V., Hendriks, G., Weisbeek, P., and Scheres, B. (1997). Short-range control of cell differentiation in the Arabidopsis root meristem. *Nature*, 390(6657):287–289.
- Vert, G. and Chory, J. (2006). Downstream nuclear events in brassinosteroid signalling. *Nature*, 441(7089):96–100.
- Vialaret, J., Di Pietro, M., Hem, S., Maurel, C., Rossignol, M., and Santoni, V. (2014). Phosphorylation dynamics of membrane proteins from Arabidopsis roots submitted to salt stress. *Proteomics*, 14(9):1058–1070.
- Vilarrasa-Blasi, J., González-García, M.-P., Frigola, D., Fàbregas, N., Alexiou, K., López-Bigas, N., Rivas, S., Jauneau, A., Lohmann, J., Benfey, P., Ibañez, M., and Caño-Delgado, A. (2014). Regulation of Plant Stem Cell Quiescence by a Brassinosteroid Signaling Module. *Developmental Cell*, 30(1):36–47.
- Vragović, K., Sela, A., Friedlander-Shani, L., Fridman, Y., Hacham, Y., Holland, N., Bartom, E., Mockler, T. C., and Savaldi-Goldstein, S. (2015). Translatome analyses capture of opposing tissue-specific brassinosteroid signals orchestrating root meristem differentiation. *Proceedings of the National Academy of Sciences of the United States of America*, 112(3):923–8.
- Vukašinović, N. and Russinova, E. (2018). BRexit: Possible Brassinosteroid Export and Transport Routes. *Trends in Plant Science*, 23(4):285–292.
- Wang, H. and Mao, H. (2014). On the Origin and Evolution of Plant Brassinosteroid Receptor Kinases. *Journal of Molecular Evolution*, 78(2):118–129.
- Wang, H., Yang, C., Zhang, C., Wang, N., Lu, D., Wang, J., Zhang, S., Wang, Z.-X., Ma, H., and Wang, X. (2011). Dual Role of BKI1 and 14-3-3 s in Brassinosteroid Signaling to Link Receptor with Transcription Factors. *Developmental Cell*, 21(5):825–834.
- Wang, J., Jiang, J., Wang, J., Chen, L., Fan, S.-L., Wu, J.-W., Wang, X., and Wang, Z.-X. (2014). Structural insights into the negative regulation of BRI1 signaling by BRI1-interacting protein BKI1. *Cell Research*, 24(11):1328–1341.

- Wang, X. and Chory, J. (2006). Brassinosteroids Regulate Dissociation of BKI1, a Negative Regulator of BRI1 Signaling, from the Plasma Membrane. *Science*, 313(5790):1118–1122.
- Wang, X., Goshe, M. B., Soderblom, E. J., Phinney, B. S., Kuchar, J. A., Li, J., Asami, T., Yoshida, S., Huber, S. C., and Clouse, S. D. (2005a). Identification and functional analysis of in vivo phosphorylation sites of the Arabidopsis BRASSINOSTEROID-INSENSITIVE1 receptor kinase. *The Plant cell*, 17(6):1685–703.
- Wang, X., Kota, U., He, K., Blackburn, K., Li, J., Goshe, M. B., Huber, S. C., and Clouse, S. D. (2008). Sequential Transphosphorylation of the BRI1/BAK1 Receptor Kinase Complex Impacts Early Events in Brassinosteroid Signaling. *Developmental Cell*, 15(2):220–235.
- Wang, X., Li, X., Meisenhelder, J., Hunter, T., Yoshida, S., Asami, T., and Chory, J. (2005b). Autoregulation and Homodimerization Are Involved in the Activation of the Plant Steroid Receptor BRI1. *Developmental Cell*, 8(6):855–865.
- Wang, Z.-Y., Nakano, T., Gendron, J., He, J., Chen, M., Vafeados, D., Yang, Y., Fujioka, S., Yoshida, S., Asami, T., and Chory, J. (2002). Nuclear-Localized BZR1 Mediates Brassinosteroid-Induced Growth and Feedback Suppression of Brassinosteroid Biosynthesis. *Developmental Cell*, 2(4):505–513.
- Wang, Z.-Y., Seto, H., Fujioka, S., Yoshida, S., and Chory, J. (2001). BRI1 is a critical component of a plasma-membrane receptor for plant steroids. *Nature*, 410(6826):380–383.
- Wilma van Esse, G., Westphal, A. H., Surendran, R. P., Albrecht, C., van Veen, B., Borst, J. W., and de Vries, S. C. (2011). Quantification of the brassinosteroid insensitive1 receptor in planta. *Plant physiology*, 156(4):1691–700.
- Winter, D., Vinegar, B., Nahal, H., Ammar, R., Wilson, G. V., and Provart, N. J. (2007). An "Electronic Fluorescent Pictograph" browser for exploring and analyzing large-scale biological data sets. *PloS one*, 2(8):e718.
- Wolf, S., Mravec, J., Greiner, S., Mouille, G., and Höfte, H. (2012). Plant Cell Wall Homeostasis Is Mediated by Brassinosteroid Feedback Signaling. *Current Biology*, 22(18):1732–1737.

- Wu, C.-H., Derevnina, L., and Kamoun, S. (2018a). Receptor networks underpin plant immunity. *Science*, 360(6395):1300–1301.
- Wu, C.-y., Trieu, A., Radhakrishnan, P., Kwok, S. F., Harris, S., Zhang, K., Wang, J., Wan, J., Zhai, H., Takatsuto, S., Matsumoto, S., Fujioka, S., Feldmann, K. A., and Pennell, R. I. (2008). Brassinosteroids regulate grain filling in rice. *The Plant cell*, 20(8):2130–45.
- Wu, D., Liu, Y., Xu, F., and Zhang, Y. (2018b). Differential requirement of BAK1 C-terminal tail in development and immunity. *Journal of Integrative Plant Biology*, 60(4):270–275.
- Wu, X. N., Rodriguez, C. S., Pertl-Obermeyer, H., Obermeyer, G., and Schulze, W. X. (2013). Sucrose-induced Receptor Kinase SIRK1 Regulates a Plasma Membrane Aquaporin in Arabidopsis. *Molecular & Cellular Proteomics*, 12(10):2856–2873.
- Xia, X.-J., Wang, Y.-J., Zhou, Y.-H., Tao, Y., Mao, W.-H., Shi, K., Asami, T., Chen, Z., and Yu, J.-Q. (2009). Reactive oxygen species are involved in brassinosteroid-induced stress tolerance in cucumber. *Plant physiology*, 150(2):801–14.
- Xia, X.-J., Zhou, Y.-H., Shi, K., Zhou, J., Foyer, C. H., and Yu, J.-Q. (2015). Interplay between reactive oxygen species and hormones in the control of plant development and stress tolerance. *Journal of Experimental Botany*, 66(10):2839–2856.
- Xie, L., Yang, C., and Wang, X. (2011). Brassinosteroids can regulate cellulose biosynthesis by controlling the expression of CESA genes in Arabidopsis. *Journal of Experimental Botany*, 62(13):4495–4506.
- Xu, F., Xi, Z.-m., Zhang, H., Zhang, C.-j., and Zhang, Z.-w. (2015). Brassinosteroids are involved in controlling sugar unloading in *Vitis vinifera* ‘Cabernet Sauvignon’ berries during véraison. *Plant Physiology and Biochemistry*, 94:197–208.
- Xu, P., Xu, S.-L., Li, Z.-J., Tang, W., Burlingame, A. L., and Wang, Z.-Y. (2014). A Brassinosteroid-Signaling Kinase Interacts with Multiple Receptor-Like Kinases in Arabidopsis. *Molecular Plant*, 7(2):441–444.
- Yan, L., Ma, Y., Liu, D., Wei, X., Sun, Y., Chen, X., Zhao, H., Zhou, J., Wang, Z., Shui, W., and Lou, Z. (2012). Structural basis for the impact of phosphorylation on the activation of plant receptor-like kinase BAK1. *Cell Research*, 22(8):1304–1308.

- Ye, H., Liu, S., Tang, B., Chen, J., Xie, Z., Nolan, T. M., Jiang, H., Guo, H., Lin, H.-Y., Li, L., Wang, Y., Tong, H., Zhang, M., Chu, C., Li, Z., Aluru, M., Aluru, S., Schnable, P. S., and Yin, Y. (2017). RD26 mediates crosstalk between drought and brassinosteroid signalling pathways. *Nature communications*, 8:14573.
- Ye, Q., Zhu, W., Li, L., Zhang, S., Yin, Y., Ma, H., and Wang, X. (2010). Brassinosteroids control male fertility by regulating the expression of key genes involved in Arabidopsis anther and pollen development. *Proceedings of the National Academy of Sciences of the United States of America*, 107(13):6100–5.
- Yin, Y., Qin, K., Song, X., Zhang, Q., Zhou, Y., Xia, X., and Yu, J. (2018). BZR1 Transcription Factor Regulates Heat Stress Tolerance Through FERONIA Receptor-Like Kinase-Mediated Reactive Oxygen Species Signaling in Tomato. *Plant and Cell Physiology*, 59(11):2239–2254.
- Yin, Y., Vafeados, D., Tao, Y., Yoshida, S., Asami, T., and Chory, J. (2005). A New Class of Transcription Factors Mediates Brassinosteroid-Regulated Gene Expression in Arabidopsis. *Cell*, 120(2):249–259.
- Yin, Y., Wang, Z.-Y., Mora-Garcia, S., Li, J., Yoshida, S., Asami, T., and Chory, J. (2002). BES1 Accumulates in the Nucleus in Response to Brassinosteroids to Regulate Gene Expression and Promote Stem Elongation. *Cell*, 109(2):181–191.
- Yokota, T., Ohnishi, T., Shibata, K., Asahina, M., Nomura, T., Fujita, T., Ishizaki, K., and Kohchi, T. (2017). Occurrence of brassinosteroids in non-flowering land plants, liverwort, moss, lycophyte and fern. *Phytochemistry*, 136:46–55.
- Yoshida, T., Mogami, J., and Yamaguchi-Shinozaki, K. (2014). ABA-dependent and ABA-independent signaling in response to osmotic stress in plants. *Current Opinion in Plant Biology*, 21:133–139.
- Yu, Q., Tian, H., Yue, K., Liu, J., Zhang, B., Li, X., and Ding, Z. (2016). A P-Loop NTPase Regulates Quiescent Center Cell Division and Distal Stem Cell Identity through the Regulation of ROS Homeostasis in Arabidopsis Root. *PLOS Genetics*, 12(9):e1006175.
- Yu, X., Li, L., Zola, J., Aluru, M., Ye, H., Foudree, A., Guo, H., Anderson, S., Aluru, S., Liu, P., Rodermel, S., and Yin, Y. (2011). A brassinosteroid transcriptional

- network revealed by genome-wide identification of BES1 target genes in *Arabidopsis thaliana*. *The Plant Journal*, 65(4):634–646.
- Yuan, W., Li, Y., Li, L., Siao, W., Zhang, Q., Zhang, Y., Liu, J., Xu, W., and Miao, R. (2018). BR-INSENSITIVE1 regulates hydrotropic response by interacting with plasma membrane H⁺-ATPases in *Arabidopsis*. *Plant Signaling & Behavior*, pages 1–5.
- Yun, H. S., Bae, Y. H., Lee, Y. J., Chang, S. C., Kim, S.-K., Li, J., and Nam, K. H. (2009). Analysis of phosphorylation of the BRI1/BAK1 complex in *Arabidopsis* reveals amino acid residues critical for receptor formation and activation of BR signaling. *Molecules and Cells*, 27(2):183–190.
- Zhang, H., Han, W., De Smet, I., Talboys, P., Loya, R., Hassan, A., Rong, H., Jürgens, G., Paul Knox, J., and Wang, M.-H. (2010). ABA promotes quiescence of the quiescent centre and suppresses stem cell differentiation in the *Arabidopsis* primary root meristem. *The Plant Journal*, 64(5):764–774.
- Zhang, S., Cai, Z., and Wang, X. (2009). The primary signaling outputs of brassinosteroids are regulated by abscisic acid signaling. *Proceedings of the National Academy of Sciences*, 106(11):4543–4548.
- Zhang, W., Morris, Q. D., Chang, R., Shai, O., Bakowski, M. A., Mitsakakis, N., Mohammad, N., Robinson, M. D., Zirngibl, R., Somogyi, E., Laurin, N., Eftekharpour, E., Sat, E., Grigull, J., Pan, Q., Peng, W.-T., Krogan, N., Greenblatt, J., Fehlings, M., van der Kooy, D., Aubin, J., Bruneau, B. G., Rossant, J., Blencowe, B. J., Frey, B. J., and Hughes, T. R. (2004). The functional landscape of mouse gene expression. *Journal of biology*, 3(5):21.
- Zhang, W., Swarup, R., Bennett, M., Schaller, G., and Kieber, J. (2013). Cytokinin Induces Cell Division in the Quiescent Center of the *Arabidopsis* Root Apical Meristem. *Current Biology*, 23(20):1979–1989.
- Zhang, X., Henriques, R., Lin, S.-S., Niu, Q.-W., and Chua, N.-H. (2006). *Agrobacterium*-mediated transformation of *Arabidopsis thaliana* using the floral dip method. *Nature Protocols*, 1(2):641–646.

- Zhiponova, M. K., Vanhoutte, I., Boudolf, V., Betti, C., Dhondt, S., Coppens, F., Mylle, E., Maes, S., González-García, M.-P., Caño-Delgado, A. I., Inzé, D., Beemster, G. T. S., De Veylder, L., and Russinova, E. (2013). Brassinosteroid production and signaling differentially control cell division and expansion in the leaf. *New Phytologist*, 197(2):490–502.
- Zhou, A., Wang, H., Walker, J. C., and Li, J. (2004). BRL1, a leucine-rich repeat receptor-like protein kinase, is functionally redundant with BRI1 in regulating Arabidopsis brassinosteroid signaling. *The Plant Journal*, 40(3):399–409.
- Zhou, J., Wang, J., Li, X., Xia, X.-J., Zhou, Y.-H., Shi, K., Chen, Z., and Yu, J.-Q. (2014). H₂O₂ mediates the crosstalk of brassinosteroid and abscisic acid in tomato responses to heat and oxidative stresses. *Journal of Experimental Botany*, 65(15):4371–4383.

Acknowledgements

I would like to dedicate this PhD thesis to all people that supported me since, during and until the thesis finalization.

I sincerely thank all the people that believed in me. It is not only science and knowledge what it is generated, but also a critical vision of our reality. Thank you for helping me conquer this personal achievement.

La ciencia...

Muchas gracias a Dra. Ana Conesa por abrirme las puertas de su laboratorio e introducirme en la estadística y bioinformática. En tu laboratorio descubrí otra forma de plantearme preguntas y otro modo de responderlas. Muchas gracias también a Prof. Baldomero Oliva por compartir sus herramientas computacionales y mostrarnos una visión estructural de la biología. Me has acercado a lo que creo que es una ciencia más teórica pero con un gran potencial. Tu punto de vista ha sido determinante en la última etapa de esta tesis y marcará futuros trabajos. Gracias también a Gonzalo por ayudarme a materializar mis abstractas ideas.

Norma es un honor para mí haber sido tu alumno y poder ser coautor de ese magnífico artículo que presento en el capítulo 3. Como habrás notado, en la tesis cito sin parar tus publicaciones y tu tesis. Es por algo. Este trabajo es una continuación natural de las bases que sentaste en este laboratorio y estoy convencido de que seguirán sustentando más descubrimientos. Gracias por ser mi mentora y enseñarme a trabajar con precisión, elegancia y diligencia. Esta tesis no hubiera sido posible sin ti. Ana, no ha sido fácil ni rápido pero parece que la cosa no ha ido mal. Te agradezco

enormemente la gran apuesta que hiciste por mí desde el primerísimo momento. Juegas fuerte, y eso lo admiro. De tu laboratorio me quedo sin duda con esa autoconfianza que inculcas y la sana ambición de querer jugar en *champions*. Gracias también por la libertad que me diste para aprender a volar. Espero que podamos seguir trabajando juntos en el futuro.

Los amigos...

Una cosa importante que aprendí durante estos años es que todos somos personas. Todos. Y finalizar la tesis sin amigos es sencillamente imposible. Por eso me gustaría agradecer y dedicar esta tesis a todas las personas que han convertido esta etapa vital en algo fascinante.

Dentro del laboratorio...

Thank you very much to all my colleagues of *cañolab*. Sharing this space-time in close proximity with you has been a wonderful experience. You are a great team. Very often we have shown to be able to save ourselves, which is admirable. This is why I totally trust in you and in the future you can count on me for anything. Dentro de este gran equipo quiero agradecer especialmente a Nadja y David. Empezamos juntos esta aventura y hemos visto crecer el laboratorio a un ritmo vertiginoso. Os agradezco todas esas discusiones tan técnicas en las que acabamos gritándonos. Fueron la base de todo el trabajo experimental bien hecho que vino después. Nadja te deseo lo mejor en tu tesis y puedes contar con mi apoyo para cualquier experimento que te propongas (incluso para hacer las estadísticas del Betis si hace falta). Un cándido agradecimiento para Ainoa y todos los estudiantes que tuve. De todos aprendí algo. Y aún más importante es que me hicisteis aprender de mí mismo. Me llevo de vosotros muchas habilidades. No figurarán en ningún CV, pero son igualmente valiosas. Gracias también a toda la gente increíble que conocí en Florida, fue como un segundo Erasmus y gracias por aquel inolvidable viaje por el *deep south*. Thank you Raymond for opening me the door of your house and helping me with the adaptation to the american life. You were an amazing roommate. Norma, otro agradecimiento enorme también en este párrafo. Porque además de mi mentora fuiste amiga y me enseñaste muchas otras cosas, por ejemplo que ser científico y fiestero es perfectamente compatible, incluso bueno. Si la ciencia avanza es porque hay científicos que, como tú, son magníficas personas. Moltes graciès Norma.

Fuera del laboratorio...

Un gran enorme GRACIAS se merecen esos *leftovers* del máster de genética (+incorporaciones). Habéis sido mi familia en Barcelona y es una relación que ha madurado a la par que la tesis. Me encanta hablar de cosas no *100tifikas* con vosotros, a pesar de ser *100tifikos*. Siempre entre risas. Me habéis enseñado que los buenos científicos son necesariamente buenas personas y aún mejores compañeros de parranda. People of *Barna shore* y amigos de la Uni, que no pare la cosa. Son muchos años ya desde *Lleideee* y seguimos compartiendo momentos. Habéis sido la red de seguridad en todo esta etapa. El jardín donde escapar y desconectar. Muchas gracias. Especial mención al físico loco con síndrome de Peter Pan: Aunque sea difícil de creer, tus pocos ortodoxos argumentos para seguir en la academia son los más convincentes de todos. Fer, si las circunstancias se dan fundaremos esa empresa, no lo dudes. En cualquier caso, gracias por estar ahí en lo bueno y en lo malo.

La familia...

Gracias Papá y Mamá por vuestro incondicional apoyo. Me habéis demostrado ser como las plantas que analizo en esta tesis. A pesar de las circunstancias, a pesar del estrés, vuestra generosidad, cariño y fé en mi han sido imperturbables. Sin duda esas son las raíces que sustentan todo lo demás, incluida esta tesis. Gracias Anita por tus lecciones de vida y perdóname por volar del nido tan pronto. Prometo pasar más tiempo contigo como *Phylosophy Doctor*, porque eres una fuente constante de ideas y porque te quiero mucho. Me gustaría especialmente que tomaras esta tesis como ejemplo de lo que somos capaces con esfuerzo y que te sirva de inspiración en los momentos de flaqueza.

Agradecimientos sinceros a la familia Figueroa por su calidez y apoyo. En esta tesis hay olor y sabor a Colombia.

Y finalmente, te quiero dedicar cada palabra de esta tesis a ti, Silvia. No hay buena ciencia si no hay buenas personas. Y no hay buenas personas sin amor. Eso me lo has enseñado tú. Si esta tesis ha sido exitosa es porque tu cariño y tu apoyo sincero, a pesar de mis temporadas en *modo piedra*, ha sido constante y ahora ha florecido con fuerza y hermosura. Que quede bien claro que detrás de los tecnicismos, cada frase de esta tesis esconde una declaración de amor y entre cada párrafo he dejado un infinito espacio para los dos. Este trabajo es fruto del amor que me has brindado. Te regalo mi tesis. Te quiero Silvia.

List of Figures

1.1	Chemical structures of sterol and brassinosteroids	4
1.2	Brassinosteroids signaling pathway	8
1.3	Extracellular structure of the BRI1 receptor	9
1.4	Confocal microscopy pictures of BR receptor reporter lines	11
1.5	Phylogenetic tree of BR receptors across different plant species	12
1.6	Brassinosteroids binding pocket of BR receptors	14
1.7	Network of abiotic stresses and the BR-induced protective effects	24
2.1	The stem cell niche of Arabidopsis roots and QC-specific expression of BR pathway components	36
2.2	BES1 transcription factor promotes QC division cell-autonomously	37
2.3	Quantification of QC division rates in QC-specific overexpression lines	38
2.4	WOX5-controlled BRI1 expression is QC-specific	39
2.5	QC-specific expression of BR components has an impact on the growth of primary roots	40
2.6	BRL1 and BRL3 receptors do not compete with BRI1 for ligand bind- ing in the QC microenvironment	41
2.7	Quantification of QC division rates of QC-specific overexpressors lines in the <i>brl1brl3</i> null background	42
2.8	Design and testing of BRI1 amiRNA lines	44
2.9	The pWOX5:BRI1-amiR construct downregulates BRI1 transcription in the root stem cell microenvironment	45
2.10	pWOX5:BRI1-amiR lines partially off-target BRL1 and BRL3 expression	46
2.11	pWOX5:BRI1-amiR lines retain sensitivity to BL	47
2.12	BRI1 is required in the stem cell niche to promote QC divisions	48
2.13	Quantification of QC division rates in pWOX5:BRI1-amiR lines	48

2.14	Root growth dynamics of pWOX5:BRI1-amiR lines	49
2.15	pWOX5:BRI1-amiR seedlings exhibit normal meristem divisions . . .	50
2.16	Quantification of EdU staining in pWOX5:BRI1-amiR lines	51
2.17	BR receptors in the stem cell niche modulate QC divisions upon DNA damage	52
2.18	Quantification of cell damage and QC division following bleomycin treatments	53
3.1	BR perception mutant's roots are less sensitive to osmotic stress . . .	62
3.2	Localization pattern of BRL3 protein in the <i>BRL3ox</i> roots	63
3.3	BR perception mutant roots are less sensitive to osmotic stress-induced PCD	64
3.4	BR perception mutant roots are less sensitive to hydrotropism	65
3.5	Overexpression of the BRL3 receptor promotes root hydrotropism . .	67
3.6	Brassinazole reverts the WT hydrotropic response	68
3.7	Differences in root curvature angles truly reflect differences in the hy- drotropic response	68
3.8	Stress multi-trait matrix	69
3.9	BRL3 overexpression confers drought tolerance	71
3.10	Days required to loose the same soil water content	72
3.11	Relative water content of plants at comparable soil water contents . .	73
3.12	Physiological parameters of mature plants under comparable drought stress conditions	74
3.13	BR signaling, size and drought resistance balance	75
3.14	Distribution of metabolite levels per sample	76
3.15	Metabolic fingerprint of WT, <i>BRL3ox</i> and <i>quad</i> shoots during drought time course	77
3.16	Metabolic fingerprint of WT, <i>BRL3ox</i> and <i>quad</i> roots during drought time course	78
3.17	Differentially accumulated metabolites at basal conditions	79
3.18	Metabolites following differential dynamics between <i>BRL3ox</i> and WT along the drought time course	80
3.19	Clustering of the metabolite dynamics along the drought time course	82

3.20	Metabolites following differential dynamics between <i>quad</i> and WT along the drought time course	83
3.21	GO enrichment analysis of differentially expressed genes in <i>BRL3ox</i> roots	85
3.22	Response to stress genes differentially expressed in <i>BRL3ox</i> roots	86
3.23	GO enrichment analysis of differentially expressed genes in <i>quad</i> plants along the drought time course	87
3.24	Response to hormone genes differentially expressed in <i>BRL3ox</i> roots	88
3.25	Hormone profiling on <i>BRL3ox</i> and <i>quad</i> shoots in control conditions and after 6 days drought	90
3.26	Transcript levels of two BR synthesis genes in <i>BRL3ox</i> and <i>quad</i> root and shoots during a 6 days drought time course	91
3.27	Deregulated genes in <i>BRL3ox</i> are enriched in root vascular tissues	93
3.28	Pericycle and Phloem Pole Pericycle specific genes deregulated in <i>BRL3ox</i>	94
3.29	Transcription factors with a differential drought response between <i>BRL3ox</i> and WT	96
3.30	Deregulated metabolic pathways in <i>BRL3ox</i> under control conditions and drought	97
4.1	Summary of TOTEM workflow and its basic inputs, processes and outputs	103
4.2	TOTEM homepage	106
4.3	TOTEM result page	107
4.4	Enrichment values upon random sampling	108
4.5	Arabidopsis root radial patterns of deregulated genes in <i>BRL3ox</i> at basal conditions	109
4.6	Arabidopsis root longitudinal patterns of deregulated genes in <i>BRL3ox</i> at basal conditions	111
4.7	Intersection of Arabidopsis root radial and longitudinal patterns of deregulated genes in <i>BRL3ox</i> at basal conditions	112
4.8	Tomato fruit enrichment pattern of drought stress genes deregulated in Micro-Tome cultivar	114

5.1	Crystal structure of the complex BRI1-BAK1 (extracellular parts) with BL bound	122
5.2	Crystal structure of the kinase domain of BRI1 in complex with BKI1 and with ATP bound	123
5.3	Number of interactions identified in CoIP experiments, PPIs modeled with confidence and type of interactor	125
5.4	Overall energy calculation for the BRL3 interactions modeled	126
5.5	Overall energy calculation for the BRL1 interactions modeled	127
5.6	Overall energy calculation for the BRI1 interactions modeled	128
5.7	Comparison between calculated ddG and ZRANK scores per model	129
5.8	Modeled interactions network	130
5.9	Remodeling of exclusive BRL3 interactors with the other BR receptors	131
5.10	Relative transcript levels of the BRL3 exclusive interactors	133
5.11	AT3G02880 RLK is more expressed than BAK1 across all Arabidopsis root tissues	134
5.12	Interaction models of BRL3-AT3G02880 and BRL3-BAK1 kinase domains	135
5.13	Representation of identified hotspots over the BRL3-BAK1 and BRL3-AT3G02880 interaction models	137
5.14	Modeling of extracellular part of BR receptors bound to BL	140
5.15	The BRL3-AT3G02880 interaction in the extracellular part is also more favorable than the BRL3-BAK1 interaction	142
6.1	Working hypothesis: BR hormone concentration as a limiting factor for QC division	152
6.2	The vascular brassinosteroid receptor BRL3 confers drought resistance through osmoprotectant production	162
6.3	Plausible mechanisms of a putative BRL3-KIN7 cross-signaling upon abiotic stress	166

List of Tables

5.1	Identification of hotspots for the BRL3-AT3G02880 and BRL3-BAK1 interactions	137
7.1	Arabidopsis plant lines used in this thesis	178
7.2	Primers used for Real-Time qPCR	188

CV and Publications

FIDEL LOZANO ELENA

E-MAIL : fidel.lozano@cragenomica.es / fidel.lozano.bio@gmail.com
Twitter: @LozanoElena_F
PHONE : (+34)650877008

EDUCATION:

(2014 – 2019): PhD Student in Center for Research in Agricultural Genomics (CRAG), Barcelona, Spain.

Dr. Ana I. Caño-Delgado laboratory. Thesis title: *Control of abiotic stress responses by brassinosteroids receptors in Arabidopsis thaliana*

(2013 - 2014): Master in Advanced Genetics; Barcelona Autonomic University, Barcelona, Spain.

Final master's thesis developed in Center for Research in Agricultural Genomics (CRAG).
Dr. Ana I Caño-Delgado laboratory. "*Characterization of drought stress responses in Arabidopsis brassinosteroid mutants*"

(2009 - 2013): Biotechnology degree; Lleida University, Lleida, Spain.

(February- July 2013): Development of final degree thesis within the ERASMUS program in Hedmark University College, Hammar, Norway. "*Multiplex amplification of parentage microsatellite panel and cost-effective SNPs genotyping of myostatin gene in cattle*".

PUBLICATIONS:

Lozano-Elena F & Caño-Delgado AI (2019) *Emerging roles of vascular brassinosteroids receptors of the BRI1-like family*. Current Opinion in Plant Biology. 51:105-113. doi: 10.1016/j.pbi.2019.06.006.

Fàbregas N, **Lozano-Elena F**, Blasco-Escámez D, Toghe T, Martínez-Andújar C, Albacete A, Osorio S, Bustamante M, Riechmann JL, Nomura T, Yokota T, Conesa A, Alfocea FP, Fernie AR, Caño-Delgado AI (2018) *Overexpression of the vascular brassinosteroid receptor BRL3 confers drought resistance without penalizing plant growth*. Nat Commun. 9(1):4680. doi: 10.1038/s41467-018-06861-3

Lozano-Elena F, Planas-Riverola A, Vilarrasa-Blasi J, Schwab R, Caño-Delgado AI (2018) *Paracrine brassinosteroid signaling at the stem cell niche controls cellular regeneration*. J Cell Sci. 131(2). doi: 10.1242/jcs.204065

Blasco-Escámez D, **Lozano-Elena F**, Fàbregas N. Caño-Delgado AI (2017) *The primary root of Sorghum bicolor (L. Moench) as a model system to study brassinosteroid signaling in crops*. Methods Mol Biol. 1564:181-192. doi: 10.1007/978-1-4939-6813-8_15

MANUSCRIPTS IN PREPARATION:

Lozano-Elena F, Vera G, & Caño-Delgado AI (2019) *TOTEM: A web tool for tissue-enrichment analysis on gene lists*. * TOTEM is an open source web tool that can be accessed here: <https://bioinformatics.cragenomica.es/totem>

ORAL COMMUNICATIONS:

Presentation in XIV Reunión de Biología Molecular de Plantas (Salamanca July 4th, 2018). System Biology panel. “Vascular brassinosteroid receptor confer drought resistance without penalizing plant growth”

Internal seminar, CRAG Auditorium (May 26th 2017): “Paracrine brassinosteroids signaling at the root stem niche controls growth and cellular regeneration”

RESEARCH STAYS:

(November-December 2017): Dr. Ana Conesa laboratory (University of Florida, Gainesville, FL. EEUU). *Statistical analysis, functional annotation of genomic data, complex experimental designs and integration of different omics data*. Stay inside the DEANN program: Developing and European American NGS Network.

(June-August 2016): Dr. Ana Conesa laboratory (University of Florida, Gainesville, FL. EEUU). *Statistical analysis and functional annotation of genomic data*. Stay inside the DEANN program: Developing and European American NGS Network.

LANGUAGES:

- Spanish (Mother language)
- English (Proficient)
- Catalan (Medium level)

Programming languages:

- R (Advanced)
- Python (Medium level)
- Bash (Unix systems, Medium)

COURSES:

- Career development for young scientist (The Paper Mill), CRAG November 21st-23rd, 2018
- Protein-Ligand Dockings: Conceptos y aplicaciones. (Servei de Genòmica I Bioinformàtica UAB), July 9th-12th, 2018
- Data Visualization and storytelling. (Fundación Estatal para la Formación de Empleo), CRAG April 3rd-4th, 2017

OTHER SKILLS:

- Advanced statistics for biology
- Communicative skills
- Teamwork

Emerging roles of vascular brassinosteroid receptors of the BRI1-like family

Fidel Lozano-Elena and Ana I Caño-Delgado



Brassinosteroids (BRs) are essential hormones for plant growth and development that are perceived at the plasma membrane by a group of Leucine Rich Repeat Receptor Like Kinases (LRR RLKs) of the BRASSINOSTEROID INSENSITIVE 1 (BRI1) family. The BRI1 receptor was first discovered by genetic screenings based on the dwarfism of BR deficient plants. There are three BRI1 homologs, named BRI1 like 1, 2 and 3 (BRLs), yet only BRL1 and BRL3 behave as functional BR receptors. Whereas the BRI1 pathway operates in the majority of cells to promote growth, BRL receptor signaling operates under specific spatiotemporal constraints. Despite a wealth of information on the BRI1 pathway, data on specific BRL pathways and their biological relevance is just starting to emerge. Here, we systematically compare BRLs with BRI1 to identify any differences that could account for specific receptor functions. Understanding how vascular and cell specific BRL receptors orchestrate plant development and adaptation to the environment will help shed light on membrane signaling and cell communication in plants, while opening up novel possibilities to improve stress adaptation without penalizing growth.

Address

Center for Research in Agricultural Genomics (CRAG) CSIC-IRTA-UAB-UB, Barcelona 08193, Spain

Corresponding author: Cano-Delgado, Ana I (ana.cano@cragenomica.es)

Current Opinion in Plant Biology 2019, 51:105–113

This review comes from a themed issue on **Cell signaling and gene regulation**

Edited by **Ildoo Hwang** and **Masaaki Umeda**

<https://doi.org/10.1016/j.pbi.2019.06.006>

1369-5266/© 2019 Published by Elsevier Ltd.

Introduction

Brassinosteroids (BRs) are the steroid hormones of plants. They control a myriad of responses during normal growth and development and enable plants to adapt to changing environments. In *Arabidopsis thaliana* (Arabidopsis), the canonical BR signaling pathway starts with the steroid hormone binding to the BRASSINOSTEROID INSENSITIVE 1 (BRI1) receptor in the extracellular space along with its co receptor BRI1 ASSOCIATED KINASE 1

(BAK1). This triggers a cytoplasmic cascade of signaling events that lead to the dephosphorylation of two homologous transcription factors, BRASSINOSTEROID EMS SUPPRESSOR 1 (BES1) and BRASSINAZOLE RESISTANT 1 (BZR1) in the nucleus [1]. In Arabidopsis, the BRI1 like family of receptors is composed of BRI1 and three additional BRI1 like receptors named BRL1, BRL2, and BRL3. BR receptors share at least 47% homology in their protein sequence and are characterized by an extracellular island domain that interrupts the leucine rich repeat (LRR) domain and is essential for steroid ligand binding [2] (Figure 1).

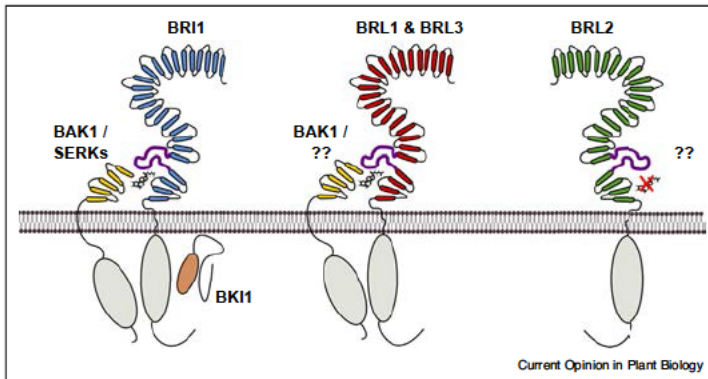
In contrast to the widely expressed BRI1 receptors, the BRLs display an enriched localization in vascular tissues and the stem cell niche at the meristem [3,4,5]. Also, BRLs appear not to play a major role in plant growth, as *bri1* single mutant plants are not dwarf like their *bri1* counterparts. This observation supports the idea that BRLs have specific roles in overall plant growth and/or have redundant roles with BRI1 [6]. Indeed, that lack of growth phenotypes along with the cell specific expression have discouraged studies examining BRL functions in plants.

Even though BRLs are thought to finetune and connect responses with BRs [7–9], and evidence suggests that different BR receptor complexes play distinct roles in different plant tissues or conditions, fundamental questions concerning the mechanisms behind such signaling coordination, including ligand transport, remain elusive [3,6,8–13]. Understanding how plants achieve growth coordination despite different tissue layers having the same hormone for a different set of receptors is a fascinating yet unanswered question. Specific studies on this topic would shed light on the evolutionary advantage of maintaining three BR receptors in addition to BRI1. However, the study of BRLs is difficult because of the probable masking effect of BRI1 itself. For these reasons, our review focuses on BRLs, systematically comparing them with BRI1 and placing a special emphasis on structural biology.

The BR receptor family

During postembryonic development, BRI1 receptor proteins are present in the majority of plant tissues (especially in the outer cell layers) [14], whereas the BRL receptors localize to vascular tissues and stem cell niches (particularly in the phloem pole pericycle cells) [3,4,5,15]. Transcriptionally, BRI1 expression does

Figure 1



Schematic representation of the BRI1-like receptor family.

BRLs have a similar structure to BRI1, with 25 LRRs in the extracellular part (blue, red, and green) interrupted by a 70-aa stretch (purple) between LRRs 21–22, which constitute the island domain. The intracellular part contains a conserved serine/threonine kinase domain (gray). Interestingly, BRL2 is not able to bind brassinolide (BL). BR signaling at the plasma membrane depends on an interaction with a coreceptor. The canonical BRI1 coreceptor is BAK1(SERK3), a small LRR–RLK (yellow). Other SERKs can also bind BRI1. BRL3 also binds BAK1 [4*]; however, it is unknown whether it can also bind other SERKs or if it possesses specific co-receptors. For BRL2, it is unknown whether it signals through other means, binding other co-receptors. In the intracellular part, BRI1 kinase activity is inhibited by BKI1 when the receptor is not active. BRL1 kinase cannot bind BKI1 [45], and based on sequence homology, it is probable that BRL3 does not bind BKI1 neither.

not overlap with the expression of BRLs, at least not in the root stem cell niche and quiescent center (Figure 2a) [4*,16]. All members of the BRI1 family of receptors share high structural similarities; they have an extracellular domain composed of 24–25 LRRs, which are interrupted by a stretch of 70 amino acids near the plasma membrane called the ‘island domain’, a transmembrane domain, and an intracellular kinase domain [2,17]. The island domain is necessary for steroid ligand binding [2]. Only BRL1 and BRL3 are functional BR receptors capable of complementing the dwarf phenotype of *bri1* mutants. In fact, BRL1 and BRL3 have a higher binding affinity for the BR hormone than BRI1 [3,18]. Interestingly, although BRL2 (*aka* VASCULAR HIGHWAY 1, VH1) is not able to bind the hormone [2], *bri2* mutants display vascular defective phenotypes [15,19]. Thus, the roles attributed to BRL2 are likely BR independent. Even more unclear, is whether BRL1 and BRL3 possess different roles. While the reason for harboring several BR receptors remains elusive, BRL compartmentalization in different plant tissues and their conservation across plant species indicate a role in specialized plant processes [20*] (Figure 1).

BRLs are conserved across plant species

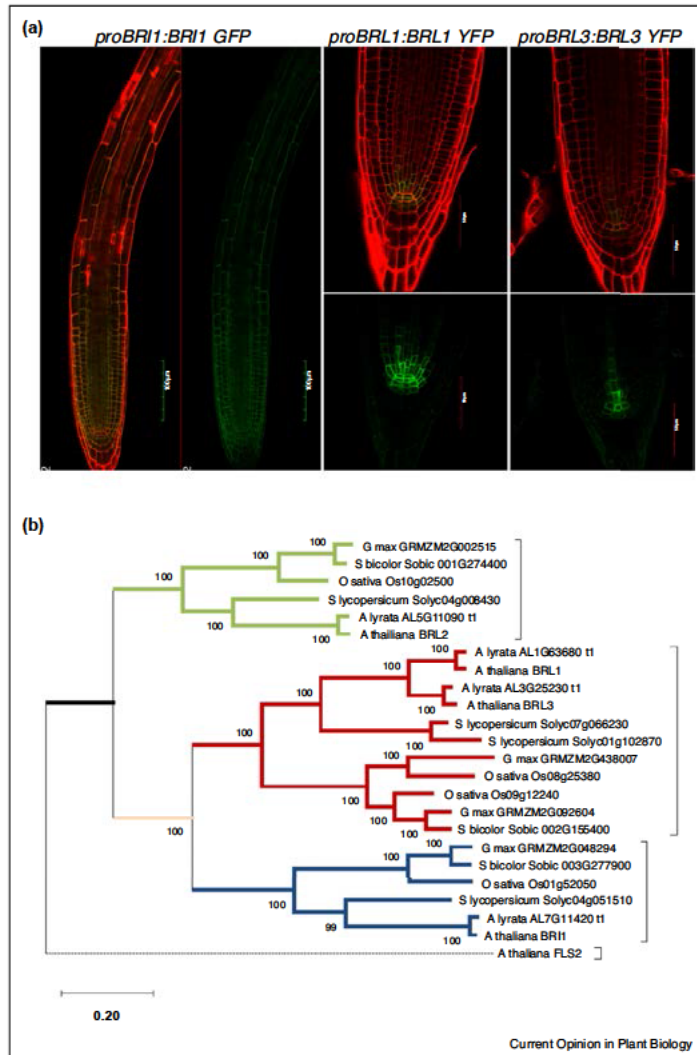
The structure of the BRI1 family in Arabidopsis, even the non functional AtBRL2 receptor is highly conserved across superior plants [20*] (Figure 2b). In fact, molecular analysis of BRLs in rice already suggests specific functions in roots [21]. Comparison of the protein sequence of BR receptors across different plant species reveals a

sequential diversification in the clades of the BRI1 BRLs family. First, there is a division between the BRL2 clade and the rest of the family members and then a division between the BRI1 and the BRL1–3 clades [20*] (Figure 2b). Remarkably, the complete receptor structure, including the island domain, LRRs, and the intracellular kinase, only appear in angiosperms and gymnosperms [20*]. This last point opens an interesting question given that BRs have been detected and quantified in non seed plants [22] but their receptor lacks the island domain. Thus, perhaps these plants have a different (ancestral) mechanism to sense and respond to steroid hormones.

Structural basis for steroid recognition and signaling

Crystals of the BRI1 ectodomain revealed a hydrophobic pocket formed by the island domain folding back into the interior of the LRR superhelix against LRRs 21–25, where the steroid hormone is bound [23*,24*] (Figure 3a). However, no major conformational changes occur upon binding of the hormone, except for a discrete fixing of the island domain loop [23*]. The mechanisms governing hormone binding in BRI1 are likely conserved in BRLs given their sequence similarity. In fact, the BRL1 ectodomain bound to brassinolide (BL) – the most active BR compound – displays a similar structure to BRI1 [25*]. The higher affinity of BRL1 to BL could be explained by the larger buried surface and very subtle residue changes in the island domain [3,25*] (Figure 3b). As for BRI1, the conformational changes are limited to the

Figure 2



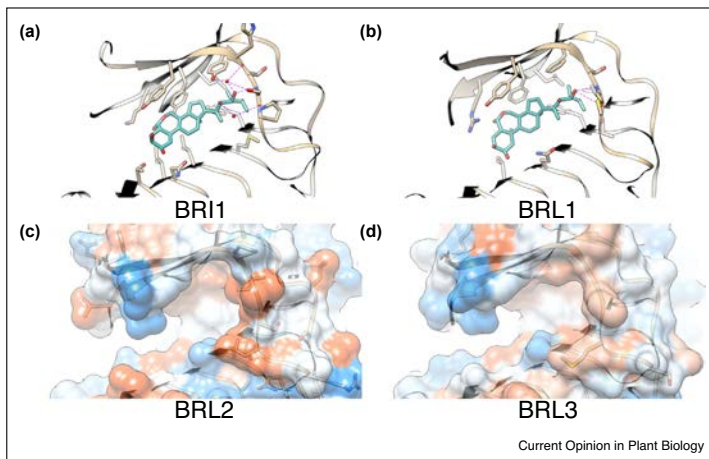
BR receptor localization and phylogeny.

(a) Confocal microscopy images of the primary root of *Arabidopsis*. Images show translational reporter lines of BRI1, BRL1, and BRL3 (left, middle, right). Merged (red: PI counter staining; green: GFP) and green channels are shown separately. Scale bars 100 μm (*proBRI1:BR1-GFP*) and 50 μm (*proBRL1/3:BRL1/3-GFP*). **(b)** Maximum-likelihood tree including all four *Arabidopsis* BR receptors and its orthologs in species of agronomic interest. Different colors denote the different clades: Green for the BRL2 clade, red for the BRL1–BRL3 clade and blue for the BRI1 clade. *Arabidopsis* LRR receptor FLS2 was included as an outgroup. Scale represents the number of substitutions per site. Numbers over the tree nodes denote the bootstrap support. Orthologous protein sequences were retrieved from Phytozome, aligned with MUSCLE, and the tree constructed with MEGAX.

island domain, which exposes part of the bound hormone to the solvent [25]. Homology models suggest a similar mechanism for BRL3 hormone binding (Figure 3d). In contrast, for BRL2, models revealed that its inability to

bind the hormone [3] is probably caused by the presence of a bulky, charged amino acid substitution at the inner end of the cavity that prevents the steroid from entering the pocket [25] (Figure 3c). The structural resolution of

Figure 3



Island domains of crystals and homology models for BR receptors.

(a) Island domain of BRI1 bound to BL (PDB: 3RGZ [23]). (b) Island domain of BRL1 bound to BL (PDB: 4J0M [25]). Purple dashed lines depict H-bonds. Fully represented residues have hydrophobic contacts with the hormone. (c) Coulombic surface of the island domain of the BRL2 homology model. (d) Coulombic surface of the island domain of the BRL3 homology model. Note the higher positive potential at the bottom of the hydrophobic pocket in BRL2. This probably avoids the hormone entering into the pocket. Fully represented residues differ from the template, the BRL1 crystal. Homology models created with Modeller v9.2 and molecular representations with UCSF Chimera.

the BR receptor ectodomains uncovered two important points: i) no major conformational changes occur upon hormone binding, and ii) hormone binding to the island domain creates a docking platform for other proteins [23,25]. These findings rationalized the evidences supporting a critical role for BAK1 in brassinosteroid signaling.

BRI1 and BRLs share the co-receptor BAK1

Apart from the BRI1 like receptors, BR signaling depends on additional components, such as BAK1, a small LRR RLK protein that contains five LRR domains [26,27]. BAK1 is considered a co receptor because it is unable to bind hormones [2,28]. BAK1 interacts with BRI1 in a BL dependent manner, and their respective kinase domains transphosphorylate each other to trigger the signaling pathway [29]. BAK1 binds to the BRI1-BL complex at its inner surface, completely burying the exposed part of the ligand and interacting with the inner part of the last LRRs. No notable conformational changes take place [30]. The current model, which is firmly supported by structural data, proposes that the extracellular part of the BRI1 receptor and BAK1 co receptor come into close proximity upon perception of the steroid hormone. This brings the kinase domains closer together and allows for subsequent transphosphorylation (Figure 1). The function of BRI1 also depends on other co receptors besides BAK1 (*aka* SOMATIC

EMBRYOGENESIS RECEPTOR LIKE KINASE3; SERK3), including other members of the SERK family of LRR kinases. Four out five SERK family members have an impact on BR signaling, they actually bind BRI1 [31-33] and share similar activation mechanisms [34]. SERKs can also bind other receptors to support their signal transduction [7,35,36]. Together, these findings support a new vision of signal transduction as an interconnected network, where the steroid receptor can associate with several co receptors to transduce the same signal, and conversely, a co receptor can support the signaling of several pathways through the association with different receptors. Accordingly, additional receptor proteins can also modulate BR signal transduction [37]. A complete *in vitro* LRR RLK interaction network revealed an important implication for small co receptors in signaling robustness, and showed that small multifunctional RLKs such as BAK1 transduce more information (through several signaling pathways) but are less essential due to redundancy [37,38].

With respect to BRLs, as they are structurally similar to BRI1, it is plausible that their specialized functions may rely on additional partners in addition to BRLs. In the abovementioned network, although BRLs clustered together with BRI1 and shared some interactors, they also showed contacts with RLKs in other subnetworks that were separated from BRI1 [37]. We hypothesize

that the actual *in vivo* interaction network of BRLs would be determined by their expression domains. In fact, the *in planta* BRL3 signalosome revealed interactions with several unannotated RLKs, with BAK1 and BRL1, but not with BRI1 [4**]. Decoding the composition of the BRI1, BRL1, and BRL2 signalosomes may reveal unique interactors for each receptor. These are potential factors determining the functional specificity of BRLs (Figure 1). As the current model of membrane signaling implies a high degree of ‘promiscuity’ between the receptors (which leads to network robustness and balanced signaling), signal specificity may be provided by kinase domains and their downstream interactors [35**]. Indeed, different parts of the BAK1 kinase domain with different phosphocodes are required for the different pathways in which it is involved [39,40*]. Taken together, these studies suggest that the specialized roles of BRLs are determined by their cell specific localization and their specific subset of interactors.

Kinase domain (KD) analysis suggests common activation mechanisms

Upon the ligand dependent binding of receptor and co-receptor, signal transmission depends on kinase activities. BRs induce BRI1 phosphorylation [41]. Although BRI1 kinase domain has autophosphorylation capability [42–44], this is kept inactive through homodimerization, auto-inhibition by its C terminal part [28] and the binding of an inhibitory kinase, BKI1 [29,42,45]. The transphosphorylation between BAK1 and BRI1 and the detachment of BKI1 are requisites for BRI1 kinase activation [29,45–47]. The existence of receptor homodimers is attributed to a resting state while heterodimerization occurs only upon BR binding and results in transphosphorylation and pathway activation [29,45,48,49]. Even the kinases activation mechanisms are known [47,49,50], how these allow for further phosphorylation on downstream components, as the BR SIGNALING KINASES (BSKs), remain poorly understood [51,52]. While no specific studies on BRLs are available, given that their kinase domains share a minimum identity of 64% (without BRL2, 74%) they could share similar activation mechanisms. Accordingly, BSKs are present in the BRL3 signalosome [4**]. The kinase domain of BRL1 does not interact with BKI1 inhibitor, at least through the BKI1 patch that binds BRI1 [45], which could yield notable differences. The same residues that avoid BKI1 binding to BRL1 are also found in BRL3. If BRL1 and BRL3 activate a different set of downstream components is currently unknown, but it could contribute to specific functions (Figure 1). Future studies on specific BRLs phosphorylation substrates is a straightforward starting point for the dissection of specific BRLs molecular pathways.

Common and specific roles of BRLs

Since the discovery of BRI, this receptor pathway has not only been linked to overall plant growth and

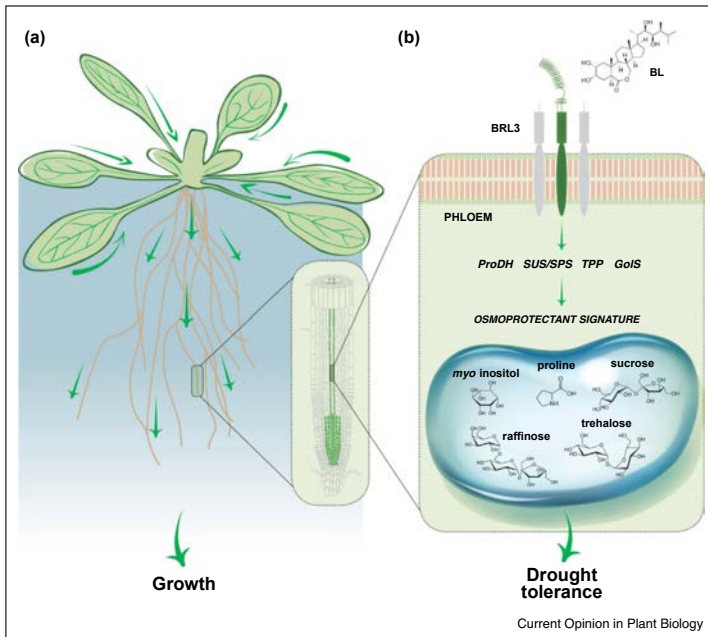
developmental processes, but also to the stress response. The roles of BRI in plant development and stress have been recently reviewed elsewhere [1]. Recent studies are narrowing down the exact tissue specific mechanisms that are triggered by BRI1 to promote plant development (such as root growth, hypocotyl elongation [53]) and responses to stress (such as stomata opening [54]). Interestingly new evidence attributes a function for BRI1 in vascular tissues differentiation that is independent of BRs [55]. Conversely, xylem and phloem differentiation requires the canonical transcription factors BES1 and BZR1 but independently of BRI1 [56]. Therefore, the notion of a canonical signaling pathway triggered by BRI1 and exclusively devoted to BRs should be reviewed.

However, the discrete localization of BRLs and the lack of any evident growth phenotypes in the mutants have hampered the understanding of the specific roles of BRLs. Interestingly, the xylem maturation phenotype of *bri1* mutants is enhanced when combined with *bri1bri3* mutants [55]. Accordingly, in other studies that account for BRLs, *bri1* vascular phenotypes are always enhanced when combined with *bri* mutants, although single or double *bri* mutants have no phenotypes themselves [4**,57]. Once again, the actual roles of BRLs are masked by the predominance of BRI1. Literature on the specific roles of BRL is extremely scarce. However, some clues of BRLs regulating vascular development and responses to stress can be extracted, for example, from BRL3 transcriptional activation under low oxygen stress [58], from induction of a differentiation regulator in xylem [59], or from the drought resistance phenotype of BRL3 over expression and its transcriptional fingerprint [60**].

In accordance with the present findings, and given the sequence and structural similarity of the BRI1 and BRL receptors, the functional specificity of BRLs may reside on: (i) specific residues in their interaction interfaces, especially in the kinase domain, that define a specific subset of interactors, and (ii) its specific localization within particular tissues, with the latter likely being the most determinant factor (Figure 4).

1. With regards to the first point, the inability of BRL1 to bind BKI1 exemplifies how BRLs could gather different subsets of interactors [45]. In fact, a specific interactor of BRL3, REGULATOR OF G PROTEIN SIGNALING (RGS1), has already been described. RGS1, which is specifically phosphorylated *in vivo* by BRL3 [61], works downstream of BRL3 in sugar sensing and ROS production and has a vascular expression pattern that highly overlaps with those of BRL3 and BRL1 [61–63]. A role for BRL3 in sugar sensing fits well with its phloem localization. We have recently shown that BRL3 overexpressor plants accumulate osmoprotectant sugars in the root, which contribute to alleviating the effects of severe drought without

Figure 4



The spatial localization of BRL receptors determine their function.

(a) The preferential vascular localization of BRLs dictates their role in the development and differentiation of xylem and phloem tissues. These roles can be taken over by BRI1 in the single and double mutants of *br1brl3*, which lack a visible phenotype (except for the case of *brl2* [15,19] or *brl1* in a background-dependent manner [3]). However, when combined with *brl1* mutants, vascular-associated phenotypes are greatly enhanced [4**,55,57]. (b) BRL3 has an impact on plant stress responses. BRL3 activates transcriptional responses in the phloem tissues that lead to a sugar-enriched metabolic signature. Many of the accumulated sugars in the roots act as osmoprotectants, which yield drought tolerant plants of normal size [60*]. In addition, BRL3 interacts specifically with RGS1, a vascular-enriched LRR-RLK that works as a sugar sensor and cooperates with BRL3 to modulate the ROS response [62,63,67].

penalizing growth [60**] (Figure 4). The possible involvement of BRL3 in other stress responses is also supported by the fact that pathogen effectors and DNA damage response transcription factors target BRL3 [38,64].

The discrete spatial localization of BRLs is informative of their biological function in the vascular tissues. For example, *brl2* mutants (despite it does not bind BL), show specifically vascular phenotype [15,19]. BRL1 or BRL3 when expressed under the control of BRI1 promoter complement the *brl1* mutant phenotype [3,18]. The fact that BR receptors are so interchangeable suggests that the control of different functions emanate from the compartmentalization. Conversely, *brl1* impaired growth is not completely restored if BRI1 is expressed only in the inner root tissues or phloem [6,65]. In addition, BR signaling from inner vascular tissues may have deep implications in development; BRI1 expressed only in protophloem cells is able to rescue most of the *brl1* dwarf phenotype in a

brl1brl1brl3 mutant background [57]. This apparent incoherence really deserves further investigation. If similar effects are not observed in a simple *brl1* background, opposing roles for BRI1 BRLs are likely. Accordingly, tissue specific transcriptomes in response to BR reveals opposite patterns that point to unique BRL functions [66]. When these tissue specific expression data [66] are combined with that derived from BRL3 overexpressors [60*], we observed that BRL1 and BRL3 cluster together in a co expression network. In contrast, BRI1 and BRL2 cluster in different modules. Interestingly, the BRL1 3 module was enriched in the cell wall metabolism and the xylem and phloem development categories. These biological processes are of special importance in vascular tissues.

Furthermore, BRL2 receptor mutants that are unable to bind BL show a specific vascular phenotype [15,19], whereas a vascular phenotype only arises in BRL knock outs when they are combined with *brl1* mutants [3,4**,57].

As such, we hypothesize that BRI1 can take over BRL1 and BRL3 functions in their absence. This suggests a BRI1 BRL mutual regulation to limit their expression domains. Indeed, the expression pattern of BRL3 is regulated by the canonical BR pathway [5], and strikingly we found a strong transcriptional activation of BRI1 in plants overexpressing BRL3 [60**]. Future work on the BRI1 BRL mutual regulation will shed light on the specific roles of BRLs, and could help to clarify the role of BRI1 signaling in inner root tissues [6,57,65].

In conclusion, BRL signaling has only just begun to emerge as a key factor for carrying out specialized functions such as vascular development or signaling to neighboring cells to promote recovery after genomic or environmental stresses (Figure 4). This kind of receptor redundancy may act to finetune plant adaptation to environmental responses. Future work aiming to elucidate specialized roles of BRLs is important because the BRI1 BRL case might be paradigmatic, with analogous examples in other pathways.

Conflict of interest statement

Nothing declared.

Acknowledgements

A.I.C-D. is a recipient of a Spanish Ministry of Economy and Competitiveness and a European Research Council (FEDER-BIO2016-78150-), ERC Consolidator Grant (ERC-2015-CoG – 683163). F.L.E. PhD thesis is funded by the FEDER-BIO2016-78150-P grant in A.I.C-D laboratory.

References and recommended reading

Papers of particular interest, published within the period of review, have been highlighted as:

- of special interest
- of outstanding interest

1. Planas-Riverola A, Gupta A, Betegon-Putze I, Bosch N, Ibanes M, Cano-Delgado AI: **Brassinosteroid signaling in plant development and adaptation to stress.** *Development* 2019, **146**:dev151894.
2. Kinoshita T, Cano-Delgado A, Seto H, Hiranuma S, Fujioka S, Yoshida S, Chory J: **Binding of brassinosteroids to the extracellular domain of plant receptor kinase BRI1.** *Nature* 2005, **433**:167-171.
3. Cano-Delgado A, Yin Y, Yu C, Vafeados D, Mora-Garcia S, Cheng J-C, Nam KH, Li J, Chory J: **BRL1 and BRL3 are novel brassinosteroid receptors that function in vascular differentiation in Arabidopsis.** *Development* 2004, **131**:5341-5351.
4. Fabregas N, Li N, Boeren S, Nash TE, Goshe MB, Clouse SD, de Vries S, Cano-Delgado AI: **The brassinosteroid insensitive1-like3 signalosome complex regulates Arabidopsis root development.** *Plant Cell* 2013, **25**:3377-3388.
- In this paper, the authors report the composition of the BRL3 complex and show that while the BRL receptors heterodimerize and interact with the BAK1 co-receptor, the BRI1 and BRL3 do not interact in native conditions.
5. Salazar-Henao JE, Lehner R, Betegon-Putze I, Vilarraza-Blasi J, Cano-Delgado AI: **BES1 regulates the localization of the brassinosteroid receptor BRL3 within the provascular tissue of the Arabidopsis primary root.** *J Exp Bot* 2016, **67**:4951-4961.
6. Hacham Y, Holland N, Butterfield C, Ubeda-Tomas S, Bennett MJ, Chory J, Savaldi-Goldstein S: **Brassinosteroid perception in the epidermis controls root meristem size.** *Development* 2011, **138**:839-848.
7. Wu C-H, Derevnina L, Kamoun S: **Receptor networks underpin plant immunity.** *Science (80-)* 2018, **360**:1300-1301.
8. Savaldi-Goldstein S, Peto C, Chory J: **The epidermis both drives and restricts plant shoot growth.** *Nature* 2007, **446**:199-202.
9. Gendron JM, Liu J-S, Fan M, Bai M-Y, Wenkel S, Springer PS, Barton MK, Wang Z-Y: **Brassinosteroids regulate organ boundary formation in the shoot apical meristem of Arabidopsis.** *Proc Natl Acad Sci U S A* 2012, **109**:21152-21157.
10. Vilarraza-Blasi J, Gonzalez-Garcia M-P, Frigola D, Fabregas N, Alexiou KG, Lopez-Bigas N, Rivas S, Jauneau A, Lohmann JU, Benfey PN *et al.*: **Regulation of plant stem cell quiescence by a brassinosteroid signaling module.** *Dev Cell* 2014, **30**:36-47.
11. Gonzalez-Garcia M-P, Vilarraza-Blasi J, Zhiponova M, Divol F, Mora-Garcia S, Russinova E, Cano-Delgado AI: **Brassinosteroids control meristem size by promoting cell cycle progression in Arabidopsis roots.** *Development* 2011, **138**:849-859.
12. Vukasinović N, Russinova E: **BRExit: possible brassinosteroid export and transport routes.** *Trends Plant Sci* 2018, **23**:285-292.
13. Lozano-Elena F, Planas-Riverola A, Vilarraza-Blasi J, Schwab R, Cano-Delgado AI: **Paracrine brassinosteroid signaling at the stem cell niche controls cellular regeneration.** *J Cell Sci* 2018, **131**:jcs204065.
14. Friedrichsen DM, Joazeiro CAP, Li J, Hunter T, Chory J: **Brassinosteroid-insensitive-1 is a ubiquitously expressed leucine-rich repeat receptor serine/threonine kinase.** *Plant Physiol* 2000, **123**:1247-1256.
15. Ceserani T, Trofka A, Gandotra N, Nelson T: **VH1/BRL2 receptor-like kinase interacts with vascular-specific adaptor proteins VIT and VIK to influence leaf venation.** *Plant J* 2009, **57**:1000-1014.
16. Wilma van Esse G, Westphal AH, Surendran RP, Albrecht C, van Veen B, Borst JW, de Vries SC: **Quantification of the brassinosteroid insensitive1 receptor in planta.** *Plant Physiol* 2011, **156**:1691-1700.
17. Li J, Chory J: **A putative leucine-rich repeat receptor kinase involved in brassinosteroid signal transduction.** *Cell* 1997, **90**:929-938.
18. Zhou A, Wang H, Walker JC, Li J: **BRL1, a leucine-rich repeat receptor-like protein kinase, is functionally redundant with BRI1 in regulating Arabidopsis brassinosteroid signaling.** *Plant J* 2004, **40**:399-409.
19. Clay NK, Nelson T: **VH1, a provascular cell-specific receptor kinase that influences leaf cell patterns in Arabidopsis.** *Plant Cell* 2002, **14**:2707-2722.
20. Wang H, Mao H: **On the origin and evolution of plant brassinosteroid receptor kinases.** *J Mol Evol* 2014, **78**:118-129.
- In this paper, the authors investigate the evolution of the binding function of the BRI1-BRL family, when it emerged and how it evolved.
21. Nakamura A, Fujioka S, Sunohara H, Kamiya N, Hong Z, Inukai Y, Miura K, Takatsuto S, Yoshida S, Ueguchi-Tanaka M *et al.*: **The role of OsBRI1 and its homologous genes, OsBRL1 and OsBRL3, in rice.** *Plant Physiol* 2006, **140**:580-590.
22. Yokota T, Ohnishi T, Shibata K, Asahina M, Nomura T, Fujita T, Ishizaki K, Kohchi T: **Occurrence of brassinosteroids in non-flowering land plants, liverwort, moss, lycophyte and fern.** *Phytochemistry* 2017, **136**:46-55.
23. Hothorn M, Belkhadir Y, Dreux M, Dabi T, Noel JP, Wilson IA, Chory J: **Structural basis of steroid hormone perception by the receptor kinase BRI1.** *Nature* 2011, **474**:467-471.
24. She J, Han Z, Kim T-W, Wang JJ, Cheng W, Chang J, Shi S, Wang JJ, Yang M, Wang Z-Y *et al.*: **Structural insight into brassinosteroid perception by BRI1.** *Nature* 2011, **474**:472-476.
25. She J, Han Z, Zhou B, Chai J: **Structural basis for differential recognition of brassinolide by its receptors.** *Protein Cell* 2013, **4**:475-482.

These three papers describe the structural basis of brassinosteroid binding to the extracellular part of the BRI1 and BRL1 receptors. These discoveries rationalized all previous knowledge of brassinosteroid signaling at the plasma membrane.

26. Li J, Wen J, Lease KA, Doke JT, Tax FE, Walker JC: **BAK1, an Arabidopsis LRR receptor-like protein kinase, interacts with BRI1 and modulates brassinosteroid signaling.** *Cell* 2002, **110**:213-222.
27. Nam KH, Li J: **BRI1/BAK1, a receptor kinase pair mediating brassinosteroid signaling.** *Cell* 2002, **110**:203-212.
28. Wang X, Li X, Meisenhelder J, Hunter T, Yoshida S, Asami T, Chory J: **Autoregulation and homodimerization are involved in the activation of the plant steroid receptor BRI1.** *Dev Cell* 2005, **8**:855-865.
29. Wang X, Kota U, He K, Blackburn K, Li J, Goshe MB, Huber SC, Clouse SD: **Sequential transphosphorylation of the BRI1/BAK1 receptor kinase complex impacts early events in brassinosteroid signaling.** *Dev Cell* 2008, **15**:220-235.
30. Sun Y, Han Z, Tang J, Hu Z, Chai C, Zhou B, Chai J: **Structure reveals that BAK1 as a co-receptor recognizes the BRI1-bound brassinolide.** *Cell Res* 2013, **23**:1326-1329.
31. Karlova R, Boeren S, Russinova E, Aker J, Vervoort J, de Vries S: **The Arabidopsis somatic embryogenesis receptor-like kinase1 protein complex includes brassinosteroid-insensitive1.** *Plant Cell* 2006, **18**:626-638.
32. He K, Gou X, Yuan T, Lin H, Asami T, Yoshida S, Russell SD, Li J: **BAK1 and BKK1 regulate brassinosteroid-dependent growth and brassinosteroid-independent cell-death pathways.** *Curr Biol* 2007, **17**:1109-1115.
33. Gou X, Yin H, He K, Du J, Yi J, Xu S, Lin H, Clouse SD, Li J: **Genetic evidence for an indispensable role of somatic embryogenesis receptor kinases in brassinosteroid signaling.** *PLoS Genet* 2012, **8**:e1002452.
34. Santiago J, Henzler C, Hothorn M: **Molecular mechanism for plant steroid receptor activation by somatic embryogenesis co-receptor kinases.** *Science* (80-) 2013, **341**:889-892.
35. Hohmann U, Santiago J, Nicolet J, Olsson V, Spiga FM, Hothorn LA, Butenko MA, Hothorn M: **Mechanistic basis for the activation of plant membrane receptor kinases by SERK-family coreceptors.** *Proc Natl Acad Sci U S A* 2018, **115**:3488-3493.

In this paper, the authors unveil the structural basis of receptor-ligand-coreceptor complex formation. Interestingly, BAK1 uses a different subset of residues when interacting with the BRI1-BL or HAESA-IDA complexes.

36. Sun Y, Li L, Macho AP, Han Z, Hu Z, Zipfel C, Zhou J-M, Chai J: **Structural basis for flg22-induced activation of the Arabidopsis FLS2-BAK1 immune complex.** *Science* (80-) 2013, **342**:624-628.
 37. Smakowska-Luzan E, Mott GA, Parys K, Stegmann M, Howton TC, Layeghifard M, Neuhold J, Lehner A, Kong J, Grunwald K *et al.*: **An extracellular network of Arabidopsis leucine-rich repeat receptor kinases.** *Nature* 2018, **553**:342-346.
- In this paper, the authors construct the complete interaction network of Arabidopsis LRR-RLK extracellular domains. The authors demonstrate how it operates as a unified regulatory network in order to finetune responses. Moreover, they predicted and validated several unknown small RLKs interacting with BRI1, showing that they actually have an effect on BR signaling.
38. Ahmed H, Howton TC, Sun Y, Weinberger N, Belkhadir Y, Mukhtar MS: **Network biology discovers pathogen contact points in host protein-protein interactomes.** *Nat Commun* 2018, **9**:2312.
 39. Wu D, Liu Y, Xu F, Zhang Y: **Differential requirement of BAK1 C-terminal tail in development and immunity.** *J Integr Plant Biol* 2018, **60**:270-275.
 40. Perraki A, DeFalco TA, Derbyshire P, Avila J, Sere D, Sklenar J, Qi X, Stransfeld L, Schwessinger B, Kadota Y *et al.*: **Phosphocode-dependent functional dichotomy of a common co-receptor in plant signaling.** *Nature* 2018, **561**:248-252.

This paper shows how BAK1 requires different and independent phosphorylation patterns for regulating the different functions in which it is involved.

41. Wang Z-Y, Seto H, Fujioka S, Yoshida S, Chory J: **BRI1 is a critical component of a plasma-membrane receptor for plant steroids.** *Nature* 2001, **410**:380-383.
42. Wang X, Chory J: **Brassinosteroids regulate dissociation of BKI1, a negative regulator of BRI1 signaling, from the plasma membrane.** *Science* (80-) 2006, **313**:1118-1122.
43. Oh M-H, Bender KW, Kim SY, Wu X, Lee S, Nou I-S, Zielinski RE, Clouse SD, Huber SC: **Functional analysis of the BRI1 receptor kinase by Thr-for-Ser substitution in a regulatory autophosphorylation site.** *Front Plant Sci* 2015, **6**:562.
44. Oh M-H, Ray WK, Huber SC, Asara JM, Gage DA, Clouse SD: **Recombinant brassinosteroid insensitive 1 receptor-like kinase autophosphorylates on serine and threonine residues and phosphorylates a conserved peptide motif in vitro.** *Plant Physiol* 2000, **124**:751-766.
45. Jaillais Y, Hothorn M, Belkhadir Y, Dabi T, Nimchuk ZL, Meyerowitz EM, Chory J: **Tyrosine phosphorylation controls brassinosteroid receptor activation by triggering membrane release of its kinase inhibitor.** *Genes Dev* 2011, **25**:232-237.
46. Yun HS, Bae YH, Lee YJ, Chang SC, Kim S-K, Li J, Nam KH: **Analysis of phosphorylation of the BRI1/BAK1 complex in Arabidopsis reveals amino acid residues critical for receptor formation and activation of BR signaling.** *Mol Cells* 2009, **27**:183-190.
47. Wang J, Jiang J, Wang J, Chen L, Fan S-L, Wu J-W, Wang X, Wang Z-X: **Structural insights into the negative regulation of BRI1 signaling by BRI1-interacting protein BKI1.** *Cell Res* 2014, **24**:1328-1341.
48. Hink MA, Shah K, Russinova E, de Vries SC, Visser AJWG: **Fluorescence fluctuation analysis of Arabidopsis thaliana somatic embryogenesis receptor-like kinase and brassinosteroid insensitive 1 receptor oligomerization.** *Biophys J* 2008, **94**:1052-1062.
49. Bojar D, Martinez J, Santiago J, Rybin V, Bayliss R, Hothorn M: **Crystal structures of the phosphorylated BRI1 kinase domain and implications for brassinosteroid signal initiation.** *Plant J* 2014, **78**:31-43.
50. Yan L, Ma Y, Liu D, Wei X, Sun Y, Chen X, Zhao H, Zhou J, Wang Z, Shui W *et al.*: **Structural basis for the impact of phosphorylation on the activation of plant receptor-like kinase BAK1.** *Cell Res* 2012, **22**:1304-1308.
51. Tang W, Kim T-W, Oses-Prieto JA, Sun Y, Deng Z, Zhu S, Wang R, Burlingame AL, Wang Z-Y: **BSKs mediate signal transduction from the receptor kinase BRI1 in Arabidopsis.** *Science* 2008, **321**:557-560.
52. Sreeramulu S, Mostizky Y, Sunitha S, Shani E, Nahum H, Salomon D, Hayun L, Ben, Gruetter C, Rauh D, Ori N *et al.*: **BSKs are partially redundant positive regulators of brassinosteroid signaling in Arabidopsis.** *Plant J* 2013, **74**:905-919.
53. Minami A, Takahashi K, Inoue S, Tada Y, Kinoshita T: **Brassinosteroid induces phosphorylation of the plasma membrane H⁺-ATPase during hypocotyl elongation in Arabidopsis thaliana.** *Plant Cell Physiol* 2019, **60**(5):935-944 <http://dx.doi.org/10.1093/pcp/pcz005>.
54. Inoue S, Iwashita N, Takahashi Y, Gotoh E, Okuma E, Hayashi M, Tabata R, Takemiya A, Murata Y, Doi M *et al.*: **Brassinosteroid involvement in Arabidopsis thaliana stomatal opening.** *Plant Cell Physiol* 2017, **58**:1048-1058.
55. Holzwart E, Huerta Al, Glockner N, Gamelo Gomez B, Wanke F, Augustin S, Askani JC, Schurholz A-K, Harter K, Wolf S: **BRI1 controls vascular cell fate in the Arabidopsis root through RLP44 and phytoсульфокine signaling.** *Proc Natl Acad Sci U S A* 2018, **115**:11838-11843.
56. Saito M, Kondo Y, Fukuda H: **BES1 and BZR1 redundantly promote phloem and xylem differentiation.** *Plant Cell Physiol* 2018, **59**:590-600.

57. Kang YH, Breda A, Hardtke CS: **Brassinosteroid signaling directs formative cell divisions and protophloem differentiation in Arabidopsis root meristems.** *Development* 2017, **144**:272-280.
58. Klok EJ, Wilson IW, Wilson D, Chapman SC, Ewing RM, Somerville SC, Peacock WJ, Dolferus R, Dennis ES: **Expression profile analysis of the low-oxygen response in Arabidopsis root cultures.** *Plant Cell* 2002, **14**:2481-2494.
59. Ohashi-Ito K, Kubo M, Demura T, Fukuda H: **Class III homeodomain leucine-zipper proteins regulate xylem cell differentiation.** *Plant Cell Physiol* 2005, **46**:1646-1656.
60. Fabregas N, Lozano-Elena F, Blasco-Escamez D, Tohge T, ●● Martínez-Andujar C, Albacete A, Osorio S, Bustamante M, Riechmann JL, Nomura T *et al.*: **Overexpression of the vascular brassinosteroid receptor BRL3 confers drought resistance without penalizing plant growth.** *Nat Commun* 2018, **9**.
- In this paper, the authors use multi-omics approaches, genetics and physiology to report that increasing BRL3 receptors, preferentially in vascular tissues, generates a metabolomic signature of osmoprotectant compounds that are transported from shoot to roots, allowing plants to maintain growth while tolerating severe drought.
61. Tunc-Ozdemir M, Li B, Jaiswal DK, Urano D, Jones AM, Torres MP: **Predicted functional implications of phosphorylation of regulator of G protein signaling protein in plants.** *Front Plant Sci* 2017, **8**:1456.
62. Ullah H, Chen JG, Young JC, Im KH, Sussman MR, Jones AM, Siderovski DP: **Modulation of cell proliferation by heterotrimeric G protein in Arabidopsis.** *Science* 2001, **292**:2066-2069.
63. Tunc-Ozdemir M, Jones AM: **BRL3 and AtRGS1 cooperate to fine tune growth inhibition and ROS activation.** *PLoS One* 2017, **12**:e0177400.
64. Ogita N, Okushima Y, Tokizawa M, Yamamoto YY, Tanaka M, Seki M, Makita Y, Matsui M, Okamoto-Yoshiyama K, Sakamoto T *et al.*: **Identifying the target genes of SUPPRESSOR OF GAMMA RESPONSE 1, a master transcription factor controlling DNA damage response in Arabidopsis.** *Plant J* 2018, **94**:439-453.
65. Hategan L, Godza B, Kozma-Bognar L, Bishop GJ, Szekeres M: **Differential expression of the brassinosteroid receptor-encoding BRI1 gene in Arabidopsis.** *Planta* 2014, **239**:989-1001.
66. Vragović K, Sela A, Friedlander-Shani L, Fridman Y, Hacham Y, Holland N, Bartom E, Mockler TC, Savaldi-Goldstein S: **Translatome analyses capture of opposing tissue-specific brassinosteroid signals orchestrating root meristem differentiation.** *Proc Natl Acad Sci U S A* 2015, **112**:923-928.
67. Tunc-Ozdemir M, Urano D, Jaiswal DK, Clouse SD, Jones AM: **Direct modulation of heterotrimeric G protein-coupled signaling by a receptor kinase complex.** *J Biol Chem* 2016, **291**:13918-13925.

RESEARCH ARTICLE

SPECIAL ISSUE: PLANT CELL BIOLOGY

Paracrine brassinosteroid signaling at the stem cell niche controls cellular regeneration

Fidel Lozano-Elena^{1,§}, Ainoa Planas-Riverola^{1,§}, Josep Vilarrasa-Blasi^{1,*}, Rebecca Schwab^{2,‡} and Ana I. Caño-Delgado^{1,¶}

ABSTRACT

Stem cell regeneration is crucial for both cell turnover and tissue healing in multicellular organisms. In *Arabidopsis* roots, a reduced group of cells known as the quiescent center (QC) act as a cell reservoir for surrounding stem cells during both normal growth and in response to external damage. Although cells of the QC have a very low mitotic activity, plant hormones such as brassinosteroids (BRs) can promote QC divisions. Here, we used a tissue-specific strategy to investigate the spatial signaling requirements of BR-mediated QC divisions. We generated stem cell niche-specific receptor knockout lines by placing an artificial microRNA against BRI1 (BRASSINOSTEROID INSENSITIVE 1) under the control of the QC-specific promoter WOX5. Additionally, QC-specific knock-in lines for BRI1 and its downstream transcription factor BES1 (BRI1-EMS-SUPPRESSOR1) were also created using the WOX5 promoter. By analyzing the roots of these lines, we show that BES1-mediated signaling cell-autonomously promotes QC divisions, that BRI1 is essential for sensing nearby inputs and triggering QC divisions and that DNA damage promotes BR-dependent paracrine signaling in the stem cell niche as a prerequisite to stem cell replenishment.

KEY WORDS: Brassinosteroid, Quiescent center, Cell division, Stem cell, DNA damage, Paracrine

INTRODUCTION

Brassinosteroids (BRs) are plant steroid hormones that were originally discovered in *Brassica napus* pollen for their ability to promote growth when exogenously applied to other vascular plants (Mitchell et al., 1970). Impaired BR biosynthesis or signaling causes reduced organ growth and abnormal development, and thereby limits plant fertility and yield (Li and Chory, 1997; Wei and Li, 2016). Despite parallels between the functions of plant and animal steroid hormones (Li and Chory, 1997; Thummel and Chory, 2002), substantial differences exist with respect to their perception and signal transduction mechanisms. Whereas animal steroid perception is mainly mediated by transcription factors inside

the cell (Aranda and Pascual, 2001), plant steroids are perceived by leucine-rich repeat (LRR) receptor kinases located at the plasma membrane (Kim and Wang, 2010).

BR signaling is initiated by the direct binding of the steroid molecule to a 93 amino acid region located within the extracellular domain of the LRR receptor kinase BRI1 (BRASSINOSTEROID INSENSITIVE 1) (Hothorn et al., 2011; Kinoshita et al., 2005; Wang et al., 2001). Upon BR binding, the heterodimerization of BRI1 with BAK1 (BRI1-ASSOCIATED RECEPTOR KINASE 1) is enhanced, and a cytoplasmic cascade of phosphorylation and dephosphorylation events is initiated (Li and Nam, 2002; Russinova et al., 2004). These events lead to the degradation of BIN2 (BRASSINOSTEROID INSENSITIVE 2) kinase (Li and Nam, 2002; Peng et al., 2008), and a consequential increase in the dephosphorylated forms of the BZR1 (BRASSINAZOLE RESISTANCE 1) (Wang et al., 2002) and BES1 (BRI1-EMS-SUPPRESSOR 1) (Yin et al., 2002) transcription factors. Dephosphorylated BZR1 and BES1 are translocated into the nucleus where they modulate the transcription of thousands of genes by directly interacting with DNA and other transcription factors (He et al., 2002). In fact, BZR1 and BES1 are known to bind specific DNA sequences: the BR-response element (BRRE, CGTGC/TG) and E-boxes (CANNTG) (He et al., 2005; Sun et al., 2010; Yu et al., 2011). Furthermore, recent work has revealed that these transcription factors are subjected to post-transcriptional regulation in response to external stimuli such as light (Kim et al., 2014) and environmental stress (Nolan et al., 2017). In this way, BR-mediated transcriptional responses are also controlled by an additional regulatory layer.

In addition to BRI1, *Arabidopsis* contains three BRI1-like (BRL) receptor kinase homologues. Interestingly, however, only BRL1 and BRL3 (BRI1-LIKE 1 and 3) are functional BR receptors capable of binding the hormone (Cano-Delgado et al., 2004). Although BRI1 is present in the majority of plant cells (Friedrichsen and Chory, 2001), the BRL1 and BRL3 receptors are enriched in vascular tissues and the stem cell niche (Cano-Delgado et al., 2004; Fábregas et al., 2013; Salazar-Henao et al., 2016).

By providing a continuous supply of precursor cells, stem cells are primarily involved in sustaining growth and replacing damaged tissues (Sablowski, 2004). Root stem cells, also known as initials, are located at the root apex and surround the quiescent center (QC) (Dolan et al., 1993) (Fig. 1A,B). The QC, which comprises a small group of cells with very low mitotic activity, not only acts as a cell reservoir for the surrounding actively dividing stem cells (Scheres, 2007; Dolan et al., 1993), but is also responsible for maintaining the stem cells in their undifferentiated state (Sabatini et al., 2003; van den Berg et al., 1997). However, upon cellular damage, the QC loses its quiescence and enters into a state of cell division to enable stem cell replenishment (Cruz-Ramírez et al., 2013; Heyman et al., 2013; Vilarrasa-Blasi et al., 2014).

Hormonal stimulation also plays an important role in governing cell division in the QC (Gonzalez-Garcia et al., 2011; Heyman et al.,

¹Department of Molecular Genetics, Centre for Research in Agricultural Genomics (CRAG) CSIC-IRTA-UAB-UB, Barcelona E-08193, Spain. ²Cold Spring Harbor Laboratory, 1 Bungtown Road, Cold Spring Harbor, NY 11724, USA.

[§]These authors contributed equally to this work. ^{*}Present address: Carnegie Institution for Science, Department of Plant Biology, 260 Panama St. Stanford, CA 94305, USA. [‡]Present address: Max Planck Institute for Developmental Biology, 72076 Tübingen, Germany.

[¶]Author for correspondence (ana.cano@cragenomica.es)

DOI: A.I.C.-D., 0000-0002-8071-6724

This is an Open Access article distributed under the terms of the Creative Commons Attribution License (<http://creativecommons.org/licenses/by/3.0/>), which permits unrestricted use, distribution and reproduction in any medium provided that the original work is properly attributed

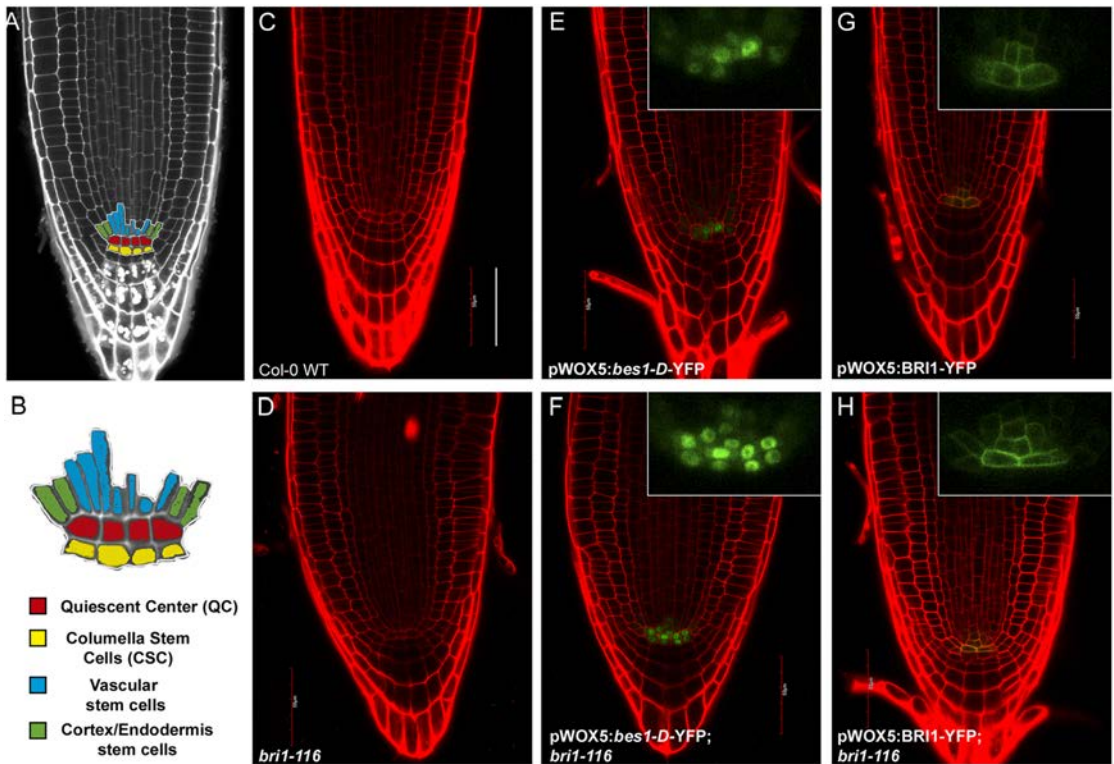


Fig. 1. The stem cell niche of Arabidopsis roots and QC-specific expression of BR pathway components. (A) A stereotypical Arabidopsis WT primary root under confocal microscopy. The root stem cell niche is highlighted in color. (B) Detailed representation of the root stem cell niche. (C–H) Confocal images of 6-day-old WT and mutant Arabidopsis roots in control conditions. Green represents YFP-tagged pathway components. Red is PI counterstaining. Insets show the YFP channels at higher magnification. Scale bar: 50 μ m.

2013; Zhang et al., 2010). For instance, BRs are known to promote both cell division in the QC and differentiation of the surrounding columella stem cells (Fàbregas et al., 2013; Gonzalez-Garcia et al., 2011; Vilarrasa-Blasi et al., 2014). More specifically, the ERF115 transcription factor, which is activated by BRs, promotes QC divisions and stem cell regeneration after DNA damage (Heyman et al., 2016, 2013). In contrast, BRAVO (BRASSINOSTEROIDS AT VASCULAR AND ORGANIZING CENTER), an R2R3-MYB transcription factor identified using cell-specific transcriptomics, acts as a repressor of QC divisions (Vilarrasa-Blasi et al., 2014). Interestingly, BRAVO is a direct transcriptional target of and interacts with the BR-regulated transcription factor BES1 at the protein level, forming a feedback loop that antagonistically regulates QC divisions (Vilarrasa-Blasi et al., 2014). Despite the importance of these transcription factors for locally safeguarding QC divisions, it is still unknown whether BR-regulated QC function is maintained in a cell-autonomous fashion or requires external signaling. Moreover, although BR receptors collectively modulate QC cell division and differentiation of surrounding stem cells under normal conditions (Fàbregas et al., 2013), the specific contribution of each receptor within the stem cell niche is not known.

These questions prompted us to investigate BR-mediated regulation of quiescence and its impact on stem cell regeneration after DNA damage at the local level. Accordingly, we used a

tissue-specific approach in order to determine the ability of QC cells to integrate exogenous steroid signals. For this purpose, we specifically overexpressed two BR signaling components – the BRI1 membrane receptor and the BES1 transcription factor – in QC cells, and specifically knocked out BRI1 in the stem cell niche using an artificial microRNA (amiRNA) (Dolan et al., 1993; Schwab et al., 2006). Altogether, we demonstrate that: (1) active BES1 is necessary for cell-autonomous QC divisions; (2) the BR hormone itself (i.e. not the receptors) is the limiting factor for BR-induced QC divisions in the root apex; (3) BRI1 is required at the stem cell niche for mediating BR-dependent QC divisions; and (4) upon stem cell death, paracrine BR signaling is required for QC divisions. Overall, our results establish a hierarchy for the different BR receptors within the stem cell niche, indicating that under normal conditions the BRI1 receptor acts as the principal player controlling QC divisions, rather than its homologous.

RESULTS

Active BES1 promotes cell-autonomous QC division

We first wanted to elucidate whether the BR-induced division signals of the QC were transduced in a cell-autonomous manner through the canonical BR signaling cascade. To this end, we used the gain-of-function BES1 mutant, *bes1-D*, which is known to be constitutively active (Yin et al., 2002). Previously, we cloned *bes1-D* under the control of the promoter of the QC-specific gene

WOX5 (Sarkar et al., 2007), and fused YFP to its C-terminus (Vilarrasa-Blasi et al., 2014). This construct, pWOX5:*bes1-D*-YFP, was transformed into both Col-0 wild-type (WT) and the null BRI1 mutant *bri1-116* (Li and Chory, 1997) (Fig. 1C–F).

Confocal microscopy of 6-day-old roots revealed an increase in the number of QC divisions in both the WT and the *bri1-116* mutant upon expressing *bes1-D* under the *WOX5* promoter (Fig. 2A,D,F,M; Table S1). This indicates that active BES1 locally promotes division at the QC in a cell-autonomous manner. Interestingly, however, the QC division rates in the *bri1-116* background were lower than those

in the WT background (Fig. 2M; Table S1), suggesting that BR signaling from surrounding tissues also participates in activation of QC divisions.

In addition, treatment of WT plants harboring the pWOX5:*bes1-D*-YFP construct with brassinolide (BL) did not result in a significant increase in cell division rates (Fig. 2D,J,M; Table S1). This is probably due to a saturated BRs signal contributed also by basal receptor-transduced signaling. Conversely, upon BL treatment, a significant increase in cell division rate was observed for the *bri1-116* plants that contained pWOX5:*bes1-D*-YFP (Fig. 2F,L,M; Table S1).

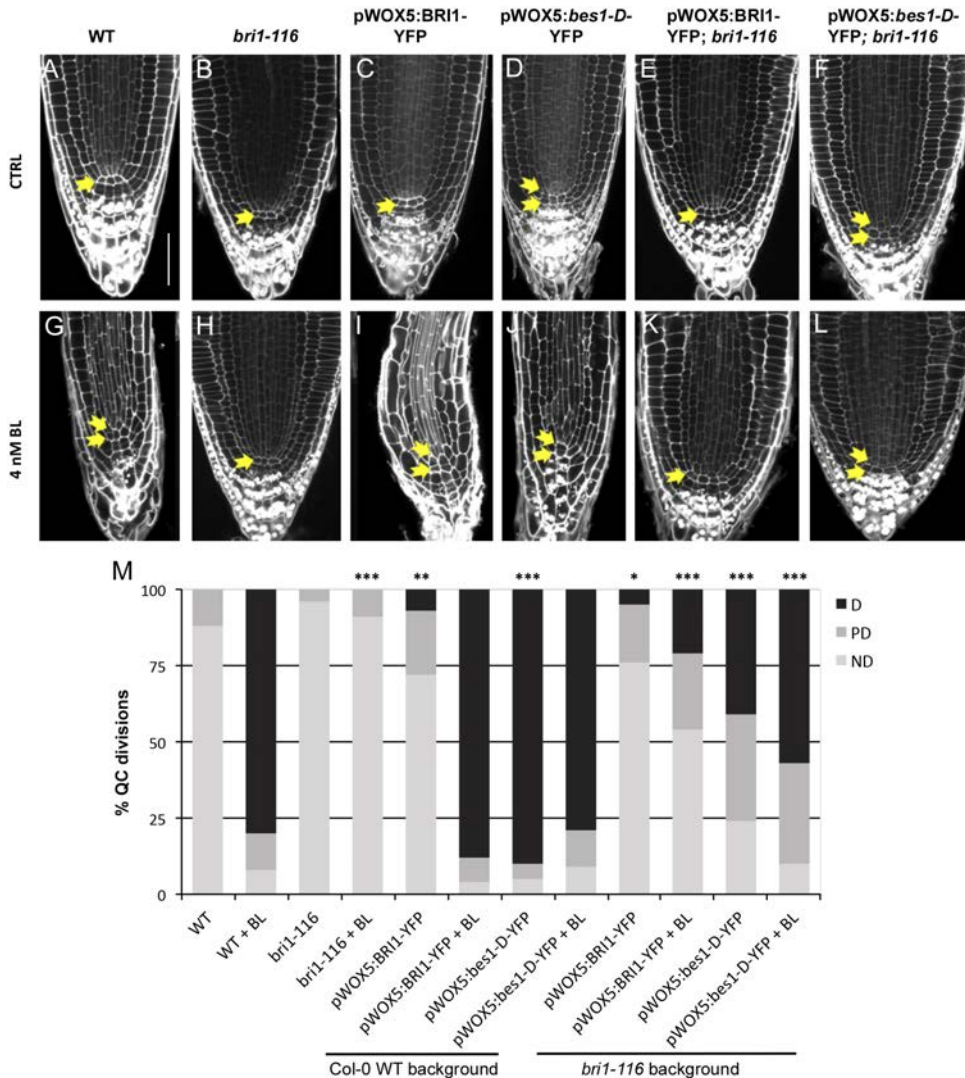


Fig. 2. The BR-regulated transcription factor BES1 promotes QC division in a cell-autonomous manner. (A–F) Confocal images of fixed 6-day-old WT and mutant Arabidopsis roots in control conditions. (G–L) Root anatomy of 6-day-old seedlings grown in medium supplemented with 4 nM BL. Arrows indicate the number of QC cell layers identified. (M) Quantification of QC division rate. ND, QC non-divided; PD, QC partially divided; D, QC totally divided. Asterisks indicate statistically significant differences due to genotype, comparing against WT either in control or 4 nM BL conditions. Frequencies in QC divisions were assessed with a two-sided Fisher's test. Values for all pairwise comparisons are provided in Table S1. Data are generated from three independent replicates ($n > 21$). * $P < 0.05$, ** $P < 0.01$, *** $P < 0.005$. Scale bar: 50 μ m.

This suggests that the signal is not saturated in these plants, and that the BRL receptors are also contributing factors.

The local BR hormone level is the main limiting factor for QC division

Next, by introducing the pWOX5:BR11-YFP transgene into both WT and *bri1-116* backgrounds, we evaluated the local contribution of the BR11 receptor to QC division (Fig. 1C,E). As the *WOX5* promoter drives relatively high expression compared with the endogenous *BR11* promoter, *WOX5*-controlled expression of the BR11 receptor resulted in its local overexpression in the QC. Confocal images comparing BR11 expression under its endogenous promoter (Geldner et al., 2007) with BR11 expression in the pWOX5:BR11-YFP lines are shown in Fig. S1.

When BR11 is locally overexpressed using the *WOX5* promoter, a small increase in QC division rate was observed in both the WT and the *bri1-116* backgrounds (Fig. 2C,E,M; Table S1). This increase, however, was substantially smaller than that observed upon expression of *bes1-D* using the same promoter (Fig. 2D,F,M; Table S1). Upon application of exogenous BL, we observed a dramatic increase in the QC division rate for those plants expressing pWOX5:BR11-YFP in the WT background but not in the *bri1-116* background (Fig. 2C,E,I,K,M; Table S1). This implies that BR11 signaling in the QC alone is not sufficient to promote QC divisions, but rather additional external signaling is required. The fact that overexpression of BR11 in the QC did not result in a large increase in QC division until exogenous BL was applied, indicates that the BR hormone itself is the limiting factor of QC division. Furthermore, only after applying BL to the pWOX5:BR11-YFP; *bri1-116* roots could a dramatic reduction in meristem cell number be observed (Fig. S2A). This typical effect of exogenous BL application was not seen when just BR11 is overexpressed. Together, these results suggest two possible scenarios: (1) there is an insufficient level of BRs in the root stem cell niche to promote QC division, or (2) BR11-like receptors (i.e. BRL1 and BRL3) act as competitors for BR ligand binding.

To address the second scenario, we crossed the pWOX5:BR11-YFP plants with double and triple mutants lacking two (*bri1bri3*) or all receptors (*bri1-116bri1bri3*), respectively, and assessed the occurrence of spontaneous QC divisions or an increased sensitivity to BL. Application of BL to the *bri1bri3* double mutant backgrounds yielded similar effects to those in the WT background, showing that the loss of these genes does not affect QC division rates even when applying lower concentrations of BL (0.04 nM) (Fig. S3, Table S2). With respect to the triple mutant, we obtained results similar to those found in the *bri1-116* background (Fig. S3, Table S2). Altogether, these results indicate that the BRL1/3 receptors do not compete with the BR11 receptor for hormone binding. Interestingly, a lack of BRL receptors attenuates the slight increase in QC division that is observed upon overexpressing BR11 in the QC (Fig. 2M; Fig. S3K, Table S2). In agreement with previously reported data (Fàbregas et al., 2013), this supports a marginal role for the BRL1 and BRL3 receptors in promoting BR-mediated QC divisions in normal conditions. These results, together with the previous ones, exclude the possibility that BRL receptors compete with BR11 for ligand binding. Thus, we conclude that the BR hormone concentration must be the limiting factor for promoting QC division.

BR11 is required in the stem cell niche for BL-triggered QC division

To more thoroughly understand the receptor requirements that drive BES1-mediated QC division, we specifically knocked out BR11

expression in the WOX5 domain. For this, we designed and cloned an amiRNA against BR11 (see Materials and Methods; Fig. S4A,B). To validate the ability of our amiRNA to knock out BR11 expression, we first placed it under the control of the constitutive promoter CaMV35S. This resulted in dwarf plants similar to null *bri1* mutants (Li and Chory, 1997) (Fig. S4C). Next, cell-specific knockouts were generated by placing the amiRNA under the control of the QC-specific promoter *WOX5*. As seen by crossing pWOX5:BR11-amiR plants with plants expressing BR11-GFP under the control of the endodermis-specific promoter *scarecrow* (*SCR*) (Hacham et al., 2011), inhibition of BR11 expression was not limited to the QC cells, but also occurred in nearby surrounding cells (Fig. 3A,B). This implies that the small size of the mature amiRNA enables it to diffuse to adjacent cells. Importantly, YFP signals observed in plants that overexpressed BR11-YFP in the QC completely disappear when crossed with pWOX5:BR11-amiR plants, indicating that our amiRNA is indeed effective at attenuating BR11 expression (Fig. 3C,D). Finally, genetic crosses between the pWOX5:BR11-amiR line and the translational reporter lines pBRL1:BRL1-GFP and pBRL3:BRL3-GFP (Fàbregas et al., 2013), showed that the BR11-amiR is partially depleting *BRL1* and *BRL3* transcripts, as consequence of sequence similarity (Fig. 3E H). A GFP intensity reduction of ~40% could be detected in the crosses (Fig. S5A,B).

Next, we analyzed two independent pWOX5:BR11-amiR lines in terms of their sensitivity towards exogenous BL. Based on root length, meristem cell number and stele width, we found that both lines expressing the amiRNA retained a BL sensitivity closely similar to that of WT plants. In contrast, the null *bri1-116* plants were insensitive to hormone application (Fig. S2C E), thereby suggesting that the effect of the mature amiRNA is strongly limited to a local level. Interestingly, both pWOX5:BR11-amiR lines were completely insensitive to BL application in terms of QC division (Fig. 4A G; Table S3). Taken together, these results indicate that the presence of BR11 receptors in the QC is essential for QC division. Additionally, pWOX5:BR11-amiR lines exhibited impaired root growth, having slightly, but significantly shorter roots than WT plants starting from 5 days after germination (Fig. 4H; Fig. S2C), suggesting that the presence of BR receptors in root stem cell niche contributes for optimal root growth.

We next asked whether the reduction in QC divisions in the pWOX5:BR11-amiR lines was a consequence of a slower cell cycle progression in the meristem. To answer this question, we stained roots with 5-ethynyl-2'-deoxyuridine (EdU), a thymidine analogue that is incorporated into actively dividing cells (Salic and Mitchison, 2008). In WT plants, we observed a uniform EdU staining in the entire root meristem except for in the QC, which owing to its quiescence, barely incorporates EdU (Fig. 5A). The same results, which are indicative of a normal cell cycle in the meristem, were also obtained for the pWOX5:BR11-amiR lines (Fig. 5B,C). Thus, the QC remains quiescent because of the absence of BR11, and not because of a meristem-wide deceleration of the cell cycle. In contrast, the *bri1-116* mutant showed a much lower extent of EdU incorporation, thereby confirming that it has a slower cell cycle compared with WT plants (Fig. 5D). Fluorescence intensity quantification confirmed that pWOX5:BR11-amiR lines incorporate EdU at the same levels as in the WT, whereas *bri1-116* does so at lower rates (Fig. S5C) and it agrees with the previously reported slow cell cycle progression of *bri1-116* (Gonzalez-Garcia et al., 2011).

Furthermore, we treated both WT and pWOX5:BR11-amiR lines with BL in order to evaluate whether BL promotes QC cell division. Upon BL treatment, WT roots incorporated EdU into the QC

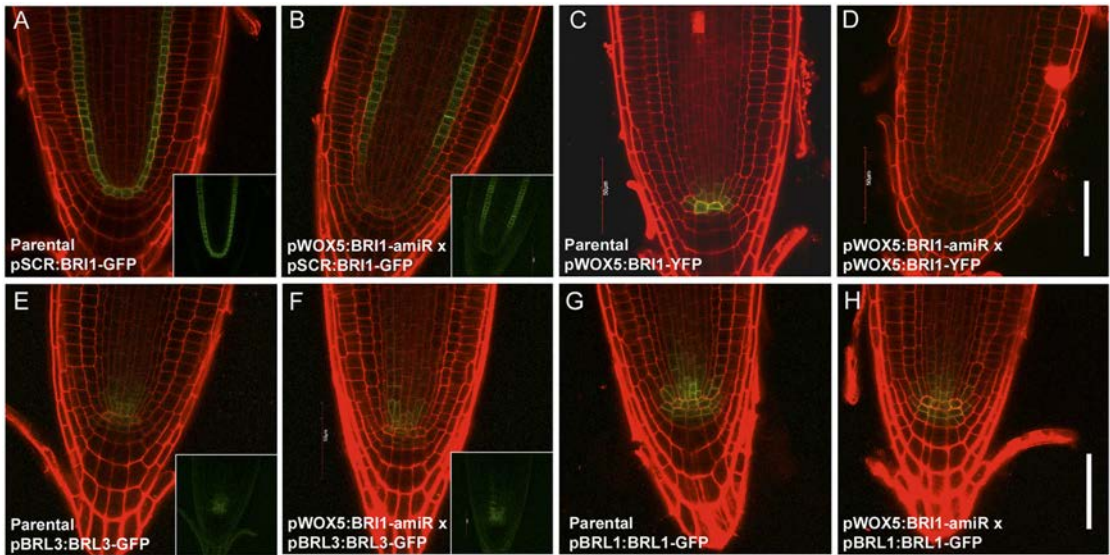


Fig. 3. The pWOX5:BR11-amiR construct targets BR1 and downregulates its transcription in the root stem cell microenvironment. Confocal images of 6-day-old Arabidopsis roots. (A,B) Genetic crosses between pWOX5:BR11-amiR and pSCR:BR11-GFP lines reveal that BR11 is knocked down in the stem cell microenvironment. (C,D) Genetic crosses between pWOX5:BR11-YFP and pWOX5:BR11-amiR lines show that the amiRNA completely depletes BR11 around the QC domain. (E–H) Genetic crosses of pWOX5:BR11-amiR lines with pBRL1:BRL1-GFP and pBRL3:BRL3-GFP lines. Insets show the GFP channel separately. All crosses are F3 double homozygous plants. Scale bar: 50 μ m.

(Fig. 5E), thereby confirming that the QC cells were undergoing cell division. In contrast, however, the pWOX5:BR11-amiR lines did not incorporate EdU into the QC after being subjected to identical BL treatment (Fig. 5F,G). This clearly supports the hypothesis that pWOX5:BR11-amiR lines are insensitive to BR-mediated signals in the QC. Along the same lines, the plant that has a constitutively dividing QC due to overexpression of active BES1 (i.e. the pWOX5: *bes1-D*-YFP line), also exhibited EdU incorporation in the QC (Fig. 5H). This, in effect, mimics the results obtained with exogenous BL treatment, and confirms that activated downstream components of BR receptors are capable of triggering QC division in a cell-autonomous manner.

Stem cell regeneration upon DNA damage entails the local action of BR receptors

Since the QC has been proposed to act as a stem cell reservoir and is known to divide in the face of environmental stresses, we decided to evaluate whether the BR receptors are essential for carrying out such stress-induced division. For this purpose, we decided to use bleomycin, a chemotherapeutic drug that has been described to preferentially harm root vascular stem cells and induce QC division (Fulcher and Sablowski, 2009; Vilarrasa-Blasi et al., 2014). As such, this system triggers QC division independently of BR treatment. We compared the local knockout lines (i.e. pWOX5: BR11-amiR) against both the null *bri1* mutant and WT roots. While the pWOX5:BR11-amiR lines were damaged at the same rate as the WT plants (Fig. 6A,B,C,I; Table S4), the *bri1* mutant remained free of any visible damage (Fig. 6D,I; Table S4). As previously described, this is probably due to its slow cell cycle progression (Gonzalez-Garcia et al., 2011; Vilarrasa-Blasi et al., 2014). Interestingly, in contrast to what was observed for the WT roots, the QC of the pWOX5:BR11-amiR lines remained undivided

following 24 h of bleomycin treatment plus 24 h of recovery (Fig. 6E,F,G,J; Table S5). In the case of *bri1*, the QC also remained undivided, but as previously mentioned, the roots were not damaged by bleomycin (Fig. 6H,J). Given that the pWOX5:BR11-amiR lines and WT show similar levels of provascular cell death after 24 h of bleomycin treatment (Fig. 6A,B,C,I; Table S4), as well as the same amount of EdU staining (Fig. 5A C; Fig. S5C), our results argue that the absence of QC divisions in bleomycin-treated pWOX5: BR11-amiR lines is due to neither an inherent resistance against DNA damage nor a slow cell cycle progression. Interestingly, our results reveal the paracrine nature of this DNA damage response: a signal that emerges from damaged stem cells triggers cell division in the adjacent QC. Moreover, according to our data, this signal must be a type of steroid molecule that is locally and mainly transduced by BR11 in the stem cell niche.

DISCUSSION

The slow-dividing nature of the cells in the QC enable it to act as a cell reservoir and organizer for surrounding stem cells (Fulcher and Sablowski, 2009; Pi et al., 2015; Sarkar et al., 2007; van den Berg et al., 1997; Vilarrasa-Blasi et al., 2014). Although recent studies have started to shed light on the molecular components behind QC quiescence, the exact mechanisms that are responsible for ensuring such a low rate of cell division remain largely unknown. One fairly recent study discovered that the interaction between RETINOBLASTOME-RELATED (RBR) and SCARECROW (SCR) is required for quiescence maintenance (Cruz-Ramirez et al., 2013). Nonetheless, rather than being completely static, the QC is in fact regulated by plant hormone signaling. For instance, while it has been shown that abscisic acid (ABA) reinforces the quiescence of this group of cells (Zhang et al., 2010), ethylene (Ortega-Martinez et al., 2007) and cytokinin (Zhang et al., 2013) are

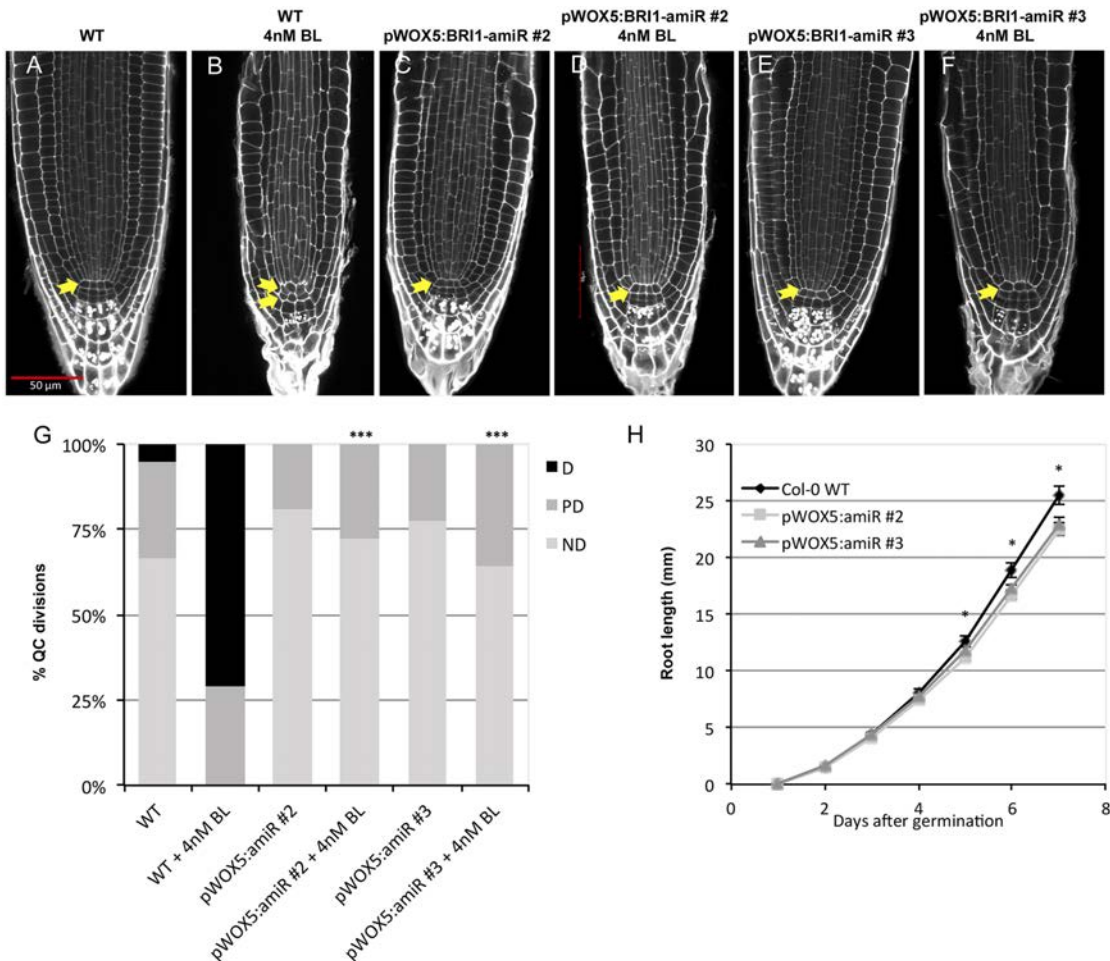


Fig. 4. BRR1 in the stem cells niche is required to promote QC divisions. (A, B) Confocal images of 6-day-old WT *Arabidopsis* roots grown in either control conditions or 4 nM BL show the change in QC division and organization. (C–F) pWOX5:BRR1-amiR transgenic lines grown in control conditions or in medium supplemented with 4 nM BL. Arrows indicate the number of QC cell layers identified. (G) Quantification of the QC divisions of WT and pWOX5:BRR1-amiR plants. ND, QC non-divided; PD, QC partially divided; D, QC totally divided. Asterisks indicate statistically significant differences due to genotype, comparing against WT either in control or 4 nM BL conditions (** $P < 0.005$). Frequencies in division occurrence were assessed with a two-sided Fisher's test. Values for all pairwise comparisons are provided in Table 3. Data generated from three independent replicates ($n > 39$). (H) Root growth dynamics of WT and pWOX5:BRR1-amiR lines. Asterisks denote significant differences with respect to the WT in a two-tailed t -test ($*P < 0.05$). Data are generated from three independent replicates ($n > 46$). Scale bar: 50 μ m.

known to disrupt their quiescence and promote division. With respect to BR hormones, they have been shown to promote QC divisions while maintaining regular cell cycle progression in the rest of the root meristem (Gonzalez-Garcia et al., 2011). The mechanisms underlying BR-mediated QC divisions are slowly being uncovered with the identification of BR-regulated and QC-specific transcription factors such as ERF115 (Heyman et al., 2013) and BRAVO (Vilarrasa-Blasi et al., 2014). However, how these signaling mechanisms are locally confined to the stem cell niche of the root is still controversial. In fact, although it has been proposed that BR action at the epidermis (Hacham et al., 2011) and vascular tissues (Kang et al., 2017) can similarly regulate meristem size and plant growth, it is unknown whether these local signals are also

capable of driving QC divisions. Here, our findings show that QC activities at the stem cell niche require the presence of BR receptors in both the QC cells themselves and nearby surrounding cells.

Activated BES1 can trigger cell-autonomous QC division but needs membrane support

Physiological analysis of QC-specific overexpression of BES1 revealed that active BES1 has the potential to trigger QC division in an autonomous manner. However, as the same QC division rates were not observed when the transgene was introduced into the *bril* mutant background (Fig. 2M; Table S1), it became apparent that BRR1 was also required for this process. It is important to note that BRR1 might also activate other downstream components besides

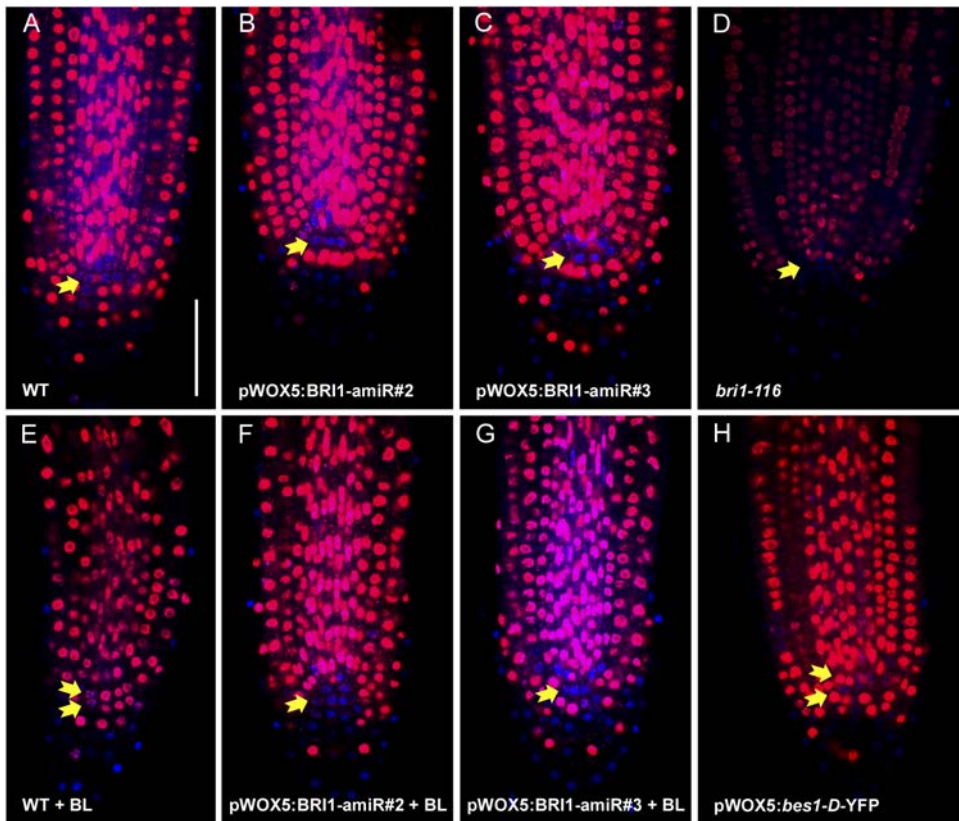


Fig. 5. pWOX5:BRI1-amiR seedlings exhibit normal meristem divisions. Confocal images of fixed and EdU-stained 6-day-old Arabidopsis roots. (A–C) WT, pWOX5:BRI1-amiR#2 and pWOX5:BRI1-amiR#3 lines grown in control conditions. (D) *bri1-116* line grown in control conditions as a negative control for QC division. (E–G) WT, pWOX5:BRI1-amiR#2, and pWOX5:BRI1-amiR#3 lines grown for 4 days in control conditions and 2 days in medium supplemented with 4 nM BL. (H) pWOX5:*bes1-D-YFP* line grown in control conditions as a positive control for QC division. Arrows indicate the number of QC cell layers identified. Scale bar: 50 μ m.

BES1. For example, one potential downstream target could be the transcription factor BZR1, which has been shown to promote autonomous QC division when activated (Chaiwanon and Wang, 2015; Lee et al., 2015). Interestingly, in the *bri1* background lines, we detected an increase in QC division frequency upon BL application (Fig. 2M; Table S1). This increase could be attributed to BRL receptors compensating for the lack of BRI1 and activating other downstream components.

The hormone is the limiting factor for promoting QC divisions

Surprisingly, when the plants that overexpressed BRI1 in the QC (pWOX5:BRI1-YFP) were assessed in terms of QC division rates, we found only a limited increase in both the WT and *bri1* backgrounds (Fig. 2M; Table S1). The fact that the roots showed signs of recovery in the *bri1* background line (i.e. longer roots) however, confirmed that BRI1 was still functional when fused to YFP (Fig. S2B). Upon BL treatment, the QC division frequency of pWOX5:BRI1-YFP plants is similar to that in WT plants treated with BL (Fig. 2M; Table S1), thus revealing that an excess of receptor has no effect until the ligand is added. As the plants overexpressing pWOX5:BRI1-YFP displayed no dramatic phenotype until exogenous hormone was applied, we concluded

that the stem cell niche microenvironment must be characterized by an excess of BRI1 and a limited amount of free hormone. We discounted competition for the ligand between BRI1 and BRLs as the reason for this (Fig. S3, Table S2), and hypothesize that, in the root stem cell niche, a threshold of available hormone has to be reached in order to promote QC divisions.

BRI1 is necessary but not sufficient to promote QC division

According to our results, the presence of BRI1 in the QC is not the limiting factor for the QC division process. In fact, very low amounts of BRI1 receptor are present within these cells (Wilma van Esse et al., 2011). Furthermore, BRL1 and BRL3, both of which bind the hormone with a higher affinity than BRI1, are also present in these cells (Cano-Delgado et al., 2004; Fàbregas et al., 2013). Accordingly, we wondered whether BRI1 was absolutely necessary in this domain. Our results show that WT lines expressing the amiRNA against BRI1 in the stem cell niche (pWOX5:BRI1-amiR) are completely insensitive towards BL-induced QC divisions (Fig. 4E). At the same time, however, BRI1 acting exclusively in the QC (i.e. pWOX5:BRI1-YFP; *bri1-116* line) is not enough to recover BL-induced QC divisions to WT levels (Fig. 2M). Taken together, these results suggest that the effects of BRI1 are reinforced

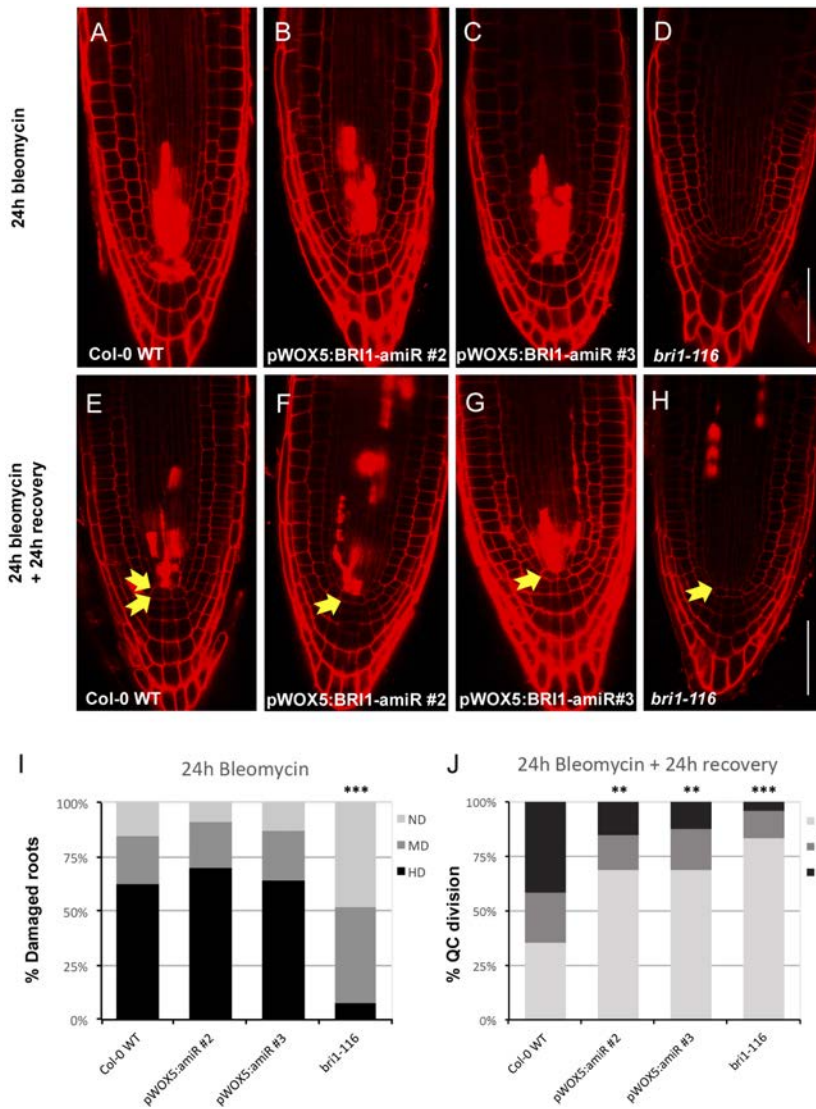


Fig. 6. BR receptors in the stem cell niche modulate QC divisions upon DNA damage. (A–D) Confocal images of 5-day-old seedlings treated with bleomycin for 24 h.

(E–H) Confocal images of 5-day-old seedlings subjected to 24 h of bleomycin treatment and a subsequent 24 h of recovery. (I) The proportion of roots showing cell death in the root apex after 24 h of bleomycin treatment. HD, hard damage; MD, mild damage; ND, no damage. Asterisks indicate statistically significant differences respect to WT (** $P < 0.005$).

Differences in the proportion of damaged roots were assessed with a two-sided Fisher's test. Values for all pairwise comparisons are provided in Table S4. Data are generated from three independent replicates ($n > 25$). (J) Quantification of QC divisions after 24 h of bleomycin treatment and 24 additional hours of recovery. ND, QC non-divided; PD, QC partially divided; D, QC totally divided. Asterisks indicate statistically significant differences with respect to WT (** $P < 0.01$, *** $P < 0.005$). Differences in division frequencies were assessed with a two-sided Fisher's test. Values for all pairwise comparisons are provided in Table S5. Data are generated from three independent replicates ($n > 24$). Scale bar: 50 μ m.

from surrounding cells. Thus, we found that BR11 signaling in the QC is necessary, but not sufficient to promote QC self-renewal, and highlight BR11 as the main driving factor for this process. Despite the fact that BRL activity is also partially downregulated in pWOX5:BR11-amiR lines, in agreement with our data, previous results showed that *bri1bri3* double mutants have a normal BR-induced QC division (Fábregas et al., 2013). On the other hand, *bri1-116* mutants, which have intact *BRL1* and *BRL3* genes, retain a quiescent QC, even upon application of high doses of BL (Gonzalez-Garcia et al., 2011) (Fig. 2M; Table S1). Our results relegate BRL receptors to a supporting action for BR11, which in turn acts as the main promoter of QC divisions in normal conditions. Moreover, QC division frequency also has an impact on the growth of primary roots, as the roots of pWOX5:BR11-amiR lines are

slightly shorter than those of the WT (Fig. 4H; Fig. S2C). Congruently, the *bri1-116* mutant lines that overexpressed BR11 or BES1 in the QC (i.e. pWOX5:BR11-YFP;*bri1-116* and pWOX5:bes1-D-YFP;*bri1-116*) not only partially recovered BR signaling in the QC, but also partially recovered seedling root length compared with that in the *bri1-116* mutant (Fig. S2D). This latter fact prompted us to hypothesize that some spontaneous QC divisions under basal conditions are required to sustain optimal root growth presumably for replenishment of the stem cell niche.

BR signaling acts in a paracrine manner to trigger QC division

It is known that the QC divides in response to environmental stresses such as the presence of DNA-damaging agents (Vilarrasa-Blasi et al., 2014) or changes in the homeostasis of reactive oxygen

species (ROS) (Yu et al., 2016). In the root, DNA-damaging agents preferentially harm vascular and columella stem cells. Cells that are unable to repair this damage activate programmed cell death (PCD) and undergo apoptosis (Fulcher and Sablowski, 2009), thereby subsequently promoting QC divisions to replenish the stem cell niche and maintain meristematic activities (Heyman et al., 2016; Vilarrasa-Blasi et al., 2014). We took advantage of this property to analyze the receptor requirements of the signaling that causes QC division. Interestingly, we found that the BRI1 receptor is necessary to trigger QC divisions after vascular cell death (Fig. 6), although we cannot discard a major contribution of BRLs under this stress scenario. Furthermore, we discounted the idea that QC quiescence observed in the pWOX5:BRI1-miR line after damage is due to a slower cell cycle (Fig. 5; Fig. S5C), as is the case for the *bri1-116* mutant. Although it has been demonstrated that downregulation of BRAVO is implicated in this type of QC division (Vilarrasa-Blasi et al., 2014), the exact nature of signal progression from the damaged cell to the QC is still unclear. Even if we cannot discern between BRI1 and the BRLs perceiving this signal, results obtained by treating the pWOX5:BRI1-miR lines with bleomycin have revealed that these signals are perceived by BR receptors acting in the stem cell niche, so the signal should be of a steroid nature and act in a paracrine manner.

It is known that by stimulating paracrine signaling, human stem cells can promote wound healing and cancer progression (Dittmer and Leyh, 2014), but in plants, the mechanisms behind autocrine and paracrine signaling are only just being uncovered (Qi et al., 2017). It has been proposed that BRs can regulate stem cell division in the roots via long-range signals originating at the epidermis (Hacham et al., 2011). However, although changes in QC markers (e.g. AGL42) were observed in response to epidermal signaling, no effect on QC divisions was reported (Hacham et al., 2011). This therefore limits direct readout of BR-mediated signaling in the QC to short-range signals. Indeed, in contrast to other hormones that act over long distances, it is accepted that BRs act at a more local level (Fridman et al., 2014) and our findings indicate that the signals that promote QC divisions come from the nearby stem cell microenvironment rather than from the outer cell layers. Nevertheless, where exactly the BR signals are driven from remains a controversy.

In summary, our findings show that (1) QC cell division activity is promoted by BES1 transcription factor in the QC; (2) BRI1 is required in both the QC and nearby cells to trigger division; and (3) paracrine steroid signaling may be regulated by the hormone's availability in the stem cell niche (Fig. 7). A plausible way to control the hormone levels in the stem cell microenvironment of the root could be to upregulate the genes controlling its biosynthesis. However, the spatial regulation of the enzymes responsible for BR biosynthesis is still poorly understood. As such, further efforts in this area are crucial for elucidating the nature and origin of BR signals, where they are synthesized and where they are driven.

MATERIAL AND METHODS

Plant material and growth conditions

All lines used in this study, along with their references are listed in Table S6. We used *Arabidopsis thaliana* (L.) Heyhn, ecotype Columbia-0 (Col-0) as the control background line.

Seeds were surface sterilized using 35% bleach, and subsequently washed five times with distilled sterile water. Seeds were vernalized at 4°C in the dark for 48 h before sowing. Plants were grown in vertical plates containing half-strength Murashige and Skoog (MS) medium with vitamins but no sucrose supplements (0.5×MS), in long day conditions (LD, 16 h light:8 h dark) at 22°C and 60% relative humidity.

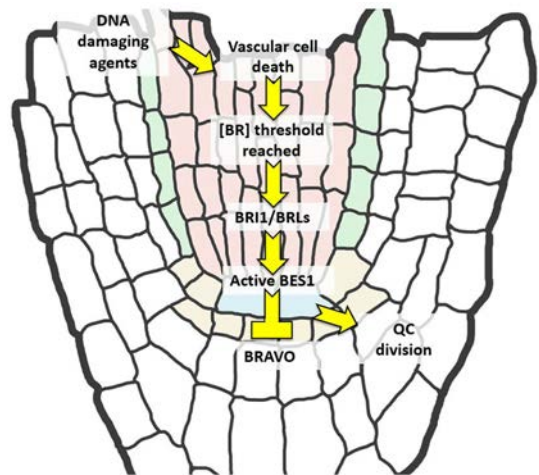


Fig. 7. Working model: BR concentration as a limiting factor for QC divisions. In order to promote QC divisions when needed, a threshold concentration of BRs has to be reached in the root apical meristem. Upon reaching this threshold, the signal is transduced via BRI1 with enough strength to promote BES1 dephosphorylation. Dephosphorylated BES1, in turn, inhibits BRAVO and triggers QC division.

amiRNA design and cloning

We designed the artificial miRNA using Web MicroRNA Designer (WMD2) as previously described (Ossowski et al., 2008; Schwab et al., 2006). Briefly, the nucleotides encoding the mature miRNA sequence, GCCCCTATCTAAGTGTCAGTT, were engineered in the miR319a precursor as described (Schwab et al., 2006). This was then subcloned under the control of the WOX5 QC promoter in the binary plasmid pH7m24GW,3, and transformed into *Arabidopsis* using the floral dip method (Zhang et al., 2006). In this work, we used two independent homozygous T4 lines named pWOX5:BRI1-miR#2 and pWOX5:BRI1-miR#3, both of which express the specific amiRNA against BRI1 under the *WOX5* promoter (4.2 kb upstream of the *WOX5* start codon). For the pWOX5:BRI1-YFP construct, the coding sequence of the *BRI1* gene was cloned under the control of the *WOX5* promoter and fused to *YFP*, all inside the binary plasmid pB7m34GW. All constructs were cloned using Gateway technology (Invitrogen) according to the manufacturer's instructions.

Confocal microscopy

For QC division analysis, 6-day-old seedlings were fixed, clarified and counterstained using modified Pseudo Schiff propidium iodide (mPS-PI) staining (Truernit and Haseloff, 2008). Then, each seedling was mounted onto a microscope slide with a drop of Hoyer's solution (30 g gum arabic, 200 g chloral hydrate, 20 g glycerol and 50 ml water). Images were obtained using a FV 1000 confocal microscope (Olympus, Tokyo, Japan). The QC division phenotypes were scored as in Vilarrasa-Blasi et al. (2014). Differences in QC division frequencies were statistically evaluated with a two-sided Fisher's exact test (Tables S2–S4).

For bleomycin assays, the percentage of damaged roots was scored after 24 h of treatment, which is a qualitative classification depending on the amount of death cells in the vasculature, identified by the incorporation of PI inside the cells: no damage means that cells did not uptake PI; mid damage indicates that some cells in the stem cell niche area were stained; hard damage indicates that all cells in the stem cell niche and some cells in the vascular system stained with PI. The percentage of QC divisions was scored after 24 h of bleomycin treatment and 24 h of recovery.

Hormone and drug treatments

For brassinolide (BL) treatment, BL (C28H48O6; Wako, Osaka, Japan) previously dissolved in ethanol was added to medium at a final concentration

of either 4 nM or 0.04 nM. For bleomycin treatment, seedlings were transferred to vertical plates supplemented with 0.6 µg/ml bleomycin (Calbiochem) 4 days after sowing. For recovery, plants were transferred back to control medium after 1 day of growth in bleomycin-containing medium and quantified under a confocal microscope after 24 h.

EdU staining

For evaluating EdU staining, we used the Click-iT EdU Alexa Fluor 555 Imaging Kit (Thermo Fisher). Five days after sowing, seedlings were transferred to vertical plates supplemented with 10 µg/ml EdU. After 24 h, seedlings were fixed in a solution containing 3.7% (w/v) paraformaldehyde and 1% (v/v) Triton X-100 in 1× PBS for 1 h in a vacuum. After fixation, the seedlings were washed twice with 3% (w/v) BSA in 1× PBS, and subsequently incubated in the Click-iT reaction cocktail (as described in the protocol of Invitrogen EdU Click-iT Reaction Imaging Kit) for 1 h in the dark. For counterstaining, seedlings were washed twice with 3% BSA in 1× PBS and incubated for 30 min with 1 µg/ml DAPI in 1× PBS in the dark. Finally, the seedlings were washed a final time in 3% BSA in 1× PBS.

Root measurements and fluorescence quantification

For root length measurements, images of seedlings were taken with a Nikon D7000 camera and roots were measured with ImageJ software (<http://imagej.nih.gov/ij/>). For meristem cell counts, 6-day-old seedlings were stained with 10 µg/ml PI and the images were obtained using a FV 1000 confocal microscope (Olympus, Tokyo, Japan), using a 20× objective. Then cells were counted by tracking the cortex, starting from QC cells. The end of the meristem was considered when a cell had >75% increase in cell length (longitudinally) than the previous one. Cell measurements were performed with ImageJ. For root stele width, measures were taken at 50 µm upstream of the QC in the root longitudinal axis. The separation between pericycle cell files (stele) was measured perpendicular to the root longitudinal axis. Measures were made with ImageJ. For fluorescence quantifications, the mean pixels/area of fluorescence in the green channel (to quantify GFP) or the red channel (to quantify EdU incorporation) were quantified with ImageJ, either on complete images for the EdU-stained samples or by measuring only the area of expression of the BRLs.

Acknowledgements

We would like to thank members of the Ana Caño-Delgado laboratory for comments, Paula Suárez-López for suggesting the use of an amiRNA in our study, Ivonne Stahl for providing the EdU staining protocol, and Tony Ferrar for critical manuscript revision and language editing.

Competing interests

The authors declare no competing or financial interests.

Author contributions

Conceptualization: F.L.-E., A.P.-R., A.I.C.-D.; Methodology: F.L.-E., A.P.-R., J.V.-B., R.S., A.I.C.-D.; Validation: F.L.-E., A.P.-R., J.V.-B., A.I.C.-D.; Formal analysis: F.L.-E., J.V.-B., A.I.C.-D.; Investigation: F.L.-E., A.P.-R., J.V.-B., A.I.C.-D.; Resources: F.L.-E., A.P.-R., R.S., A.I.C.-D.; Data curation: F.L.-E., A.P.-R., R.S., A.I.C.-D.; Writing - original draft: F.L.-E., A.P.-R., A.I.C.-D.; Writing - review & editing: F.L.-E., A.P.-R., J.V.-B., R.S., A.I.C.-D.; Visualization: A.I.C.-D.; Supervision: A.I.C.-D.; Project administration: A.I.C.-D.; Funding acquisition: A.I.C.-D.

Funding

F.L.-E is funded by a PhD fellowship from the Ministerio de Economía, Industria y Competitividad (BIO2013-43873). A.P.-R is a recipient of a PhD fellowship from the Severo Ochoa Programme for Centers of Excellence in R&D 2016-2019 (SEV-2015-0533). R.S. would like to thank EMBO for financial support through a long-term postdoctoral fellowship (ALTF 864-2005) and Rob Martienssen for continuous support and guidance related to the amiRNA work. A.I.C.-D. is the recipient of BIO2013-43873 and BIO2016-78955 grants from the Ministerio de Economía, Industria y Competitividad and a European Research Council consolidator grant (ERC-2015-CoG-683163). Deposited in PMC for immediate release.

Supplementary information

Supplementary information available online at <http://jcs.biologists.org/lookup/doi/10.1242/jcs.204065.supplemental>

References

- Aranda, A. and Pascual, A. (2001). Nuclear hormone receptors and gene expression. *Physiol. Rev.* **81**, 1269.
- Cano-Delgado, A., Yin, Y., Yu, C., Vaezados, D., Mora-Garcia, S., Cheng, J. C., Nam, K. H., Li, J. and Chory, J. (2004). BRL1 and BRL3 are novel brassinosteroid receptors that function in vascular differentiation in Arabidopsis. *Development* **131**, 5341-5351.
- Chaiwanon, J. and Wang, Z.-Y. (2015). Spatiotemporal brassinosteroid signaling and antagonism with auxin pattern stem cell dynamics in Arabidopsis roots. *Curr. Biol.* **25**, 1031-1042.
- Cruz-Ramírez, A., Díaz-Triviño, S., Wachsmann, G., Du, Y., Arteaga-Vázquez, M., Zhang, H., Benjamins, R., Bliou, I., Neef, A. B., Chandler, V. et al. (2013). A SCARECROW-RETINOBLASTOMA protein network controls protective quiescence in the Arabidopsis root stem cell organizer. *PLoS Biol.* **11**, e1001724.
- Dittmer, J. and Leyh, B. (2014). Paracrine effects of stem cells in wound healing and cancer progression (Review). *Int. J. Oncol.* **44**, 1789-1798.
- Dolan, L., Janmaat, K., Willemsen, V., Linstead, P., Poethig, S., Roberts, K. and Scheres, B. (1993). Cellular organisation of the Arabidopsis thaliana root. *Development* **119**, 71-84.
- Fábregas, N., Li, N., Boeren, S., Nash, T. E., Goshe, M. B., Clouse, S. D., de Vries, S. and Cano-Delgado, A. I. (2013). The brassinosteroid insensitive1-like3 signalosome complex regulates Arabidopsis root development. *Plant Cell* **25**, 3377-3388.
- Fridman, Y., Elkouby, L., Holland, N., Vragovic, K., Elbaum, R. and Savaldi-Goldstein, S. (2014). Root growth is modulated by differential hormonal sensitivity in neighboring cells. *Genes Dev.* **28**, 912-920.
- Friedrichsen, D. and Chory, J. (2001). Steroid signaling in plants: from the cell surface to the nucleus. *BioEssays* **23**, 1028-1036.
- Fulcher, N. and Sablowski, R. (2009). Hypersensitivity to DNA damage in plant stem cell niches. *Proc. Natl. Acad. Sci. USA* **106**, 20984-20988.
- Geldner, N., Hyman, D. L., Wang, X., Schumacher, K. and Chory, J. (2007). Endosomal signaling of plant steroid receptor kinase BRI1. *Genes Dev.* **21**, 1598-1602.
- Gonzalez-Garcia, M.-P., Vilarrasa-Blasi, J., Zhiponova, M., Divol, F., Mora-Garcia, S., Russinova, E. and Cano-Delgado, A. I. (2011). Brassinosteroids control meristem size by promoting cell cycle progression in Arabidopsis roots. *Development* **138**, 849-859.
- Hacham, Y., Holland, N., Butterfield, C., Ubeda-Tomas, S., Bennett, M. J., Chory, J. and Savaldi-Goldstein, S. (2011). Brassinosteroid perception in the epidermis controls root meristem size. *Development* **138**, 839-848.
- He, J.-X., Gendron, J. M., Wang, Y., Li, J. and Wang, Z.-Y. (2002). The GSK3-like kinase BIN2 phosphorylates and destabilizes BZR1, a positive regulator of the brassinosteroid signaling pathway in Arabidopsis. *Proc. Natl. Acad. Sci. USA* **99**, 10185-10190.
- He, J.-X., Gendron, J. M., Sun, Y., Gampala, S. S., Gendron, N., Sun, C. Q. and Wang, Z. Y. (2005). BZR1 is a transcriptional repressor with dual roles in brassinosteroid homeostasis and growth responses. *Science* **307**, 1634-1638.
- Heyman, J., Cools, T., Vandenbussche, F., Heyndrickx, K. S., Van Leene, J., Vercauteren, I., Vanderauwera, S., Vandepoel, K., De Jaeger, G., Van Der Straeten, D. et al. (2013). ERF115 controls root quiescent center cell division and stem cell replenishment. *Science* **342**, 860-863.
- Heyman, J., Cools, T., Canher, B., Shavialenka, S., Traas, J., Vercauteren, I., Van den Daele, H., Persiau, G., De Jaeger, G. et al. (2016). The heterodimeric transcription factor complex ERF115-PAT1 grants regeneration competence. *Nat. Plants* **2**, 16165.
- Hothorn, M., Belkhadir, Y., Dreux, M., Dabi, T., Noel, J. P., Wilson, I. A. and Chory, J. (2011). Structural basis of steroid hormone perception by the receptor kinase BRI1. *Nature* **474**, 467-471.
- Kang, Y. H., Breda, A. and Hardtke, C. S. (2017). Brassinosteroid signaling directs formative cell divisions and protophloem differentiation in Arabidopsis root meristems. *Development* **144**, 272-280.
- Kim, T.-W. and Wang, Z.-Y. (2010). Brassinosteroid signal transduction from receptor kinases to transcription factors. *Annu. Rev. Plant Biol.* **61**, 681-704.
- Kim, B., Jeong, Y. J., Corvalán, C., Fujioka, S., Cho, S., Park, T. and Choe, S. (2014). Darkness and gulliver2/phyB mutation decrease the abundance of phosphorylated BZR1 to activate brassinosteroid signaling in Arabidopsis. *Plant J.* **77**, 737-747.
- Kinoshita, T., Caño-Delgado, A., Seto, H., Hiranuma, S., Fujioka, S., Yoshida, S. and Chory, J. (2005). Binding of brassinosteroids to the extracellular domain of plant receptor kinase BRI1. *Nature* **433**, 167-171.
- Lee, H.-S., Kim, Y., Pham, G., Kim, J. W., Song, J.-H., Lee, Y., Hwang, Y.-S., Roux, S. J. and Kim, S.-H. (2015). Brassinazole resistant 1 (BZR1)-dependent brassinosteroid signalling pathway leads to ectopic activation of quiescent cell division and suppresses columella stem cell differentiation. *J. Exp. Bot.* **66**, 4835-4849.
- Li, J. and Chory, J. (1997). A putative leucine-rich repeat receptor kinase involved in brassinosteroid signal transduction. *Cell* **90**, 929-938.
- Li, J. and Nam, K. H. (2002). Regulation of brassinosteroid signaling by a GSK3/SHAGGY-like kinase. *Science* **295**, 1299-1301.

- Mitchell, J. W., Mandava, N., Worley, J. F., Plimmer, J. R. and Smith, M. V. (1970). Brassins—a new family of plant hormones from rape pollen. *Nature* **225**, 1065–1066.
- Nolan, T. M., Brennan, B., Yang, M., Chen, J., Zhang, M., Li, Z., Wang, X., Bassham, D. C., Walley, J. and Yin, Y. (2017). Selective autophagy of BES1 mediated by DSK2 balances plant growth and survival. *Dev. Cell* **41**, 33–46.e37.
- Ortega-Martinez, O., Pernas, M., Carol, R. J. and Dolan, L. (2007). Ethylene modulates stem cell division in the Arabidopsis thaliana root. *Science* **317**, 507–510.
- Ossowski, S., Schwab, R. and Weigel, D. (2008). Gene silencing in plants using artificial microRNAs and other small RNAs. *Plant J.* **53**, 674–690.
- Peng, P., Yan, Z., Zhu, Y. and Li, J. (2008). Regulation of the Arabidopsis GSK3-like kinase BRASSINOSTEROID-INSENSITIVE 2 through proteasome-mediated protein degradation. *Mol. Plant* **1**, 338–346.
- Pi, L., Aichinger, E., van der Graaff, E., Llavata-Peris, C. I., Weijers, D., Hennig, L., Groot, E. and Laux, T. (2015). Organizer-Derived WOX5 signal maintains root columella stem cells through chromatin-mediated repression of CDF4 expression. *Dev. Cell* **33**, 576–588.
- Qi, X., Han, S. K., Dang, J. H., Garrick, J. M., Ito, M., Hofstetter, A. K. and Torii, K. U. (2017). Autocrine regulation of stomatal differentiation potential by EPF1 and ERECTA-LIKE1 ligand-receptor signaling. *Elife* **6**, e24102.
- Russinova, E., Borst, J.-W., Kwaaitaal, M., Caño-Delgado, A., Yin, Y., Chory, J. and de Vries, S. C. (2004). Heterodimerization and endocytosis of Arabidopsis brassinosteroid receptors BRI1 and AtSERK3 (BAK1). *Plant Cell* **16**, 3216–3229.
- Sabatini, S., Heidstra, R., Wildwater, M. and Scheres, B. (2003). SCARECROW is involved in positioning the stem cell niche in the Arabidopsis root meristem. *Genes Dev.* **17**, 354–358.
- Sablowski, R. (2004). Plant and animal stem cells: conceptually similar, molecularly distinct? *Trends Cell Biol.* **14**, 605–611.
- Salazar-Henao, J. E., Lehner, R., Betegón-Putze, I., Vilarrasa-Blasi, J. and Caño-Delgado, A. I. (2016). BES1 regulates the localization of the brassinosteroid receptor BRL3 within the provascular tissue of the Arabidopsis primary root. *J. Exp. Bot.* **67**, 4951–4961.
- Salic, A. and Mitchison, T. J. (2008). A chemical method for fast and sensitive detection of DNA synthesis in vivo. *Proc. Natl. Acad. Sci. USA* **105**, 2415–2420.
- Sarkar, A. K., Luijten, M., Miyashima, S., Lenhard, M., Hashimoto, T., Nakajima, K., Scheres, B., Heidstra, R. and Laux, T. (2007). Conserved factors regulate signalling in Arabidopsis thaliana shoot and root stem cell organizers. *Nature* **446**, 811–814.
- Scheres, B. (2007). Stem-cell niches: nursery rhymes across kingdoms. *Nature Rev. Mol. Cell Biol.* **8**, 345.
- Schwab, R., Ossowski, S., Riester, M., Warthmann, N. and Weigel, D. (2006). Highly specific gene silencing by artificial microRNAs in Arabidopsis. *Plant Cell* **18**, 1121–1133.
- Sun, Y., Fan, X.-Y., Cao, D.-M., Tang, W., He, K., Zhu, J.-Y., He, J.-X., Bai, M.-Y., Zhu, S., Oh, E. et al. (2010). Integration of brassinosteroid signal transduction with the transcription network for plant growth regulation in Arabidopsis. *Dev. Cell* **19**, 765–777.
- Thummel, C. S. and Chory, J. (2002). Steroid signaling in plants and insects—common themes, different pathways. *Genes Dev.* **16**, 3113–3129.
- Truernit, E. and Haseloff, J. (2008). A simple way to identify non-viable cells within living plant tissue using confocal microscopy. *Plant Methods* **4**, 15.
- van den Berg, C., Willemsen, V., Hendriks, G., Weisbeek, P. and Scheres, B. (1997). Short-range control of cell differentiation in the Arabidopsis root meristem. *Nature* **390**, 287–289.
- Vilarrasa-Blasi, J., González-García, M.-P., Frigola, D., Fàbregas, N., Alexiou, K. G., López-Bigas, N., Rivas, S., Jauneau, A., Lohmann, J. U., Benfey, P. N. et al. (2014). Regulation of plant stem cell quiescence by a brassinosteroid signaling module. *Dev. Cell* **30**, 36–47.
- Wang, Z.-Y., Seto, H., Fujioka, S., Yoshida, S. and Chory, J. (2001). BRI1 is a critical component of a plasma-membrane receptor for plant steroids. *Nature* **410**, 380–383.
- Wang, Z.-Y., Nakano, T., Gendron, J., He, J., Chen, M., Vafeados, D., Yang, Y., Fujioka, S., Yoshida, S., Asami, T. et al. (2002). Nuclear-localized BZR1 mediates brassinosteroid-induced growth and feedback suppression of brassinosteroid biosynthesis. *Dev. Cell* **2**, 505–513.
- Wei, Z. and Li, J. (2016). Brassinosteroids regulate root growth, development, and symbiosis. *Mol. Plant* **9**, 86–100.
- Wilma van Esse, G., Westphal, A. H., Surendran, R. P., Albrecht, C., van Veen, B., Borst, J. W. and de Vries, S. C. (2011). Quantification of the brassinosteroid insensitive1 receptor in planta. *Plant Physiol.* **156**, 1691.
- Yin, Y., Wang, Z.-Y., Mora-García, S., Li, J., Yoshida, S., Asami, T. and Chory, J. (2002). BES1 accumulates in the nucleus in response to brassinosteroids to regulate gene expression and promote stem elongation. *Cell* **109**, 181–191.
- Yu, X., Li, L., Zola, J., Aluru, M., Ye, H., Foudree, A., Guo, H., Anderson, S., Aluru, S., Liu, P. et al. (2011). A brassinosteroid transcriptional network revealed by genome-wide identification of BES1 target genes in Arabidopsis thaliana. *Plant J.* **65**, 634–646.
- Yu, Q., Tian, H., Yue, K., Liu, J., Zhang, B., Li, X. and Ding, Z. (2016). A P-loop NTPase regulates quiescent center cell division and distal stem cell identity through the regulation of ROS homeostasis in Arabidopsis root. *PLoS Genet.* **12**, e1006175.
- Zhang, X., Henriques, R., Lin, S.-S., Niu, Q.-W. and Chua, N.-H. (2006). Agrobacterium-mediated transformation of Arabidopsis thaliana using the floral dip method. *Nat. Protoc.* **1**, 641–646.
- Zhang, H., Han, W., De Smet, I., Talboys, P., Loya, R., Hassan, A., Rong, H., Jurgens, G., Paul Knox, J. and Wang, M.-H. (2010). ABA promotes quiescence of the quiescent centre and suppresses stem cell differentiation in the Arabidopsis primary root meristem. *Plant J.* **64**, 764–774.
- Zhang, W., Swarup, R., Bennett, M., Schaller, G. E. and Kieber, J. J. (2013). Cytokinin induces cell division in the quiescent center of the Arabidopsis root apical meristem. *Curr. Biol.* **23**, 1979–1989.

ARTICLE

DOI: 10.1038/s41467-018-06861-3

OPEN

Overexpression of the vascular brassinosteroid receptor BRL3 confers drought resistance without penalizing plant growth

Norma Fàbregas^{1,9}, Fidel Lozano-Elena¹, David Blasco-Escámez¹, Takayuki Tohge^{2,10}, Cristina Martínez-Andújar³, Alfonso Albacete³, Sonia Osorio⁴, Mariana Bustamante⁵, José Luis Riechmann^{1,5}, Takahito Nomura⁶, Takao Yokota⁷, Ana Conesa⁸, Francisco Pérez Alfocea³, Alisdair R. Fernie² & Ana I. Caño-Delgado¹

Drought represents a major threat to food security. Mechanistic data describing plant responses to drought have been studied extensively and genes conferring drought resistance have been introduced into crop plants. However, plants with enhanced drought resistance usually display lower growth, highlighting the need for strategies to uncouple drought resistance from growth. Here, we show that overexpression of BRL3, a vascular-enriched member of the brassinosteroid receptor family, can confer drought stress tolerance in *Arabidopsis*. Whereas loss-of-function mutations in the ubiquitously expressed BRI1 receptor leads to drought resistance at the expense of growth, overexpression of BRL3 receptor confers drought tolerance without penalizing overall growth. Systematic analyses reveal that upon drought stress, increased BRL3 triggers the accumulation of osmoprotectant metabolites including proline and sugars. Transcriptomic analysis suggests that this results from differential expression of genes in the vascular tissues. Altogether, this data suggests that manipulating BRL3 expression could be used to engineer drought tolerant crops.

¹Centre for Research in Agricultural Genomics (CRAG) CSIC IRTA UAB UB, 08193 Barcelona, Spain. ²Max Planck Institute of Molecular Plant Physiology, D 14476 Potsdam Golm, Germany. ³Department of Plant Nutrition, CEBAS CSIC, 30100 Murcia, Spain. ⁴Instituto de Hortofruticultura Subtropical y Mediterránea “La Mayora”, University of Málaga Consejo Superior de Investigaciones Científicas. Department of Molecular Biology and Biochemistry, 29071 Málaga, Spain. ⁵Institució Catalana de Recerca i Estudis Avançats (ICREA), 08010 Barcelona, Spain. ⁶Center for Bioscience Research and Education, Utsunomiya University, MinemachiUtsunomiya 321 8505, Japan. ⁷Department of Biosciences, Teikyo University, Toyosatodai Utsunomiya 320 8551, Japan. ⁸Microbiology and Cell Science Department, IFAS, Genetics Institute, University of Florida, Gainesville 32603, USA. ⁹Present address: Max Planck Institute of Molecular Plant Physiology, D 14476 Potsdam Golm, Germany. ¹⁰Present address: NAIST Graduate school of Biological Sciences, 8916 5 Takayama, Ikoma, Nara 630 0192, Japan. These authors contributed equally: Norma Fàbregas, Fidel Lozano Elena. Correspondence and requests for materials should be addressed to A.I.C. D. (email: ana.cano@cragenomica.es)

Drought is responsible for at least 40% of crop losses worldwide and this proportion is dramatically increasing due to climate change¹. Understanding cellular responses to drought stress represents the first step toward the development of better adapted crops, something which is a great challenge for the field of plant biotechnology². Classical approaches aimed at examining how plants cope with limited water led to the identification of regulators involved in the signal transduction cascades of the abscisic acid (ABA) dependent and ABA independent pathways³. Adaptation to drought stress has been associated with the presence of proteins that protect cells from dehydration, such as late embryogenesis abundant (LEA) proteins, osmoprotectants, and detoxification enzymes^{4,5}. These studies provided deep insights into the molecular mechanisms underlying abiotic stress², showing that drought resistance is a complex trait simultaneously controlled by many genes. While genetic approaches have succeeded in conferring stress resistance to plants, this generally comes at the cost of reduced growth^{6,7}. Therefore, understanding how cellular growth is coupled to drought stress responses is essential for engineering plants with improved growth in rain fed environments.

Receptor like kinases (RLKs) play an important role in optimizing plant responses to stress^{8,9}. Brassinosteroid (BR) hormones directly bind to BR INSENSITIVE 1 (BRI1) leucine rich repeat (LRR) RLK family members on the plasma membrane^{10–14}. Ligand perception triggers BRI1 to interact with the co receptor BRI1 ASSOCIATED RECEPTOR KINASE 1 (BAK1)^{15–17}, which is essential for early BR signaling events¹⁸. This BRI1 BAK1 heterodimerization initiates a signaling cascade of phosphorylation events that control the expression of multiple BR regulated genes mainly via the BRI1 EMS SUPPRESSOR1 (BES1) and BRASSINAZOLE RESISTANT1 (BZR1) transcription factors^{19–21}.

Although BRs modulate multiple developmental and environmental stress responses in plants, the exact role of BRs under stress conditions remains controversial. Whereas the exogenous application of BRs and the overexpression of the BR biosynthetic enzyme DWF4 both confer increased plant adaptation to drought stress^{22–24}, suppression of the BRI1 receptor also results in drought resistant phenotypes^{25,26}. Intriguingly, ABA signaling inhibits the BR signaling pathway after BR perception, and crosstalk between the two pathways upstream of the BRASSINOSTEROID INSENSITIVE 2 (BIN2) kinase has been reported^{27,28}. Further crosstalk has been described downstream mediated by the overlapping transcriptional control of multiple BR regulated and ABA regulated genes^{29,30}, such as *RESPONSE TO DESICCATION 26 (RD26)*²⁶.

Recently, greater attention is being placed on the spatial regulation of hormonal signaling pathways in attempt to further understand the coordination of plant growth and stress responses^{26,31–34}. For instance, while the BRI1 receptor is widely localized in many tissues³⁵, the BRI1 LIKE receptor homologs BRL1 and BRL3 signal from the innermost tissues of the plant and thereby contribute to vascular development^{12,33,36}. BR receptor complexes are formed by different combinations of BRI1 like LRR RLKs with the BAK1 co receptor in the plasma membrane³³. Despite BRI1 being a central player in plant growth and adaptation to abiotic stress^{26,37,38}, the functional relevance of vascular BRL1 and BRL3 is only just beginning to be explored^{33,39}. For example, in previous proteomic approaches we found abiotic stress related proteins within BRL3 signalosome complexes³³, but the exact role of the BRL3 pathway in drought remains elusive.

Here, we show that knocking out or overexpressing different BR receptors modulate multiple drought stress related traits in both the roots and shoots. While the traits controlled by the BRI1

pathway are intimately linked to growth arrest, we found that overexpressing the vascular enriched BRL3 receptors can confer drought resistance without penalizing overall plant growth. Moreover, metabolite profiling revealed that the overexpression of the BRL3 receptor triggers the production of an osmoprotectant signature (i.e., proline, trehalose, sucrose, and raffinose family oligosaccharides) in the plant and the specific accumulation of the osmoprotectant metabolites in the roots during periods of drought. Subsequent transcriptomic profiling showed that this metabolite signature is transcriptionally regulated by the BRL3 pathway in response to drought. An enrichment of deregulated genes in root vascular tissues, especially in the phloem, further supports a preferential accumulation of osmoprotectant metabolites to the root. Overall, this study demonstrates that overexpression of the BRL3 receptor boosts the accumulation of sugar and osmoprotectant metabolites in the root and overcomes drought associated growth arrest, thereby uncovering a strategy to protect crops against drought.

Results

BR receptors control osmotic stress sensitivity in the root. To determine the contribution of the BR complexes in the response to drought, we performed a comprehensive characterization of different combinations of mutants of all the BR receptors and the BAK1 co receptor. For each combination, we first analyzed primary root growth (Fig. 1a). As previously described^{17,33,40}, 7 day old roots of *bak1*, *brl1brl3bak1*, *brl1*, and *brl1brl3* displayed shorter roots than the Col 0 wild type (WT). We also found that the primary roots of the quadruple mutant *brl1brl3bak1* (hereafter *quad*) were the shortest and the most insensitive to BRs (Fig. 1a, b and Supplementary Fig. 1). Conversely, plants overexpressing BRL3 (*35S::BRL3 GFP*, hereafter *BRL3ox*) not only exhibited longer roots than WT (Fig. 1a, b) but also showed increased receptor levels in root vascular tissues³³ (Supplementary Fig. 2). These results agree with the previously reported role of BR receptors in promoting root growth^{40,41}. We then subjected *Arabidopsis* seedlings to osmotic stress by transferring them to sorbitol containing media and subsequently quantified the level of inhibition of root growth in sorbitol relative to control conditions (see Methods). A significantly lower level of relative root growth inhibition mediated by osmotic stress was observed in *brl1* (27%), *brl1brl3* (28%), and *quad* (27%) mutants compared to the WT (39%; Fig. 1a, b). In contrast, no differences were found in *brl1brl3* and *brl1br3bak1* root growth inhibition when compared to WT (Fig. 1a, b). Similarly, the roots of *BRL3ox* plants were like those of WT in terms of relative root growth inhibition (Fig. 1a, b).

Previous experimental evidences unveiled that water stress induced cell death in *Arabidopsis* roots is localized and occurs via programmed cell death (PCD)⁴². As shown by the incorporation of propidium iodide (PI) into the nuclei (Fig. 1c, d), a short period of osmotic stress (24 h) caused cell death in the elongation zone of WT roots. In comparison, a reduced amount of cell death was observed in the roots of *brl1*, *brl1brl3*, and *quad* mutants (Fig. 1c, d), thereby indicating less sensitivity towards osmotic stress. Conversely, plants with increased levels of BRL3 showed a massive amount of cell death in root tips compared to WT, indicating an increased sensitivity to short osmotic stress (Fig. 1c, d). These results point towards a role for BR receptors in triggering osmotic stress responses in the plant root.

Since root hydrotropism represents a key feature for adaptation to environments scarce in water⁴³, we investigated the capacity of roots to escape imposed osmotic stress by bending towards water available media (Fig. 2a). We found that BR receptor loss of

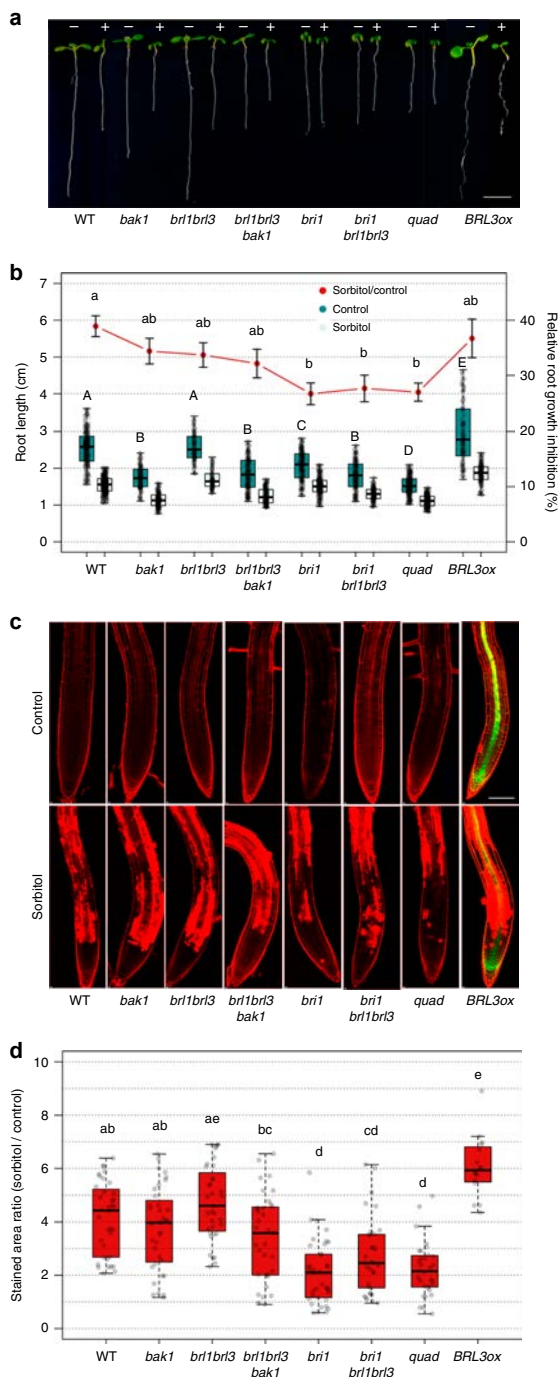


Fig. 1 BR perception mutant roots are less sensitive to osmotic stress.

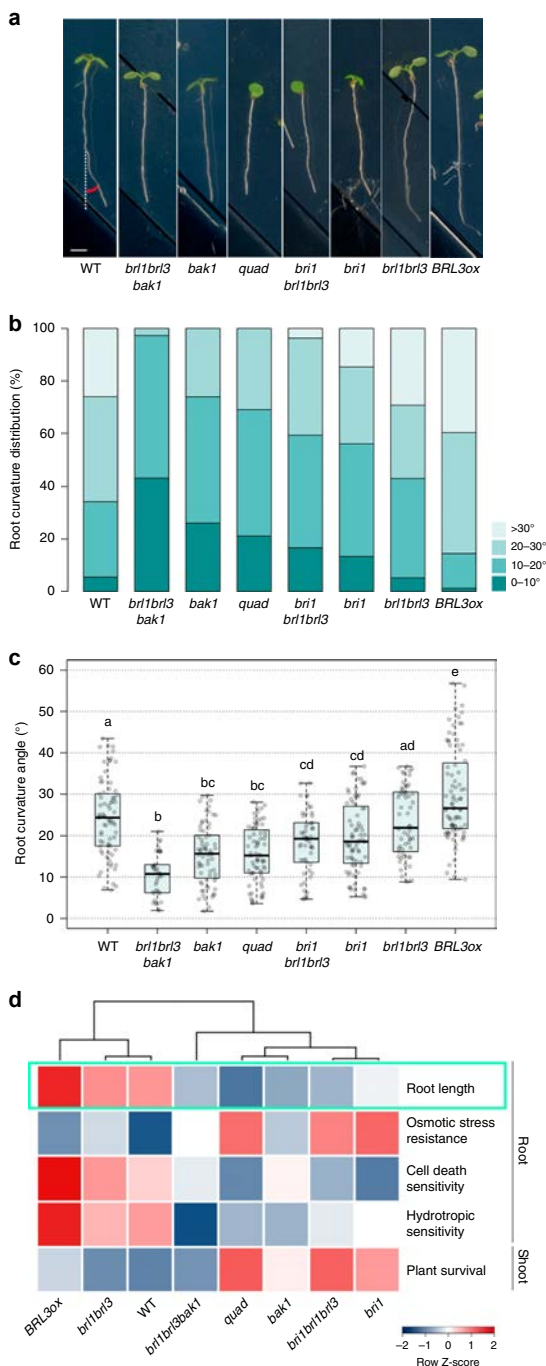
a Seven day old roots of WT, BR mutants *bak1*, *brl1brl3*, *brl1brl3bak1*, *bri1*, *bri1brl1brl3*, and *bri1brl1brl3bak1* (*quad*), and BR overexpressor line 35S:*BRL3* GFP (*BRL3ox*) grown in control (-) or 270 mM sorbitol (+) conditions. Scale bar: 0.5 cm. **b** Boxplots depict the distribution of 7 day old root lengths in control (dark green) or sorbitol (light green) conditions. Red line depicts relative root growth inhibition upon stress (ratio sorbitol/control \pm s.e.m.). Data from five independent biological replicates ($n > 150$). Different letters represent significant differences (p value < 0.05) in an ANOVA plus Tukey's HSD test. **c** Four day old roots stained with propidium iodide (PI, red) after 24 h in control (top) or sorbitol (bottom) media. Green channel (GFP) shows the localization of the BRL3 membrane protein receptor in the vascular tissues in primary roots. Scale bar: 100 μ m. **d** Quantification of cell death in sorbitol treated root tips. Boxplots show the relative PI staining (sorbitol/control) for each genotype. Averages from five independent biological replicates ($n > 31$). Different letters represent significant differences (p value < 0.05) in an ANOVA plus Tukey's HSD test. Boxplots represent the median and interquartile range (IQR). Whiskers depict $Q1 - 1.5 \cdot IQR$ and $Q3 + 1.5 \cdot IQR$ and points experimental observation.

brl1brl3bak1 mutants were the least sensitive to osmotic stress in terms of hydrotropism, showing lower root curvature angles than the *quad* roots (Fig. 2b). Consistently, compared to WT roots, an enhanced hydrotropic response was observed in *BRL3ox* (Fig. 2a c). Furthermore, exogenous application of the BR synthesis inhibitor brassinazole⁴⁴ reverted the hydrotropic response of WT roots (Supplementary Fig. 3). For better visualization, we generated a drought multi trait matrix for all the BR receptor mutants analyzed in this study (Fig. 2d; Supplementary Table 1). From this matrix, it can be seen that overexpression or mutation of BRL3/BRL1/BAK1 receptors in the vascular tissues alters drought response related traits.

BRL3ox confers drought resistance without penalizing growth.

To investigate if the impaired responses to abiotic stress observed in root seedling were preserved in mature plants, we next analyzed the phenotypes of plants exposed to severe drought. After 12 days of withholding water, dramatic symptoms of drought stress were observed in WT, *brl1brl3*, and *brl1brl3bak1* mutants. In contrast, other BR mutants showed a remarkable degree of drought resistance. In particular, *bak1*, *bri1*, *bri1brl1brl3*, and *quad* mutant plants were the most resistant to the severe water withholding regime (Fig. 3a). As these mutants exhibited some degree of dwarfism (Fig. 3a), we confirmed their resistance to drought by examining their survival rates after re watering (Fig. 3b). To correct for the delayed growth seen in BR deficient mutants, plants were submitted to a time course of drought stress in which water use, photosynthesis and transpiration parameters were monitored under similar relative soil water content (Fig. 3c e). The WT plants took just 9 days to use 70% of the available water (field capacity) during the drought period (Fig. 3c). In comparison, BR loss of function mutant plants *bri1*, *bri1brl1brl3*, and *quad* took 15 days. All subsequent measurements were done at the same soil water content for each genotype. We found that the relative water content (RWC) in WT plants was reduced during drought, while RWC in BR mutant leaves remained as in well watered conditions (Fig. 3d). In addition, compared to WT plants, BR mutants sustained higher levels of photosynthesis and transpiration during the drought period (Fig. 3e and Supplementary Fig. 4). Altogether our results indicate that the dwarf BR receptor mutant plants are more resistant while consuming less water, likely through avoiding the effects of drought (Fig. 3f).

function mutants showed reduced hydrotropic responses compared to WT plants. For instance, while no significant differences were found under control conditions (mock) (Supplementary Fig. 3), the roots of BR receptor mutants grew straighter than WT roots towards sorbitol containing media (Fig. 2a c). Interestingly,



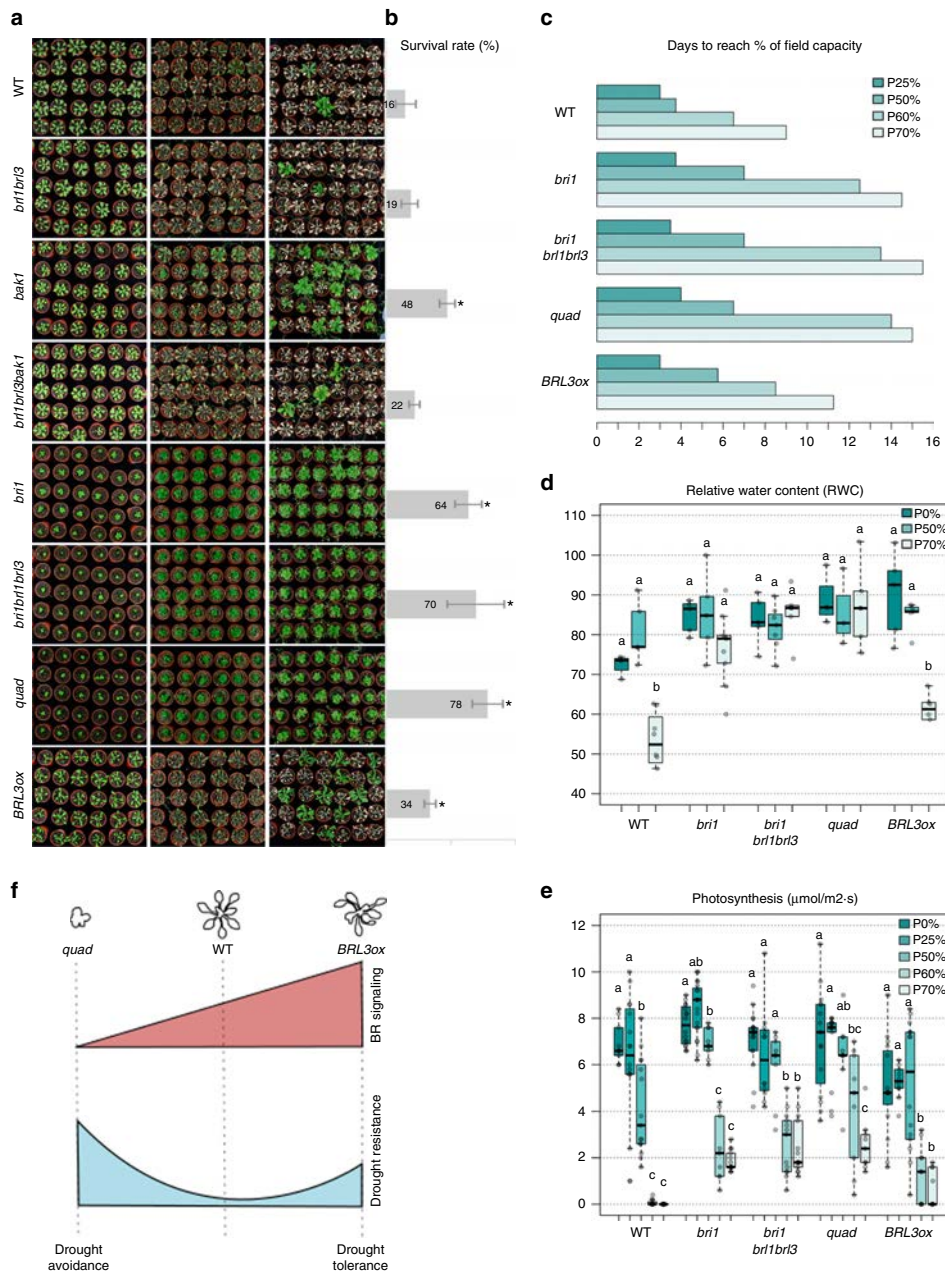
Strikingly, we found that *BRL3ox* plants were more resistant than WT plants to severe drought stress as shown by increased survival rates (Fig. 3a, b). Plants with increased BRL3 receptors showed reduction of RWC during drought similarly to WT plants (Fig. 3d). Interestingly the rate of photosynthesis was lower in

Fig. 2 Overexpression of the BRL3 receptor promotes root hydrotropism. **a** Root curvature (hydrotropic response) in 7 day old roots after 24 h of sorbitol induced osmotic stress (270 mM). Scale bar: 0.2 cm. **b** Discrete distribution of root hydrotropic curvature angles in the different genotypes. Lightest green depicts roots curved between 0° and 10°, light green between 10° and 20°, dark gray between 20° and 30°, and darkest green depicts roots that have a curvature of more than 30°. **c** Continuous distribution of root curvature angles. Different letters indicate a significant difference (p value < 0.05) in a one way ANOVA test plus Tukey's HSD test. Boxplot represent the median and interquartile range (IQR). Whiskers depict $Q1 - 1.5 \times IQR$ and $Q3 + 1.5 \times IQR$ and points experimental observations. Data from four independent biological replicates ($n > 50$). **d** Stress traits matrix for all physiological assays performed on the roots and shoots of WT, BR loss of function mutants and *BRL3ox*. Root growth in control conditions is highlighted in green. Color bar depicts values for scaled data

BRL3ox compared to WT at basal conditions, but together with transpiration, was more stable than in WT plants during the drought period (Fig. 3e and Supplementary Fig. 4). This indicates that *BRL3ox* plants are healthier than WT under the same water consumption conditions. These results suggest that the BRL3 overexpression actively promotes drought tolerance without penalizing plant growth (Fig. 3f).

***BRL3ox* plants accumulate osmoprotectant metabolites.** To further investigate the cause behind drought tolerance conferred by BRL3 overexpression, we performed metabolite profiling of *BRL3ox* plants and compared it to the profile of WT and *quad* plants in a time course drought experiment. Roots were separated from shoots to address possible changes in metabolite accumulation from source to sink tissues. The complete metabolic fingerprints are provided in Supplementary Figs. 5 and 6 and Supplementary Data 1 and 2. Metabolite profiling of mature *BRL3ox* plants grown in control conditions (time 0) revealed an increment in the production of osmoprotectant metabolites. Both shoots (Fig. 4a) and roots (Fig. 4b) of the *BRL3ox* plants exhibited metabolic signatures enriched in proline and sugars, metabolites which have previously been reported to confer resistance to drought^{45–47}. This suggests that the BRL3 receptor promotes priming⁴⁸. Importantly, the levels of these metabolites were lower in *quad* mutant plants (Fig. 4a, c).

Compared to WT, sugars including fructose, glucose, galactinol, galactose, maltose, and raffinose overaccumulated in the shoots of *BRL3ox* (Fig. 4a). Conversely, whereas glucose levels were lower in the roots, sucrose, trehalose, *myo* inositol, and maltose appeared to accumulate there (Fig. 4b) suggesting that the BRL3 pathway promotes sugar accumulation preferentially in the roots. We then analyzed the dynamics of each metabolite in response to drought (see Methods). In this time course, a rapid accumulation of osmoprotectant metabolites was observed in *BRL3ox* plants (Fig. 4c, d). In the shoot of *BRL3ox*, proline maintained higher levels than in WT along the drought time course, following an exponential increase (Fig. 4c, f). In contrast, in *BRL3ox* shoots glucose, galactose, and *myo* inositol increased at similar or slightly lower rates than WT (Fig. 4c, e, g). However, in roots, an accumulation of trehalose, sucrose, proline, and raffinose was observed in *BRL3ox* mutants subjected to drought stress (Fig. 4d), and this accumulation showed steeper exponential dynamics than in WT plants (Fig. 4h). Additionally, glucose, galactose, fructose, and *myo* inositol linearly increased in WT roots but exponentially increased in *BRL3ox* roots (Fig. 4j). Interestingly, throughout this time course, the levels of these metabolites were lower in the *quad* mutant plants compared to in WT (Supplementary Fig. 7). Altogether, these findings uncover a



key role for BR receptors in promoting sugar metabolism, and support the idea that BRL3 triggers the accumulation of osmoprotectant metabolites in the root to promote growth during periods of drought.

Transcriptional control of metabolite production in *BRL3ox*. We next investigated whether metabolic pathways are transcriptionally regulated in *BRL3ox* roots. RNAseq of *BRL3ox* roots revealed 759 deregulated genes at basal conditions (214

upregulated and 545 downregulated; FC > 1.5, FDR < 0.05; Supplementary Data 3) and 1068 deregulated genes in drought conditions (378 upregulated and 690 downregulated; FC > 1.5, FDR < 0.05; Supplementary Data 4). In control conditions, a high proportion of the deregulated genes belonged to the response to water stress, oxygen containing compounds (ROS) and response to ABA GO categories (Fig. 5a, c and Supplementary Data 5 and 6). We next deployed the genes falling into the response to stress category, which included classical drought stress markers, such as

Fig. 3 BRL3 overexpression confers drought tolerance. **a** From top to bottom, 3 week old plant rosette phenotypes of WT, *brl1brl3*, *bak1*, *brl1brl3bak1*, *brl1*, *brilbrl1brl3*, *quad*, and *BRL3ox* grown in well watered conditions (left column), after 12 days of drought stress (middle column) and after 7 days of re watering (right column). **b** Plant survival rates after 7 days of re watering. Averages of five independent biological replicates \pm s.e.m. ($n > 140$). Asterisk indicates a significant difference (p value < 0.05) in a chi squared test for survival ratios compared to WT. **c** Bar plot shows the days needed to reach different percentages of the soil field capacity for each genotype used in the study. **d** Relative water content (RWC) of mature rosettes at 0% (field capacity), 50% and 70% soil water loss. **e** Photosynthesis efficiency ($\mu\text{mol}/\text{m}^2/\text{s}$) at different percentages of soil water loss. **d, e** Boxplot represent the median and interquartile range (IQR). Whiskers depict $Q1 - 1.5 \times \text{IQR}$ and $Q3 + 1.5 \times \text{IQR}$ and points experimental observations ($n = 6$). Different letters depict significant differences within each genotype in a one way ANOVA plus a Tukey's HSD test. **f** Schematic representation of BR signaling levels, adult plant size and drought resistance. Loss of function mutants passively avoid stress (drought avoidance), whereas plants with increased levels of BRL3 act actively to avoid drought stress (drought tolerance)

RD22 and *RAB18* that were already upregulated in basal conditions (Fig. 5b). An enrichment of genes belonging to the response to hormone category indicated altered hormonal responses in *BRL3ox* plants under drought (Fig. 5a, c and Supplementary Data 7 and Supplementary Data 8). Further analyses of specific hormonal responses revealed that the ABA and jasmonic acid (JA) were the most altered responses (Supplementary Fig. 8). Repression of JA biosynthesis genes may be responsible for decreased levels of JA in basal conditions (Supplementary Fig. 8).

In order to uncover differential drought responses between WT and *BRL3ox* roots, we constructed a linear model accounting for the interaction between genotype and drought (Supplementary Data 9). Taking the 200 most significantly affected genes, we grouped them in (i) genes more activated in *BRL3ox* under drought compared to WT (Supplementary Data 10) and (ii) genes more repressed in *BRL3ox* under drought compared to WT (Supplementary Data 11). GO enrichment analysis of this genotype drought interaction revealed (i) secondary metabolism, response to stress, and response to water deprivation in the first group and (ii) BR mediated signaling pathway in the second group (Fig. 5d). Importantly, the expression levels of dehydration response genes remained repressed in *quad* mutant plants during drought (Supplementary Fig. 7 and Supplementary Data 12–15). The expression levels of two key BR biosynthesis genes, *CPD* and *DWF4* were analyzed by RT-qPCR. Consistently, within the drought time course, transcription levels of *CPD* and *DWF4* were increased in *quad* and reduced in *BRL3ox* compared to WT plants. Quantification of the bioactive BR hormone Castasterone (CS) showed similar trends and we could only detect BL in *quad*, suggesting that BL is accumulated in *quad* more than in WT and *BRL3ox* plants (Supplementary Fig. 9).

Analysis of transcription factors revealed 29 of them with differential responses to drought between *BRL3ox* and WT roots. Interestingly, the drought responsive transcription factor *RD26* showed an enhanced response in *BRL3ox* roots during stress, whereas several vascular specific transcription factors remained repressed under drought (Supplementary Fig. 10). Given that the BRL3 receptor is natively expressed at the phloem pole pericycle and enriched in vascular tissues when overexpressed³³, we analyzed the spatial distribution of the deregulated genes within the root tissues in our RNAseq dataset⁴⁹. The deregulated genes were enriched for genes that are preferentially expressed in specific vascular tissues, such as the pericycle and phloem pole pericycle but also in lateral root primordia (which initiates from pericycle) and root hair cells (Fig. 6a, see Methods). Interaction affected genes were enriched in pericycle and phloem but also in columella and cortex expressed genes (Fig. 6b). Among the phloem enriched genes, we found two trehalose phosphate phosphatases (*TPPs*) and one galactinol synthases (*GolS2*) that show increased expression in *BRL3ox* roots at basal conditions and in response to drought (Fig. 6d). These enzymes are involved in the synthesis of the osmoprotectant metabolites trehalose, myo inositol and raffinose that overaccumulated in *BRL3ox*

roots. Together, these results suggest the importance of changes in expression of phloem associated genes for sustaining drought resistance.

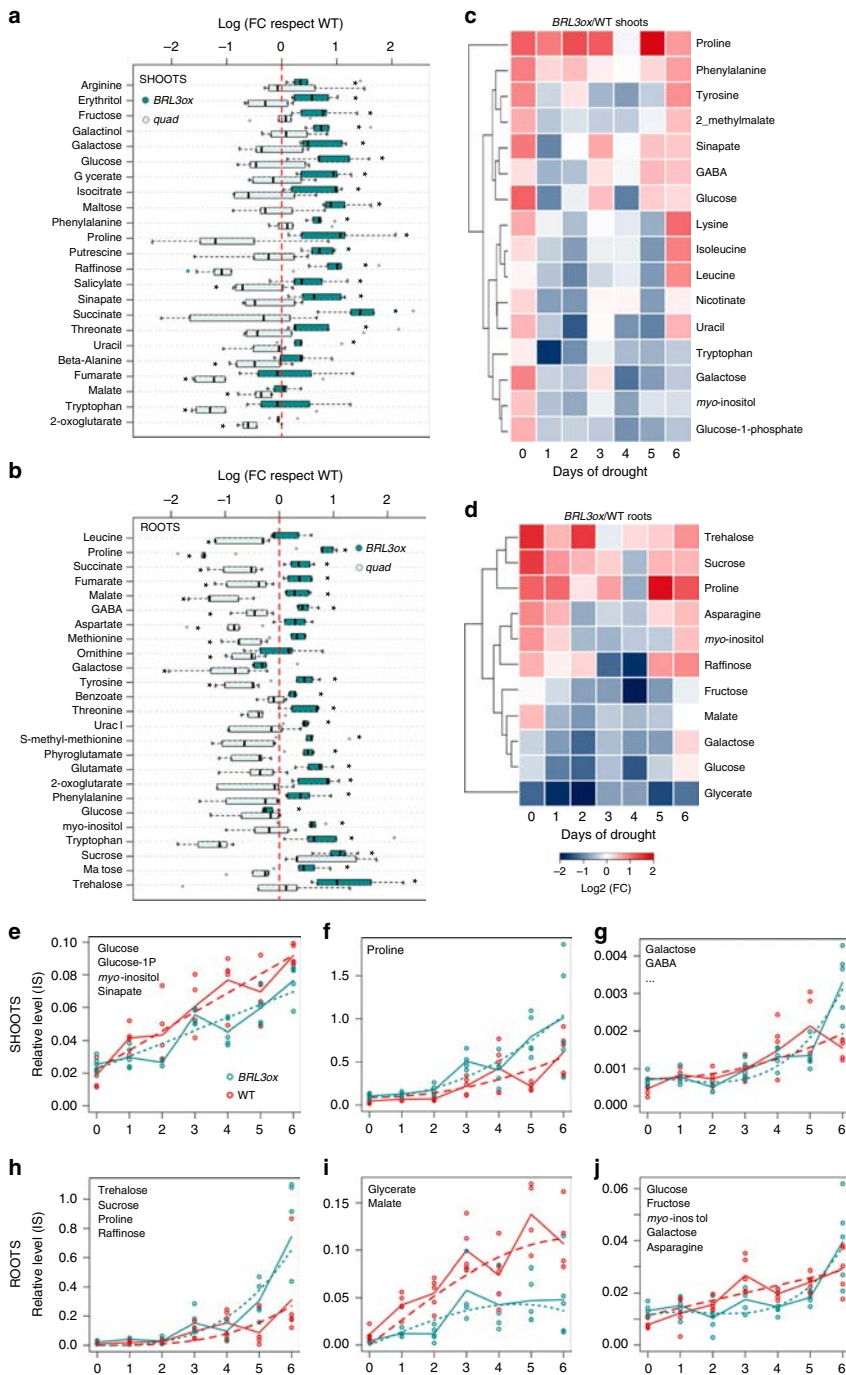
Furthermore, a statistical analysis revealed a significant link between the whole transcriptomic and metabolomic signatures, both in basal conditions and under drought ($p = 0.017$ and $p = 0.001$, respectively; see Methods), suggesting that the metabolic signature of *BRL3ox* plants is transcriptionally controlled. We used the metabolic and transcriptomic signatures to identify deregulated metabolic pathways using Paintomics⁵⁰. This analysis suggests constitutive deregulation of sucrose metabolism in *BRL3ox* plants that was enhanced during drought stress. We also found that BRL3 overexpression affects galactose metabolism under periods of drought, including the raffinose family of oligosaccharides (RFOs) synthesis pathway (Supplementary Fig. 11, Supplementary Data 16 and 17). Collectively, these results suggest that BRL3 overexpression promotes drought tolerance, mainly by controlling sugar metabolism.

Discussion

Our study shows that overexpression of the BRL3 receptor can prevent growth arrest during drought. We suggest that this is accomplished through the transcriptional control of metabolic pathways that produce osmoprotectant metabolites that accumulate in the roots. While spatial BR signaling has been shown to contribute to stem cell replenishment in response to genotoxic stress^{31,34}, here we show that ectopic expression of vascular enriched BRL3 receptors can promote growth during drought. Altogether, our results suggest that spatial regulation of BR signaling can affect plant stress responses.

The exogenous application of BR compounds has been used widely in agriculture to extend growth under different abiotic stresses^{22,51}, yet how these molecules precisely activate growth in challenging conditions remains largely unknown. The analysis of BR signaling and BR synthesis mutant plants subjected to stress failed to provide a linear picture of the involvement of BR in drought stress adaptation. For instance, although overexpression of the canonical BRI1 pathway and the BR biosynthesis gene *DWF4* can both confer abiotic stress resistance^{24,38}, *BRI1* loss of function mutants also showed drought stress resistance^{25,26}. However, increased levels of BR regulated transcription factors trigger antagonistic effects in drought stress responses^{26,52}, thus depicting a complex scenario for the role of BRs in abiotic stress. Given the spatiotemporal regulation of the BR signaling components³⁹ and the complexity of drought traits⁷, it is plausible to hypothesize that drought traits are under the control of cell type specific BR signaling.

Our study unveils that the BR family of receptors, in addition to promoting growth, guide phenotypic adaptation to drought by influencing a myriad of drought stress related traits. The drought resistance phenotypes of BR loss of function mutants (Fig. 3a) are likely caused by a reduced exposure of these plants to the effect of drought. This phenomenon, known as drought avoidance, is linked



to growth arrest and stress insensitivity that maintains transpiration, leaf water status, and photosynthesis along the drought (Fig. 3 and Supplementary Fig. 4). The reduced levels of ABA and canonical stress related metabolites, together with the downregulation of stress related genes, further support the insensitivity of *quad* plants to stress (Supplementary Figs. 7 and 8).

In contrast, the phenotypes observed in *BRL3ox* plants indicate an active drought tolerance mechanism driven by overexpression of the BRL3 receptor. First, *BRL3ox* roots showed increased water stress induced PCD in the root tip compared to WT (Fig. 1c, d), which has been proposed to modify the root system architecture and thereby enhance drought tolerance⁴⁹. Second, the enhanced

Fig. 4 BRL3 overexpression plants show a primed metabolic signature. **a** Metabolites differentially accumulated in *BRL3ox* (dark green) or *quad* (light green) shoots relative to WT at basal conditions. **b** Metabolites differentially accumulated in *BRL3ox* (dark green) or *quad* (light green) roots relative to WT at basal conditions. **a, b** Boxplot represent the median and interquartile range (IQR). Whiskers depict Q1 - 1.5*IQR and Q3 + 1.5*IQR and points experimental observations ($n = 5$). Asterisks denote statistical differences in a two tailed t test (p value < 0.05) for raw data comparisons *BRL3ox* vs. WT (panel right side) or *quad* (panel left side). **c** Metabolites following differential dynamics between *BRL3ox* and WT shoots along the drought time course. **d** Metabolites following differential dynamics between *BRL3ox* and WT roots along the drought time course. **e** Heatmap represents the \log_2 ratio of *BRL3ox*/WT. **e, j** Clustering of the dynamics of relative metabolite levels along the drought time course in shoots and roots. Solid lines show the actual metabolic profile (averages) of the representative metabolite for each cluster while dashed lines represent the polynomial curve that best fit the profile. Statistical significance was evaluated with the maSigPro package. **e** Metabolites following a linear increase during drought in shoots include glucose, glucose 1P, *myo* inositol, and sinapate. **f** Proline follows a steeper exponential increase in *BRL3ox* shoots. **g** Metabolites following an exponential increase in *BRL3ox* shoots but nearly a linear increase in WT include galactose, GABA, phenylalanine, tyrosine, 2 methylmalate, lysine, isoleucine, leucine, nicotinate, uracil, and tryptophan. **h** Metabolites following a steeper exponential increase in *BRL3ox* roots include trehalose, sucrose, proline, and raffinose. **i** Metabolites following a reduced linear increase until a certain maximum in *BRL3ox* roots include glycerate and malate. **j** Metabolites following an exponential increase in *BRL3ox* roots but a linear increase in WT include glucose, fructose, *myo* inositol, galactose, and asparagine

hydrotropic response of *BRL3ox* roots (Fig. 2a, c) could function during water limited conditions by modifying root architecture for increased acquisition of water, favoring plant growth and survival under drought conditions as previously described⁵³. Third, at same RWC in leaves, the rate of photosynthesis and transpiration were more stable in *BRL3ox* than in WT plants during drought (Fig. 3d, e and Supplementary Fig. 4). Altogether, these findings indicate that BRL3 overexpression actively promotes drought tolerance without penalizing plant growth.

We found the expression of the drought response transcription factor *RD26* to be enhanced in *BRL3ox* roots when subjected to drought (Supplementary Fig. 10). *RD26* has been shown to antagonize the BR canonical transcription factor BES1²⁶, thereby suggesting that BRL3 overexpression activates alternative pathways. These alternative pathways may be derived from a spatial specialization of BR functions within the root. Indeed, we found that genes preferentially expressed in vascular tissues, especially within phloem related cell types, were overrepresented among deregulated genes in *BRL3ox* roots (Fig. 6a, b). The localization of the native BRL3 protein in phloem cells³³ and the metabolic signature found in *BRL3ox* suggests a possible role in phloem loading during drought. Moreover, metabolic enzymes implicated in trehalose and RFO metabolism were enriched in vascular tissues and either upregulated in *BRL3ox* roots in basal conditions or strongly responding to drought (Fig. 6c, d). Thus, BRL3 overexpression may affect not only loading and unloading of the phloem, but may also directly control metabolic pathways. This is the case for the *TPPs* family^{54,55} and galactinol synthase 2 (*GolS2*)⁵⁶, which are both described to impact drought responses and are involved in trehalose and RFO synthesis, respectively. In addition to controlling expression in vascular tissues, our analyses also suggest that BRL3 overexpression regulates non vascular enzymes important for metabolism and drought responses. These enzymes include hexokinases, such as *HXX3* or *HKL1*, the sucrose synthases *SUS3* and *SPS2F*, and proline dehydrogenase genes such as the early response to dehydration 5 (*ERD5*) which is involved in stress tolerance⁵⁷. In light of our findings and given that *Bes1 D* gain of function mutants exhibit drought hypersensitivity²⁶, we propose that overexpression of the vascular BRL3 receptors may act independently of the canonical growth promoting BR11 pathway.

Our data further suggest that *BRL3ox* plants accumulate sugars in the sink tissues to enable plant roots to grow and escape drought by searching for water within the soil. In support of these findings, we also observed reduced levels of photosynthesis in well watered leaves of *BRL3ox* plants (Fig. 3e). These results, together with the higher levels of sucrose in roots compared with in shoots (Fig. 4a), and higher levels of glucose and fructose in the shoots suggest that the BRL3 pathway promotes sugar

mobilization from the leaves (source) to the roots (sink). In fact, previous work reported that BRs promote the flow of assimilates in crops from source to sink via the vasculature⁵⁸ and via sucrose phloem unloading⁵⁹.

In control conditions, *BRL3ox* plants exhibited a metabolic signature enriched in proline and sugars. Proline and sugar accumulation classically correlates with drought stress tolerance, osmolytes, ROS scavengers, and chaperone functions^{5,45–47,60,61}, suggesting that overexpression of the BRL3 receptor promotes priming^{48,62}. In addition, *BRL3ox* plants also accumulated succinate, fumarate, and malate. Importantly, all these metabolites were decreased in *quad* mutant plants. Altogether, these data suggest a role for BRL3 signaling in the promotion of the tricarboxylic acid (TCA) cycle, sugar, and amino acid metabolism.

In drought stress conditions, *BRL3ox* shoots displayed increased levels of the amino acids proline, GABA, and tyrosine. In contrast, trehalose, sucrose, *myo* inositol, raffinose, and proline were the most abundant metabolites in the *BRL3ox* roots along the stress time course. Importantly, all these metabolites have previously been linked to drought resistance^{45,46,60}. In addition, the levels of the RFO metabolites raffinose and *myo* inositol, which are involved in membrane protection and radical scavenging⁶³, were higher in the roots of *BRL3ox* plants under drought, yet reduced in the roots of *quad* plants.

Our data suggest that the roots of *BRL3ox* plants are loaded with osmoprotectant metabolites and are thus better prepared to alleviate drought stress via a phenomenon previously referred to as priming^{48,62}. Altogether these findings suggest that drought stress responses are correlated with BRL3 receptor levels in the root vasculature, especially within the phloem, and that this is important for the greater survival rates of *BRL3ox* plants. Future cell type specific engineering of signaling cascades stands out as a promising strategy to circumvent growth arrest caused by drought stress.

Methods

Plant materials. Seeds were sterilized with 35% NaClO for 5 min and washed five times for 5 min with sterile dH₂O. Sterile seeds were vernalized 48 h at 4 °C and grown in half-strength agar Murashige and Skoog (MS1/2) media with vitamins and without sucrose. Plates were grown vertically in long day (LD) conditions (16 h of light/8 h of dark; 22 °C, 60% relative humidity). Genotypes used in this study: Columbia-0 WT (Col-0 WT), *brl1-1brl3-1* (*brl1brl3*), *bak1-3* (*bak1*), *bril1-301* (*bril1*), *bril1-301brl1-1brl3-1* (*bril1brl1brl3*), *bril1-301bak1-3brl1-1brl3-1* (*quad*), and *35S:BRL3-GFP* (*BRL3ox*)³³. DNA rapid extraction protocol⁶⁴ was used for all the plant genotyping experiments. Supplementary Table 2 describes the primers used for genotyping of the BR mutant plants.

Brassinolide (BL) and sorbitol sensitivity assays in roots. For hormone treatments, seeds were continuously grown in concentration series of BL (Wako, Japan). For sorbitol assays, 3-day-old seedlings were transferred to either control or 270

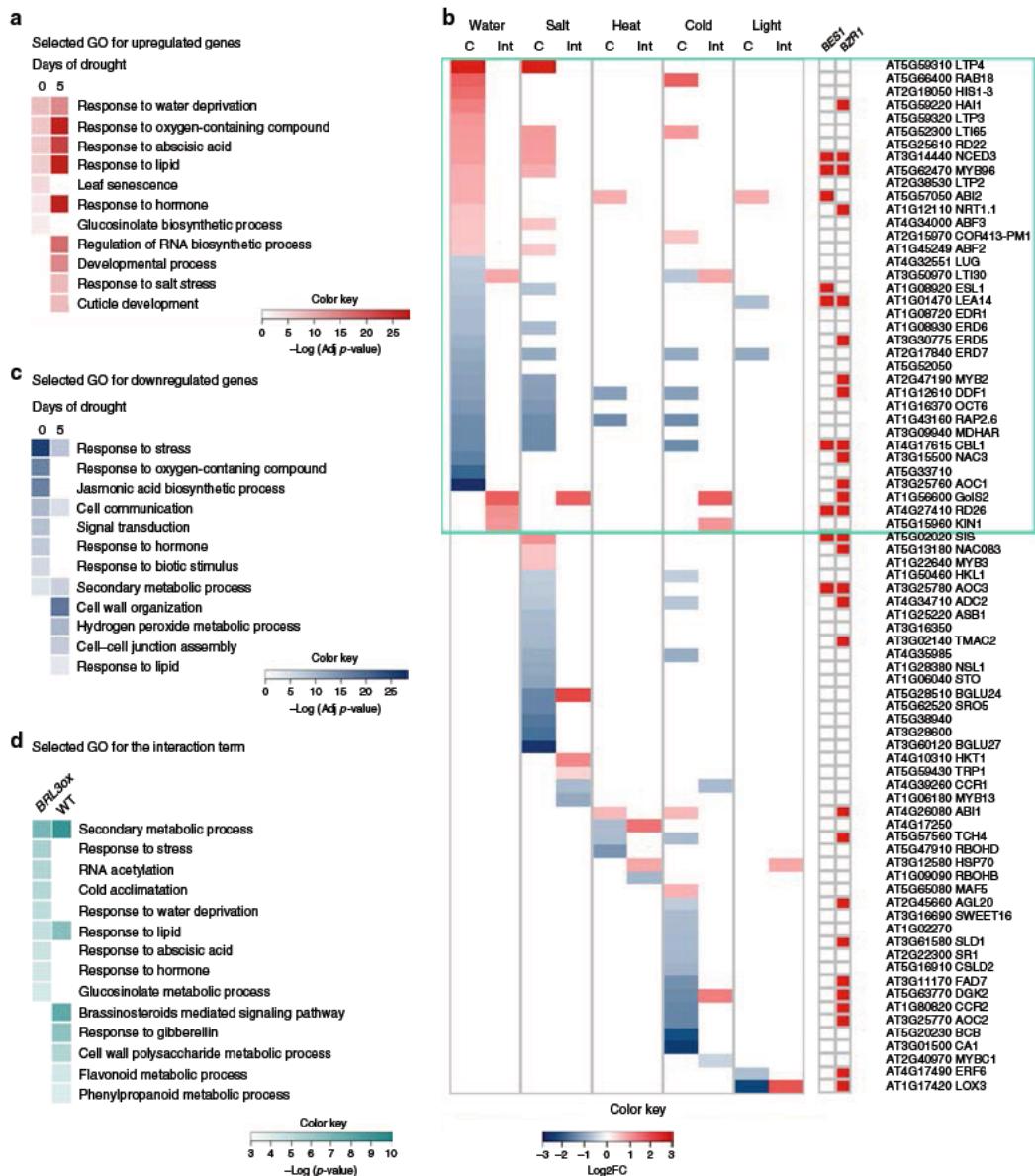


Fig. 5 Stress genes are constitutively activated in *BRL3ox* roots. **a** Most representative GO categories enriched in *BRL3ox* roots from the upregulated genes at time 0 and after 5 days of drought. **b** Deployment of genes within “Response to stress” (GO:0006950) term that are also annotated as responsive to water, salt, heat, cold, and light stress. Colors in the heatmap represent the log₂ fold change of *BRL3ox* vs. WT roots in control conditions (C) or the differential drought response (log₂(FC drought/CTRL in *BRL3ox*)) (log₂(FC drought/CTRL in WT)) if the gene is affected by the interaction genotype*drought (Int.). Red color in the squared heatmaps on the right shows that the gene has been previously identified as a direct target of BES1 or BZR1 transcription factors. **c** Most representative GO categories enriched in *BRL3ox* roots from the upregulated genes at time 0 and after 5 days of drought. **d** Most representative GO categories enriched among genes affected by the interaction genotype drought. GO categories enriched in genes activated in *BRL3ox* under drought compared to WT (left column) in genes repressed in *BRL3ox* under drought compared to WT (right column). Color bars: log of *p* value (adjusted by Benjamini Hochberg or non adjusted)

mM sorbitol media for four additional days. The root length of 7-day-old seedlings was measured using Image J (<http://rsb.info.nih.gov/ij/>) and compared with automatically acquired data from the MyROOT²⁵ software (Supplementary Fig. 12). Four-day-old roots grown in control conditions or in 24 h of sorbitol were stained with propidium iodide (10 µg/ml, PI, Sigma). PI stains the cell wall

(control) and DNA in the nuclei upon cell death (sorbitol). Images were acquired with a confocal microscope (FV1000 Olympus). Cell death damage in primary roots was measured in a window of 500 µm from QC in the middle root longitudinal section (Image J). As an arbitrary setting to measure the stained area, a color threshold ranging from 160 to 255 in brightness was selected.

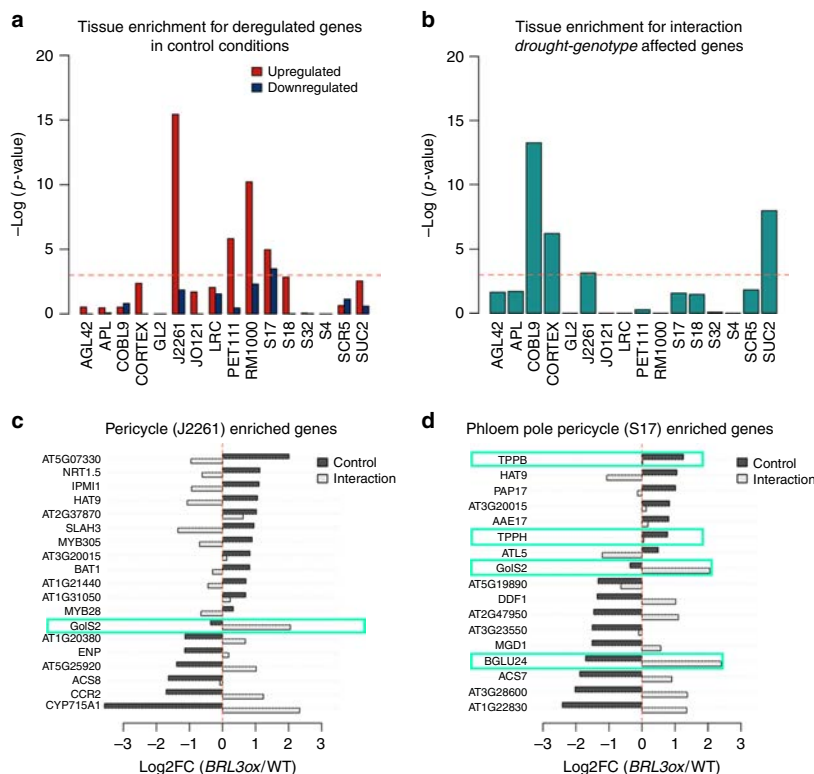


Fig. 6 Enrichment of deregulated genes in *BRL3ox* root vasculature. **a** Tissue enrichment for upregulated (red) or downregulated (blue) genes in control conditions. Bars trespassing the p value threshold (0.05) were considered enriched in the dataset. **b** Tissue enrichment for genes affected by the interaction genotype*drought. Bars trespassing the threshold p value < 0.05 were considered enriched in the dataset. **a, b** Deregulated genes tissue enrichment. AGL42: quiescent center, APL: phloem + companion cells, COBL9: root hair cells, CORTEX: cortex, GL2: non hair cells, J2261: pericycle, JO121: xylem pole pericycle, LRC: lateral root cap, PET111: columella, RM1000: lateral root primordia, S17: phloem pole pericycle, S18: maturing Xylem, S32: protophloem, S4: developing xylem, SCR5: endodermis, and SUC2: phloem. y axis represent the negative logarithm of one tailed Fisher's test. **c** Deregulated genes enriched in the Pericycle (J2261 marker). **d** Deregulated genes enriched in the Phloem Pole Pericycle (S17 marker). **c, d** Bars represent the \log_2 fold change of *BRL3ox* vs. WT roots in control (black) or the difference of drought responses between *BRL3ox* and WT (FC drought/CTRL in *BRL3ox* - FC drought/CTRL in WT) in the lineal model (gray). Blue boxes highlight enzymes directly involved in the metabolism of deregulated metabolites

Root hydrotropism. Seedlings were germinated in MS1/2 without sucrose for 6 days. Then, the lower part of the agar was removed from the plates and MS1/2 with 270 mM sorbitol was added to simulate a situation of reduced water availability. The media was placed in 45° angle to scape gravitropism effect. When indicated, 1 μ M of brassinazole⁴⁴ was added to sorbitol media. Root curvature angles were measured and analyzed using the Image J software (<http://rsb.info.nih.gov/ij/>).

Drought stress for scoring plant survival. One-week-old seedlings grown in MS1/2 agar plates were transferred individually to pots containing 30 \pm 1 g of substrate (plus 1:8 v/v vermiculite and 1:8 v/v perlite). For each biological replicate, 40 plants of each genotype were grown in LD conditions for 3 weeks. Three-week-old plants were subjected to severe drought stress by withholding water for 12 days followed by re-watering. After the 7-day recovery period, the surviving plants were photographed and manually counted (two-sided chi-squared test, p -value < 0.01).

Metabolite profiling analyses. One-week-old seedlings were placed in individual pots with 30 g of autoclaved soil and grown under LD photoperiodic conditions. After 3 weeks growing, half of the plants were subjected to severe drought (withholding water) for 6 days and the other half were watered normally (well-watered control conditions). A total of five biological replicates were collected every 24 h during the time course (from day 0 to day 6) both in drought and watered conditions, and for each genotype (WT, *quad*, and *BRL3ox*). Four independent plants were bulked in each biological replicate. Roots were manually separated from shoots. Four entire shoots were grinded using the Frosty Cryogenic grinder

system (Labman). Four entire root samples were grinded in the Tissue Lyser Mixer-Mill (Qiagen). Roots were aliquoted into 20 mg samples and shoot into 50 mg samples (the exact weight was annotated for data normalization). Primary metabolite extraction was carried as follows⁶⁶. One zirconia and 500 μ l of 100% methanol premixed with ribitol (20:1) were added and samples were subsequently homogenized in the Tissue Lyser (Qiagen) 3 min at 25 Hz. Samples were centrifuged 10 min at 14,000 rpm (10 °C) and resulting supernatant was transferred into fresh tubes. Addition of 200 μ l of $CHCl_3$ and vortex ensuring one single phase followed by the addition of 600 μ l of H_2O and vortex 15 s. Samples were centrifuged 10 min at 14,000 rpm (10 °C). 100 μ l from the upper phase (polar phase) were transferred into fresh eppendorf tubes (1.5 ml) and dried in the speed vacuum for at least 3 h without heating. 40 μ l of derivatization agent (methoxyaminhydrochloride in pyridine) were added to each sample (20 mg/ml). Samples were shaken for 3 h at 900 rpm at 37 °C. Drops on the cover were shortly spun down. One sample vial with 1 ml MSTFA + 20 μ l FAME mix was prepared. Addition of 70 μ l MSTFA + FAMES in each sample was done followed by shaking 30 min at 37 °C. Drops on the cover were shortly spun down.

Samples were transferred into glass vials specific for injection in GC-TOF-MS. The GC-TOF-MS system comprised of a CTC CombiPAL autosampler, an Agilent 6890N gas chromatograph, and a LECO Pegasus III TOF-MS running in EI+ mode. Metabolites were identified by comparing to database entries of authentic standards⁶⁷. Chromatograms were evaluated using Chroma TOF 1.0 (Leco) Pegasus software was used for peak identification and correction of RT. Mass spectra were evaluated using the TagFinder 4.0 software⁶⁸ for metabolite annotation and quantification (peak area measurements). The resulting data matrix was normalized using an internal standard, Ribitol, in 100% methanol (20:1),

followed by normalization with the fresh weight of each sample. Metabolomics data from control (well-watered) conditions at day 0 were analyzed with a two-tailed t -test, p -value < 0.05 (no multiple testing correction). Data from the time course was analyzed with R software using the maSigPro package⁶⁹. Briefly, the profile of each metabolite under each condition was fitted to a polynomial model of maximum degree 3. The curves of each genotype were statistically compared taking into account the fitting value and correcting the p -value (Benjamini–Hochberg method). Significant metabolites (p -value < 0.05) having a differential profile between genotypes were plotted to visualize their behavior under the drought time course. Clustering analysis was performed using the maSigPro package and the *hclust* R core function.

Transcriptomic profiling analysis. For microarray analysis, a drought stress time course was carried out in WT and *quad* mutant 3-week-old plants. Entire plants grown under drought stress and control conditions were collected every 48 h during the time course (Day 0, Day 2, and Day 4). Two biological replicates composed of five independent rosettes were collected. RNA was extracted with the Plant Easy Mini Kit (Qiagen) and quality checked using the Bioanalyser. A Genome-Wide Microarray platform (Dual color, Agilent) was performed by swapping the color hybridization of each biological replicate (Cy3 and Cy5). Statistical analysis was performed with the package “limma”⁷⁰, and the “mle2/” “normexp” background correction method was used. Different microarrays were quantile-normalized and a Bayes test used to identify differentially expressed probes. The results were filtered for adjusted p -value < 0.05 (after Benjamini–Hochberg correction) and $\text{Log}_2 \text{FC} > |1.5|$. For RNAseq analysis, 3-week-old roots were detached from mature plants grown in soil under control conditions and 5 days of drought. RNA was extracted as described above. Stranded cDNA libraries were prepared with TruSeq Stranded mRNA kit (Illumina). Single-end sequencing, with 50-bp reads, was performed in an Illumina HiSeq500 sequencer, at a minimum sequencing depth of 21 M. Reads were trimmed 5 bp at their 3' end, quality filtered and then mapped against the TAIR10 genome with “HISAT2”. Mapped reads were quantified at the gene level with “HTSeq”. For differential expression, samples were TMM normalized and statistical values calculated with the “EdgeR” package in R. Results were filtered for adjusted p -value (FDR) < 0.05 and $\text{FC} > |2|$ in the pairwise comparisons. For the evaluation of differential drought response between WT and *BRL3ox* roots, a linear model accounting for the interaction genotype and drought was constructed with “EdgeR” package. The interaction term was evaluated. A gene was considered to be affected by the interaction if p -value (uncorrected) < 0.0025. Heatmaps were performed in R with the heatmap2 function implemented in the “gplots” package.

For the Rt qPCR, cDNA was obtained from RNA samples by using the Transcriptor First Strand cDNA Synthesis Kit (Roche) with oligo dT primers. qPCR amplifications were performed from 10 ng of cDNA using LightCycler 480 SYBR Green I master mix (Roche) in 96-well plates according to the manufacturer's recommendations. The real-time PCR was performed on a LightCycler 480 System (Roche). Ubiquitin (AT5G56150) was used as housekeeping gene for relativizing expression. Primers used are described in Supplementary Table 3.

Statistical methods and omics data integration. For root tissue enrichment analysis, deregulated genes were queried against available lists of tissue-enriched genes⁴⁹. For each tissue, a 2×2 contingency table was constructed, counting the number of deregulated genes in the tissue that were enriched and non-enriched and also the number of non-deregulated genes (for either $\text{FDR} > 0.05$ or $\text{logFC} > |1|$ in the RNAseq gene universe) that were enriched and non-enriched. Statistical values of the enrichment were obtained using a one-sided Fisher's test. To statistically evaluate the influence of transcriptomic changes on the metabolic signature, both deregulated enzymes and metabolites were queried in an annotation file of the metabolic reactions of *Arabidopsis thaliana*, which included merged data from the KEGG (<http://www.genome.jp/kegg/>) and BRENDA (www.brenda-enzymes.org) databases. Then, the same approach of constructing a 2×2 contingency table was taken. Significant and non-significant metabolites annotated in the database were matched with differentially and non-differentially expressed genes annotated in the database. The statistical value of the association between regulated metabolites and genes was obtained through a two-sided Fisher's exact test. Genes and metabolites were mapped onto the KEGG pathways using the PaintOmics3 (<http://bioinfo.cipf.es/paintomics/>) according to the developer's instructions⁵⁰.

Physiological parameters and chlorophyll fluorescence. One-week-old seedlings were placed in individual pots and watered with the same volume of a modified Hoagland solution (one-fifth strength). Pots were weighed daily during the experiment. Well-watered control plants were grown in 100% field capacity (0% of water loss). The time course drought stress assay was started by withholding the nutrient solution until reaching 25%, 50%, 60%, and 70% water loss. Photosynthesis (A) and transpiration (E) were measured in control and drought plants at those time points. Four plants of each genotype were harvested at 0%, 50%, and 70% water loss for biomass, water content, and hormone analyses. Drought experiments were repeated three times and at least four plants per genotype and

treatment were used in each experiment. RWC was calculated according to the formula: $\text{RWC} (\%) = \frac{[(\text{FW} - \text{DW}) / (\text{TW} - \text{DW})] \times 100$.

Plant hormones quantification. Plant hormones cytokinins (*trans*-zeatin), gibberellins (GA1, GA4, and GA3), indole-3-acetic acid (IAA), ABA, salicylic acid (SA), JA, and the ethylene precursor 1-aminocyclopropane-1-carboxylic acid (ACC) were analyzed as follows. 10 μl of extracted sample were injected in a UHPLC–MS system consisting of an Accela Series U-HPLC (ThermoFisher Scientific, Waltham, MA, USA) coupled to an exactive mass spectrometer (ThermoFisher Scientific, Waltham, MA, USA) using a heated electrospray ionization (HESI) interface. Mass spectra were obtained using the Xcalibur software version 2.2 (ThermoFisher Scientific, Waltham, MA, USA). For quantification, calibration curves were constructed for each analyzed hormone (1, 10, 50, and 100 $\mu\text{g l}^{-1}$) and corrected for 10 $\mu\text{g l}^{-1}$ deuterated internal standards. Recovery percentages ranged between 92% and 95%.

For endogenous BR analysis plant materials (4 g fresh weight) were lyophilized and grinded. BL and CS were extracted with methanol and purified by solvent partitions by using a silica gel column and ODS-HPLC as follows. The endogenous levels of BL and CS were quantified by LC–MS/MS using their deuterated internal standards (2 ng).

LC–MS/MS analysis was performed with a triple quadrupole/linear ion trap instrument (QTRAP5500; AB Sciex, USA) with an electrospray source. Ion source was maintained at 300 °C. Ion spray voltage was set at 4500 V in positive ion mode. MRM analysis were performed at the transitions of m/z 487–433 (collision energy (CE) 30 V) and 487–451 (CE 21 V) for 2H 6 -BL, m/z 481 to 427 (CE 30 V) and 481–445 (CE 30 V) for BL, m/z 471–435 (CE 23 V) and 471–453 (CE 25 V) for 2H 6 -CS and m/z 465–429 (CE 23 V) and 465–447 (CE 25 V) for CS. Enhanced product ion scan was carried out at CE 21 V. HPLC separation was performed using a UHPLC (Nexera X2; Shimadzu, Japan) equipped with an ODS column (Kinetex C18, $\text{f}_2.1$ 150 mm, 1.7 μm ; Phenomenex, USA). The column oven temperature was maintained at 30 °C. The mobile phase consisted of acetonitrile (solvent A) and water (solvent B), both of which contained 0.1% (v/v) acetic acid. HPLC separation was conducted with the following gradient at flow rate of 0.2 ml/min: 0–12 min, 20% A–80% A; 12–13 min, 80% A–100% A; 13–16 min, 100% A.

Data availability

RNAseq and microarray data that support the findings of this study have been deposited in Gene Expression Omnibus (GEO) with the [GSE119382](https://www.ncbi.nlm.nih.gov/geo/query/acc.cgi?acc=GSE119382) and [GSE119383](https://www.ncbi.nlm.nih.gov/geo/query/acc.cgi?acc=GSE119383) accession codes.

Received: 19 June 2017 Accepted: 26 September 2018

Published online: 08 November 2018

References

- Boyer, J. S. Plant productivity and environment. *Science* **218**, 443–448 (1982).
- Todaka, D., Shinozaki, K. & Yamaguchi-Shinozaki, K. Recent advances in the dissection of drought-stress regulatory networks and strategies for development of drought-tolerant transgenic rice plants. *Front. Plant Sci.* **6**, 84 (2015).
- Yoshida, T., Mogami, J. & Yamaguchi-Shinozaki, K. ABA-dependent and ABA-independent signaling in response to osmotic stress in plants. *Curr. Opin. Plant Biol.* **21**, 133–139 (2014).
- Graether, S. P. & Boddington, K. F. Disorder and function: a review of the dehydrin protein family. *Front. Plant Sci.* **5**, 576 (2014).
- Seki, M., Umezawa, T., Urano, K. & Shinozaki, K. Regulatory metabolic networks in drought stress responses. *Curr. Opin. Plant Biol.* **10**, 296–302 (2007).
- Shao, H. B., Chu, L. Y., Jaleel, C. A. & Zhao, C. X. Water-deficit stress-induced anatomical changes in higher plants. *C. R. Biol.* **331**, 215–225 (2008).
- Tardieu, F. Any trait or trait-related allele can confer drought tolerance: just design the right drought scenario. *J. Exp. Bot.* **63**, 25–31 (2012).
- Marshall, A. et al. Tackling drought stress: receptor-like kinases present new approaches. *Plant Cell* **24**, 2262–2278 (2012).
- Smakowska-Luzan, E. et al. An extracellular network of *Arabidopsis* leucine-rich repeat receptor kinases. *Nature* **553**, 342–346 (2018).
- Li, J. & Chory, J. A putative leucine-rich repeat receptor kinase involved in brassinosteroid signal transduction. *Cell* **90**, 929–938 (1997).
- Wang, Z. Y., Seto, H., Fujioka, S., Yoshida, S. & Chory, J. BRI1 is a critical component of a plasma-membrane receptor for plant steroids. *Nature* **410**, 380–383 (2001).
- Kinoshita, T. et al. Binding of brassinosteroids to the extracellular domain of plant receptor kinase BRI1. *Nature* **433**, 167–171 (2005).
- Hothorn, M. et al. Structural basis of steroid hormone perception by the receptor kinase BRI1. *Nature* **474**, 467–471 (2011).

14. She, J. et al. Structural insight into brassinosteroid perception by BRI1. *Nature* **474**, 472–476 (2011).
15. Karlova, R. et al. The *Arabidopsis* somatic embryogenesis receptor-like Kinase1 protein complex includes Brassinosteroid-insensitive1. *Plant Cell* **18**, 626–638 (2006).
16. Li, J. et al. BAK1, an Arabidopsis LRR receptor-like protein kinase, interacts with BRI1 and modulates brassinosteroid signaling. *Cell* **110**, 213–222 (2002).
17. Nam, K. H. & Li, J. BRI1/BAK1, a receptor kinase pair mediating brassinosteroid signaling. *Plant Physiol.* **123**, 93–100 (2000).
18. Gou, X. et al. Genetic evidence for an indispensable role of somatic embryogenesis receptor kinases in brassinosteroid signaling. *PLoS Genet.* **8**, e1002452 (2012).
19. Yin, Y. et al. BES1 accumulates in the nucleus in response to brassinosteroids to regulate gene expression and promote stem elongation. *Cell* **109**, 181–191 (2002).
20. Wang, Z. Y. et al. Nuclear-localized BZR1 mediates brassinosteroid-induced growth and feedback suppression of brassinosteroid biosynthesis. *Dev. Cell* **2**, 505–513 (2002).
21. He, J. X., Gendron, J. M., Yang, Y., Li, J. & Wang, Z. Y. The GSK3-like kinase BIN2 phosphorylates and destabilizes BZR1, a positive regulator of the brassinosteroid signaling pathway in Arabidopsis. *Proc. Natl Acad. Sci. USA* **99**, 10185–90 (2002).
22. Kagale, S., Divi, U. K., Krochko, J. E., Keller, W. A. & Krishna, P. Brassinosteroid confers tolerance in *Arabidopsis thaliana* and *Brassica napus* to a range of abiotic stresses. *Planta* **225**, 353–364 (2007).
23. Krishna, P. Brassinosteroid-mediated stress responses. *J. Plant Growth Regul.* **22**, 289–297 (2003).
24. Sahni, S. et al. Overexpression of the brassinosteroid biosynthetic gene DWF4 in *Brassica napus* simultaneously increases seed yield and stress tolerance. *Sci. Rep.* **6**, 28298 (2016).
25. Feng, Y., Yin, Y. & Fei, S. Down-regulation of BdBRI1, a putative brassinosteroid receptor gene produces a dwarf phenotype with enhanced drought tolerance in *Brachypodium distachyon*. *Plant Sci.* **234**, 163–173 (2015).
26. Ye, H. et al. RD26 mediates crosstalk between drought and brassinosteroid signalling pathways. *Nat. Commun.* **8**, 14573 (2017).
27. Zhang, S., Cai, Z. & Wang, X. The primary signaling outputs of brassinosteroids are regulated by abscisic acid signaling. *Proc. Natl Acad. Sci. USA* **106**, 4543–4548 (2009).
28. Gui, J. et al. OsREM4.1 interacts with OsSERK1 to coordinate the interlinking between abscisic acid and brassinosteroid signaling in rice. *Dev. Cell* **38**, 201–213 (2016).
29. Huang, D., Wu, W., Abrams, S. R. & Cutler, A. J. The relationship of drought-related gene expression in *Arabidopsis thaliana* to hormonal and environmental factors. *J. Exp. Bot.* **59**, 2991–3007 (2008).
30. Chung, Y., Kwon, S. I. & Choe, S. Antagonistic regulation of *Arabidopsis* growth by brassinosteroids and abiotic stresses. *Mol. Cells* **37**, 795–803 (2014).
31. Vilarrasa-Blasi, J. et al. Regulation of plant stem cell quiescence by a brassinosteroid signaling module. *Dev. Cell* **30**, 36–47 (2014).
32. Fábregas, N. & Caño-Delgado, A. I. Turning on the microscope turret: a new view for the study of brassinosteroid signaling in plant development. *Physiol. Plant* **151**, 172–183 (2014).
33. Fábregas, N. et al. The brassinosteroid insensitive1-like3 signalosome complex regulates *Arabidopsis* root development. *Plant Cell* **25**, 3377–3388 (2013).
34. Lozano-Elena, F., Planas-Riverola, A., Vilarrasa-Blasi, J., Schwab, R. & Cano-Delgado, A. I. Paracrine brassinosteroid signaling at the stem cell niche controls cellular regeneration. *J. Cell. Sci.* **131**, jcs204065 (2018).
35. Friedrichsen, D. M., Joazeiro, C. A., Li, J., Hunter, T. & Chory, J. Brassinosteroid-insensitive-1 is a ubiquitously expressed leucine-rich repeat receptor serine/threonine kinase. *Plant Physiol.* **123**, 1247–1256 (2000).
36. Caño-Delgado, A. et al. BRL1 and BRL3 are novel brassinosteroid receptors that function in vascular differentiation in *Arabidopsis*. *Development* **131**, 5341–5351 (2004).
37. Belkhadir, Y. & Jaillais, Y. The molecular circuitry of brassinosteroid signaling. *New Phytol.* **206**, 522–540 (2015).
38. Eremina, M. et al. Brassinosteroids participate in the control of basal and acquired freezing tolerance of plants. *Proc. Natl Acad. Sci. USA* **113**, E5982–E5991 (2016).
39. Vragovic, K. et al. Transcriptome analyses capture of opposing tissue-specific brassinosteroid signals orchestrating root meristem differentiation. *Proc. Natl Acad. Sci. USA* **112**, 923–928 (2015).
40. González-García, M. P. et al. Brassinosteroids control meristem size by promoting cell cycle progression in *Arabidopsis* roots. *Development* **138**, 849–859 (2011).
41. Hacham, Y. et al. Brassinosteroid perception in the epidermis controls root meristem size. *Development* **138**, 839–848 (2011).
42. Duan, Y. et al. An endoplasmic reticulum response pathway mediates programmed cell death of root tip induced by water stress in *Arabidopsis*. *New Phytol.* **186**, 681–695 (2010).
43. Takahashi, N., Goto, N., Okada, K. & Takahashi, H. Hydrotropism in abscisic acid, wavy, and gravitropic mutants of *Arabidopsis thaliana*. *Planta* **216**, 203–211 (2002).
44. Asami, T. et al. Characterization of brassinazole, a triazole-type brassinosteroid biosynthesis inhibitor. *Plant Physiol.* **123**, 93–100 (2000).
45. Singh, T. N., Aspinall, D. & Paleg, L. G. Proline accumulation and varietal adaptability to drought in barley: a potential metabolic measure of drought resistance. *Nat. New Biol.* **236**, 188–190 (1972).
46. Szabados, L. & Savoure, A. Proline: a multifunctional amino acid. *Trends Plant Sci.* **15**, 89–97 (2010).
47. Durand, M. et al. Water deficit enhances C export to the roots in *Arabidopsis thaliana* plants with contribution of sucrose transporters in both shoot and roots. *Plant Physiol.* **170**, 1460–1479 (2016).
48. Conrath, U., Pieterse, C. M. & Mauch-Mani, B. Priming in plant-pathogen interactions. *Trends Plant Sci.* **7**, 210–216 (2002).
49. Brady, S. M. et al. A high-resolution root spatiotemporal map reveals dominant expression patterns. *Science* **318**, 801–806 (2007).
50. Garcia-Alcalde, F., Garcia-Lopez, F., Dopazo, J. & Conesa, A. Paintomics: a web based tool for the joint visualization of transcriptomics and metabolomics data. *Bioinformatics* **27**, 137–139 (2011).
51. Shakirova, F. et al. Involvement of dehydrins in 24-epibrassinolide-induced protection of wheat plants against drought stress. *Plant Physiol. Biochem.* **108**, 539–548 (2016).
52. Chen, J. et al. Arabidopsis WRKY46, WRKY54, and WRKY70 transcription factors are involved in brassinosteroid-regulated plant growth and drought responses. *Plant Cell* **29**, 1425 (2017).
53. Iwata, S., Miyazawa, Y., Fujii, N. & Takahashi, H. MIZ1-regulated hydrotropism functions in the growth and survival of *Arabidopsis thaliana* under natural conditions. *Ann. Bot.* **112**, 103–114 (2013).
54. Ge, L.-F. et al. Overexpression of the trehalose-6-phosphate phosphatase gene OSTPP1 confers stress tolerance in rice and results in the activation of stress responsive genes. *Planta* **228**, 191–201 (2008).
55. Nuccio, M. L. et al. Expression of trehalose-6-phosphate phosphatase in maize ears improves yield in well-watered and drought conditions. *Nat. Biotechnol.* **33**, 862 (2015).
56. Himuro, Y. et al. Arabidopsis galactinol synthase AtGolS2 improves drought tolerance in the monocot model *Brachypodium distachyon*. *J. Plant Physiol.* **171**, 1127–1131 (2014).
57. Nanjo, T. et al. Antisense suppression of proline degradation improves tolerance to freezing and salinity in *Arabidopsis thaliana*. *FEBS Lett.* **461**, 205–210 (1999).
58. Wu, C. Y. et al. Brassinosteroids regulate grain filling in rice. *Plant Cell* **20**, 2130–2145 (2008).
59. Xu, F., Xi, Z.-M., Zhang, H., Zhang, C.-J. & Zhang, Z.-W. Brassinosteroids are involved in controlling sugar unloading in *Vitis vinifera* 'Cabernet Sauvignon' berries during véraison. *Plant Physiol. Biochem.* **94**, 197–208 (2015).
60. Krasensky, J. & Jonak, C. Drought, salt, and temperature stress-induced metabolic rearrangements and regulatory networks. *J. Exp. Bot.* **63**, 1593–608 (2012).
61. Urano, K. et al. Characterization of the ABA-regulated global responses to dehydration in *Arabidopsis* by metabolomics. *Plant J.* **57**, 1065–78 (2009).
62. Ding, Y., Fromm, M. & Avramova, Z. Multiple exposures to drought 'train' transcriptional responses in *Arabidopsis*. *Nat. Commun.* **3**, 740 (2012).
63. Nishizawa, A., Yabuta, Y. & Shigeoka, S. Galactinol and raffinose constitute a novel function to protect plants from oxidative damage. *Plant Physiol.* **147**, 1251–1263 (2008).
64. Aljanabi, S. M. & Martinez, I. Universal and rapid salt-extraction of high quality genomic DNA for PCR-based techniques. *Nucleic Acids Res.* **25**, 4692–4693 (1997).
65. Betegón-Putze, I., González, A., Sevillano, X., Blasco-Escámez, D. & Caño-Delgado, A. I. MyROOT: a novel method and software for the semi-automatic measurement of plant root length. Preprint at *bioRxiv* <https://doi.org/10.1101/309773> (2018).
66. Liseč, J., Schauer, N., Kopka, J., Willmitzer, L. & Fernie, A. R. Gas chromatography mass spectrometry-based metabolite profiling in plants. *Nat. Protoc.* **1**, 387–396 (2006).
67. Kopka, J. et al. GMD@CSB.DB: the golm metabolome database. *Bioinformatics* **21**, 1635–1638 (2005).
68. Luedemann, A., Strassburg, K., Erban, A. & Kopka, J. TagFinder for the quantitative analysis of gas chromatography-mass spectrometry (GC-MS)-based metabolite profiling experiments. *Bioinformatics* **24**, 732–737 (2008).

69. Conesa, A., Nueda, M. J., Ferrer, A. & Talon, M. maSigPro: a method to identify significantly differential expression profiles in time-course microarray experiments. *Bioinformatics* **22**, 1096–1102 (2006).
70. Ritchie, M. E. et al. limma powers differential expression analyses for RNA-sequencing and microarray studies. *Nucleic Acids Res.* **43**, e47 (2015).

Acknowledgements

We thank Ricardo Aiese Cigliano (Sequentia Biotech) for help with microarray analysis, Tony Ferrar for critical manuscript revision and language editing (<http://www.theeditorsite.com>) and Olga Moreno Pradas for graphic design support. We acknowledge financial support from the Spanish Ministry of Economy and Competitiveness, through the “Severo Ochoa Programme for Centres of Excellence in R&D” 2016 2019 (SEV 2015 0533), the CERCA Programme from the Generalitat de Catalunya, and the Agencia de Gestió d’Ajuts Universitaris i de Recerca (2014 SGR 1406). N.F. was funded by Fundación Renta Corporación, by EMBO short term postdoctoral fellowship (ASTF 422 2015) and by BIO2013 43873; F.L.E. was funded by BIO2013 43873 and BIO2016 78150 P; and D.B. was funded by BIO2013 43873 and ERC 2015 CoG GA 683163. C.M.A., A.A., and F.P.A. acknowledge financial support from the Spanish MINECO FEDER (project AGL2014 59728 R) and from the European Union’s Seventh Framework Program for research technological development and demonstration under grant agreement no. 289365 (project ROOTOPOWER). S.O. was supported by Ministry of Science and Innovation and University of Malaga (Spain) through the grant Ramón y Cajal program (Sonia Osorio, RYC 09170). M.B. was funded by BES 2012 053274 and J.L.R. laboratory is supported by grant BFU2014 58289 P from the Spanish Ministry of Economy and Competitiveness. A.I.C. D. A.C. collaboration was funded by the European Regional Development Funds and Marie Curie IRSES Project DEANN (PIRSES GA 2013 612583). A.I.C. D. is a recipient of BIO2013 43873 and BIO2016 78150 P grants from the Spanish Ministry of Economy and Competitiveness. A.I.C. D. is recipient of an ERC Consolidator Grant; this project has received funding from the European Research Council (ERC) under the European Union’s Horizon 2020 research and innovation program (grant agreement no. 683163).

Author contributions

A.I.C. D. conceived, designed and supervised the study. N.F., F.L.E., D.B., C.M.A., and F.P.A. performed the genetics and stress phenomic experiments and data analyses. N.F.,

F.L.E., M.B., J.L.R., and A.I.C. D. designed the genome wide experiments. N.F., F.L.E., A.C., and A.I.C. D. performed the genome wide experiments and data analysis. N.F., F.L.E., T.T., S.O., and A.R.F. carried out the metabolic profiling and data analysis. A.A. performed the hormone profiling experiments. T.N. and T.Y. carried the CS and BL quantification assays. N.F., F.L.E., and A.I.C. D. wrote the manuscript. All authors discussed the results and the manuscript.

Additional information

Supplementary Information accompanies this paper at <https://doi.org/10.1038/s41467-018-06861-3>.

Competing interests: The authors declare no competing interests.

Reprints and permission information is available online at <http://npg.nature.com/reprintsandpermissions/>

Publisher’s note: Springer Nature remains neutral with regard to jurisdictional claims in published maps and institutional affiliations.



Open Access This article is licensed under a Creative Commons Attribution 4.0 International License, which permits use, sharing, adaptation, distribution and reproduction in any medium or format, as long as you give appropriate credit to the original author(s) and the source, provide a link to the Creative Commons license, and indicate if changes were made. The images or other third party material in this article are included in the article’s Creative Commons license, unless indicated otherwise in a credit line to the material. If material is not included in the article’s Creative Commons license and your intended use is not permitted by statutory regulation or exceeds the permitted use, you will need to obtain permission directly from the copyright holder. To view a copy of this license, visit <http://creativecommons.org/licenses/by/4.0/>.

© The Author(s) 2018

